Activation of Hydrocarbons and their Catalytic Oxidation by Heterogeneous Catalysis

Thesis submitted in accordance with the requirements of Cardiff University for the degree of

Doctor of Philosophy

VIRGINIE PENEAU

December 2014

Acknowledgements

Having completed this PhD, I would like to extend my gratitude to a number of people, who made these three years possible.

First of all I would like to express my gratitude to my supervisor Prof. Graham Hutchings for giving me the opportunity to do this PhD, for his support and guidance throughout the period of my research.

I am also very happy to acknowledge my post doc Drs Michael Forde, Greg Shaw and Simon Freakley as well as Drs Rob Armstrong and Nikolaos Dimitratos, for their continued encouragement, support and advice. I would also like to thank Prof. Christopher Kiely and his students for the microscopy analysis of my catalyst.

I extend my gratitude to Cardiff University for the financial support. I would like to acknowledge Evonik industries, sponsor of one of the projects I worked on. And I would like to thank Dr Horst-Werner Zanthaff and Dr Holger Wiederhold for their help given during the last year of my PhD.

Thanks must be given to Steven Morris and Dr Robert Jenkins for their continued technical assistance and advice throughout the time of my PhD.

A special thank you goes to Dr Greg Shaw for all the long hours spent on my thesis corrections. I am also very grateful to Clara, Ewa, Amie, Alastair, James and Kevin who took the time to read my thesis.

I would also like to acknowledge my fellow PhD student and friend, Rebecca McVicker who helped me at the start with languages and British culture.

Many thanks go to all my friends in Cardiff especially Clara Erice Jurecky for believing in me and for their support all these years.

Finally I would like to thank my family and loved ones for their constant support, encouragement and patience throughout the past 3 years.

Abstract

The targets of this thesis were the selective oxidation of hydrocarbons under mild conditions, using cheap and environmentally friendly oxidants and initiators. Three projects are treated; the oxidation of an alkane using O_2 and a co-oxidant, the oxidation of toluene using TBHP (*tert*-butyl hydroperoxide) and finally the oxidation of propane using hydrogen peroxide. C-H bond activation, O_2 activation and high conversion with high selectivity were essential points to investigate.

In the first project, alkane oxidation was studied in presence of a co-oxidant. The co-oxidant has for purpose to initiate the activation of the alkane and O_2, as well as prevent the over-oxidation of the alkane. The co-oxidation of octane using benzaldehyde has been investigated using 1 wt. % AuPd/ C catalyst; the hypothesis is that benzaldehyde oxidation would use a radical mechanism able to activate octane to octanol. Also, the coupling of octanol with activated benzaldehyde would prevent the over-oxidation of octanol by the formation of an ester; octylbenzoate.

The aim of the second study was to investigate the selective oxidation of toluene using TBHP at 80 °C with supported noble metal nanoparticle catalysts prepared by sol-immobilisation techniques. Au, Pd and Pt have been use to form mono, bi and trimetallic catalysts of different morphology supported on C and TiO_2. These catalysts have been tested for toluene oxidation. The catalyst showing the best activity has been used for further investigation such as reuse test, using H_2O_2 as oxidant or O_2 activation.

The third project target was to oxidise propane using H_2O_2 in mild conditions. 2.5 wt. % Fe/ ZSM-5 (30) has been used to investigate reaction conditions in order to optimise the system. This catalyst has been acid treated; standard and treated catalysts were characterised and analysed to identify the structure and active sites. Role of supports and metals (mono and bimetallic) has been explored in order to improve this system.

List of abbreviations

Å	Angstrom i.e. 10^{-10} metres
acac	Acetylacetonate
at. %	Atomic percent
BET	Brunauer, Emmett, Teller; Surface area analysis
C_n	n carbon(s) per alkane molecule
°C	Degrees Celsius
cm	Centimetre
cm^{-1}	Reciprocal centimetre
CVI	Chemical Vapour Impregnation
DRIFTS	Diffuse Reflectance Infrared Fourier Transform Spectroscopy
EDX	Energy Dispersive X-ray Spectroscopy
EPR	Electron Paramagnetic Resonance
eV	Electron Volts
FID	Flame Ionisation Detector
g	Gram
GC	Gas Chromatography
h	Hour
HAADF	High Angle Annular Dark Field
HPLC	High-Performance Liquid Chromatography
HOMO	Highest Occupied Molecular Orbital
ICP	Inductively Coupled Plasma
IR	Infrared Spectroscopy
λ	Wavelength
KBr	Potassium bromide
kHz	Kilohertz
kV	Kilovolts
LUMO	Lowest Unoccupied Molecular Orbital
M	Molar (moles per litre)
mA	Milliampere
MAS-NMR	Magic Angle Spin Nuclear Magnetic Resonance
MFI	Mordenite Framework Inverted
MHz	Megahertz
Min	Minute
mL	Millilitre

mm	Millimetre
MMO	Methane Monooxygenase
Mol	Moles
MS	Mass Spectroscopy
mV	Millivolts
NH_3-TPD	Temperature Programmed ammonia Desorption
NMR	Nuclear Magnetic Resonance
Nm	Nanometre i.e. 10^{-9} metres
Oh	Octahedral
PTFE	Polytetrafluoroethylene
PVA	Polyvinyl alcohol
rpm	Revolutions per minute
SEM	Scanning Electron Microscopy
SI	Sol Immobilisation
$SiO_2/Al_2O_3 = X$	Moles of SiO_2 to 1 mole of Al_2O_3 in a specific zeolite
STEM	Scanning Transmission Electron Microscopy
TBHP	*tert*-Butyl hydroperoxide
TBOT	Titanium (IV) tetrabutoxide
Td	Tetrahedral
TCD	Thermal Conductivity Detector
TEM	Transmission Electron Microscopy
TEOS	Tetraethylorthosilicate,
TMS	Tetramethyl Silane
TPAOH	Tetrapropylammonium hydroxide
TGA	Thermogravimetric Analysis
TPR/ TPO	Temperature Programme Reduction/ Oxidation
TON	Turnover number
TOF	Turnover frequency
TS-1	Titanium silicalite-1
UV-Vis	Ultraviolet-Visible Electromagnetic Radiation Spectroscopy
W	Watt
wt. %	Weight percent
XPS	X-Ray Photoelectron Spectroscopy
XRD	X-Ray Diffraction
ZSM-5	Zeolite ZSM-5
μmol	Micromole i.e. 10^{-6} moles

Table of contents

Chapter 4: Toluene Oxidation using TBHP

Chapter 5: Propane Oxidation using H_2O_2

Chapter 6: Conclusions and Future work

General Introduction 1

1. Introduction

1.1. Concept of catalysis

Since the end of the 18th century, catalytic reactions have been studied. It was Berzelius who first introduced the concept of catalysis in 1835. It was explained as the ability of a molecule, without being changed, to help a reaction to occur in conditions that it wouldn't occur in without this molecule.[1] He defined this term based on many other scientific research papers and also stated that the transformation "cannot be explained by any chemical action" with the catalyst. A general definition of catalysis is the increase of the rate of reaction by an additional substance, namely a catalyst. Despite its role in the reaction, a catalyst is not consumed during the reaction.[2, 3]

Many scientists studied the use of catalysis, including industrialists. For example a patent from Phillips proposed the use of Pt as a catalyst for sulfuric acid production.[4] The studies of reactions using catalyst grew and scientists soon realised that catalysis was applicable for a broad range of processes. In 1877, Lemoine elucidated the thermodynamics of catalysis. He explained that the rate of reaction is the only parameter to change, whereas the equilibrium of reaction stays the same.[5]

Catalysis was, and still is, widely studied. It also has many applications in industrial processes and manufacture. Catalysis is everywhere in life, even in the human body as proteins called enzymes. In every case a catalyst acts in the same way, by providing an

alternative pathway with lower activation energy (E_a) as shown in Figure 1.1. Hence, the energy of transition state is decreased allowing the reaction to occur.
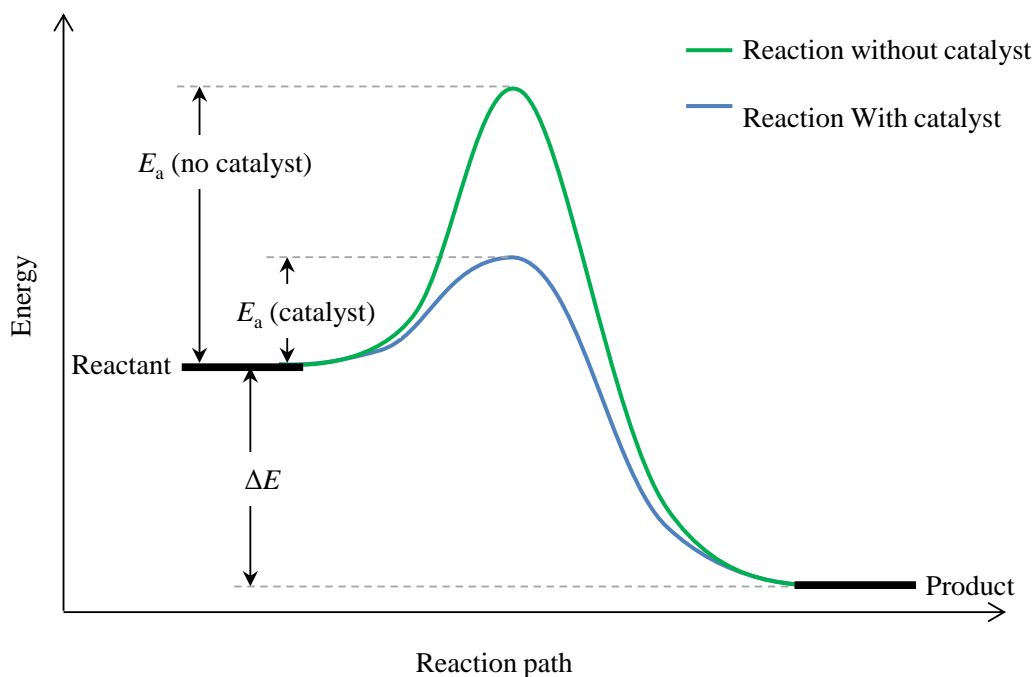
Figure 1.1: Potential energy diagram for reactions with and without catalyst

Three types of catalyst exist: enzymatic, homogeneous, and heterogeneous catalysts. An enzyme is a natural catalyst; a protein synthesised by cells. Their structure has a specific site called an 'active site' able to bond with the substrate. Once bonded, the reaction occurs and the products are formed.

Homogeneous catalysts are molecules that are in the same phase as the reactant, usually in liquid phase. Heterogeneous catalysts are molecules that are in a different phase from the reactant, for example a solid catalyst with the reactants in the liquid phase. Both homogeneous and heterogeneous catalysts have their advantages. However, for industrial processes heterogeneous catalysts are crucial as they can be separated and recycled.[6]

1.2. Heterogeneous catalysis

Heterogeneous catalysis has been studied since catalysis was first discovered. Van Marum, Davy, Dobereiner and others reported catalytic reactions using metals such as Pt, Ag, Fe or Cu.[7] As stated previously, heterogeneous catalysis implies the use of a catalyst which is in a different phase to the reactant; it can be liquid or solid. Most catalysts are solid with the reactants in the liquid or gas phase. Hence it is essential to

understand surface interactions and molecular adsorption in order to understand a reaction involving a heterogeneous catalyst.

A molecule can interact with a solid catalyst surface via two different types of adsorption, physisorption and chemisorption. Physisorption involves low energy Van Der Waals forces. This does not cause a significant change to the electronic structure of the adsorbate. Chemisorption is higher energy with bond dissociation and changes in electronic structure such as the sharing of an electron between the adsorbate and the surface.[8-10]

Three mechanisms are proposed for the chemisorption of molecules to a surface; Langmuir-Hinshelwood, Rideal-Eley and Mars-Van Krevelen mechanisms. For the Langmuir-Hinshelwood mechanism, two molecules are adsorbed onto the surface and interact together to give a product which will then desorb as shown Figure 1.2. An example of this is the reaction between NO_2 and NH_4^+ on the surface of V_2O_5 catalyst to form N_2 and H_2O.[11]
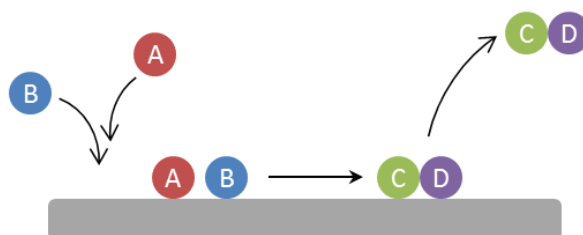
Figure 1.2: Langmuir-Hinshelwood mechanism

Figure 1.3 shows the Rideal-Eley mechanism, where one of the molecules (A) is adsorbed to the surface. A second molecule (B) will interact with (A) but is not adsorbed to the surface. The new products formed will then desorb. Petrov *et al.* reported the selective oxidation of ethene to ethylene oxide in presence of Ag and Ca catalyst supported on Al_2O_3. The empirical kinetic model shows that this reaction proceeds by a Rideal-Eley mechanism.[12]
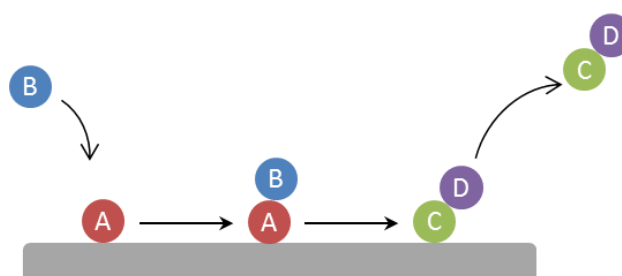
Figure 1.3: Rideal-Eley mechanism

3

Finally, the mechanism Mars-Van Krevelen involves the surface of the catalyst. The reactant interacts with the active surface to form the product. After reaction the product desorbs leaving a vacancy on the surface of the catalyst. The catalyst is regenerating by filling the vacancy as described in Figure 1.4.[13] This mechanism is used for the total oxidation of methanol, toluene and 2-propanol using Au/ CeO$_2$. The Au nanoparticles have the ability to decrease the strength of Ce-O bonds. Hence, the oxygen involved in the oxidation of the substrate is removed from the surface of the catalyst.[14]
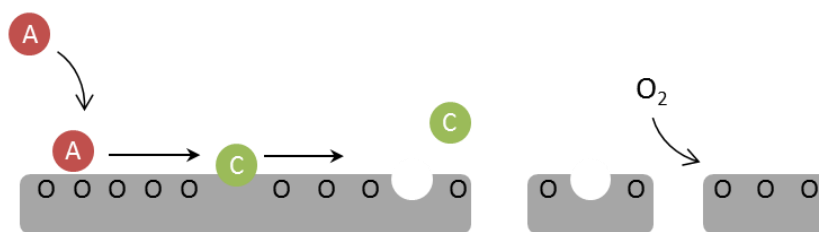
Figure 1.4: Mars-Van Krevelen mechanism

2. Preparation and use of catalysts

2.1. Preparation of catalysts

A catalyst can be synthesised from a number of different materials such as TiO$_2$, carbon and zeolites which are used to support active metals or metal oxides. The materials are chosen for properties such as porosity, surface area, thermal stability or photocatalytic properties. The components of a catalyst, i.e. the metals or supports, have specific properties which can be modified when the metal is supported.

Solymosi reported that the electronic properties of a support can play a role on the catalytic activity of supported metals due to their electronic interactions.[15] However, he also explains that the metal has to be a thin layer in order to be affected by these electronic effects. Hence the type of supports, as well as the morphology of the metal particles, is crucial to obtain an active catalyst.

Changing the interface between metal and support can also influence the catalytic activity of a material. This can be achieved by changing to a different support or by a variation of the preparation or pre-treatment method. Zhang and co-workers studied the efficiency of a NiO catalyst using various supports and different pre-treatments for the photocatalytic generation of hydrogen. It was reported that the diffusion and shape of Ni particles was different depending on the support, and was also affected by treatments which modified

the metal-support interface. A smaller particle size increased the metal surface area and the amount of active sites, increasing the photocatalytic activity.[16]

All characteristics of a catalyst come from the properties of the support and the metal particles (such as morphology and composition) and how they interact together. Hence the catalyst preparation method is very important as the activity of a catalyst can be sensitive to changes. Martin and co-workers showed the effects of using different precursors and changing the conditions of deposition for the preparation of ZnO films doped with alumina. It was reported that morphology and crystallinity were affected by the precursor used. It was also shown that Al concentration was higher when Zn acetate was used instead of $ZnCl_2$.[17]

2.2. Noble metal catalysts

Noble metal catalysts have played a significant role in modern catalysis, as for highly active catalysts only a very small amount of the costly metal is necessary, and if it can be recovered the cost of use is mitigated. Additionally, noble metal catalysts have found a place in green chemistry because of the ability to activate molecular O_2, a preferred oxidant.[18] Au, Pd and Pt are noble metals and they are used for various chemical transformations. For example, these metals have been shown to be the most active for the direct synthesis of H_2O_2,[19] selective alkane activation,[20, 21] alkene epoxidation,[22, 23] and selective alcohol oxidation.[24-26]

As noble metals are expensive, a low loading is important to decrease the cost involved. Ideally, all the deposited nanoparticles would be active for the target reaction in order to allow the lowest loading possible. It is now known that smallest particles size lead to highest activity for Au nanoparticles.[27] Lopez *et al.* proposed that decreasing the Au particle size increases the concentration of low-coordinated Au atoms which are the active sites for CO oxidation.[28] The size and shape of nanoparticles also has an important effect on reactions occurring at the interface between the particle and support. The smaller the particles are, the higher the number of interface sites.[29]

Research has shown the addition of a second metal to a monometallic supported catalyst can have a promoting effect. Prati and co-workers found that bimetallic catalysts (AuPd or AuPt) show better activity than the corresponding monometallic catalysts for the oxidation of glycerol. The presence of Pd or Pt also shows a difference in the selectivity of the products. Later, the same set of catalysts was tried for the oxidation of various alcohols. A positive synergistic effect was found for AuPd while a negative synergistic effect was found for AuPt.[30]

The support material used is also important, as metal particles show different activity depending on the support. Unsupported and supported Pt have been tested for the hydrogenation of aldehyde to alcohol. Pt was supported on various oxides, and it was shown that reducible support are able the change the catalytic behaviour. Pt catalysts supported on TiO_2, SnO_2, CeO_2 or ZnO show 60 % to 90 % selectivity for alcohol. Not more than 10 % alcohol selectivity could be reached using unsupported Pt, as well as with Pt supported on Al_2O_3 or MgO.[31]

Support materials can be catalytically active, and can also have an effect on the metal particles size and shape during the preparation of the catalyst.

Titania and carbon supports are frequently used as they show advantages when used as supports in catalytic reactions. Both are used in many catalytic processes due to their properties and low cost. Different types of carbon show different properties such as inertness, stability, high surface area, and porosity. All these properties allow carbon to be an appropriate support.[32, 33]Titania is used as raw material for photocatalytic processes and it is also used as support. A strong metal-support interaction (SMSI) has been reported between titania and noble metals.[34, 35] Vannice reported that SMSI between noble metals and titania led to an increase of activity for CO hydrogenation.[36]

Interaction of the support with the metal nanoparticles can cause changes to the properties of the material. It is been shown that colloidal AuPd particles with a mean particle size of 2.9 nm increase in particle size to 3.7 nm and 3.9 nm when they are supported on carbon and TiO_2 respectively. Furthermore, the morphology of the AuPd particles changes depending on which support is used; icosahedral AuPd colloids will possess the same morphology when supported on carbon, but become cuboctahedral when supported on TiO_2.[20, 21] Changing the shape of a nanoparticle can have an effect on the catalytic activity. Somorjai *et al.* reported that benzene hydrogenation gave different products depending on the shape of Pt nanoparticle; cyclohexane and cyclohexene were formed on cuboctahedral nanoparticles while only cyclohexane was formed on cubic nanoparticles.[37, 38]

The structure and morphology of a catalyst has an important role in the activity. Metal-support interactions, addition metals and all compounds used for the preparation of a catalyst can have consequences. Hence, size and shape of particles, interactions with support and oxidation state have to be well controlled during the preparation and reproducible methods have to be developed.

Colloidal methods to form metals nanoparticles with a well-controlled size have been well studied. This method allows the formation of controlled size nanoparticles with high

metal dispersion using various reactants such as stabiliser or reducer. These materials can then be immobilised onto a support with minimal change. Reactants play a role on the size, dispersion and oxidation state of the nanoparticles.[38-40] Homogeneous alloy bimetallic catalysts and core-shell materials can be prepared using the sol immobilisation method.[41] The order of reduction of metals during the preparation will define whether a homogeneous or core-shell catalyst will be made. The simultaneous reduction of metals will lead to a homogeneous catalyst whilst a consecutive reduction will lead to a core–shell catalyst. These various nanoparticles supported on TiO_2 and carbon have been used to oxidise toluene and benzyl alcohol using molecular O_2, indicating the activation of O_2 under mild condition.[21, 42]

2.3. Fe supported on zeolite catalyst

Zeolites are microporous aluminosilicate crystalline materials which belong to the molecular sieves family. This family is characterised by the existence of channels and cavities whose diameter varies between 5 Å and 20 Å. The uniform pore size distribution allows the zeolite to discriminate between molecules with dimensions only 0.1 Å apart. Zeolites are composed of TO_4 tetrahedra (where T = Si, Al) which are connected by bridging oxygen atoms. The general formula is $M_{m/z}[mAlO_2.nSiO_2].qH_2O$ where M is a cation (Na^+, NH_4^+, H^+) of charge z and q is the number of sorbed water molecules.[43-45] A pure SiO_2 zeolite structure would be electrically neutral. However, the substitution of Si^{4+} by Al^{3+} will cause negative charges, requiring a counter ion. If the counter cation is a proton H^+, the zeolite will display Brønsted acidity (Figure 1.5). The presence of Al atoms induces Lewis acidity. These properties can be changed with a heat treatment which leads to dealumination, which is a migration of the Al from the framework to the extra-framework.[44, 46] A wide range of Si/Al ratios are possible giving different properties due to the differences in acidity.
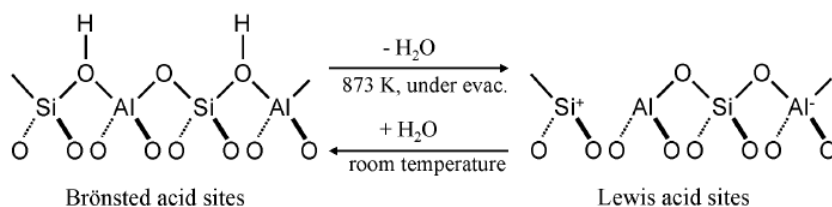
Figure 1.5: Structural representation of zeolite materials, Brønsted acidity and Lewis acid [47]

ZSM-5 is part of the MFI (Mordenite Framework Inverted) family of zeolites. MFI-type zeolites are based upon a 5-membered pentasil unit (Figure 1.6 (a)) which condenses with 5 other pentasil units to form the secondary building unit (SBU) (Figure 1.6 (b)). The ZSM-5 framework is composed of two 10-ring channel systems. The first one is sinusoidal along the [001] axis and its ring opening has a dimensions of 5.1 x 5.5 Å. The second one is straight, running parallel to [010] with rings openings of dimensions 5.4 x 5.6 Å.[48, 49]
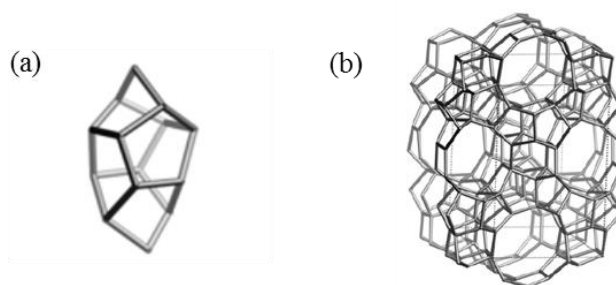
Figure 1.6: MFI composite building unit (a) and fusion of 5 pentasil units to yield the SBU of the MFI structure (b) [48]

Chemical vapour infiltration (CVI) is a controlled method for the introduction of metals into porous materials via sublimation of the metal precursor into the support.[50] This method, and others, has been used to support Fe on ZSM-5. CVI preparation gives high activity for the partial oxidation of methane.[51]

Zecchina *et al.* studied the structure and nuclearity of active sites in Fe/ zeolite. Figure 1.7 is a representation from their study. Three different Fe species were found; Fe_2O_3 nanoparticles, Fe_xO_y clusters, grafted Fe^{2+} and Fe^{3+} in framework position.
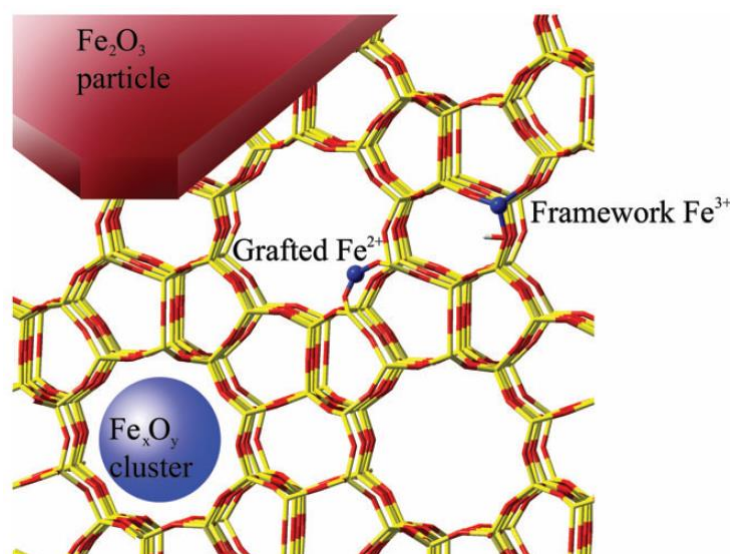
Figure 1.7: Representations of Fe$_2$O$_3$ particles, Fe$_x$O$_y$ clusters, grafter Fe^{2+} and Fe^{3+} in framework position [52]

3. *Potential oxidants for hydrocarbon oxidation*

In order to oxidise a hydrocarbon to an alcohol, aldehyde or acid, the presence of an O$_2$ source is crucial. According to Roger A. Sheldon three mechanisms can be distinguished for oxidation reactions: (i) auto-oxidation via a free radical chain reaction; (ii) oxidation of the substrate coordinated to the metal ion followed by re-oxidation of the reduced metal, and (iii) catalytic O$_2$ transfer.[53] The reaction conditions and the nature of the reactants (catalyst, oxidant) determine which mechanism will take place. Different oxidising agents can be utilised in an oxidation reaction. Oxygen that is incorporated into products can come from an oxidant which is not part of the catalyst, or it can be taken from the catalyst via reduction. Hence, an oxidant can interact directly with the substrate or be used in order to regenerate a catalyst as with the Mars-Van Krevelen mechanism.[54]

Often it is the formation of a peroxide species which will initiate the oxidation regardless of the oxidant used. Hence, some reactions can have similar activity using different oxidants, while other reactions will be dependent on the reagent used and variations in solvent, catalyst and oxidant.[53, 55]

In addition to being an oxidant, some species (H$_2$O$_2$ and TBHP) can also act as radical initiators. The homolytic cleavage of the molecule allows the formation of radical species which can easily activate other molecules. A radical mechanism is a three-step process and a general scheme is shown below. The first step, Equation 1, is initiation of the

molecule, in which an oxidant or radical initiator is subject to homolytic cleavage giving two radical molecules. The second step is the propagation of radical species to the target molecule. A radical molecule will react with a new molecule which will cleave to give another molecule and radical molecule as shown Equation 2. The propagation step carries on as long as radical molecules are in the system. Finally, any two radical species from the system can bond in order to form a final molecule, in a process called termination, Equation 3. Depending on which radical/ oxidant used, the mechanism will be slightly different within three steps. However, each step can include several reactions.[56, 57]

$$(1) \ \text{Initiation} \qquad R_1 - R_1 \longrightarrow 2 \ R_1^{\bullet}$$

$$(2) \ \text{Propagation} \qquad R_1^{\bullet} + R_2 - R_3 \longrightarrow R_1 - R_3 + R_2^{\bullet}$$

$$R_2^{\bullet} + R_4 - R_5 \longrightarrow R_2 - R_4 + R_5^{\bullet}$$

$$(3) \ \text{Termination} \qquad R_2^{\bullet} + R_5^{\bullet} \longrightarrow R_2 - R_5$$

$$2 \ R_2^{\bullet} \longrightarrow R_2 - R_2$$
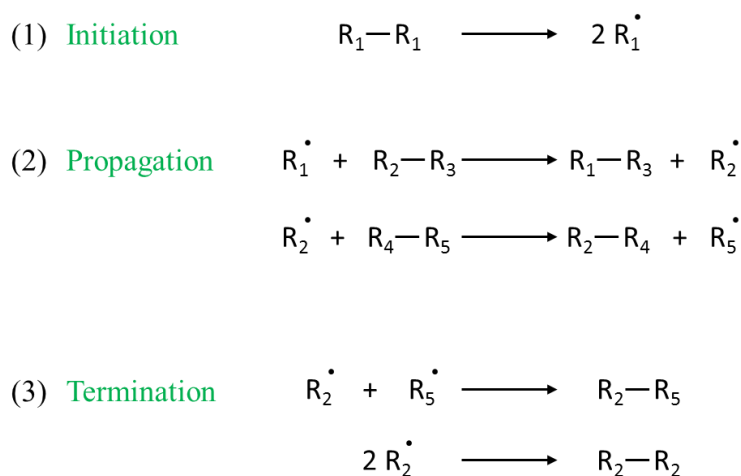
The use of stoichiometric oxidant such as $KMnO_4$, Ag_2O and CrO_3 is not considered environmentally friendly; hence the challenge is to replace them with cheap and available oxidants such as O_2, H_2O_2 and TBHP that are the focus of this study.

The use of these oxidants involved, in most cases, a radical pathway. Radical reactions are quite difficult to control. Hence it is important to design a catalyst able to initiate the radical mechanism as well as control the propagation. Understanding the mechanism of the reaction occurring on the surface of catalyst is crucial to the development of new systems. The choice between different oxidants is made depending on the reaction conditions, the substrate and the known mechanism. H_2O_2 and TBHP are relatively cheap and environmentally friendly oxidant, while O_2 is an abundant resources which is extremely cheap. However, O_2 is a more difficult oxidant to activate.

3.1. Hydrogen peroxide (H_2O_2)

H_2O_2 is a non-organic simple molecule widely used in the fine chemical industry but also in everyday life as a bleaching agent or disinfectant. From a chemistry point of view,

H_2O_2 is interesting as its decomposition gives only one by-product, water. This specificity gives to this molecule an undeniable green aspect. Shulpin and Nizova have shown the formation of peroxy radical species using O_2 with transition metal complex as catalyst.[58] H_2O_2 can form radical species with a high activity, simplifies the reaction by avoiding the step of making the peroxy species from O_2. The inconvenience with H_2O_2 is that it is thermodynamically unstable and decomposes to form water and O_2. High temperatures, concentrations, changes in pH and certain catalysts can increase the rate of decomposition making the use of H_2O_2 difficult and specific to certain reaction conditions.

A reaction of H_2O_2 with some species, such as Fe based catalysts, has been reported as Fenton's reaction. Fenton reagents decompose H_2O_2 into free radical HO· and HOO· as shown in equation 1 and 2.[57, 59]

$$(1) \quad Fe^{2+} + HO{-}OH \longrightarrow Fe^{3+} + HO^{\bullet} + HO^{-}$$

$$(2) \quad Fe^{3+} + HO{-}OH \longrightarrow Fe^{2+} + O^{\bullet}{-}OH + H^{+}$$
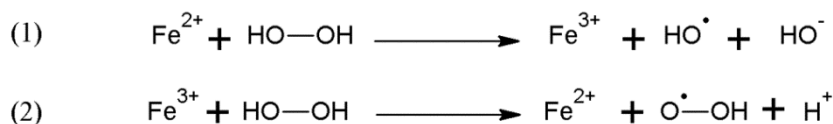
Homogeneous and heterogeneous Fe catalysts have been shown to be active for this reaction. Gallard and Laat described the kinetic decomposition of H_2O_2 at 25 ℃ by a homogeneous ferric solution. Araujo *et al.* reported the discolouration of reactive dye using hematite powder (Fe_2O_3) at 25 ℃ after 2 hours.[60, 61]

It is important to find a system where H_2O_2 is not decomposed to form water and O_2 in order to use H_2O_2 efficiently. The challenge is to decompose H_2O_2 into free radical species which will be introduced into products and recycle the H_2O_2 not used during the reaction. The formation of H_2O_2 has been studied in order to find a one-step reaction from H_2 and O_2 gas. Controlling the direct synthesis of H_2O_2 would permit the *in situ.* formation of H_2O_2 and be used to oxidise a target substrate. Hutchings *et al.* found that AuPd catalysts were able to form H_2O_2 by switching off subsequent decomposition and hydrogenation pathways.[62] It was found that AuPd supported on heteropolyacid catalysts show the greatest H_2O_2 productivity.[63]

3.2. Tert-butyl hydroperoxide (TBHP)

TBHP is an organic molecule which is more complex than H_2O_2. This molecule is widely used for oxidation processes. Compared to H_2O_2, the presence of the *tert*-butyl group gives the molecule organic properties, which allows it to be soluble in aqueous but also organic substrates. The use of catalysts, such as transition metals, coupled with TBHP is

quite active for oxidation reactions. It is assumed that the function of the catalyst is to activate TBHP, generating free radical species. Singh *et al.* showed the ability of their catalyst, LaMO$_3$ (where M = Cr, Co, Fe, Mn, Ni), to generate radicals from TBHP which then oxidised alkylaromatics molecules to benzylic ketones.[64]

The main reason to choose TBHP over H$_2$O$_2$ is its increased activation potential. H$_2$O$_2$ and TBHP need different energies to be activated via radical or heterolytic cleavage. As such the role of the catalyst and reaction condition is crucial. TBHP is a strong oxidant and often it is more effective than H$_2$O$_2$ and O$_2$. Many explanations have been given for this behaviour.[65, 66] Alirio E. Rodrigues reported a system where the decomposition of H$_2$O$_2$ was fast but TBHP was stable allowing it to initiate the reaction.[67] Escola *et al.* found that using TBHP over H$_2$O$_2$ gave better results for the oxidation of 1-dodecene to 2-dodecanone. In their system the formation of complexes between TBHP and Pd are reported. These complexes show varying oxidising properties which can explain the high oxidising performance of TBHP.[68] In contrast to this, A.P. Singh and co-workers reported a system where H$_2$O$_2$ was approximately three times more active than TBHP due to the more aqueous properties of H$_2$O$_2$ which would allow it to interact with the hydrophilic sites of the catalyst.[69] Often the decomposition into radical species of TBHP or H$_2$O$_2$ implies the formation of by-products. However, the by-product of H$_2$O$_2$ is water and usually does not interfere with the target products. In the case of TBHP few by-products can be formed such as *tert*-butanol or methanol which can be reactive depending on the reaction conditions.[56] Hence, the choice of oxidant should depend on the substrate used, the target products expected and the reaction conditions.

3.3. Oxygen (O$_2$)

Many researchers have been studying oxidation reactions using molecular O$_2$. It is a challenge to activate molecular O$_2$ compared to other oxidant due to the strong O=O double bond. However, the demand to use a green, cheap and abundant oxidant such as molecular O$_2$ is increasing. Other oxidants are frequently used because of their ability to be more easily activated. Usually stronger conditions, such as high temperature, are needed to activate O$_2$ whereas only mild conditions allow the activation of other oxidant such as H$_2$O$_2$. Understanding the activation mechanism and how O$_2$ interacts with the catalyst and substrate would help to develop a system able to activate O$_2$.

The use of O$_2$ as an oxidant in homogeneous catalysis has been studied and is better understood than for heterogeneous catalysis. Boisvert and Goldberg reported a few examples of homogeneous systems with O$_2$ as an oxidant.[70] The insertion of O$_2$ in late

metal complexes showed different mechanisms depending on the metal, its environment, and its oxidation state. Radical chain reactions, the formation of peroxy species by oxygen insertion, and reductive elimination are some of the mechanisms reported and compared in several studies with similar mechanisms. Heyduk *et al.* describes many systems using Pt complexes with different oxidation states such as $[PtCl_4]^{2-}$ or $(N-N)PtMe_2$, (N = tetramethylethylenediamine). These systems activate the C-H bond of alkanes in presence of O_2 under mild conditions.[71] Homogeneous Pd catalysts such as Pd acetate/ benzoquinone/ molybdo-vanado-phosphoric acid have also been reported active for the oxidation of methane to methanol using O_2 and mild conditions.[72]

Another catalytic system, using a mixture of homogeneous and heterogeneous catalysts, uses $CuCl_2$ with metallic Pd in the presence of O_2 and CO. This system has been shown to activate O_2 under mild conditions (150 ºC), and oxidise methane and other low chain alkanes. Activation of C-H and C-C bond leading to C-C cleavage has been observed.[73] In the case of heterogeneous catalysis, the activation of molecular O_2 requires higher temperature which often leads to over-oxidation of the products.[74]

Some metals have been shown to be active under milder conditions using O_2 as an oxidant. However, only low conversion is reached and the mechanism is not well understood. Robert G. Bell and co-workers used aluminophosphate molecular sieves containing Co^{III} or Mn^{III} ions to oxidise alkane chains (C_5, C_6 and C_8) at 100 ºC. A conversion of 8.8 % was reached for pentane using O_2; nevertheless, the mechanism has not been elucidated.[75] Many papers reported the ability of Au based catalysts to activate O_2. Schroeder and co-workers reported the activation of O_2 by Au/ TiO_2 for CO oxidation at room temperature.[76] The addition of a second metal such as Pd, Fe or Ag can promote O_2 activation at mild temperatures (80 ºC to 120 ºC).[77-79] Various Au/ TiO_2 catalysts have also been characterised to investigate O_2 activation depending on the size and shape of the Au clusters and their interaction with TiO_2. Hence, a part of mechanism can be understood.[80]

In the presence of certain catalysts and under the right conditions, a Fenton-type reaction can be observed using molecular O_2. Sasaki and co-workers reported that a Cu catalyst, in presence of O_2 and proton donor molecule, will form H_2O_2 which will then react as Fenton reagent.[81] Later this group tried the same experiments with other metals (Fe, Cr, Pb and Sn) and observed similar reactions with lower rate but the formation of H_2O_2 was not detected.[82]

Sometimes O_2 is used as the oxidant but it is not able to directly activate the reaction. Hence the addition of a non-oxidant radical initiator can activate the reaction using O_2.

Ishii *et al.* added *N*-hydroxyphthalimide (NHPI) to their catalyst system. NHPI is activated, forming the radical species phthalimide-*N*-oxyl (PINO). This is key to the reaction as it is able to activate the substrate, toluene.[83] The use of sacrificial aldehyde has also been investigated. The presence of an aldehyde in the system is able to activate O_2 by forming peroxy radical species which would then react with the substrate.[84]

4. *Activation of hydrocarbons*

Hydrocarbon molecules are organic compounds made from carbon and hydrogen which can be classified into various sub-divisions. They can be linear or cyclic, and saturated or unsaturated. Hydrocarbons can be gaseous (methane), liquid (hexane) or solid (polymer) and as such cover a large range of different properties. Hydrocarbons are also found in nature, being the principal constituent of fossil fuel in the form of natural gas and petroleum. They are also present in trees and plants. As such they are primarily used as a source of energy.

In the current work aromatic toluene and various saturated linear hydrocarbons including methane, propane and octane have been studied. These are simple molecules found in fossil fuels and although some of them can be used as raw materials for chemical processes, their oxidation products are often more valuable.

4.1. Selective oxidation of hydrocarbon

The oxidation of hydrocarbons can be divided in two categories: total oxidation to CO_2, (namely combustion), and partial and selective oxidation. Both have been studied for centuries, with a recent large expansion of research into the selective oxidation of hydrocarbons to form more valuable products, avoiding the formation of CO_2. Different methods can be used for oxidation including biological and biomimetic catalysis, which investigate the properties of natural catalysts (enzymes) in order to apply these properties in industrial applications. Often, homogeneous catalysis oxidises more selectively with lower energy whereas heterogeneous catalysis is less selective and requires more energy. However, heterogeneous catalysis is the most economical way as the catalyst can be recycled and reused.[85]

Factors affecting the properties of the catalyst play a role on their activity for both the total oxidation of alkanes and for the selective oxidation. The products formed depend on the adsorption site, as shown in Figure 1.8. When the alkane is adsorbed on the oxygen, α-H elimination will produce an aldehyde, while β-H elimination will produce an olefin.

If the molecule is adsorbed on the metal there is no elimination reaction; the intermediates, being stable, stay on the surface and are further oxidised to CO_x.[86]

$$M\text{-}O\text{-}CH_2\text{-}CH_3 \longrightarrow CH_2=CH_2 + CH_3\text{-}CHO$$

$$M\text{-}O + CH_3\text{-}CH_3$$

$$M\text{-}CH_2CH_3 \longrightarrow n\ CO_x$$
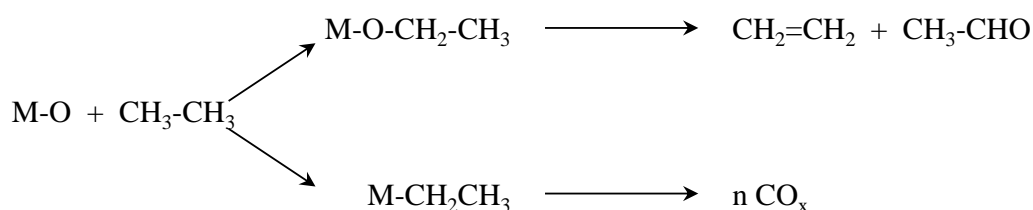
Figure 1.8: Different pathways due to the adsorption of ethene on the surface by oxygen bonded or metal bonded [86]

In order to oxidise an alkane only partially, the system has to be able to stop the reaction before over-oxidation. After activation of the C-H bond further oxidations are energetically favourable due to the highly negative standard free energy of formation of oxidation products.[87] The challenge is (i) to decrease the rate of the over-oxidation, (which also implies that being selective often decreases the total rate of reaction) or (ii) to find a catalyst which uses a reaction pathway able to desorb the product before its oxidation.

Homogeneous catalysis has been widely used, due to the fact that homogeneous catalysis not only showed promising results but are also easier to characterise and understand. Biochemical- and biomimetic-based reactions usually involve a radical pathway. Homogeneous metal-based systems are non-radical and the C-H bond cleavage occurs at the metal centre. Similar to a Mars-Van Krevelen mechanism, the substrate stays bound to the metal complex leading to stoichiometric activation. Hence, to obtain a catalytic reaction system, an additional elimination step of the product is required with regeneration of the homogeneous complex. The use of transition metal centres have been shown to be very efficient. Shilov and Shul'pin intensively studied the activation of the C-H bond by transition metal complexes, leading to a review reporting it. They reported the widespread use of Pt salt metal complex to activate saturated hydrocarbons. Pt complexes possess nucleophilic and electrophilic properties. Since the mechanism is different to the standard pathway (Figure 1.9), it is still not totally understood.[88]

Various mechanisms have been reported for the activation of the C-H bond such as an electrophilic system, oxidative addition,[89] σ-complexes and σ-bond metathesis.[90] However, according to Periana, four general mechanisms have been reported for the oxidation of C-H bonds by homogeneous catalysis as shown in Figure 1.9.[91] All these

mechanism have been, and are still being, investigated in order to improve understanding of the catalysts and the conditions required to selectively oxidise an alkane.

(i) Shilov type catalytic cycle

(ii) O-atom insertion cycle

(iii) High valence metals cycle

(iv) Low valence metals cycle
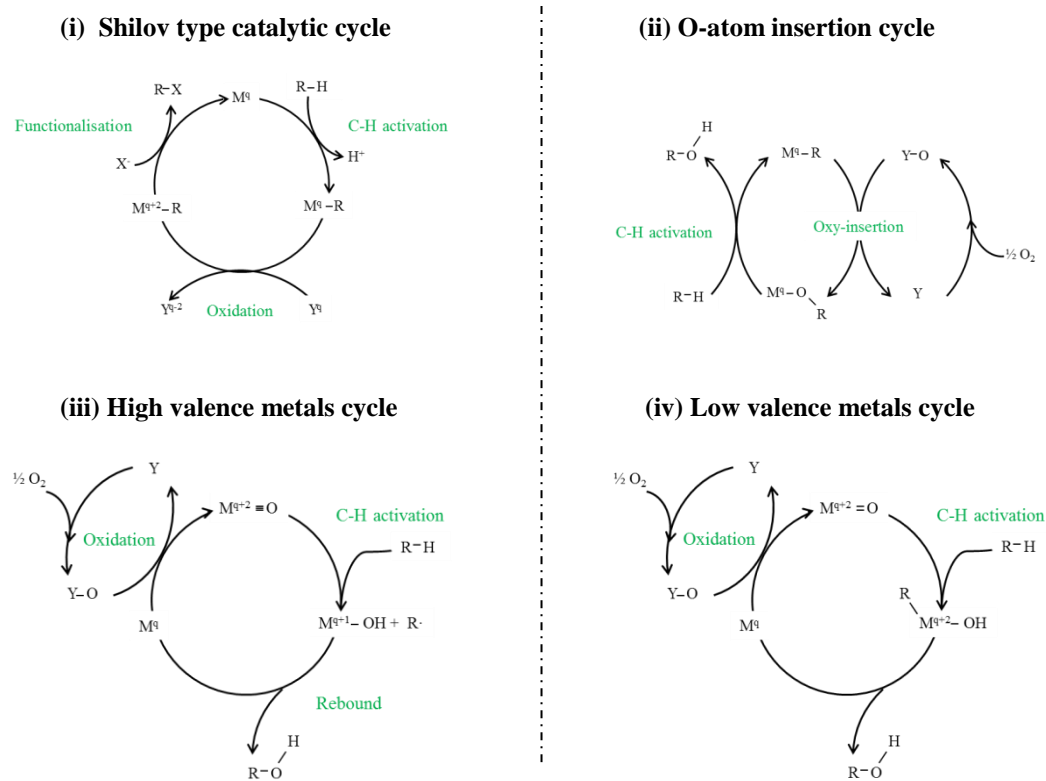
Figure 1.9: General mechanisms for the catalytic oxidation of alkane

(i)   Shilov mechanism, (which uses late transition metals), where the C-H bond is activated, followed by oxidation and release of the products.

(ii)   O-atom insertion involving an insertion of oxygen into an M-R bond after C-H activation. The M-O-R formed will then react with a hydrocarbon (RH) to release the product.

(iii) The use of high-valence metals for the activation of C-H with metal oxo species to form M-OH and alkyl radicals. The alkyl radical will then react with the hydroxyl to give an alcohol and the reduced metal. The metal is reoxidised using molecular O_2 in a different step.

(iv)   Using low-valence metals for the addition of R-H to the metal oxide forming one complex (M-alkyl (hydroxo)). Reductive elimination will then produce the alcohol and reduce the metal, which will then be reoxidised by molecular O_2.

The primary C-H bond is the most difficult bond to activate as the energy of other C-H bonds in the alkane chain are weaker, as shown in Figure 1.10. The difference between the primary and secondary bond is 11.7 kJ/ mol. The lighter the alkane is, the more inert it is, with methane being the most inert. Depending on the alkane, a catalyst can be designed in order to create steric interaction or to create a specific reactive site able to functionalise the primary C-H bond without over-oxidation.
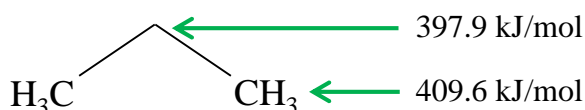
Figure 1.10:Bonds strength for propane [92]

In nature, cytochrome P450 is able to selectively oxidise the primary C-H bond to C-OH by physical constraint. A steric interaction between the enzyme and the substrate causes the oxidation of C-H bonds other than the primary are unfavourable.[93]

Dias *et al.* found a way to increase the selectivity toward the primary C-H bond; the silver complex catalyst used was modified by increasing the number of acidic silver sites or changing the ligands.[94] In another study an iridium catalyst with chemo-selective properties reacted with primary C-H bonds in preference to secondary C-H bonds using a mildly reducing reagent.[95] Recently theoretical studies have shown the possibility of activating the primary C-H bond of propane on PdO (101). The interaction of propane with the surface and the heterolytic cleavage of the C-H bond are two factors responsible for the preference toward primary C-H bond activation.[96] These examples show that it is possible to oxidise the primary C-H bond selectively by tailoring the catalyst and controlling the reaction conditions.

4.2. Methane

Methane (CH_4) is a principal component in natural gas and can also be found in coal beds. The global reserves of methane are colossal and have been rapidly increasing, especially in the last two decades.[91, 97] Methane is a greenhouse gas which contributes to global warming; the increase of the greenhouse effect is due to an increase of gases such as CO_2, methane or nitrous oxide that are able to trap the heat in the atmosphere.[98] Methane can be used as fuel and chemical feedstock but it is difficult to transport in the raw gaseous state. One solution is to convert methane into oxygenates, in particular

methanol.[97] However, methane is hard to activate, as the C-H bonds are difficult to cleave, but it is not completely inert.[99] The C-H bond in methane is stronger than the C-H bond in methanol, 438.8 kJ/ mol and 373.5 kJ/ mol respectively, hence when methane is oxidised to methanol the over-oxidation reaction to form formaldehyde, formic acid or carbon dioxide prevails.[97, 100]

In nature, enzymes like cytochromes P450 monooxygenase are able to oxidise an alkane to an alcohol under physiological pressure and temperature. Methane monooxygenase (MMO) shows the presence of a heme, which is considered to be the active site to oxidise methane. Studies reported that the active site is due to the Fe species of the heme.[101, 102] A representation of the active centre is shown in Figure 1.11 and a catalytic cycle is shown in Figure 1.12. More investigations on MMO mention the possible role of Cu as well as Fe in particulate MMO (pMMO) compare to soluble MMO (sMMO). [103] Balasubramanian *et al.* extracted all metal species from pMMO. The activity was tested, and the enzyme was restored to 90 % of its original activity by adding Cu ions. With addition of Fe, pMMO was inactive.[104]
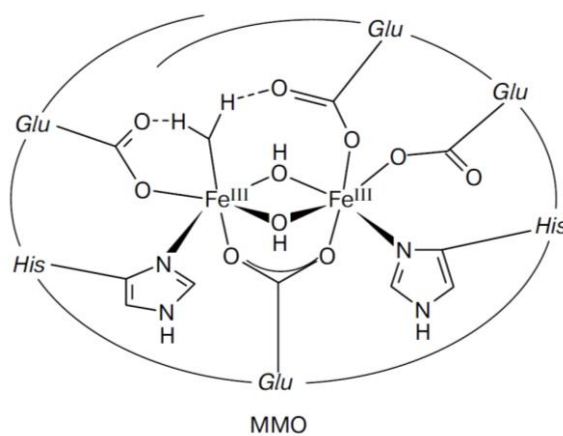
Figure 1.11: Active centre of methane monooxygenase enzyme [101]
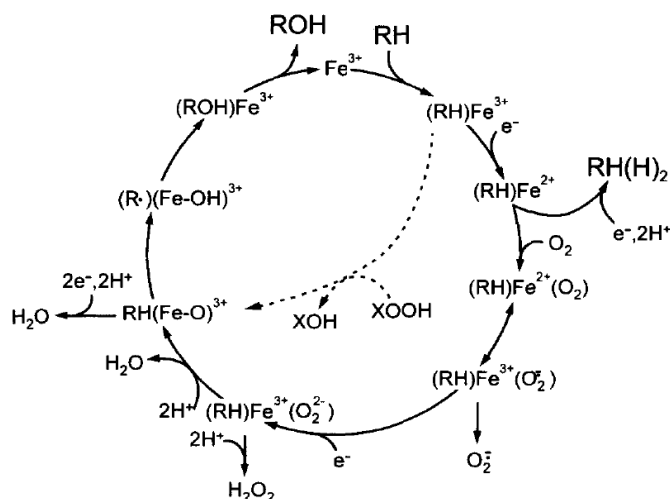
Figure 1.12: The catalytic cycle for cytochrome P450 for the oxidation of alkane to alcohol [105]

With the knowledge of the activity of P450 oxygenase, studies on biomimetic catalysts have been run. Fish *et al.* reported biomimetic catalysts able to oxidise hydrocarbons with TBHP and O_2 as oxidant using Fe complexes.[106] Working on the fact that one of the MMO intermediates is the oxidant responsible for cleaving the C-H bond, Xue *et al.* prepared an Fe complex catalyst [$Fe_2(\mu-O)_2$]. This complex was reported to be able to be activated by water or methanol, which caused a more active catalyst for the cleavage of the C-H bond.[107]

Panov studied Fe complexes stabilised in a ZSM-5 matrix as a mimic model for MMO. He found this system able to activate oxygen from N_2O at room temperature. By decomposing N_2O Fe adsorbed α-oxygen which gave oxidative properties to the Fe species. α-oxygen was then as reactive as oxygen from MMO.[108, 109] The presence of dinuclear Fe complexes was found to be the reason of the α-oxygen formation. Both Fe atoms generated an α-oxygen able to then interact with methane at room temperature.[110]

Hutchings' group reported the oxidation of methane and ethane using Fe and Fe-Cu based catalysts.[51, 111] Fe/ ZSM-5 and Fe/ Silicalite-1 catalysts were shown to be active for the liquid phase oxidation of methane to methanol using H_2O_2 as the oxidant. Despite that, over-oxidation products were also present.[112] The catalytic cycle is represented in Figure 1.13. Fe content studies and analysis techniques such as UV-Vis, XANES, EXAFS and DFT calculation showed that oligomeric Fe species are the active component.[113] In other experiments Cu was added into the previous Fe/ ZSM-5 catalyst. Both conversions were similar (0.7 %). However, in presence of Cu 85 %

selectivity towards methanol with no formic acid was reported, whereas the Fe catalyst produced 10 % methanol and 72 % selectivity for formic acid. These results were attributed to the incorporation of Cu and its ability to minimise the production of OH radicals.[111, 113]
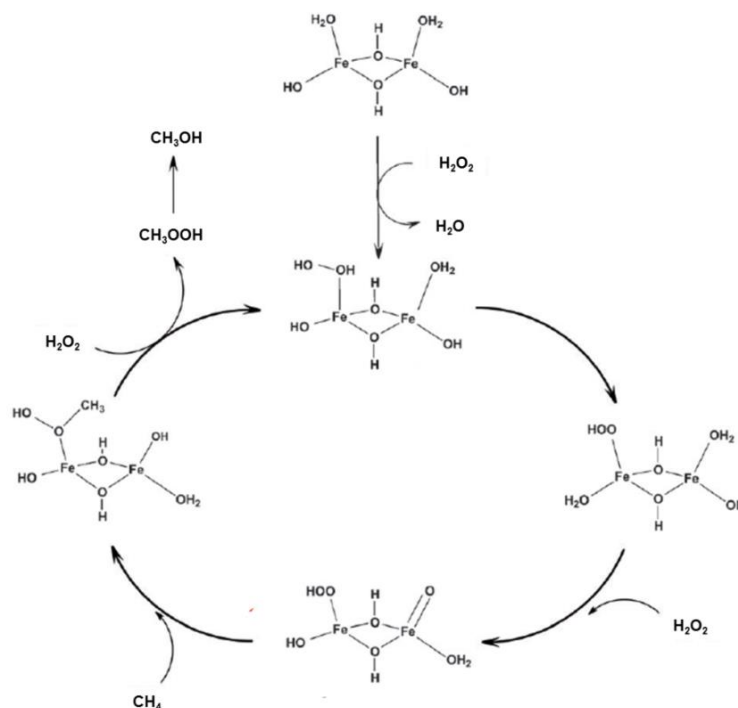
Figure 1.13: Proposed catalytic cycle for the oxidation of methane to methanol using H_2O_2 and Fe/ ZSM-5 [111]

Periana and co-workers developed catalysts able to selectively oxidise methane to methanol. It was reported that transition metal complexes were able to activate methane whilst preventing the formation of radical species. Three different systems were investigated.

The first system used electrophilic catalysts and acidic solvents to remove the electron from the HOMO (highest occupied molecular orbital) of the C-H bond and used the solvent to prevent CH_3OH from forming an ester or $[CH_3OH_2]^+$ by protonation. The presence of the acid solvent permits the activation of electrophilic catalysts by protonation of the ligands, which increased the electrophilicity of the metal centre.

The second system used nucleophilic catalysts with basic solvents to produce the reverse effect to the previous system; an electron was donated to the LUMO (lowest unoccupied molecular orbital) of the C-H bond. The ligands were deprotonated by the solvent and the nucleophilicity of the catalyst increased, then CH_3OH was deprotonated to $[CH_3O]^-$.

The last system used was a system able to react with both the HOMO and the LUMO of C-H bond. It was called an ambiphilic catalyst and a neutral solvent was necessary.[114]

The first system has been studied with several catalysts under mild condition. Hg, Pt and Au are used as example of their work. Hg^{II} and concentrated sulfuric acid converted 50 % of the methane, producing methyl bisulphate with 85 % selectivity and the side products water and sulphur dioxide. An hydrolysis of methyl bisulphate to methanol and the reoxidation of sulphur dioxide with air completed the catalytic mechanism.[115] Pt complexes were used under the same conditions and it was reported that the dichloro(η-2-[2,29-bipyrimidyl])Pt^{II} complex was the most effective catalyst with 90 % methane conversion and 81 % selectivity for methyl bisulphate. H_2SO_4 and other strong acids, such as CF_3SO_3H or $HB(HSO_4)_4$, were successfully used as solvents and reactants to form methyl ester from methane oxidation.[116] Au catalysts were also tested and it was reported that Se^{VI} was needed as an oxidant. A small amount of H_2SeO_4 in sulfuric acid allowed the oxidation of methane with Au^{III}. Se^{VI} oxidised the Au^0 formed during the reaction to Au^{III}, the active species for methane oxidation.[117]

From Periana's work, the most effective system for methane oxidation was the electrophilic catalysts with acid solvent, particularly the Pt complex. However, the acidity of the system caused deactivation.

Later, Ferdi Schüth's group created a heterogeneous catalyst able to oxidise methane under similar condition to the Periana catalyst. Their catalyst was a polymer formed from 2, 6-dicyanopyridine with accessible bipyridyl structure units. Pt was introduced to this polymer to give a similar catalyst to the dichloro (η-2-[2, 29-bipyrimidyl])Pt^{II} complex from Periana. Under the same conditions, these heterogeneous and homogeneous catalysts were compared; based on Pt content, the highest TON (turnover number) of 355 was reported for the homogeneous, and a TON of 246 was reported for the heterogeneous catalyst. Hence, even though the reported TON was lower, Schüth *et al.* showed it was possible to oxidise methane with a reusable catalyst.[118]

Computational studies show that a MoO_3-supported Pt catalyst could activate the C-H bond of methane. The calculations show a reaction barrier of 0.32 eV which is lower than for Pt (111), and that CH_3 dissociation is difficult on this catalyst. Since the oxidation of CH_3 from methanol would be unlikely on this type of catalyst, the over-oxidation would not occur, which gives the possibility of selectively oxidising methane to methanol.[119]

4.3. Propane

Propane is a C_3 linear alkane chain. It is a widely-used fuel with a low carbon footprint and oxidation products that are valuable for industrial processes and chemical synthesis. Most oxygenate products are more useful and more environmentally friendly than the alkane. For example, propene is a raw material for plastic, and acetone and isopropanol are used as solvents and chemical intermediates.

From 1929, Peace studied the oxidation of propane. He reported the difference of products formed depending of the temperature in the gas phase and liquid phase.[120, 121] Studies were done on thermal oxidation but the use of a catalyst was introduced to oxidise propane selectively. The catalytic oxidation of propane to different products has been studied; total oxidation, oxidative dehydrogenation (ODP), and oxidation to acrylic acid and oxygenated products such as acetone, propene, propanol, isopropanol, propanal and propanoic acid.

Total oxidation of propane usually requires high temperature, between 250 ºC and 800 ºC. These reactions were carried out in the gas phase with O_2 as oxidant. Co, Ru, CuO, CeO_2, and noble metal catalysts were found to be effective for the total oxidation of propane.[122-125] The use of high temperature conditions usually led to total oxidation. Nevertheless, some catalysts can allow these conditions to be used to give small alkane molecules. Rossini and co-workers studied propane oxidation with O_2 using a V-K/ Al_2O_3 catalyst. Below 680 ºC the major products were propene, ethene, CO_2 and CO. Above 680 ºC ethene and methane are the predominant products.[126]

 The modification of the catalyst in order to avoid over or total oxidation has been investigated and showed the possibility to control the partial oxidation of propane to propene.[127]

The oxidative dehydrogenation of propane (ODP) to form propene is also one of the important propane reactions and has been widely studied. Vanadium-based catalysts were found to be active with high selectivity. Putra *et al*. reported 19.1 % conversion of propane with 80 % selectivity for propene over Al_2O_3-supported Sr-V-Mo catalysts under atmospheric pressure and 500 ºC.[128] Some systems used a Mars-Van Krevelen mechanism, in which propane is oxidised by oxygen from the catalyst, which is then regenerated by O_2.[129] Other metals such as Au have also been used for the ODP reaction.[130] However, propene production involved the co-production of ethene and the best productivity for propane was near to 10 g/ (g_{cat}.h) while for ethane the productivity reached 24 g/ (g_{cat}.h). This makes ODP unattractive for use at an industrial level.[131]

The direct formation of acrylic acid from propane was also investigated in order to use a less expensive raw material compare to the two steps process from propene.[132, 133] Propane oxidation to oxygenated products (acetone, propanol, isopropanol, propanal and propanoic acid) requires milder conditions such as low temperature or liquid phase oxidation. The challenge is to avoid over-oxidation and C-C scission. The conditions needed to obtain oxygenate products change depending on the ability of the oxidants to be activated at lower temperatures, (such as H_2O_2 with Fenton reagent),[134] the use of different acidity [135] and also the intervention of light.[136] Oyama and co-workers reported the formation of H_2O_2 *in situ.* from H_2 and O_2 over Au/ TS-1 catalyst. This system was used to oxidise propane to acetone and isopropanol.[137]

4.4. Octane

Octane is a hydrocarbon with formula C_8H_{18}. Many isomers exist such as 2, 2, 4-trimethylpentane, also known as isooctane or 2, 2-dimethylhexane. In the current work linear octane has been studied, which is liquid under atmospheric pressure and temperature. Linear octane has been chosen rather than an isomer of octane to prevent effects from the branched groups. In the current literature only a few studies can be found regarding the oxidation of octane, which has been studied under thermal oxidation and catalytic oxidation parameters. In this work, the interest is to selectively oxidize octane to octanol; 1-octanol being of greatest interest due to the necessity of the activation of the primary C-H bond. Octanol is used for the synthesis of esters for flavoring, essential oils and pharmaceuticals.

O_2 and TBHP have been studied as initiators to understand the thermal oxidation of octane. Different possible reaction pathways were identified as a function of the conditions used, with a variety of different products found. Aldehyde has not been detected in liquid phase, but it was the primary product in gas phases.

Pope *et al.* studied the mechanism of the vapour phase auto-oxidation of octane at temperatures higher than 200 ℃. It was shown that the first oxidation product of octane is the aldehyde, which was oxidised further to CO and CO_2 by successive C-C scission forming smaller alkane until total decomposition.[138] Gould and co-workers investigated the auto-oxidation of octane between 100 ℃ and 125 ℃ in the presence of TBHP. The formation of octyl hydroperoxide and octanediols was reported.[139] Other experiments showed the cleavage of C-C bonds during the auto-oxidation of octane from 135 ℃ to 145 ℃. Octanal, octanol and octanone were formed, as well as smaller acids such as formic acid, propanoic acid, heptanoic acid and acetic acid.[140]

Computational studies showed a molecular scheme for octane oxidation using a radical mechanism in the presence of O_2.[141, 142] However, other papers proved the negligible effect of radicals depending on the catalysts. Kumar and co-workers used VO^{2+} and $Co^{II}V^{IV}L^{2+}$, (L= ligand) supported on modified Al_2O_3. It was shown that a mechanism involving radical species could not occur, instead their catalyst reacted directly with the substrate leading to the formation of a carbonium ion.[143, 144]

Many reactions over 100 ºC were studied in the presence of catalyst. Low conversions were reported, (under 10 %), but a certain control of selectivity was achieved. C-C scissions were prevented [144] and alcohol, aldehyde and acid were selectively produced.[75]

4.5. Toluene

Toluene is an aromatic hydrocarbon also known as methylbenzene. It is a natural molecule which can be found in crude oil and as a by-product in gasoline processes. It is also produced from naphthenes by hydroforming.[145, 146] Toluene is widely used in chemical reactions as a precursor for benzene formation, and as a solvent in paints, adhesives, cleaning agents, coatings, synthetic fragrances and inks.[147-149] The oxidation of toluene is interesting for various reasons. Benzaldehyde, benzyl alcohol, benzoic acid and benzyl benzoate are the direct products of toluene oxidation and are used in flavours, flagrances, cosmetics, preservatives, medications and also as raw material for other chemical reactions such as the formation of phenol from benzoic acid.[150-155]

The second reason to investigate toluene oxidation is that the methyl group of toluene has often been considered as a model for the primary C-H bond. If the oxidation of the CH_3 group can be achieved, and understood properly, it could indicate ways to oxidise primary C-H bond in smaller alkanes such as methane.

Many studies have been reported for toluene oxidation. Without a catalyst, toluene oxidation shows a high selectivity for benzaldehyde and benzoic acid. Huang and co-workers used a graphene-hemin hybrid catalyst to selectively oxidise the primary C-H bond of toluene using TBHP as initiator and O_2 as an oxidant at 60 ºC. Hemin is an iron protoporphyrin and the active site of the heme of a protein. Depending on time and amount of catalyst, 40 % conversion was reached. At low conversion benzaldehyde was the major product, and benzoic acid was the major product at higher conversion.[156] This implies that avoiding the over-oxidation of benzyl alcohol usually involves a low conversion. Zhao *et al.* reported more than 65 % selectivity for benzyl alcohol and

benzaldehyde keeping a low conversion; under 9 %.[157] Gong-de and co-workers achieved 81.4 % selectivity for benzyl alcohol using a F-modified CuNiAl hydrotalcite compounds, despite a low conversion of 8.4 %.[158] Other research groups found different ways to oxidise toluene into other products with high selectivity. Kesavan *et al.* developed a system that used molecular O_2 and 1 wt. % AuPd/ C. A conversion of 94 % was reported with 95 % selectivity towards benzyl benzoate. This product was not a direct product of toluene oxidation; a different pathway is used involving the formation of benzyl benzoate by the coupling of two molecules from toluene oxidation.[20]

5. *Aims of the thesis*

The aims of my PhD were to study the selective oxidation of hydrocarbon in liquid phase using a solid catalyst in mild reaction conditions. Three distinct projects with common objectives were investigated. To study these projects, various points have been followed:

- The development of a heterogeneous catalyst able to oxidise the substrate with high conversion and selectivity.
- Systematic studies to understand the effect of reaction conditions on catalytic activity and selectivity.
- Modification of the catalyst and reaction condition in order to improve conversion, selectivity and oxidant utilisation
- Elucidation of the active site.

However, they all have been studied separately and with different approach depending on previous work.

(i)   Co-oxidation of alkane using molecular O_2.

The aim of the project was to use a well-known system, toluene oxidation using O_2, and introduce an alkane, methane in order to oxidise it. Inconclusive data have been reported as preliminary work. Hence, the system have been change, octane has been co-oxidise using benzaldehyde. Systematic studies on reaction condition have been carried out in order to establish the best reaction condition for this system. Later the improved system has been applied using various alkane and aldehyde in order to generalise the concept.

(ii)   Toluene oxidation using TBHP

This project had for purpose to oxidise toluene using mild condition. Various Au, Pd and Pt catalyst has been investigated using TBHP, initiator and oxidant. These catalysts have

been prepared and characterised in order to confirm size, shape and oxidation state of the nanoparticles. After testing these catalysts for toluene oxidation, various studies have been carried out with the most active catalyst. Subsequently, the introduction of O_2 in the system reveals its possible activation.

(iii)   Propane oxidation using H_2O_2.

Finally, propane oxidation has been investigating using H_2O_2 and zeolite catalyst. Various support and metal have been tested. Systematic studies on reaction condition have been carried out using Fe/ ZSM-5 (30) in order to increase conversion and selectivity. Subsequently, this catalyst has been acid treated removing the Fe on surface, characterised and tested. With this investigation the active site for propane oxidation can be determined.

6. References

1.   Berzelius, J.J., *Edinburgh New Philosophical Journal,* 1936. **21**, p. 223-228.

2.   Chorkendorff, I. and Niemantsverdriet, J.W., *Concepts of Modern Catalysis and Kinetics*. 2003: Wiley-VCH.

3.   *Iupac, Gold Book: Catalyst*.   [cited 2014 20/10]; Available from: http://goldbook.iupac.org/C00876.html.

4.   Phillips, P. *Vinegar Maker, for an Improvement in Manufacturing Sulphuric Acid*. 1831. British patent 6096

5.   Lemoine, M.G., *Annales de Chimie et de physique,* 1877. **12**, p. 145.

6.   Fadhel, A.Z., Pollet, P., Liotta, C.L. and Eckert, C.A., *Molecules,* 2010. **15**, p. 8400-8424.

7.   Campbell, I.M., *Catalysis at Surfaces*. 1988, London: Cahpman and Hall Ltd.

8.   Gabor, A. and Somorjai, Y.L., *Introduction to Surface Chemistry and Catalysis*. 2010, New Jersey: Wiley & Sons.

9.   Ibach, H., *Physics of Surfaces and Interfaces*. 2006, Berlin: Springer.

10.   Ross, J.R.H., *Heterogeneous Catalysis: Fundamentals and Applications*. 2012, Oxford: Elsevier.

11.   Takagi, M., Kawai, T., Soma, M., Onishi, T. and Tamaru, K., *Journal of Catalysis,* 1977. **50** (3), p. 441-446.

12.   Petrov, L., Eliyas, A. and Shopov, D., *Applied Catalysis,* 1985. **18** (1), p. 87-103.

13. Doornkamp, C. and Ponec, V., *Journal of Molecular Catalysis A: Chemical,* 2000. **162**, p. 19-32.

14. Scirè, S., Minicòa, S., Crisafullia, C., Satrianoa, C. and Pistone, A., *Applied Catalysis B: Environmental,* 2003. **40** (1), p. 43-49.

15. Solymosi, F., *Catalysis Reviews Science and Engineering,* 1968. **1** (1), p. 233-255.

16. Zou, J.-J., Liu, C.-J. and Zhang, Y.-P., *Langmuir : the ACS journal of surfaces and colloids,* 2006. **22**, p. 2334-2339.

17. Romero, R., Leinen, D., Dalchiele, E.A., Ramos-Barrado, J.R. and Martín, F., *Thin Solid Films,* 2006. **515**, p. 1942-1949.

18. Bond, G.C., Louis, C. and Thompson, D.T., *Catalysis by Gold*, in *Catalytic Science Series*, G.J. Hutchings, Editor. 2006, Imperial College Press: London.

19. Edwards, J.K., Carley, A.F., Herzing, A.A., Kiely, C.J. and Hutchings, G.J., *Faraday Discussions,* 2008. **138**, p. 225-239.

20. Kesavan, L., Tiruvalam, R., Ab Rahim, M.H., bin Saiman, M.I., Enache, D.I., Jenkins, R.L., Dimitratos, N., Lopez-Sanchez, J.A., Taylor, S.H., Knight, D.W., Kiely, C.J. and Hutchings, G.J., *Science,* 2011. **331** (6014), p. 195-199.

21. Saiman, M.I.b., Brett, G.L., Tiruvalam, R., Forde, M.M., Sharples, K., Thetford, A., Jenkins, R.L., Dimitratos, N., Lopez-Sanchez, J.A., Murphy, D.M., Bethell, D., Willock, D.J., Taylor, S.H., Knight, D.W., Kiely, C.J. and Hutchings, G.J., *Angewandte Chemie, International Edition,* 2012. **51**, p. 5981-5985.

22. Haruta, M., *catalysis Science & Technology,* 2002. **6** (3), p. 102-115.

23. Hashmi, A.S.K. and Hutchings, G.J., *Angewandte Chemie, International Edition,* 2006. **45**, p. 7896-7936.

24. Biella, S. and Rossi, M., *Chemical Communications,* 2003, p. 378-379.

25. Mori, K., Hara, T., Mizugaki, T., Ebitani, K. and Kaneda, K., *Journal of the American Chemical Society,* 2004. **126** (36), p. 10657-10666.

26. Abad, A., Concepción, P., Corma, A. and García, H., *Angewandte Chemie, International Edition,* 2005. **44** (26), p. 4066-4069.

27. Hvolbæk, B., Janssens, T.V.W., Clausen, B.S., Falsig, H., Christensen, C.H. and Nørskov, J.K., *Nanotoday,* 2007. **2** (4), p. 14-18.

28. Lopez, N., Janssens, T.V.W., Clausen, B.S., Xu, Y., Mavrikakis, M., Bligaard, T. and Nørskov, J.K., *Journal of Catalysis,* 2004. **223**, p. 232-235.

29. Vaarkamp, M., Miller, J.T., Modica, F.S. and Koningsberger, D.C., *Journal of Catalysis,* 1996. **163**, p. 294-305.

30.   Dimitratos, N., Villa, A., Wang, D., Porta, F., Su, D. and Prati, L., *Journal of Catalysis,* 2006. **244** (1), p. 113-121.

31.   Abid, M., Ammari, F., Liberkova, K. and Touroude, R., *Studies in Surface Science and Catalysis,* 2003. **145**, p. 267-270.

32.   Auer, E., Freund, A., Pietsch, J. and Tacke, T., *Applied Catalysis A: General,* 1998. **173**, p. 259-271.

33.   Reinoso, F.R., *Carbon,* 1998. **36** (3), p. 159-175.

34.   Hadjiivanov, K.I. and Klissurski, D.G., *Chemical society reviews,* 1996, p. 61-69.

35.   Tauster, S.J., Fung, S.C. and Garten, R.L., *Journal of the American Chemical Society,* 1978. **100** (1), p. 170-175.

36.   Vannice, M.A., *Journal of Catalysis,* 1982. **74** (1), p. 199-202.

37.   Bratlie, K.M., Lee, H., Komvopoulos, K., Yang, P. and Somorjai, G.A., *Nanoletters,* 2007. **7** (10), p. 3097-3101.

38.   Prati, L. and Villa, A., *Accounts of Chemical Research,* 2014. **47** (3), p. 855-863.

39.   Kaidanovych, Z., Kalishyn, Y. and Strizhak, P., *Advances in Nanoparticles,* 2013. **2**, p. 32-38.

40.   Prati, L. and Villa, A., *Catalysts,* 2012. **2**, p. 24-37.

41.   Tiruvalam, R.C., Pritchard, J.C., Dimitratos, N., Lopez-Sanchez, J.A., Edwards, J.K., Carley, A.F., Hutchings, G.J. and Kiely, C.J., *Faraday Discussions,* 2011. **152**, p. 63.

42.   Dimitratos, N., Lopez-Sanchez, J.A., Morgan, D., Carley, A.F., R.Tiruvalam, Kiely, C.J., Bethella, D. and Hutchings, G.J., *Physical Chemistry Chemical Physics,* 2009. **11**, p. 5142-5153.

43.   Murakami, Y., Iijima, A. and Ward, J.W., *New Developments in Zeolite Science and Technology*. Vol. **28**. 1986: Elsevier Science.

44.   Corma, A., *Chemical Reviews,* 1995. **95**, p. 559-614.

45.   Auerbach, S.M., Carrado, K.A. and Dutta, P.K., *Handbook of Zeolite Science and Technology*. 2003: Marcel Dekker.

46.   Cejka, J., Corma, A. and Zones, S., *Zeolites and Catalysis: Synthesis, Reactions and Applications*. Vol. **1**. 2010: Wiley-VCH.

47.   Kondo, J.N., Nishitani, R., Yoda, E., Yokoi, T., Tatsumi, T. and Domen, K., *Physical Chemistry Chemical Physics,* 2010. **12**, p. 11576-11586.

48.   Baerlocher, C.H., McCusker, L.B. and Olson, D.H., *Atlas of Zeolite Framework Types*. 2007: Elsevier.

49.   Meier, W.M., *Nature,* 1978. **272**, p. 437-438.

50.   Lee, K.-B., Lee, S.-M. and Cheon, J., *Advanced Materials,* 2001. **13** (7), p. 517-520.

51.   Forde, M.M., Armstrong, R.D., Hammond, C., He, Q., Jenkins, R.L., Kondrat, S.A., Dimitratos, N., Lopez-Sanchez, J.A., Taylor, S.H., Willock, D., Kiely, C.J. and Hutchings, G.J., *Journal of the American Chemical Society,* 2013. **135**, p. 11087-11099.

52.   Zecchina, A., Rivallan, M., Berlier, G., Lambertia, C. and Ricchiardi, G., *Physical Chemistry Chemical Physics,* 2007. **9**, p. 3483-3499.

53.   Arends, I.W.C.E., Sheldon, R.A., Wallau, M. and Schuchardt, U., *Angewandte Chemie, International Edition,* 1997. **36**, p. 1144-1163.

54.   Cheng, M.-J., Chenoweth, K., Oxgaard, J., Duin, A.v. and Goddard, W.A., *Journal of Physical Chemistry,* 2007. **111**, p. 5115-5127.

55.   Vaino, A.R., *Journal of Organic Chemistry,* 2000. **65**, p. 4210-4212.

56.   Bennett, J.E., *Journal of the Chemical Society, Faraday Transactions,* 1990. **86** (19), p. 3247-3252.

57.   Barb, W.G., Baxendale, J.H., George, P. and Hargrave, K.R., *Nature,* 1949. **163**, p. 692-694.

58.   Shulpin, G.B. and Nizova, G.V., *Reaction Kinetics and Catalysis Letters,* 1992. **48** (1), p. 333-338.

59.   Barb, W.G., Baxendale, J.H., George, P. and Hargrave, K.R., *Transactions of the Faraday Society,* 1951. **47**, p. 591-616.

60.   Araujo, F.V.F., Yokoyama, L., Teixeira, L.A.C. and Campos, J.C., *Brazilian Journal of Chemical Engineering,* 2011. **28** (4), p. 605-616.

61.   Laat, J.D. and Gallard, H., *Environmental Science and Technology,* 1999. **33**, p. 2726-2732.

62.   Edwards, J.K., Solsona, B., Ntainjua, E.N., Carley, A.F., Herzing, A.A., Kiely, C.J. and Hutchings, G.J., *Science,* 2009. **323**, p. 1037-1041.

63.   Freakley, S.J., Lewis, R.J., Morgan, D.J., Edwards, J.K. and Hutchings, G.J., *Catalysis Today,* 2014.

64.   Singh, S.J. and Jayaram, R.V., *Catalysis Communication,* 2009. **10**, p. 2004-2007.

65.   Dhakshinamoorthy, A., Alvaro, M. and Garcia, H., *Journal of Catalysis,* 2009. **267**, p. 1-4.

66.   Zhang, J., Wang, Z., Wang, Y., Wan, C., Zheng, X. and Wang, Z., *Green Chemistry,* 2009. **11**, p. 1973-1978.

67. Kishore, D. and Rodrigues, A.E., *Catalysis Communication,* 2009. **10**, p. 1212-1215.

68. Escola, J.M., Botas, J.A., Aguado, J., Serrano, D.P., Vargas, C. and Bravo, M., *Applied Catalysis A: General,* 2008. **335** (2), p. 137-144.

69. Jha, R.K., Shylesh, S., Bhoware, S.S. and Singh, A.P., *Microporous and Mesoporous Materials,* 2006. **95**, p. 154-163.

70. Boisvert, L. and Goldberg, K.I., *Accounts of Chemical Research,* 2012. **45** (6), p. 899-910.

71. Heyduk, A.F., Zhong, H.A., Labinger, J.A. and Bercaw, J.E., *Activation and Functionalization of C-H Bonds*, in *Chapter 15. C-H Bond Activation at Pt(II): A Route to Selective Alkane Oxidation?*, K.I.G.a.A.S. Goldman, Editor. 2004, American Chemical Society.

72. Yuan, J., Wang, L. and Wang, Y., *Industrial & Engineering Chemistry Research,* 2011. **50** (10), p. 6513-6516.

73. Lin, M., Hogan, T. and Sen, A., *Journal of the American Chemical Society,* 1997. **119**, p. 6048-6053.

74. Wang, X., Wang, Y., Tang, Q., Guo, Q., Zhang, Q. and Wan, H., *Journal of Catalysis,* 2003. **217**, p. 457-467.

75. Thomas, J.M., Raja, R., Sankar, G. and Bell, R.G., *Nature,* 1999. **398**, p. 227-230.

76. Weiher, N., Beesley, A.M., Tsapatsaris, N., Delannoy, L., Louis, C., Bokhoven, J.A.v. and Schroeder, S.L.M., *Journal of the American Chemical Society,* 2007. **129**, p. 2240-2241.

77. Abad, A., Almela, C., Corma, A. and Garcia, H., *Tetrahedron,* 2006. **62**, p. 6666-6672.

78. Zhu, J., Carabineiro, S.A.C., Shan, D., Faria, J.L., Zhu, Y. and Figueiredo, J.L., *Journal of Catalysis,* 2010. **274**, p. 207-214.

79. Huang, Y.-F., Zhang, M., Zhao, L.-B., Feng, J.-M., Wu, D.-Y., Ren, B. and Tian, Z.-Q., *Angewandte Chemie, International Edition,* 2014. **53**, p. 2353-2357.

80. Boronat, M. and Corma, A., *Dalton Transactions,* 2010. **39**, p. 8538-8546.

81. Ito, S., Yamasaki, T., Okada, H., Okino, S. and Sasaki, K., *Journal of the Chemical Society, Perkin Transactions 2,* 1988 (3), p. 285-293.

82. Zhi-Hu, G., Yamaguchi, F., Itoh, A., Kitani, A. and Sasaki, K., *Electrochimica Acta,* 1992. **37** (2), p. 345-347.

83. Yoshino, Y., Hayashi, Y., Iwahama, T., Sakaguchi, S. and Ishii, Y., *Journal of Organic Chemistry,* 1997. **62**, p. 6810-6813.

84. Yamada, T., Takai, T., Rhode, O. and Mukaiyama, T., *Chemistry Letters,* 1991 (1), p. 1-4.

85. Labinger, J.A., *Journal of Molecular Catalysis A: Chemical,* 2004. **220**, p. 27-35.

86. Oyama, S.T., *Factors Affecting Selectivity in Catalytic Partial Oxidation and Combustion Reactions*, in *Heterogeneous Hydrocarbon Oxidation*. 1996, ACS Symposium Series. p. 2-19.

87. Dean, J.A., *Lange's Handbook of Chemistry*, ed. R. Esposito. 1952: McGraw-Hill, inc.

88. Shilov, A.E. and Shul'pin, G.B., *Chemical Reviews,* 1997. **97** (8), p. 2879-2934.

89. Goldman, A.S. and Goldberg, K.I., *Activation and Functionalization of C-H Bonds*, in *Chapter 1. Organometallic C-H Bond Activation: An Introduction*, K.I.G.a.A.S. Goldman, Editor. 2004, American Chemical Society.

90. Crabtree, R.H., *Journal of Organometallic Chemistry,* 2004. **689**, p. 4083-4091.

91. Golisz, S.R., Brent Gunnoe, T., Goddard, W.A., Groves, J.T. and Periana, R.A., *Catalysis Letters,* 2010. **141** (2), p. 213-221.

92. Weinberg, W.H. and Sun, Y.-K., *Science,* 1991. **253**, p. 542-545.

93. Johnston, J.B., Ouellet, H., Podust, L.M. and Montellano, P.R.O.d., *Archives of Biochemistry and Biophysics,* 2011. **507**, p. 86-94.

94. Rangan, K., Fianchini, M., Singh, S. and Dias, H.V.R., *Inorganica Chimica Acta,* 2009. **362**, p. 4347-4352.

95. Simmons, E.M. and Hartwig, J.F., *Nature,* 2012. **483**, p. 70-73.

96. Antony, A., Asthagiri, A. and Weaver, J.F., *Physical Chemistry Chemical Physics,* 2012. **14**, p. 12202-12212.

97. Michalkiewicz, B., *Journal of Catalysis,* 2003. **215** (1), p. 14-19.

98. Milich, L., *Global Environmental Change,* 1999. **9**, p. 179-201.

99. Shilov, A.E. and Shul'pin, G.B., *American Chemical Society,* 1997. **97**, p. 2879-2932.

100. Arndtsen, B.A., BERGMAN, R.G., MOBLEY, T.A. and PETERSON, T.H., *American Chemical Society,* 1995. **28**, p. 154-162.

101. Shteinman, A.A., *Russian Chemical Bulletin, International Edition,* 2001. **50** (10), p. 1795-1810.

102. Wong, L.-L., *Current Opinion in Chemical Biology,* 1998. **2** (2), p. 263-268.

103. Jr, J.M.B., *Nature Chemistry,* 2010. **465**, p. 40-41.

104. Balasubramanian, R., Smith, t.M., Rawat, S., Yatsunyk, L.A., Stemmler, T.L. and Rosenzweig, A.C., *Nature,* 2010. **465**, p. 115-121.

105. Halkier, B.A., *Phytochemistry,* 1996. **43** (1), p. 1-21.

106. Fish, R.H., Oberhausen, K.J., Chen, S., Richardson, J.F., Pierce, W. and Buchanan, R.M., *Catalysis Letters,* 1993. **18**, p. 357-365.

107. Xue, G., Pokutsa, A. and L. Que, J., *Journal of the American Chemical Society,* 2011. **133**, p. 16657-16667.

108. Panov, G.I., Sobolev, V.I., Dubkov, K.A., Parmon, V.N., Ovanesyan, N.S., Shilov, A.E. and Shteinman, A.A., *Reaction Kinetics and Catalysis Letters,* 1997. **61** (2), p. 251-258.

109. Panov, G.I., Uriarte, A.K., Rodkin, M.A. and Sobolev, V.I., *Catalysis Today,* 1998. **41**, p. 365-385.

110. Dubkov, K.A., Ovanesyan, N.S., Shteinman, A.A., Starokon, E.V. and Panov, G.I., *Journal of Catalysis,* 2002. **207**, p. 341-352.

111. Hammond, C., Forde, M.M., Rahim, M.H.a., Thetford, A., He, Q., Jenkins, R.L., Dimitratos, N., Lopez-Sanchez, J.A., Dummer, N.F., Murphy, D.M., Carley, A.F., Taylor, S.H., Willock, D.J., Eric E. Stangland, Kang, J., Hagen, H., Kiely, C.J. and Hutchings, G.J., *Angewandte Communications,* 2012. **51**, p. 5129-5133.

112. Hammond, C., Dimitratos, N., Lopez-Sanchez, J.A., Jenkins, R.L., Whiting, G., Kondrat, S.A., Rahim, M.H.a., Forde, M.M., Thetford, A., Hagen, H., Stangland, E.E., Moulijn, J.M., Taylor, S.H., Willock, D.J. and Hutchings, G.J., *ACS Catalysis,* 2013. **3**, p. 1835-1844.

113. Hammond, C., Dimitratos, N., Jenkins, R.L., Lopez-Sanchez, J.A., Kondrat, S.A., Rahim, M.H.a., Forde, M.M., Thetford, A., Taylor, S.H., Hagen, H., Stangland, E.E., Kang, J.H., Moulijn, J.M., Willock, D.J. and Hutchings, G.J., *ACS Catalysis,* 2013. **3**, p. 689-699.

114. Hashiguchi, B.G., Bischof, S.M., Konnick, M.M. and Periana, R.A., *Accounts of Chemical Research,* 2012. **45** (6), p. 885-898.

115. Periana, R.A., Taube, D.J., Evitt, E.R., Loffler, D.G., Wentrcek, P.R., Voss, G. and Masuda, T., *Science,* 1993. **259**, p. 340-343.

116. Periana, R.A., Taube, D.J., Gamble, S., Taube, H., Satoh, T. and Fujii, H., *Science,* 1998. **280** (5363), p. 560-564.

117. Jones, C.J., Taube, D., Ziatdinov, V.R., Periana, R.A., Nielsen, R.J., Oxgaard, J. and Goddard, W.A., *Angewandte Chemie,* 2004. **116** (35), p. 4726-4729.

118. Palkovits, R., Antonietti, M., Kuhn, P., Thomas, A. and Schuth, F., *Angewandte Chemie, International Edition,* 2009. **48**, p. 6909-6912.

119. Zhang, C.J. and Hu, P., *Journal of Chemical Physics,* 2002. **116**, p. 4281-4285.

120.   Pease, R., *Journal of the American Chemical Society,* 1929. **51**, p. 1839-1856.

121.   Pease, R.N. and Munro, W.P., *Journal of the American Chemical Society,* 1934. **56** (10), p. 2034-2038.

122.   Wu, X., Zhang, L., Weng, D., Liu, S., Si, Z. and Fan, J., *Journal of Hazardous Materials,* 2012. **225-226**, p. 146-154.

123.   Solsona, B., Davies, T.E., Garcia, T., Vazquez, I., Dejoz, A. and Taylor, S.H., *Applied Catalysis B: Environmental,* 2008. **84**, p. 176-184.

124.   Debecker, D.P., Farin, B., Gaigneaux, E.M., Sanchez, C. and Sassoye, C., *Applied Catalysis A: General,* 2014. **481**, p. 11-18.

125.   Heynderickx, M.P., Thybaut, J.W., Poelman, H., Poelman, D. and Marin, G.B., *Applied Catalysis B: Environmental,* 2010. **95**, p. 26-38.

126.   Resini, C., Panizza, M., Arrighi, L., Sechi, S., Busca, G., Miglio, R. and Rossini, S., *Chemical Engineering Journal,* 2002. **89**, p. 75-87.

127.   Zanthoff, H.W., Lahmer, M., Baerns, M., Klemm, E., Seitz, M. and Emig, G., *Journal of Catalysis,* 1997. **172**, p. 203-210.

128.   Putra, M.D., Al-Zahrani, S.M. and Abasaeed, A.E., *Catalysis Communication,* 2011. **14**, p. 107-110.

129.   Fukudome, K., Ikenaga, N.-O., Miyake, T. and Suzuki, T., *catalysis Science & Technology,* 2011. **1**, p. 987-998.

130.   Bravo-Suárez, J.J., Bando, K.K., Lu, J., Fujitani, T. and Oyama, S.T., *Journal of Catalysis,* 2008. **255**, p. 114-126.

131.   Cavani, F., Ballarini, N. and Cericola, A., *Catalysis Today,* 2007. **127**, p. 113-131.

132.   Ishchenko, E.V., Popova, G.Y., Kardash, T.Y., Ishchenko, A.V., Plyasova, L.M. and Andrushkevich, T.V., *Catalysis for Sustainable Energy,* 2013. **1**, p. 75-81.

133.   Ieda, S., Phiyanalinmat, S., Komai, S.-I., Hattori, T. and Satsuma, A. *Role of Promoters on Active Sites of Vanadyl Pyrophosphate for Selective Oxidation of Propane*. in *15th Saudi-Japan Joint Symposium*. 2005. Dhahran, Saudi Arabia.

134.   Espro, C., Marini, S., Mendolia, F., Frusteri, F. and Parmaliana, A., *Catalysis Today,* 2009. **141**, p. 306-310.

135.   Xu, J., Mojet, B.L., Ommen, J.G.v. and Lefferts, L., *Journal of Catalysis,* 2005. **232**, p. 411-423.

136.   Sun, H., Blatter, F. and Frei, H., *Catalysis Letters,* 1997. **44**, p. 247-253.

137.   Bravo-Suárez, J.J., Bando, K.K., Fujitani, T. and Oyama, S.T., *Journal of Catalysis,* 2008. **257**, p. 32-42.

138.   Pope, J.C., Dykstra, F.J. and Edgar, G., *Journal of the American Chemical Society,* 1929. **51** (6), p. 1875-1889.

139.   Sickle, D.E.V., Mill, T., Mayo, F.R., Richardson, H. and Gould, C.W., *Journal of Organic Chemistry,* 1973. **38** (26), p. 4435-4440.

140.   Garcia-Ochoa, F., Romero, A. and Querol, J., *Industrial & Engineering Chemistry Research,* 1989. **28** (1), p. 43-48.

141.   Pfaendtner, J. and Broadbelt, L.J., *Industrial & Engineering Chemistry Research,* 2008. **47**, p. 2886-2896.

142.   Pfaendtner, J. and Broadbelt, L.J., *Industrial & Engineering Chemistry Research,* 2008. **47**, p. 2897-2904.

143.   Mishra, G.S. and Kumar, A., *Reaction Kinetics and Catalysis Letters,* 2003. **80** (2), p. 223-231.

144.   Kishore, M.J.L., Mishra, G.S. and Kumar, A., *Indian Journal of Chemistry,* 2005. **44B**, p. 349-355.

145.   Antos, G.J. and Aitani, A.M., *Catalytic Naphtha Reforming, Revised and Expanded*. 2005: Taylor and Francis e-Library.

146.   Myers, C.G., Lang, W.H. and Welsz, P.B., *Industrial and engineering chemistry,* 1961. **33** (4), p. 299-302.

147.   *Manufacturing Processes*.   [cited 2014 9th october]; Available from: http://www.sbioinformatics.com/design_thesis/Toluene/Toluene_Methods-2520of-2520Production.pdf.

148.   *Toluene Production and Manufacturing Process* 2007 [cited 2014 9th october]; Available   from: http://www.icis.com/resources/news/2007/11/07/9076551/toluene-production-and-manufacturing-process/

149.   Foxall, K. *Toluene: General Information*. 2010   [cited 2014 9th october]; Available   from: https://www.gov.uk/government/uploads/system/uploads/attachment_data/file/338278/hpa_toluene_general_information_v2.pdf.

150.   Denis, W. and Dunbar, P.B., *The journal of industrial and engineering chemistry,* 1909. **1** (4), p. 256-257.

151.   Wilson, L. and Martin, S., *ANNALS OF EMERGENCY MEDICINE*. **33** (5), p. 495-499.

152.   Kalpaklioglu, A.F., Ferizli, A.G., Misirligil, Z., Demirel, Y.S. and Gurbuz, L., *Allergy,* 1996. **51**, p. 164-170.

153.   Hazan, R., Levine, A. and Abeliovich, H., *Applied and environmental microbiology,* 2004. **70** (8), p. 4449-4457.

154. Fraga-Dubreuil, J., Garcia-Serna, J., Garcia-Verdugo, E., Dudd, L.M., Aird, G.R., Thomas, W.B. and Poliakoff, M., *Journal of Supercritical Fluids,* 2006. **39**, p. 220-227.

155. Duma, V., Popp, K.E., Kung, M.C., Zhou, H., Nguyen, S., Ohyama, S., Kung, H.H. and Marshall, C.L., *Chemical Engineering Journal,* 2004. **99**, p. 227-236.

156. Li, Y., Huang, X., Li, Y., Xu, Y., Wang, Y., Zhu, E., Duan, X. and Huang, Y., *Scientific Reports,* 2013. **3**, p. 1-7.

157. Huang, G., Wang, A.P., Liu, S.Y., Guo, Y.A., Zhou, H. and Zhao, S.K., *Catalysis Letters,* 2007. **114**, p. 174-177.

158. Wen, S., Xiao-li, W., Zhen-hua, Z., Ke-qiang, D., Xian-feng, L. and Gong-de, W., *Journal of Molecular Catalysis,* 2013.

Experimental 2

1. Introduction

This chapter describes the experimental procedures used during this study. Details on catalyst preparation are given in the first part of this chapter, followed by the theory and procedures used to characterise the prepared catalysts. The last section is dedicated to a description of catalytic reactions and subsequent analysis of the products formed.

2. Materials

The following compounds were used during this project. All reagents were used as received without further purification, unless otherwise stated.

Toluene (> 99.9 %, Sigma-Aldrich)

Tert-butyl Hydroperoxide (TBHP) (70 % in water, Sigma-Aldrich)

Methane (99.999 %, BOC gases)

Methanol (HPLC grade, Sigma-Aldrich)

Octane (> 99 %, Sigma-Aldrich)

Decane (99 %, Alfa Aesar)

Dodecane (99 %, Aldrich)

Cyclooctane (> 99 %, Aldrich)

Benzaldehyde (98 %, Acros organic)

Formaldehyde (37 wt. % in H_2O, Sigma-Aldrich)

Propanal (97 %, Sigma-Aldrich)

Butanal (redistilled, 99.5 %, Aldrich)

Propane (99.999 %, BOC gases)

Hydrogen peroxide (H_2O_2) (50 wt. % in water, Sigma Aldrich)

Zeolite NH_4-ZSM-5 (SiO_2/ Al_2O_3 = 23, 30, 50 and 250, Zeolyst)

Iron (III) acetylacetonate (Fe(acac)$_3$, 98 %, Sigma Aldrich)

Copper (II) acetylacetonate (Co(acac)$_2$, 98 %, Sigma Aldrich)

Zeolite β (Zeolyst)

Zeolite Y (SiO_2/ Al_2O_3 = 5.1, 30, Zeolyst)

Aluminium oxide (puriss, 98 %, Sigma Aldrich)

Silica mesostructured MCM 41 (Sigma Aldrich)

Silica nanopowder (99.8 %, Sigma Aldrich)

Titania (TiO_2, P25, Degussa)

Tetraethylorthosilicate, (TEOS) (99.999 %, Sigma Aldrich)

Tetrapropylammonium hydroxide, (TPAOH) (1 M in water, Sigma Aldrich)

Titanium (IV) tetrabutoxide (TBOT) (97 %, Sigma Aldrich)

Aluminum isopropoxide (> 98 %, Sigma Aldrich)

Other metal acetylacetonates, Mn (III), Co (III), Ni (II), Zn (II), (all 98 %, Sigma Aldrich)

$HAuCl_4.3H_2O$ (Johnson Matthey)

$PdCl_2$ (Johnson Matthey)

$PtCl_2$ (Johnson Matthey)

Polyvinyl alcohol (PVA, MW = 10 kDa, Aldrich)

Sodium borohydride ($NaBH_4$, Sigma Aldrich)

Sulfuric acid (H_2SO_4, Fischer Scientific)

Carbon (Darco GC60, Sigma Aldrich)

Titania (TiO_2, P25, Degussa)

1,3,5-trimethyl benzene (Sigma Aldrich)

α,α,α-Trifluorotoluene (99 %, Acros Organic)

Sodium thiosulfate (Sigma Aldrich)

Potassium iodide (99 %, Sigma Aldrich)

Ferroin indicator (0.1 wt. % in water, Sigma Aldrich)

Cerium sulphate (Sigma Aldrich)

Deuterium Oxide (99.9 %), Sigma Aldrich)

3. Definitions

3.1. Conversion

3.1.1.   Octane reaction

$$\text{Octane conversion} = \frac{\text{Moles of Octane left after reaction}}{\text{Moles of Octane charge in reaction}} * 100$$

3.1.2.   Toluene/ Propane reaction

$$\text{Conversion} = \frac{\text{Moles of carbon in products formed}}{\text{Moles of initial carbon in reaction}} * 100$$

3.2. Oxygenate Selectivity

$$\text{Oxy. Selec.} = \frac{\text{Moles of carbon in liquid products formed}}{\text{Moles of carbon in total products formed}} * 100$$
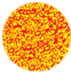
3.3. Turn Over Frequency (TOF)

$$\text{Mol}_{\text{(products formed)}} \, \text{Mol}^{-1}_{\text{(metal)}} \, \text{H}^{-1}$$

4. Catalyst preparation

4.1. Sol immobilisation

Catalysts made for toluene and octane oxidation (refer to section 6.3 to 6.5 for details) were prepared by a sol immobilisation (SI) method. This method allows the formation of nanoparticles with a good dispersion across the support. Different nanoparticle structures can be made by the addition of one, two or three different metals. Homogeneous monometallic, bimetallic or trimetallic alloys as well as heterogeneous core-shell structures are represented in Table 2.1.

Table 2.1: Representation of Au, Pd and Pt nanoparticles structures

Structures		
Homogeneous alloy		Heterogeneous
Monometallic	Bi/Trimetallic	Core-shell

Gold, palladium and platinum precursors were used in the preparation of monometallic bimetallic and trimetallic nanoparticles supported on carbon or Titania. Each catalyst was prepared to have a total final metal loading of 1 wt. %. A schematic of the preparation is shown in Figure 2.1.

Figure 2.1: Sol-immobilisation preparation for Mono, Bi and Tri metallic catalysts

The preparation of trimetallic 1 wt. % AuPdPt/ C is described as an example:

An aqueous solution of $PdCl_2$ (9.94 mg/ mL, 0.705 mL) $HAuCl_4.3H_2O$ (4.94 mg/ mL, 1.417 mL) and $PtCl_2$ (10.17 mg/ mL, 0.6882 mL), of the desired concentration was prepared. Subsequently, polyvinyl alcohol (PVA) solution (1 wt. % aqueous solution, 2.4 mL, PVA/ (total metal) (wt/ wt) = 1.2) was freshly prepared and added as the stabiliser. Next, a freshly prepared $NaBH_4$ solution (0.1 M aqueous solution, 7.24 mL, $NaBH_4$/ (total metal) (mol/ mol) = 5) was added to form a dark-brown sol. After 30 min of sol generation the colloid was acidified to pH 1 with H_2SO_4 and immobilized by adding carbon under vigorous stirring conditions (2 h). The slurry was filtered and the catalyst washed thoroughly with distilled water before drying (120 °C for 16 h).[1]

4.2. Chemical Vapour Infiltration (CVI)

CVI was used to prepare catalysts for the oxidation of propane (refer to section 6.6 for details). Most catalysts were supported on zeolite ZSM-5 (30), unless otherwise stated. The commercial zeolites being the ammonium form were first treated to activate and obtain the acidic form (H-ZSM-5 (30)). NH_4-ZSM-5 (30) were calcined in a ceramic boat (flowing air, 550 ºC, 3 h, 20 ºC/ min).

Prior to the addition of the metal the support was dried (160 ºC, 3 h) in a vacuum flask under vacuum (lowest pressure 10^{-3} mbar) prior to sieving (< 0.42 mm).
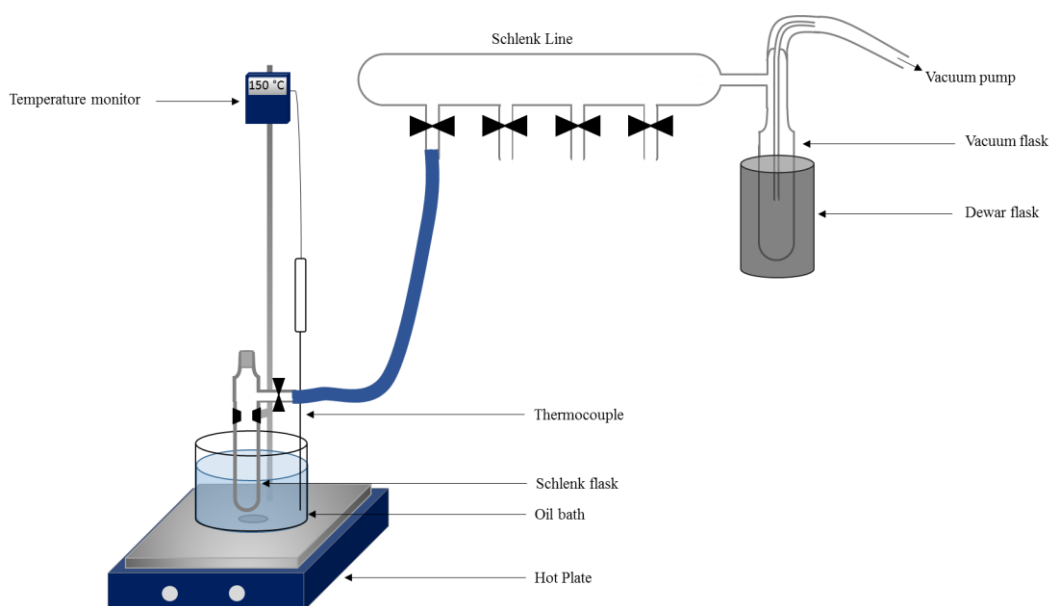

Figure 2.2: Schematic representation of the CVI method

A preparation of 2 g of 2.5 wt. % Fe/ ZSM-5 (30) is given as an example:

This preparation was performed in a vacuum flask connected to a Schlenk line as shown in Figure 2.2. H-ZSM-5 (30) (1.95 g) and iron (III) acetylacetonate ($Fe(acac)_3$) (0.316 g) were mixed until uniform in appearance and placed in the flask. The flask was then evacuated (lowest pressure 10^{-3} mbar) and its contents heated under dynamic vacuum (150 ºC, 2 h). The sample was removed after cooling and attaining atmospheric pressure. A calcination furnace fitted with a quartz tube was used to heat treat the sample (static air, 550 ºC, 3 h, 20 ºC/ min).

4.3. Solid-state ion-exchange

A number of catalysts were prepared by solid-state ion-exchange of a zeolite support (H-ZSM-5 (30)) with the relevant metal acetylacetonate precursor. The full procedure for 2.5 wt. % Fe/ ZSM-5 (30) is outlined. Fe(acac)$_3$ (0.158 g) was added to the desired amount of H-ZSM-5 (30) (1.95 g) and ground with a pestle and mortar for 30 minutes. The catalyst was subsequently activated by calcination (static air, 550 °C, 3 h).

4.4. Sol gel preparation: SiO$_2$/ Al$_2$O$_3$

For this preparation the mass of product was calculated in order to obtain a ratio of SiO$_2$/ Al$_2$O$_3$ 10 and 100. Aluminum isopropoxide (98 %, 0.27 or 2.7 g) was dissolved in tetrapropylammonium hydroxide (TPAOH, 1 M, 6.4 mL) at 60 °C. The solution was cooled to room temperature, then tetraethylorthosilicate (TEOS, 98 %, 13.75 g) and ethanol (30 mL) was added. After about 5 minutes the monophasic clear solution was transformed to a homogeneous lightly opalescent gel. After ageing (15 h) at room temperature, the gel was dried (100 °C) and calcined (static air, 550 °C, 8 h, 2 °C/ min).[2]

4.5. Synthesis of Silicalite

Tetrapropylammonium hydroxide (TPAOH, 20 wt. %, 49.9 mmoles) was stirred vigorously at room temperature for 1 h. To this solution tetraethylorthosilicate (TEOS, 98 %, 49.4 mmoles) was added drop wise. The resulting gel was homogenised for 5 h at 60 °C prior to crystallisation in a Teflon lined stainless steel Parr autoclave (175 °C, 48 h). The as synthesised material was later recovered by filtration, washed with deionised water (1 L) and dried in air (110 °C, 16 h). The dried sample was then ground, prior to heat treatments to remove the template (flowing N$_2$, 550 °C, 5 h, 1 °C/ min, then flowing air, 550 °C, 3 h).[3]

4.6. Synthesis of TS-1 (Si/ Ti molar ratio = 50)

Tetraethylorthosilicate (TEOS, 98 %, 57.6 mmoles) was added to an aqueous solution of hydrochloridric acid (10 mL, 0.05 M). To this solution titanium (IV) tetrabutoxide (TBOT, 97 %, 1.15 mmoles) dissolved in isopropanol (99.5 %, 6.67 mL) was added drop wise. After 15 min stirring tetrapropylammonium hydroxide (TPAOH, 20 % solution, 2.5 mmoles) was added drop wise to form a transparent gel which was aged (2 h) at room

temperature, dried (110 ºC, 16 h) and finely ground. A quantity of TPAOH two times the weight of the solid was added and the mixture was crystallized in a Teflon lined stainless steel Parr autoclave (175 ºC, 24 h). The as synthesised material was later recovered by filtration, washed with deionised water (1 L) and calcined to remove the template (static air, 550 ºC, and 16 h, 2 ºC/ min).

5. *Catalyst characterisation*

5.1. Electron Microscopy

Microscopy is a non-destructive method and gives the possibility of seeing, studying, and examining small, subatomic particles or compositions of a sample. Transmission electronic microscopy (TEM) was used to characterise heterogeneous catalysts as it allows the determination of catalyst particle size, dispersion and chemical composition. TEM has a resolution of 5 Å.[4]

TEM uses primary high voltage electron beams which pass through a condenser to produce parallel rays. The rays are then transmitted through a thin sample, interacting with the sample as it passes through. Electrons which are transmitted or diffracted will be detected in TEM; the detectable signals are represented in Figure 2.3. The attenuation of the beam depends on the density and the thickness of the sample. The transmitted diffracted electrons form a 2-dimensional projection of the sample mass distribution.

STEM (Scanning Transmission Electron Microscope) was also used to characterise samples. STEM works in a similar way to a scanning electron microscope (SEM). A focused beam of electrons scanned the sample and interacted with the atoms to produce backscattered electrons, secondary electrons and X-ray as shown in Figure 2.3. STEM collects different signals which allow a variety of imaging modes. However, higher signal levels and better spatial resolution are available by detecting transmitted electrons. High Angle Annular Dark Field (HAADF) was used as the detector to collect scattered transmitted electrons. The inner angle of the annular dark field detector is made large enough so no Bragg diffracted electrons are collected. The images therefore come from elastically scattered electrons which have passed very close to the atomic nuclei in the sample.

TEM and STEM images were collected at Lehigh University by Christopher J. Kiely's group. These images were collected on a JEOL JEM-2100 transmission electron microscope fitted with a LaB_6 filament. Samples were prepared by dispersing powdered

catalyst in high purity ethanol, before adding a drop of the suspension to a porous carbon film supported by a meshed copper TEM grid.
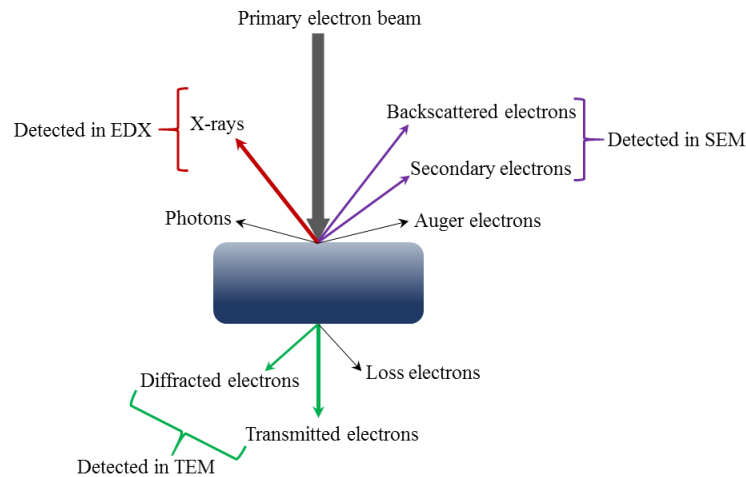

Figure 2.3: Scheme of detectable signals in electron microscopy of a sample bombarded by a primary electron beam

5.2. Energy Dispersive X-ray Spectroscopy (EDX/ EDS)

EDX is a quantitative technique for bulk samples. When an electron beam hits the sample an electron from the inner shell is ejected leaving an electron vacancy. An electron from an outer shell fills the vacancy by lowering its energy. The excess of energy is released through X-ray emission as shown in Figure 2.4.[5]

As each atom from the periodic table has a different electronic structure the emission of excess energy will be different and characteristic of each atom.

EDX data were collected on a SEM EVO 40VP fitted with a tungsten filament. The SEM is coupled with an oxford instrument detector in order to detect the X-ray emission. Samples were deposited on a carbon disc for analysis.
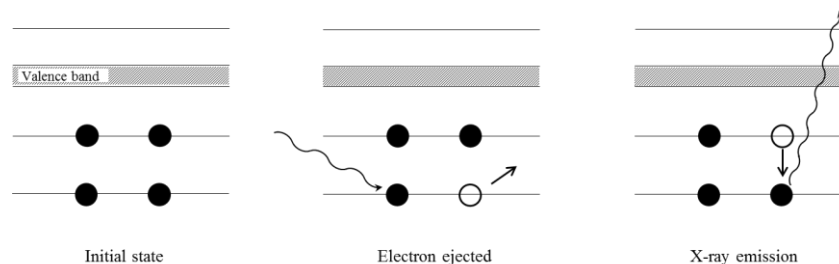

Figure 2.4: Schematic representation of energy dispersive X-ray spectroscopy

5.3. X-ray Photoelectron Spectroscopy (XPS)

XPS is a technique used for surface (1.5 to 6 nm) analysis. It gives information on the elemental composition and the oxidation state of the element. A monochromatic X-ray photoelectron irradiation hits the sample. A photon (hv) is absorbed by an atom of the sample which will emit a photoelectron with the lowest energy (can be core or valence electron). (Figure 2.5)[4] The energy E_k can be calculated following the equation:

$$E_k = hv - E_b - \varphi$$

E_k : is the kinetic energy of the photoelectron

h : is the Plank's constant (6.626×10^{-34} J.s)

v : is the frequency of the exciting radiation

E_b : is the binding energy of the photoelectron with respect to the Fermi level of the sample

φ : is the work function of the spectrometer
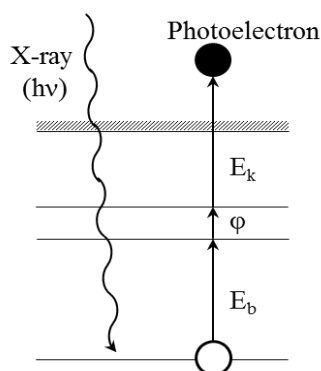
Figure 2.5: Schematic representation of X-ray photoelectron spectroscopy

Binding energies are characteristic of an element; the energy depends on the environment and oxidation state of the atom. Binding energy changes with oxidation state, in general it increases with the oxidation state.

XPS spectra were collected using a Kratos Axis Ultra DLD System using monochromatic Al Kα X-ray source operating at 120 W. Data was collected in the hybrid mode of operation, using a combination of magnetic and electrostatic lenses, and at pass energies of 40 and 160 eV for high resolution and survey spectra respectively. Magnetically

confined charge compensation was used to minimize sample charging and the resulting spectra were calibrated to the Si (2p) line at 103.2 eV.

5.4. Inductively Coupled Plasma (ICP)

Iron content of zeolite samples were obtained using ICP technique by Warwick Analytical Services. As prepared samples were accurately weighed (50 mg usually) and digested in concentrated hydrofluoric acid (HF) followed by digestion in aqua regia after evaporation of HF. The solution was then neutralised and infused into an ICP machine for analysis.

5.5. X-Ray Diffraction (XRD)

X-ray diffraction is used to identify crystalline phases of a material. In powder X-ray diffraction, the diffraction pattern is obtained from a powder of the material, rather than an individual crystal. This technique can identify bulk phase (amorphous or crystalline phase) and give an indication of the particles size. X-rays have wavelengths of an equal order to molecular bond lengths (10^{-10} m) and are sufficiently energetic to penetrate solids and probe their internal structure. The sample is bombarded with X-rays; two types of emitted rays are produced. X-rays are partially reflected by the first layer of atoms on the surface, the other part of the X-rays passes through to the next layer and are reflected which cause an overall diffraction pattern. (Figure 2.6) The diffraction of X-ray follows Bragg's law:

$$n\lambda = 2d \sin\theta \, ; \; n = 1,2,\ldots$$

λ : is the wavelength of the X-rays

d : is the distance between two lattice planes (or atom layers)

θ : is the angle of incidence of the X-ray

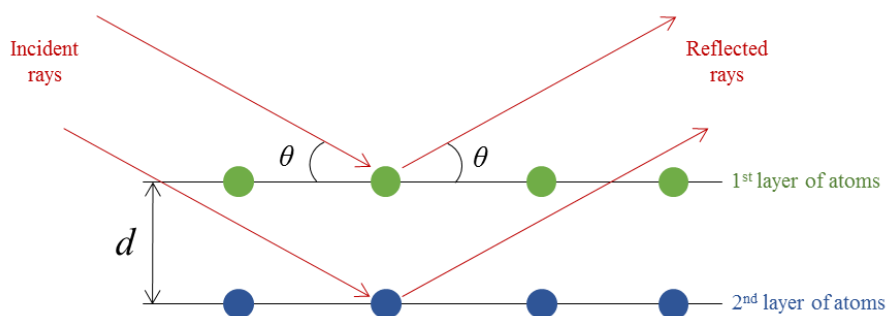n : is an integer called the order of the reflection

Figure 2.6: Schematic representation of X-ray diffraction

For diffraction to occur, a regular structure is needed. Amorphous materials do not show a diffraction pattern. Through comparison with a database of XRD patterns, the phases which are present within a sample may be identified and crystallite sizes may be determined from a peak's width via the Scherrer equation, though the latter is limited to species with particle sizes of greater than 10 nm.
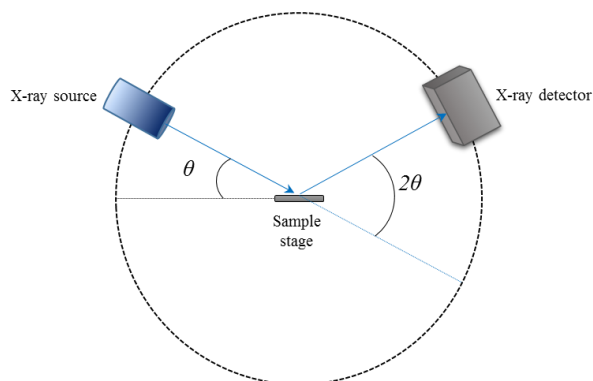
Figure 2.7: Schematic representation of X-ray diffraction system

Powder X-ray diffraction was performed using a PANalytical X'PertPRO X-ray diffractometer, with a CuKα radiation source (40 kV and 40 mA) and Ni attenuator. Diffraction patterns were recorded across a range of 5-70 degrees, 0.0167 step size (time/ step = 150 seconds).[4, 5]

5.6. Thermogravimetric Analysis (TGA)

TGA analysis is a method involving change in weight with respect to temperature. This technique is used on heterogeneous catalysis to obtain information on adsorbents present

on the catalyst and the decomposition temperature of the material. Used catalysts can also be analysed to give information about potential contamination. During analysis, a high precision microbalance and temperature control are used so that the change in mass can be monitored as the sample temperature is increased. By comparing mass changes to specific temperatures and reference materials, the identification and quantification of adsorbents or species present in a sample can be deduced.[6]

5.7. Temperature programme Reduction/ Oxidation (TPR/ TPO)

TPR/ TPO is a useful technique to determine the ability of reduction/ oxidation of a heterogeneous catalyst. It is a technique in which a chemical reaction is monitored while the temperature increases linearly with time. This analysis gives information on the phase present on the catalyst.

This is achieved by flowing a reducing or oxidising gas, for example 10 % H_2/ Ar or 10 % O_2/ He, over a sample whilst heating the sample according to a programmed, linear temperature ramp. The area under a TPR/ TPO represents the total H_2/ O_2 consumption. Interaction between the support and metals may change the reduction/ oxidation potential of the metals.[4]

Temperature programmed reduction/ oxidation was carried out using a TPDRO 1100 series analyser. Samples (80 mg) were pre-treated for 1 h at 130 ºC (20 ºC/ min) in a flow of Argon (20 mL/ min). Following this the gas flow was changed to 10% H_2/ Ar or 10 % O_2/ He and the temperature was ramped to 800 ºC (10 ºC/ min) with a 5 min hold at the T_{max}. H_2/ O_2 uptake was monitored using a TCD detector.

5.8. Temperature Programme Desorption (TPD)

Thermal desorption spectroscopy (TDS) or TPD is used in surface science. It is the study of gas desorption from the surface. TPD is an excellent technique for determining surface coverage and to give information on the strength of the bond between adsorbate and substrate (adsorption energies of adsorbents from the surface).

Different gases can be adsorbed which can give unique information. In this work, ammonia was employed in order to determine the different acid sites. NH_3 is first adsorbed on the surface. The sample is then subjected to a temperature ramp and NH_3 desorption is recorded by TCD at different temperatures. The temperature of desorption shows the energy needed to break the bond, thus the strength of the bond.[4]

NH$_3$-TPD was carried out using a CHEMBET TPR/ TPD chemisorption analyser, Quantachrome Industries fitted with a TCD. The samples (50 mg) were pre-treated for 1 h at 130 ℃ (15 ℃/ min) in a flow of helium (80 mL/ min). Following this, the sample was cooled to ambient temperature and pure ammonia flowed through for 20 min to ensure saturation. The system was then heated 1 h at 100 ℃ (15 ℃/ min) under a flow of helium (80 mL/ min) to remove physisorbed ammonia. Subsequently, chemisorbed ammonia was desorbed by heating to a temperature maximum of 900 ℃ (15 ℃/ min) in a flow of helium (80 mL/ min) during which period desorbed ammonia was monitored using a TCD, current 180 mV and attenuation of 1.

5.9. Brunauer Emmett Teller (BET) surface area analysis

BET technique allows measurement of the specific surface area and pore volume of a solid sample by the adsorption of a monolayer of nitrogen. The adsorption occurs on the outer surface and in the pores in case of porous materials. The sample is first pre-treated in order to clean the surface removing adsorbents such as water or solvent. In a second step a physical adsorption of adsorbate is carried out involving different pressures of nitrogen. The relationship between pressure and quantity of nitrogen adsorbed is given by the following equation.[7, 8]

$$\frac{P}{v(P_0 - P)} = \frac{1}{v_m C} + \frac{C - 1}{v_m C}\frac{P}{P_0}$$

P: is the equilibrium pressure

Po: is the saturation pressure

v : is the volume

v_m: is the volume required to cover the surface in a monolayer

C: is a constant

This equation is an adsorption isotherm and can be linearised by plotting $\frac{P}{v(P_0-P)}$ versus $\frac{P}{P_0}$. This straight line intercepts $\frac{1}{v_m C}$.

The surface area can finally be determined from υ_m and the equation:

$$Surface\ Area = \frac{v_m * N_a * S}{M}$$

υ_m : is the volume required to cover the surface in a monolayer

N_a : is the Avogadro's number (6.023×10^{23})

S : is the cross sectional area of N_2 ($0.162\ nm^2$)

BET analysis of materials was conducted on an Autosorb-1 Quantachrome instruments system at 77 K. A Monte Carlo based model was used in determining pore volumes. Points in the range of 0.06 to 0.35 were used in the BET multipoint surface area quantification.

5.10. Solid State - Nuclear Magnetic Resonance (NMR)

Magic angle spinning (MAS)-NMR spectroscopy is a technique that provides information on the chemical environment of atoms present in a solid sample. This technique allows the study of molecules with a magnetic moment. A nucleus possesses a magnetic moment when its spin quantum number (I) is not zero (uneven number of protons and/ or neutrons present). If a nucleus with a magnetic moment is exposed to a magnetic field the energy levels will be split following the equation $m = 2I + 1$.
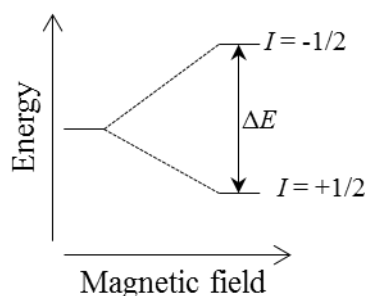

Figure 2.8: Schematic representation of energy splitting when the sample is under a magnetic field

The magnetic field causes a splitting of degenerate energy levels as represented in Figure 2.8. The energy splitting for a nucleus $I = 1/2$ with a difference in energy ΔE is given by:

$$\Delta E = \frac{\gamma h B_0}{2\pi}$$

B_0 : is the strength of the magnetic field

γ : is the gyromagnetic ratio of the nucleus studied

h : is the Planck's constant (6.626 x 10^{-34} J.s)

Electromagnetic radiation causes the molecule to resonate between these two energy levels bringing about a resonance frequency (ν) which relates to the magnetic field strength and the gyromagnetic ratio of the nucleus according to the following equation:

$$2\pi\nu = \gamma B_0$$

The resonance frequency is characteristic of the environment around the nucleus and leads to the chemical shift (δ) which is the signal present on NMR spectra.

In solid samples, molecules are locked into a certain configuration in contrast with liquid samples. This anisotropic system causes broad peak signals. In order to eliminate this effect, the solid sample is spun rapidly (> 5 kHz) at an angle of 54.7 ° to the magnetic field called magic angle which mimics the rapid movement of species in the liquid phase, and allows spectra of higher resolution to be obtained.[9]

^{27}Al MAS-NMR measurements were performed during this study in order to investigate the role of alumina in the zeolite samples after addition of metals or treatment. The solid-state NMR experiments were carried out on a 400 MHz Varian CMX infinity spectrometer, equipped with 4.0 mm probe with resonance frequencies of 400.1 and 100.4 MHz for ^{1}H and ^{27}Al respectively. Single-pulse ^{27}Al experiments were performed with a pulse length of 1 μs and a pulse delay of 1 s. The magic angle spinning rate was set to be 8 kHz. The chemical shift was referenced to Kaolin as a second reference to 1 M Al(NO_3)$_3$ solution.

5.11. UV-Visible

UV-Vis is based on the coloured transition metal complexes. It is known that for a particular oxidation state a metal has a particular colour which will change with the oxidation state. The rearrangement of valence electrons is responsible for the transition studied in UV-Vis. In heterogeneous catalysis, UV-Vis spectroscopy is used to study transition metal ions within catalysts. Electronic spectroscopy is an absorption technique

where the colour of a sample depends on which energy of visible light is absorbed. When the sample is irradiated by electromagnetic radiation (200-800 nm) some energy is absorbed and causes electronic transitions from a lower energy state to an excited state with higher energy. Signals on UV-Vis spectra show the absorbed energy which causes a transition energy as shown in Figure 2.9.[9]
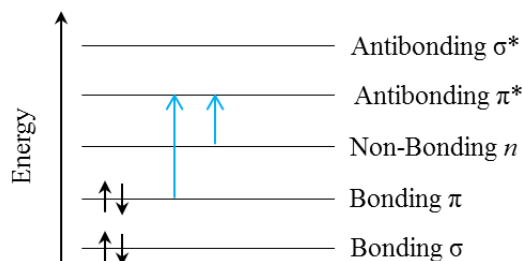

Figure 2.9: Schematic representation of transition energy in UV-Visible

Only π → π* and *n* → π* transition occurring in the UV-vis region are observed.

UV-Vis spectra were collected using a Varian 4000 UV-Vis spectrophotometer. Scans were collected across the wavelength range 200-800 nm, at a scan rate of 150 nm/ min, with a UV-vis changeover wavelength of 260 nm. Background scans were taken using a high purity PTFE disc. Prior to analysis catalyst samples were ground to a fine powder.

5.12. Diffuse Reflectance Infrared Fourier Transform Spectroscopy (DRFITS)

Infra-red spectroscopy is a useful technique to elucidate the structure of a chemical compound. Various forms of IR spectroscopy are in use. DRIFTS allow the measurement of loose powders. The DRIFT cell allows the control of temperature and the environment during analysis. In comparison to other IR techniques, only the diffusely scattered radiation from the sample, as shown in Figure 2.10, is collected by a special mirror. This allows functional groups and adsorbed molecules on the surface of the catalyst to be investigated.
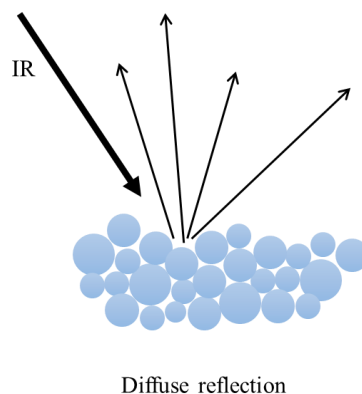
Diffuse reflection

Figure 2.10: Schematic representation of the diffuse reflection in vibrational microscopy

IR is a vibrational spectroscopy and studies the changes in the vibrational state of molecules. Molecules possess discrete levels of rotational and vibrational energy. The transition between levels occurs by absorption of a photon with frequency ν (IR radiations are between $\nu = 4000$ and 200 cm^{-1}) as shown in Figure 2.11. The frequencies of the vibration bond (or functional group) are a signature of the type of bond. Vibrational frequencies increase with increasing bond strength and with decreasing mass of the vibrating atoms.[4, 6, 9, 10]
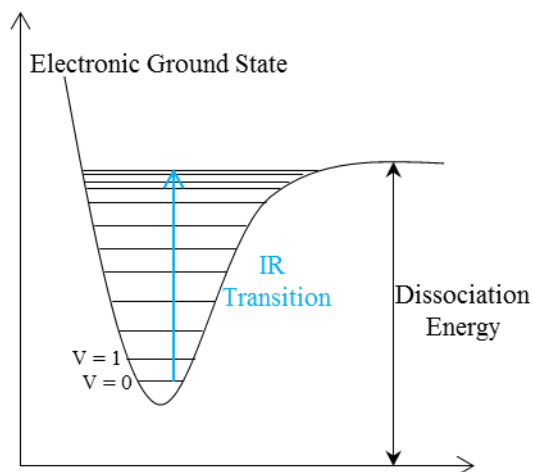

Figure 2.11: Schematic representation of infrared transition

IR spectra were collected on a Bruker Tensor 27 spectrometer fitted with a liquid nitrogen-cooled Mercury Cadmium Telluride (MCT) detector. Samples were housed within a Praying Mantis high temperature diffuse reflection environmental reaction chamber (HVC-DRP-4) fitted with zinc selenide windows. Background scans were taken

using finely ground KBr. Prior to analysis, samples were mixed with KBr 1:1 by volume, and subsequently ground to a fine powder. Samples were pretreated prior to acquisition by heating the cell to 200 ℃ (10 ℃/ min) under continuous vacuum (10^{-3} mbar) and maintained at this temperature for 2 h to ensure removal of residual water. Scans were collected across the range 4000 cm^{-1} to 1500 cm^{-1}, 4 cm^{-1} frequency, 64 scans.

6. Catalytic testing

6.1. Reactor design (Parr reactor and batch reactor)

6.1.1. Parr reactor

All reactions were performed in a stainless-steel autoclave (Parr reactor) containing a Teflon liner vessel with total volume of 50 mL (working volume of 35 mL), a schematic is shown in Figure 2.12.
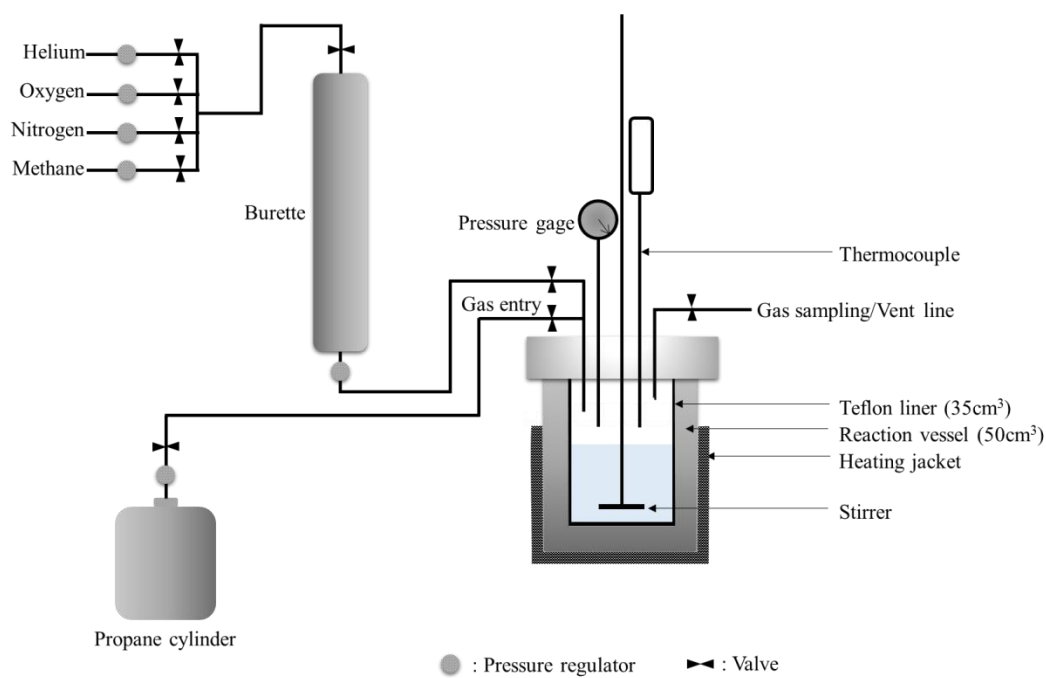

Figure 2.12: Schematic representation an autoclave batch reactor

6.1.2. Bench reactor

All bench reactions were performed in a glass round bottom flask with a volume of 50 mL (working volume of 25 mL); a schematic is shown in Figure 2.13.
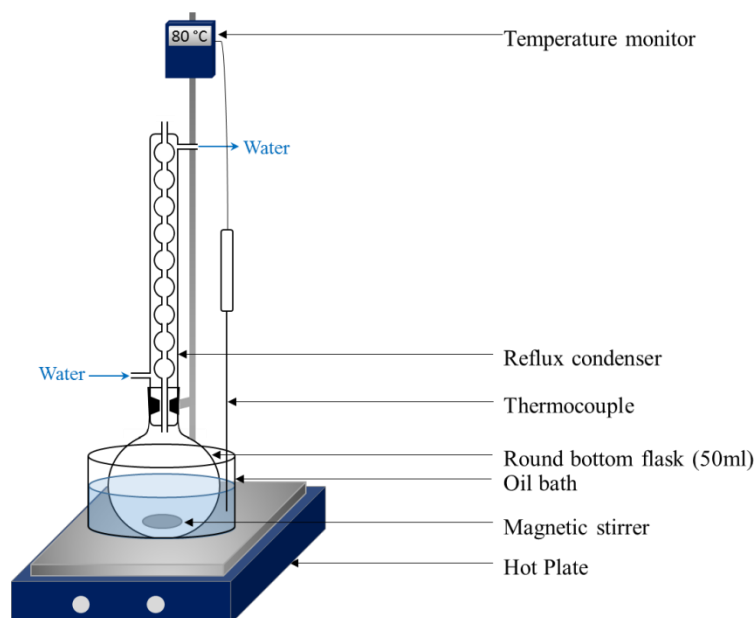
Figure 2.13: Schematic representation of a set up for bench reactions

At the end of each reaction the autoclave or flask was cooled in ice to a temperature below 10 °C to minimise loss of volatile products. The reaction mixture was filtered and analysed by GC or ^{1}H-NMR. For reaction occurring in autoclave, the reaction gas was removed for analysis using a gas sampling bag fitted to the outlet line.

6.2. Gas Chromatography

Gas chromatography was used in every study as a technique to analyse the products in gas and/ or liquid phases. The technique allows the identification and quantification of products.

Liquid samples are vaporised in the injector. A mobile gas phase carries the products on to the column. This carrier gas has to be an inert, typically He, to avoid any interaction with products. In the column the stationary phase is an adsorbent or a liquid phase on an inert material. It is the interactions (H-bonding, dipole-dipole) between products and stationary phase which allow the separation. When products arrive at the end of the

column they are detected. Many types of detectors can be used, in this study flame ionisation detector (FID) and mass spectra were used. (Figure 2.14)
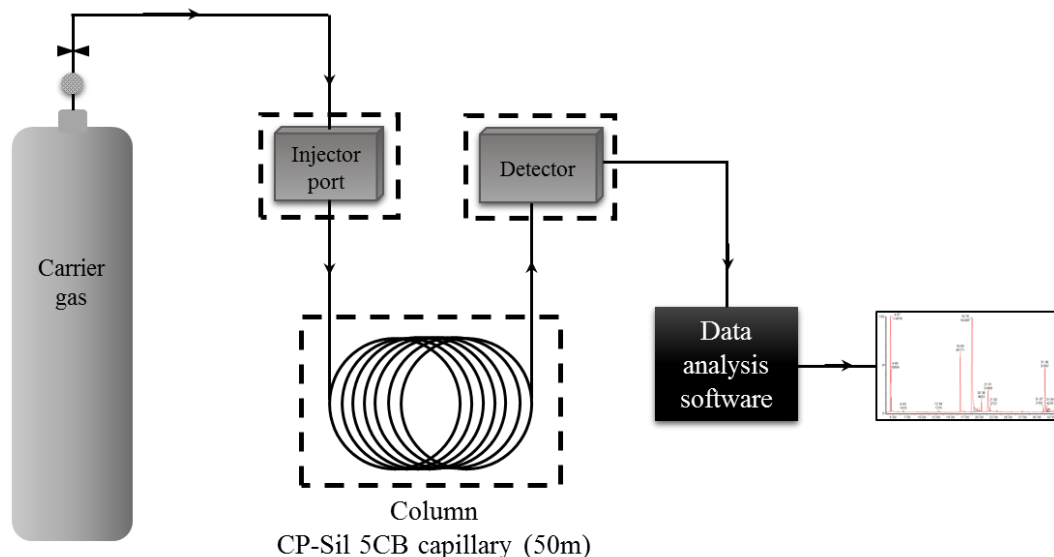
Figure 2.14: Schematic representation of gas chromatograph

FID detector: A FID detector detects compounds through pyrolysis. Hydrogen and compressed air are injected in the detector with the sample. Organic compounds will be pyrolysed by the flame and produce fragmented ions which can be detected between two oppositely charged plates. The response of the detector being proportional to the number of moles responsible for the signal, thus the sample can be quantified.[11, 12]

Mass spectrometry: This technique is used to identify unknown products thanks to their molecular mass. The compound is ionised by bombarding the sample with electrons to generate charged molecules and measuring their mass to charge ratio (m/z). Gas chromatography and mass spectroscopy combined allow the separation, identification and quantification of a mixture of unknown products.[13]

Once known the compounds were calibrated in each GC in order to quantify them. The details of the machine and sample preparation are described below.

6.3. Toluene oxidation with *tert*-butyl hydroperoxide (TBHP)

6.3.1. Catalytic testing

6.3.1.1. Bench reactor

All reactions were performed in a stirred glass round bottom flask (50 mL) fitted with a reflux condenser and heated in an oil bath. Typically, toluene and TBHP (molar ratio toluene/ TBHP = 1) and the required amount of catalyst were suspended in the solution. The reactions were carried out at 80 °C for 24 h (unless otherwise stated). The reaction was carried out in air at atmospheric pressure.

6.3.1.2. Parr reactor

The reactions were carried out in a 50 mL autoclave. The vessel was charged with the mixture toluene-TBHP (10 mL) and catalysts (0.05g). The autoclave was purged 5 times with nitrogen and 2 times with the gas mixture leaving the vessel at 20 bar pressure. The reactions were carried out at 80 °C for 24 h (unless otherwise stated).

6.3.2. Identification and analysis

6.3.2.1. Gas Chromatography

The identification and analysis of the products was carried out using GC-MS (a Waters GCT Premier and a HP 6890 N with a 30 m Agilent DB-5ms column) and GC (a Varian star 3400 cx with a 30 m CP-Wax 52 CB column). The products were identified by comparison with known standards. For the quantification of the amounts of reactants consumed and products generated, the external calibration method using a standard (1, 3, 5-trimethyl benzene, Sigma Aldrich) was used. 1,3,5-trimethyl benzene was added after the reaction and before the samples were analysed. All reaction mixtures were dissolved in methanol (5 mL) before analysis due to the solid form of the product obtained after longer reaction times.

The gas phase was analysed with a GC (Varian 450-GC equipped with FID & TCD detectors, methaniser and CP-SiL5CB column (50 m, 0.33 mm diameter, He carrier gas)).

6.3.2.2. TBHP titration

After reaction, TBHP was titrated in order to calculate the amount of TBHP converted. This titration was done by adding sodium thiosulfate. Prior to this addition the reaction mixture (typically 0.5 mL) was added to a solution of potassium iodine (10 mL mixture

of Acetone, acetic acid and water with a ratio 2: 1: 1). It is a back titration where sodium thiosulfate titrates iodine.[14]

$$(1) \qquad I_2 + 2\ S_2O_3{}^{2-} \longrightarrow 2\ I^- + S_4O_6{}^{2-}$$

$$(2) \qquad ROOH + 2\ I^- + 2\ H^+ \longrightarrow ROH + H_2O + I_2$$
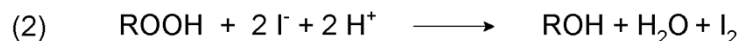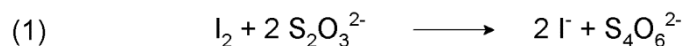
The first step causes a change of colour of the mixture (Equation 1). The mixture becomes colourless when the volume of titration is reached. (Equation 2)

6.3.2.3.Reuse studies

To determine the reusability of the catalyst, the following procedure was applied. Fresh catalyst (300 mg) was tested for catalytic activity under standard conditions described in this chapter section 6.3.1. Upon completion of the reaction, the solution was filtered and the solid catalyst was wash with acetone and air dried overnight at room temperature. Two portions of the dried sample (50 mg each) were subsequently tested for catalytic activity under standard conditions, representing the second use of the catalyst. The two portions of spent catalyst were then combined, dried and reused in a third use. When this reuse process had been completed three re-use cycles were done.

6.4. Methane-Toluene oxidation

6.4.1. Catalytic testing

Typically, in the reaction involving methane and toluene the reaction was performed in a 50 mL autoclave. The vessel was charged with toluene (10 mL) and catalyst (0.05 g to 0.1 g). The autoclave was purged 5 times with nitrogen followed by 2 times with methane: oxygen mixture taking care to avoid the explosive limits of this mixture. Then the reactor was filled with the required pressure of the methane: oxygen mixture. Most of the reactions were run for 20 h (unless otherwise stated) with a temperature range from 80 °C to 160 °C and stirred at 1500 rpm.

6.4.2. Identification and analysis GC

The identification of the products was carried out using GC-MS (a Waters GCT Premier and a HP 6890 N with a 30 m Agilent DB-5 ms column) for the liquid phase. The gas phase was analysed with a GC (Varian 450-GC equipped with FID & TCD detectors,

methaniser and CP-SiL5CB column (50 m, 0.33 mm diameter, He carrier gas)). In this part no quantification was done as the target product was not present.

6.5. Octane/ benzaldehyde/ O_2 system

6.5.1. Catalytic testing

The reactions involving alkanes and aldehydes were carried out in a 50 mL autoclave (working volume of 35 mL). The vessel was charged with an alkane: aldehyde mixture (10 mL, 9:1 molar) and catalyst (0.05 g). The autoclave was purged 5 times with nitrogen and 2 times with pure oxygen leaving the vessel at 20 bar pressure, time and temperature used will be stated in chapter 3.

6.5.2. Identification and analysis

The subsequent final reaction mixtures were dissolved in 5 mL isopropanol before analysis due to the formation of solid products during reaction. The identification and analysis of the products were carried out using GC-MS (a Waters GCT Premier and a HP 6890 N with a 30 m Agilent DB-5 ms column) for the liquid phase and GC (Varian 450-GC equipped with FID & TCD detectors, methaniser and CP-SiL5CB column (50 m, 0.33 mm diameter, He carrier gas)) for liquid and gas phase. For quantification of the amount of reactants (alkanes and aldehydes) consumed an external calibration method was utilised with 1, 3, 5-trifluorotoluene (sigma Aldrich) as the standard.

6.6. Propane oxidation

6.6.1. Catalytic testing

In a typical experiment, catalyst (27 mg, unless otherwise stated) was added to pure water (10 mL) containing a measured amount of H_2O_2, typically 5000 µmol. The system was pressurised with propane to a fixed pressure (4 bar, 4000 µmol) after air in the reactor was removed by purging three times with helium and two times with propane. A pressure of 20 bar total was reached by adding helium. The autoclave was heated to the desired reaction temperature (30 °C to 90 °C). The solution was vigorously stirred at 1500 rpm from the beginning. Once the reaction temperature was attained the time was started (0.5 h to 20 h).

6.6.2. Analysis of products and quantification

6.6.2.1. Nuclear Magnetic Resonance

NMR is a powerful technique principally used to identify organic molecules in solution. ^{1}H-NMR spectroscopy was used to identify and quantify products in the liquid phase. This technique allows the quantification of each product as it is associated with the protons present in the molecules and their environment. Hence any compound, regardless of its chemical shift, produces a signal with a magnitude that is proportional to the number of nuclei responsible for the signal. Section 5.10 of this chapter described the theory behind NMR spectroscopy. However, in the case of liquid samples there is no need for spinning at magic angle as the molecules are not locked in position.[6, 9]

Room temperature NMR spectra were recorded on a Bruker DPX 500 MHz Ultra- Shield NMR spectrometer ([1]H 500.13 MHz). A solvent suppression program was performed in order to minimise the signal arising from the solvent (water). NMR spectra of the liquid products formed during the oxidation of propane are shown in Figure 2.15

^{1}H NMR analysis was performed after filtration of the reaction. Typically, 0.7 mL of sample, 0.1 mL of D_2O and a glass ampule containing Tetramethyl Silane (TMS) in $CDCl_3$ were placed in an NMR tube for analysis. TMS was used as an internal standard in order to quantify each product. This internal standard was calibrated using various concentrations of products. The calibration curve of acetone is shown in Figure 2.16.

Each product does not have only one signal on NMR spectra and some of them are overlapping as shown Figure 2.15. The chemical shifts and splitting for the protons used in quantifying the various C_1, C_2 and C_3 products formed are shown in Table 2.2.
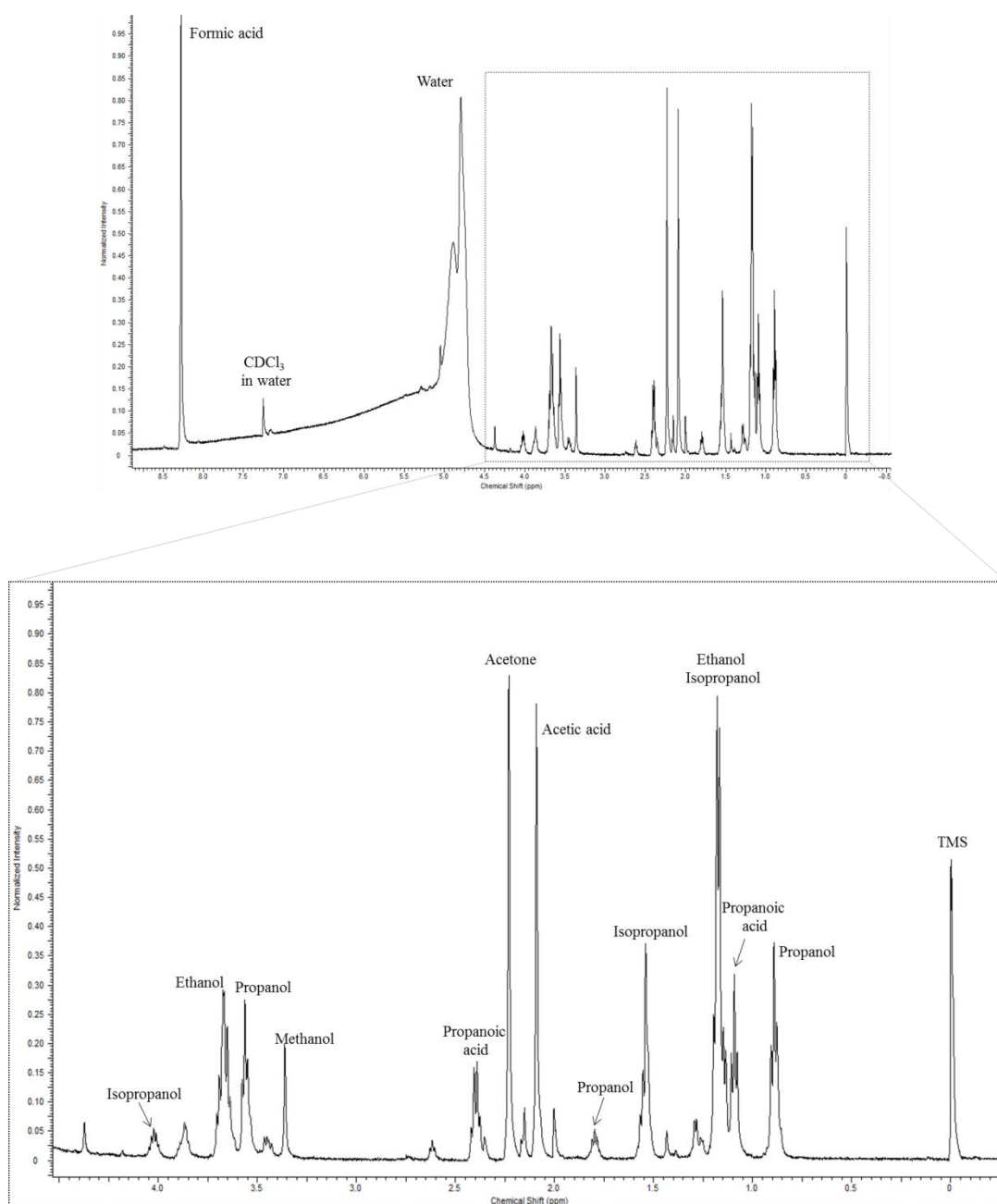
Figure 2.15: ¹H-NMR, water suppressed spectra for products from propane oxidation reaction.
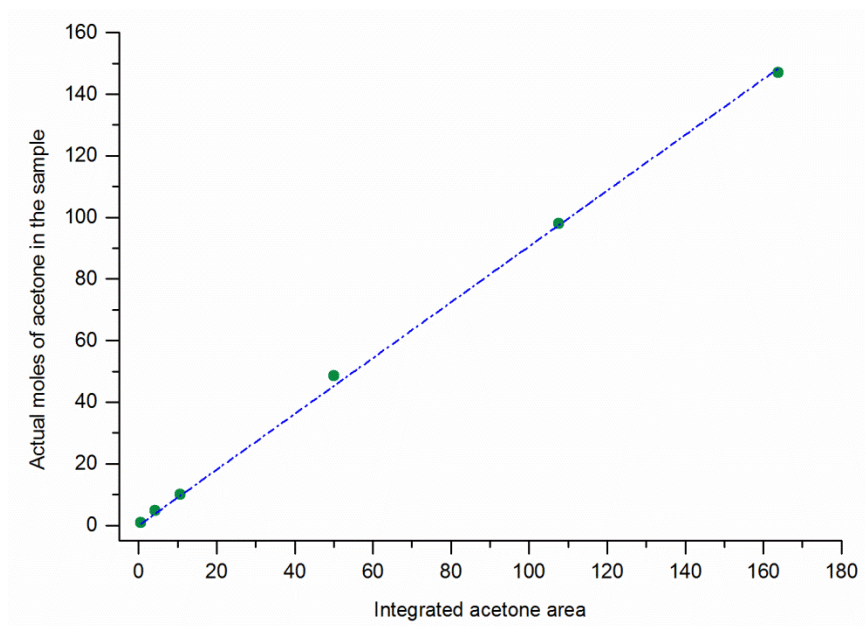
Figure 2.16: Acetone calibration curve

Table 2.2: ^{1}H NMR chemical shifts of liquid phase propane oxidation products

Compound	Formula	Chemical shift δ (ppm)	Multiplicity
Propanol	$CH_3CH_2CH_2OH$	3.55	Triplet
Propanoic Acid	CH_3CH_2CHOOH	1.08	Triplet
Isopropanol	$(CH_3)_2CHOH$	4.02	Multiplet
Acetone	$(CH_3)_2CO$	2.23	Singlet
Ethanol	CH_3CH_2OH	3.65	Quartet
Acetic Acid	CH_3COOH	2.07	Singlet
Methanol	CH_3OH	3.37	Singlet
Formic Acid	$CHOOH$	8.2	Singlet

6.6.2.2. Gas Chromatography

The identification of the gas products were analysed with a Varian 450-GC equipped with FID & TCD detectors, methaniser and CP-SiL5CB column (50 m, 0.33 mm diameter, He carrier gas).

6.6.2.3. H_2O_2 titration

H_2O_2 was quantified through titration of the reaction solution (typically 0.1 mL) against an acidified solution of $Ce(SO_4)_2$ (8 x 10^{-3} mol/ L) which was standardised versus $(NH_4)_2Fe(SO_4)_2 \cdot 9H_2O$, with a Ferroin indicator.[15]

6.6.3. Catalyst treatment

6.6.3.1. Acid treatment

Acid treatment was done on bare zeolite in order to investigate the potential dealumination. This treatment was also investigated on 2.5 wt. % Fe/ ZSM-5 (30) to remove iron from the catalyst.

The sample (typically 1 g) was stirred in an aqueous solution of nitric acid (50 mL, 10 % volume in water, unless otherwise stated) for 15 min to 120 min at a temperature between 50 ºC and 120 ºC. The sample was filtered and washed with deionised water until neutral pH and dried at 110 ºC for 4 h.

6.6.3.2. Alkali treatment

Alkali treatment was done on bare zeolite in order to increase the presence of Lewis acid sites.[16] The sample (typically 1 g) was stirred in an aqueous solution of sodium hydroxide (10 mL, 2 M) for 2 h at 50 ºC. The sample was filtered and washed with deionised water until neutral pH and dried at 110 ºC for 4 h.

7. References

1.   Dimitratos, N., Lopez-Sanchez, J.A., Morgan, D., Carley, A., Prati, L. and Hutchings, G.J., *Catalysis Today,* 2007. **122**, p. 317-324.

2.   Rizzo, C., Carati, A., Tagliabue, M. and Perego, C., *Studies in Surface Science and Catalysis,* 2000. **128**, p. 613-622.

3.   Taramasso, M., Perego, G. and Notari, B., *United States Patent 4410501,* 1982.

4.   Niemantsverdriet, J.W., *Spectroscopy in Catalysis: An Introduction*. Second Completely Revised Edition ed. Wiley-Vch. 2000.

5.   Guozhong, C., *Nanostructures & Nanomaterials Synthesis, Properties & Applications*. 2004: Imperial College Press.

6.   Khopkar, S.M., *Basic Concept of Analytical Chemistry*. 2009: New Age Science.

7.   Leofantia, G., Padovanb, M., Tozzolac, G. and Venturellic, B., *Catalysis Today,* 1998. **41**, p. 207-219.

8.   Brunauer, S., Emmett, P.H. and Teller, E., *Journal of the American Chemical Society,* 1938. **60**, p. 309.

9.   Brisdon, A.K., *Inorganic Spectroscopic Method*. 1998: Oxford University Press.

10.   Fuller, M.P. and Griffiths, P.R., *Analytical Chemistry,* 1978. **50** (13), p. 1906–1910.

11.   Fifield, F.W. and Kealey, D., *Principles and Practice of Analytical Chemistry*. 2000: Blackwell Science Ltd.

12.   Skoog, D.A., West, D.M. and Holler, F.J., *Fundamentals of Analytical Chemistry*. 7th ed. 1996: Saunders College Publishing.

13.   Hoffmann, E. and Stroobant, V., *Mass Spectrometry: Principles and Applications*. 3rd ed. 2007: John Wiley &Sons , Ltd.

14.   Malr, R.D. and Graupner, A.J., *Analytical Chemistry,* 1964. **36** (1), p. 194-204.

15.   Lopez-Sanchez, J.A., Dimitratos, N., Miedziak, P., Ntainjua, E., Edwards, J.K., Morgan, D., Carley, A.F., Tiruvalam, R., Kiely, C.J. and Hutchings, G.J., *Physical Chemistry Chemical Physics,* 2008. **10**, p. 1921-1930.

16.   Jia, A., Lou, L.-L., Zhang, C., Zhang, Y. and Liu, S., *Journal of Molecular Catalysis A: Chemical,* 2009. **306** (1-2), p. 123-129.

Octane Oxidation using O$_2$

<div style="text-align: right">*3*</div>

1. Introduction

The selective oxidation of alkanes to valuable oxygenated products such as alcohols, aldehydes, carboxylic acids and derivatives has been well studied. However, this stays a real challenge as C-H bond in alkanes molecules are difficult to activate selectively. Alkane oxidation using H_2O_2 have shown interesting results.[1-3] Nevertheless, the use of molecular oxygen is desirable due to its low environmental impact and cost.[4] Kumano and co-worker selectively oxidised cyclohexane to the alcohol and ketone using ruthenium, iron and copper catalysts at room temperature. They used various sources of oxidant including O_2.[5] Theyssen *et al.* used molecular oxygen and acetaldehyde to oxidise various alkane in supercritical CO_2. No catalysts were used and acetaldehyde was acting as a sacrificial co-reducer.[6]

Noble metals catalysts have shown potential for various reactions such as alcohol oxidation.[7, 8] The sol immobilisation method allows the formation of nanoparticles with well controlled size and oxidation state. It has been previously shown that Au-Pd catalysts prepared by sol immobilisation on a carbon support are particularly effective for the oxidation of toluene.[9] The same catalyst has also been reported as effective for the oxidation of methane to methanol using *in situ.* H_2O_2. [10, 11]

The first aim of this project was the oxidation of methane using oxygen by adding methane to the toluene oxidation reaction.

Toluene is often considered as a molecule model for C-H bond activation. A reaction system where O_2 is used for toluene oxidation in combination with supported noble

metals has been reported. Kesavan *et al.* used AuPd supported on C to oxidise toluene what resulted in 94 % conversion and 95 % selectivity for benzyl benzoate at 160 °C.[9] This system has been used with two ideas. First, we reasoned that the activation of toluene by AuPd catalyst could initiate the activation of alkane to form the alcohol; the radical species from toluene oxidation would be able to activate the C-H bond of alkane, especially the primary C-H bond. Second, assuming that the pathway to oxidise toluene involves the formation of benzoic acid, the production of an ester from alcohol and benzoic acid would prevent the over-oxidation of the alcohol.

Benzaldehyde is a reaction product from toluene oxidation. It has previously been used in studies as a sacrificial aldehyde to oxidise various substrates. In presence of oxygen, benzaldehyde formed a peroxy radical species able to initiate other molecules.[12, 13] In principle, the peroxy radical species formed during the oxidation of toluene to benzaldehyde should be able to activate C-H bonds.

In this chapter, the activation of methane using toluene was first investigated. Next, octane oxidation using benzaldehyde as co-oxidant has been studied to prove the concept of co-oxidation. Systematic studies of reaction condition have been carried out in order to determine the best condition for high conversion but also high selectivity for C1 oxygenate. Finally other reactants; alkane and aldehyde, have been tried in order to test the general applicability of the system.

2. Preliminary work: Co-oxidation of methane with toluene

2.1. Coupling reaction with methane and toluene

The addition of methane to the oxidation of toluene by molecular oxygen at 160 °C was investigated. Under these conditions toluene is assumed to be oxidized by a radical mechanism. The products are benzaldehyde, benzoic acid and benzyl benzoate. It was proposed that these radical compounds could initiate the activation of methane (which has also been shown to involve a radical based mechanism).[14] In the presence of oxygen, this activation could lead to the formation of methanol which would subsequently couple with benzyl products to form methyl benzoate as shown in the reaction scheme 3.1
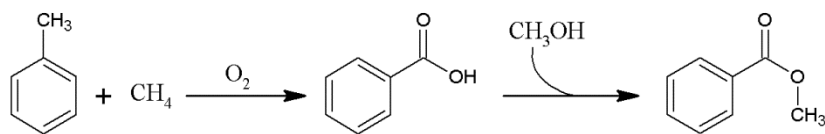
Scheme 3.1: Hypothetic reaction scheme for the coupling methane-toluene

The reaction between methane and toluene was initially investigated under the optimal conditions developed for toluene oxidation: 160 °C and using a 1 wt. % AuPd/ C catalyst prepared by sol immobilisation as describe chapter 2 section 4.1. The limit of flammability of methane in pure oxygen is between 5.1 % and 61 % which constrains to change some conditions; 10 bar total pressure was used for a mixture of methane/ oxygen of 9:1.The analysis sample of this reaction was not diluted in order to detect all products even in small amounts. However, the GC-MS graph in Figure 3.1 didn't show any signal corresponding to the desired product, methyl benzoate.

Figure 3.1: GC-MS spectrum of methane-toluene oxidation with 1 wt. % AuPd/ C and O₂
Reaction conditions: Toluene = 90 mmol, methane = 10 mmol, ratio methane/ oxygen = 9:1, 1 wt. % AuPd/ C = 0.2 g, time = 20 h, temperature = 160 °C, stirring = 1500 rpm

The feasibility of the coupling between methanol and the toluene activated products was tested by omitting the methane and adding methanol into the liquid phase. As previously stated the sample for analysis was not diluted. The experiment between toluene and

methanol under the same conditions (nitrogen instead of methane) showed a GC-MS signal for methyl benzoate as represented in Figure 3.2. This demonstrates the feasibility of coupling methanol with toluene under these conditions. Therefore if methanol was present from the activation of methane, methyl benzoate would be formed. Which proves that methanol is not formed during the methane-toluene reaction, hence methane is not activated under the conditions utilised.
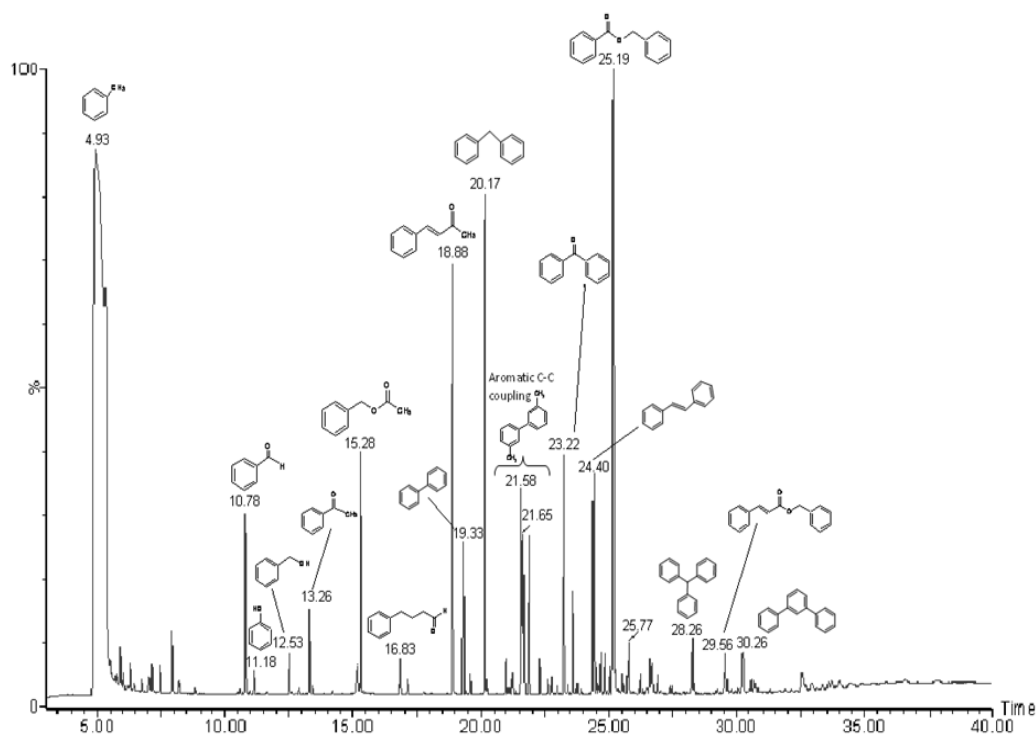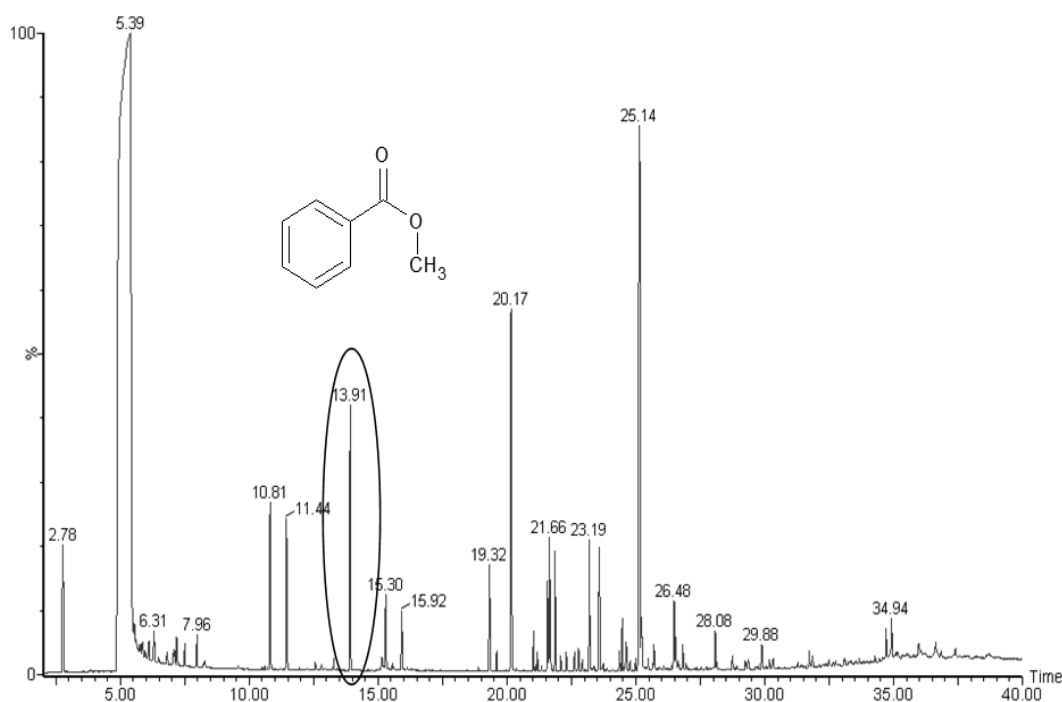

Figure 3.2: GC-MS spectrum of methanol-toluene oxidation with 1 wt. % AuPd/ C and O$_2$

Reaction conditions: Toluene = 90 mmol, methanol = 2 mmol, oxygen = 2 mmol, 1 wt. % AuPd/ C = 0.2 g, time = 20 h, temperature = 160 °C, stirring = 1500 rpm

2.2. Possible mechanism

As shown previously, the coupling of methane and toluene under the reaction conditions utilised is not occurring and ultimately the target product methyl benzoate is not formed. However, other products are formed. These products could come from different coupling reactions between toluene and a number of other species. In the mixture only toluene, methane, oxygen and the catalyst are present. It is known that toluene oxidation can involve a radical mechanism in the presence of TBHP.[15] O$_2$ is a di-radical and could initiate the oxidation of toluene via a radical mechanism. Kesavan *et al.* proposed a

mechanism showing the formation of the direct products of toluene oxidation, benzaldehyde, benzyl alcohol, benzoic acid and benzyl benzoate. This mechanism is represented in scheme 3.2.[9]
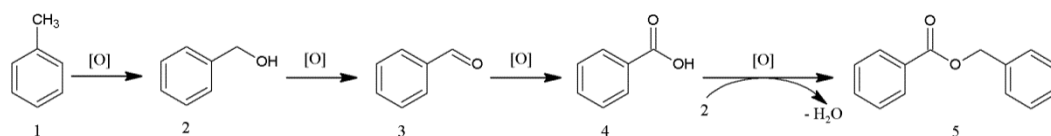
Scheme 3.2: Reaction scheme for toluene oxidation at 160 ºC using O_2 as oxidant

The dissociation of toluene by radical mechanism under certain conditions can give different radical species. The possibility to form phenyl or benzyl radical has been shown theoretically and experimentally where different irradiations were used in order to form these radicals.[16, 17] The possible production of these intermediates can lead to the formation of other molecules present in this work. Schemes 3.3.a-d show hypothetically possible routes forming radical species. The coupling of these species can lead to the formation of different products which were found in this study, for example the formation of biphenyl from benzene radicals shown in scheme 3.3.e.[18] Although radical mechanisms are occurring, other reaction could also occur as shown in scheme 3.3.f; after formation of diphenylmethane a catalytic oxygen transfer allows the formation of benzophenone.[19, 20]
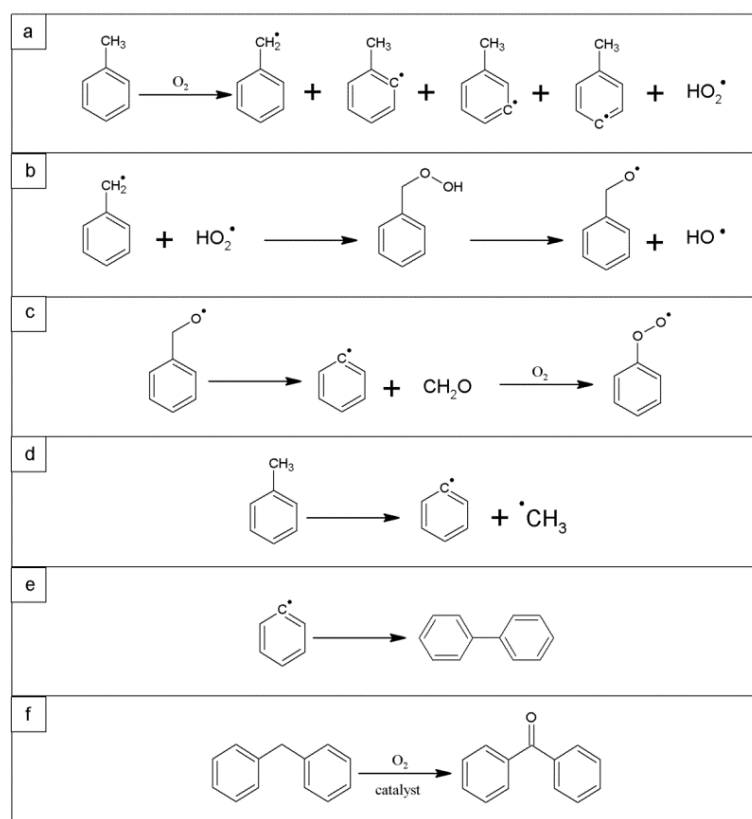
Scheme 3.3: Hypothetic reaction schemes of radicals and products formation from toluene

3. *Co-oxidation of octane*

The activation of methane is known to be very difficult. So as a proof of concept and to find more suitable conditions for coupling the oxidation of alkane, octane was investigated. Under atmospheric condition, octane is in a liquid phase with boiling point 125 ℃ which means that octane will still be in liquid phase in the condition used (until 160 ℃ and 10 bar to 30 bar pressure).[21] Also C-C scission being expected, the variety of products formed by C-C scission will increase with the size of alkane. Hence, the choice of octane was based on the fact that under the highest condition used for this work (160 ℃, 30 bar) octane is the lower alkane which will stay in liquid phase. Giving that, the mixture octane/ oxygen would not be explosive. The oxidation of octane in the presence of toluene was performed, and analysed by GCMS. Figure 3.3 shows only the formation of benzyl benzoate which is the major products of toluene oxidation under similar conditions.[9] The formation of radical species from toluene was expected to activate octane with no success. It can be concluded that octane is not activated in the present work conditions.
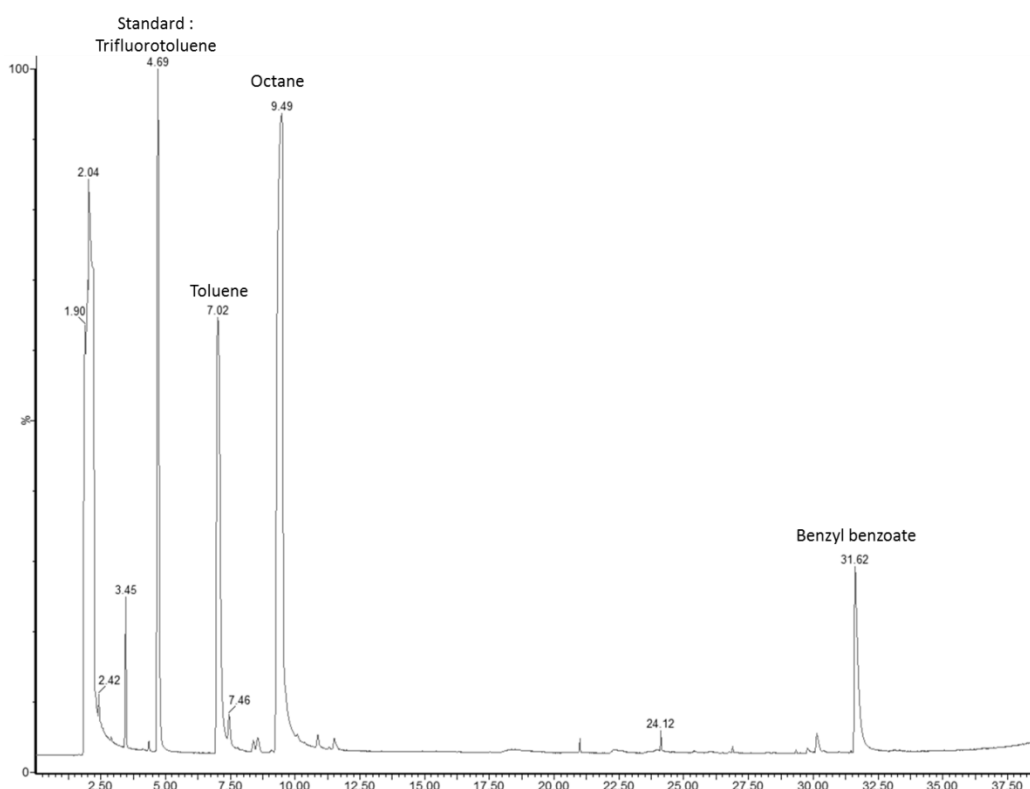
Figure 3.3: GC-MS spectrum of octane-toluene oxidation with 1 wt. % AuPd/ C and O_2

Reaction conditions: Octane = 60 mmol, ratio octane/ toluene = 9:1, 10 bar oxygen, 1 wt. % AuPd/ C = 0.05 g, time = 20 h, temperature = 160 °C, stirring = 1500 rpm

A revised proposal was to investigate benzaldehyde as a co-oxidant for the oxidation of alkane. The oxidation of benzaldehyde to benzoic acid has been shown to occur at a faster rate than the oxidation of toluene to benzoic acid under similar conditions and does not require as high temperature to proceed. Also the oxidation of benzaldehyde to benzoic acid can be initiated by an oxidant like O_2 able to decompose and produce free radical such as perbenzoic acid as intermediate.[22] It was proposed that this intermediate would be able to initiate the oxidation of octane.

From this study the activation of octane to ketones, aldehydes and alcohols was expected as well as the formation of cracking products. Four alcohol's (octan-1-ol, octan-2-ol, octan-3-ol and octan-4-ol) could be formed from this oxidation from the different carbons in the chain. The subsequent coupling between these alcohols and benzoic acid to form four octyl benzoates should follow as shown in scheme 3.4
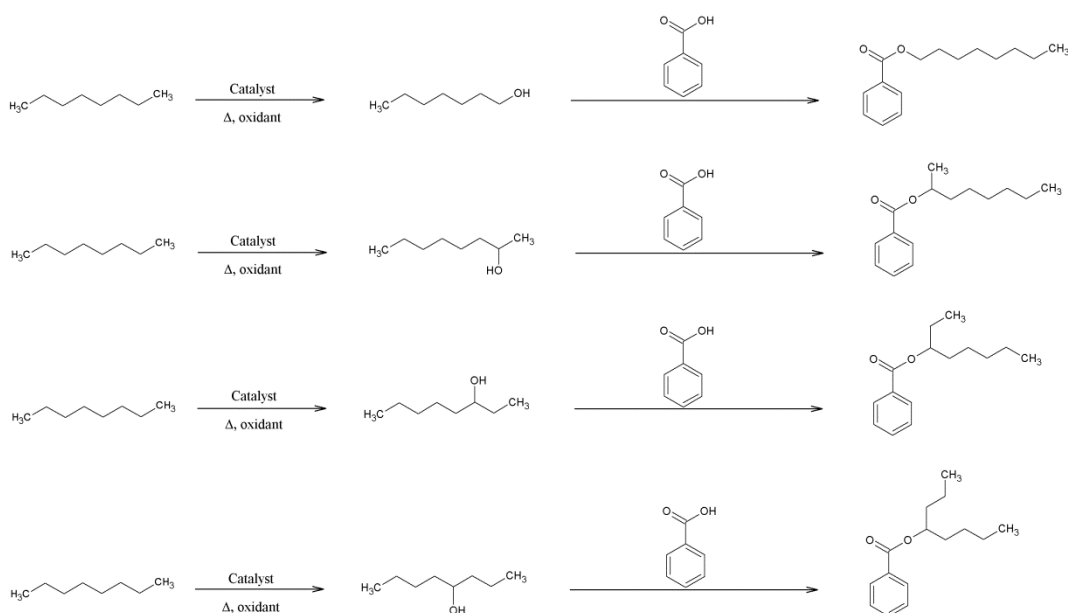
Scheme 3.4: Hypothetic scheme of reaction between octane and benzoic acid

3.1. Proof of concept

3.1.1. Investigation at atmospheric pressure

The first step was to prove the feasibility of the reaction between octane and benzaldehyde. The first set of reactions were done under atmospheric pressure as described in the experimental chapter section 6.1.2, which means the only oxidant would be the oxygen from air. Three different temperatures were tested: 80 °C, 120 °C and 160 °C for 20 h in the presence of catalyst. The GCMS chromatograph is shown in Figure 3.4. At 80 °C and 160 °C the major products are from benzaldehyde oxidation, with octanone being the only product present from the oxidation of octane. However, at 120 °C there is a greater amount of octane oxidation products namely octanone, octanol and two different types of esters. The first esters are alkyl-octanoate, formed from the oxidised cracking products of octane and octanoic acid. The second esters are the target products, octyl-benzoates. At lower and higher temperature a smaller amount of oxidative products (octanol and octanone) are detected. At 80 ℃ this can be explain by the lower activation due to the lower temperature while at 160 ℃ a larger amount of cracking products were detected resulting into a smaller amount of octanol and octanone formed. In both cases, the small amount of target products suggests that condition might not be optimum.
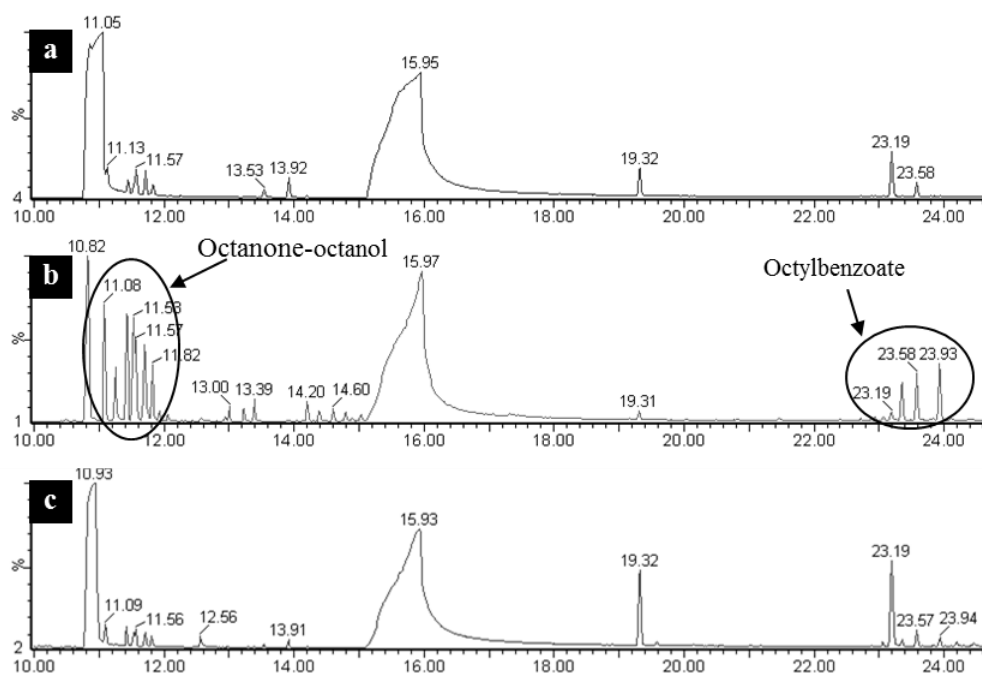
Figure 3.4: GC-MS spectrum of octane oxidation at 80°C (a), 120°C (b) and 160°C (c)
Reaction conditions: Octane = 60mmol, ratio octane/ benzaldehyde = 9:1, atmospheric pressure,
1 wt. % AuPd/ C = 0.05 g

3.1.2. Investigation in autoclave under oxygen pressure

The following reactions were performed under an oxygen pressure in a high pressure autoclave, typically 20 bar unless otherwise stated as described in chapter 2 section 6.1.1. The oxidation of octane was firstly investigated in the absence of a catalyst at 120 °C. The GCMS spectrum in Figure 3.5.a shows the presence of oxidation products, octanone, octanol and alkyl ester. No acid were detected; however, Garcia-Ochoa *et al.* run studies on octane oxidation between 135 °C and 145 °C. They reported the formation of octanol and octanone products but also the presence of smaller acid.[23] Hence, alkyl ester could be the product of a coupling between alcohol and acid coming from cracking products from octane. This suggests that the auto-oxidation of octane occurs at 120 °C or below. The auto-oxidation will be investigated further in the following section.

Subsequently the addition of benzaldehyde was investigated under the same condition as previously used; the result is shown in Figure 3.5.b. In the presence of benzaldehyde the formation of octanol and octanone is still occurring. However, the formation of alkyl esters disappears. This implies that the products to form the alkyl ester were not present in solution. Hence, at least some products from octane were not formed from C-C scission. The presence of benzaldehyde is believed to generate a competition reaction between the oxidation of benzaldehyde and the oxidation of octane. Thus, C-C scission

and oxidation of octane wouldn't occur as much as without benzaldehyde. Hence, at 120 °C information about the effect of benzaldehyde in this system is limited.
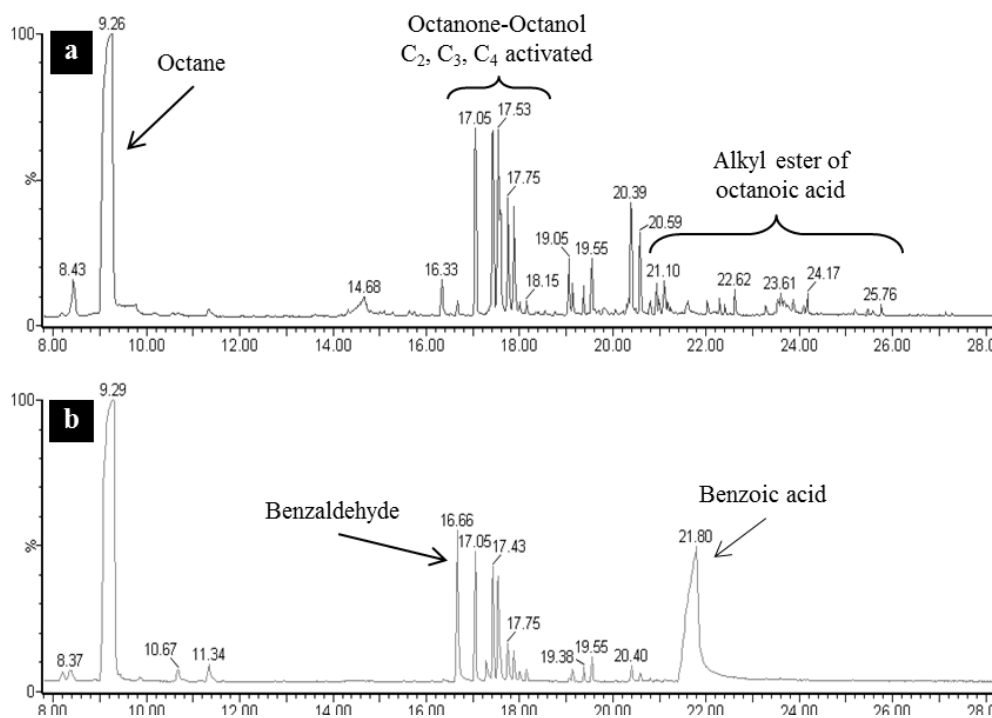
Figure 3.5: GC-MS spectrum of octane oxidation without (a) and with (b) benzaldehyde in absence of catalyst
Reaction conditions: Octane = 60 mmol, ratio octane/ benzaldehyde = 9:1, 10 bar oxygen, temperature = 120 °C, no catalyst

3.2. Octane/ aldehyde/ O_2 system: Preliminary work

3.2.1. Autoxidation of octane and the role of benzaldehyde

From now on all reactions have been performed in an autoclave in order to study the oxidation of octane with molecular oxygen as describe in the experimental chapter section 6.5. Firstly blank reactions, in the absence of benzaldehyde and catalyst, in a range of temperatures between 50 and 120 °C were performed.

Figure 3.6 shows that in the absence of benzaldehyde no products were detected until 80 ℃, at 100 °C the conversion of octane is approximately 1 % going up to 6.5 % at 120 °C. Hence, it is thought the auto-oxidation of octane starts occurring at approximately 100 °C. The products detected were C-C scission products from octane along with the alcohol (1, 2, 3 and 4-octanol) and ketone (2, 3 and 4-octanone).
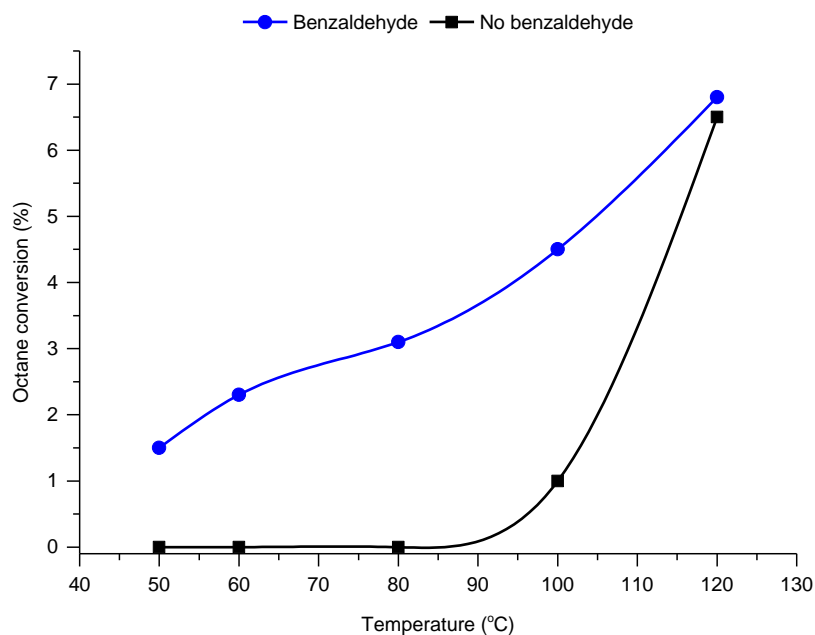
Figure 3.6: Octane conversion for the oxidation of octane with and without benzaldehyde in absence of catalyst at various temperatures
Reaction conditions: Octane = 60 mmol, ratio octane/ benzaldehyde = 9:1, 10 bar oxygen, no catalyst

This range of temperature was then tested with the addition of benzaldehyde in the reaction and compared to the previous results. At 50 °C, 1.5 % of octane was converted going up to 6.8 % at 120 °C. The addition of benzaldehyde to the octane oxidation reaction at low temperatures initiates the activation of octane. At higher temperature, the conversion of octane is similar in the presence or absence of benzaldehyde. However, the selectivity for oxygenated and target products increases. Figure 3.7 shows the amount of octanol-octanone and octylbenzoate products. From 50 ºC to 80 ºC the formation of octanol and octanone decreases slightly then increases with temperature, 28 % of the octane converted forms octanone/ octanol at 80 °C, rising to 45 % at 120 °C. The formation of octyl benzoate is first seen at 100 °C and increases with temperature. At lower temperature the formation of the ester would be slower due to the smaller amount of octanol produced.

The presence of benzaldehyde in the system allows the activation of octane from 50 ºC and the formation of octylbenzoate. As seen previously in this section, the mixture benzaldehyde/ O₂ can form benzyl peroxide. This suggests that in absence of catalyst, this system is able to activate octane.
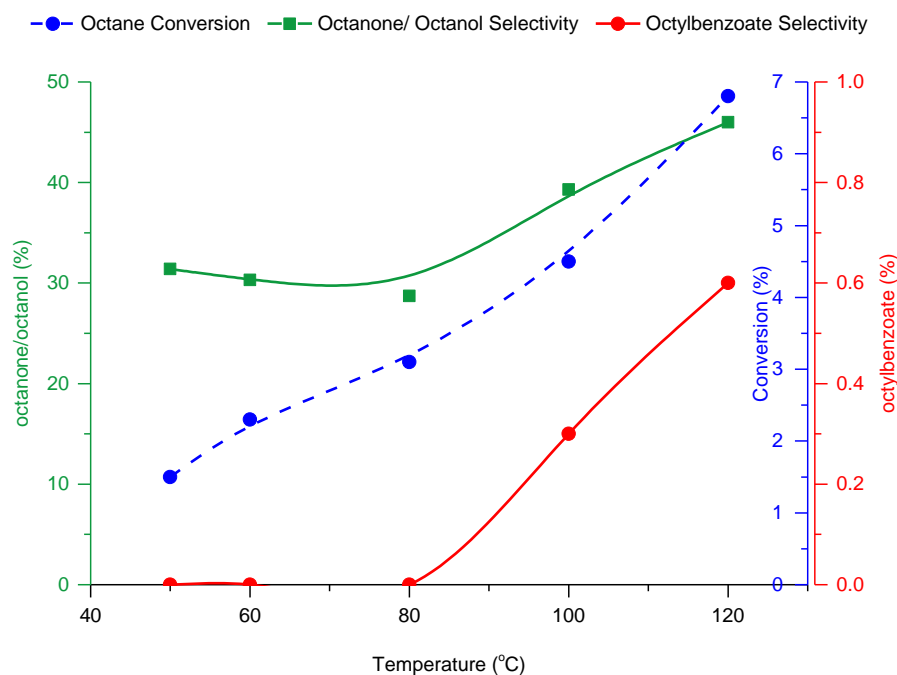
Figure 3.7: Products of oxidation of octane in presence of benzaldehyde at different temperature

Reaction conditions: Octane = 60 mmol, ratio octane/ benzaldehyde = 9:1, 10 bar oxygen, no catalyst

3.2.2. Addition of catalyst

The oxidation of octane with molecular oxygen was then studied in the presence of catalyst at 80 ºC. Under these conditions without catalyst we observed a conversion of 3.1 % with the formation of oxygenated products but no formation of the target ester, octyl benzoate. 1 wt. % AuPd/ C prepared by sol immobilisation is known to activate oxygen for toluene oxidation reaction at 160 ºC and under 10 bar O$_2$.[9] Hence, this catalyst was used for the present reaction.

The catalyst was characterised using XPS, the data concerning binding energies and surface atomic metal ratios are presented in Table 3.1.The measured binding energies of Au and Pd indicate that the metal is in the zero-valent state, i.e. all the nanoparticles are metallic in nature. XPS data also shows that this catalyst has a surface atomic ratio Pd/Au of 1.39. This value confirms the higher amount of Pd atoms than Au atoms as expected. The ratio Pd/Au has been chosen from Kesavan *et al.* studies where it is shown the atomic ratio Pd/Au = 1.85, corresponding to a weight ratio Pd/Au = 1, has the best activity.[9]

Table 3.1: XPS surface compositional data from Au–Pd catalysts supported on C

Catalyst	Binding energy (eV)*		Surface content (Atom %)		Ratio Pd/Au
	Au $4f_{7/2}$	Pd $3d_{5/2}$	Au $4f_{7/2}$	Pd $3d_{5/2}$	
1 wt. % AuPd/ C	83.6	334.8	0.81	1.53	1.39

*All binding energies referenced to C 1s = 284.7 eV.

Au-Pd/ C bimetallic samples were also examined by STEM analysis as shown in Figure 3.8. Figure 3.9 presents the particles size distribution. The metal particle size ranged between 1 and 10 nm with a mean value of 3.7 nm. Nanoparticles size has an effect on the catalytic activity. It has been reported that small nanoparticles show great activity; Goodman and co-workers showed that the catalyst activity for CO oxidation using Au cluster supported on TiO_2 reaches the highest activity with particle size of 3.5 nm.[24]
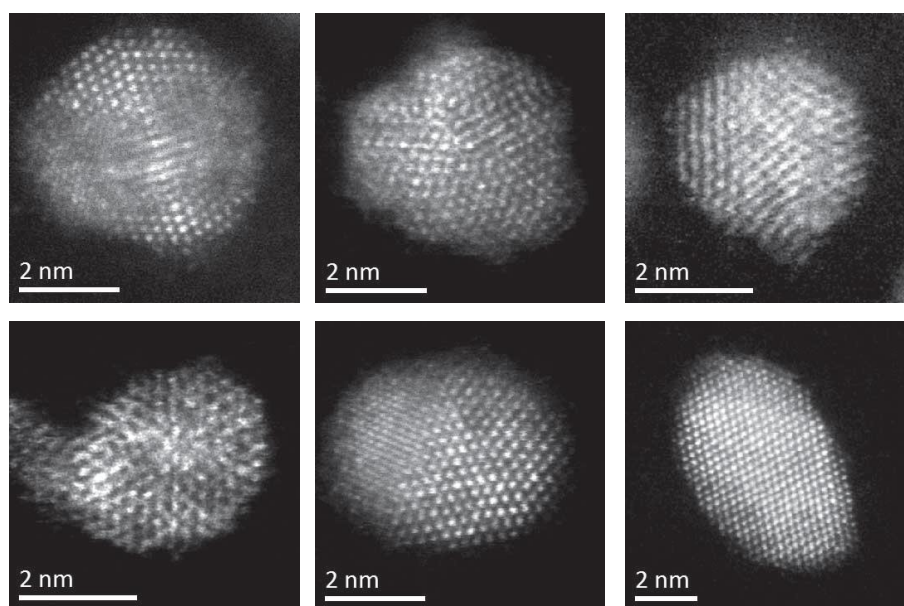
Figure 3.8: Representative STEM HAADF of Au-Pd nanoparticles in the 1 wt. % Au-Pd/ C sol-immobilized sample (Image from reference [9])
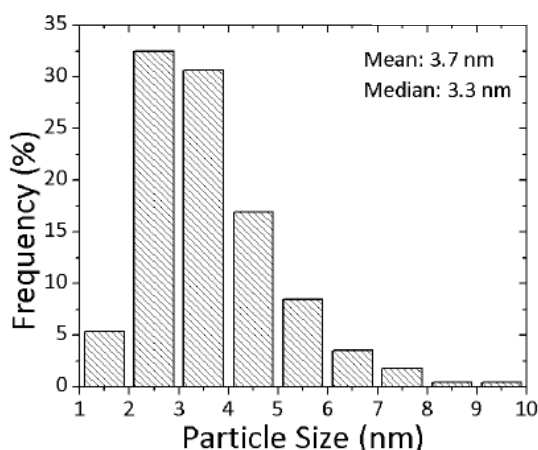
Figure 3.9: Particle size distributions for sol–immobilized 1 wt. % AuPd/ C (Image from reference [9])

The addition of 1 wt. % AuPd/ C catalyst to the reaction mixture increased the formation of products (octanone, octanol). The conversion of octane goes up to 5 % and octyl benzoate is formed albeit at a low level, selectivity 0.7 %, as shown in Table 3.2. A reaction in the absence of benzaldehyde with catalyst was run to confirm the role of benzaldehyde. No products were detected confirming that benzaldehyde is necessary to oxidise octane at 80 ℃.

The presence of benzaldehyde and catalyst combined allows the activation of octane at 80 ℃ increasing the conversion, as well as helping to control the selectivity to oxygenated C$_8$ products and octylbenzoate.

Table 3.2: Oxidation of octane in presence of benzaldehyde at 80 °C with and without catalyst

	octane conversion %	octylbenzoate selectivity %	Octanol/octanone selectivity %
no catalyst	3.1	–	29
1 wt. % AuPd/ C	5	0.7	58

Reaction conditions: Octane = 60 mmol, ratio octane/ benzaldehyde = 9:1, 10 bar oxygen, 1 wt. % AuPd/ C = 0.05 g, time = 20 h, temperature = 80 °C, stirring = 1500 rpm

4. *Octane/ benzaldehyde/ O_2 system: Investigation of reaction conditions*

The basic conditions to activate octane and control the selectivity were found in the previous sections of this chapter. Reaction parameters were subsequently varied including catalyst mass, oxygen pressure, reaction time and reaction temperature, in order to gain a greater understanding of the system. Typically the standard conditions were: 20 bar of O_2 pressure, 80 ℃, 20 h reaction and 0.05 g catalyst.

4.1. Effect of oxygen pressure PO_2

The effect of pressure is shown in Figure 3.10. From 10 bar to 30 bar O_2 pressure, the conversion increases from 4.6 % to 8.4 %. This indicates that the increased solubility of oxygen in octane, with increased pressure, allows the reaction to occur at a greater rate. For oxygen pressures above 20 bar the selectivity to oxygenated products decreases while the conversion increases indicating a higher formation of products from C-C bonds scission. The selectivity towards octylbenzoate decreases slightly as a function of the pressure.

Figure 3.10: Effect of pressure for octane oxidation

Reaction conditions: Octane = 60 mmol, ratio octane/ benzaldehyde = 9:1, **10 bar to 30 bar oxygen**, 1 wt. % AuPd/ C = 0.05 g, time = 20 h, temperature = 80 °C, stirring = 1500 rpm

The formation of octylbenzoate is depending on octanol which also decrease with pressure. Increasing the pressure of O_2 would increase the total number of molecules (octane, benzaldehyde and O_2) in the liquid phase. Hence, increase the number of molecule will increase the collision which could involve the C-C scission of octane.

4.2. Effect of catalyst mass

Increasing the amount of catalyst should increase the amount of active sites, therefore causing an increase in conversion. In fact the conversion of octane increases from 5 % to 7.7 % as the mass of catalyst is increased as shown in Figure 3.11. The selectivity towards oxygenates decreases while the formation of smaller alkanes and smaller oxygenated products increases. No change in the amount of octylbenzoate can be seen.

The increase in conversion confirmed the presence of higher number of active sites due to higher amount of catalyst. However, increasing the activity decreases the selectivity towards the target products octylbenzoate and C-C scission increases. This indicates that the active sites are not only specific for the oxidation of the C-H bond, but also are active to break C-C bonds.

Figure 3.11: Effect of catalyst mass for octane oxidation

Reaction conditions: Octane = 60 mmol, ratio octane/ benzaldehyde = 9:1, 10 bar oxygen, **1 wt. % AuPd/ C = 0.05 g to 0.2 g**, time = 20 h, temperature = 80 °C, stirring = 1500 rpm

4.3. Effect of temperature

As a next part of experimental investigation, the effect of temperature has been studied. Temperature was increased until 160 ℃ as shown in Figure 3.12. The conversion increases to a maximum of 24 % at 140 ℃. However, 140 ℃ is high enough temperature to activate octane and a higher temperature does not increase conversion. C-C scission increased at higher temperature corresponding to oxygenate product selectivity dramatically decreasing from 58 % to 15 %. However, after 140 ℃ the selectivity for octylbenzoate increased to 12 % suggesting the need of heat to increase the rate of ester formation.

In the case of these reactions two possibilities could explain the increase of ester formation. Either the formation of ester between octanol and benzoic acid depends on the temperature or the temperature has an effect on other parameters (acidity for instance) which would indirectly increase the rate of ester formation. Further investigation on the kinetic could be useful to understand the mechanism of reaction.
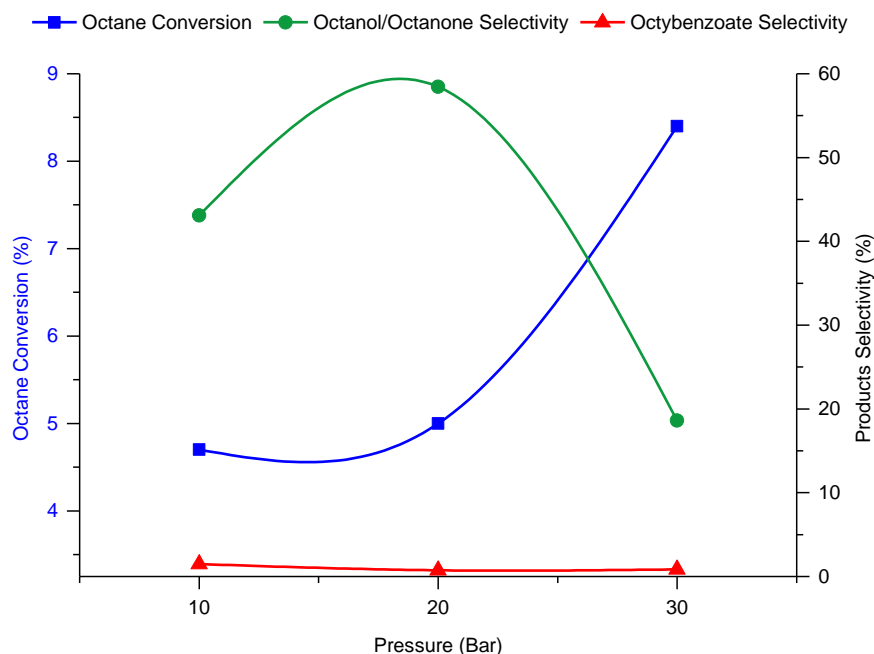

Figure 3.12: Effect of temperature for octane oxidation

Reaction conditions: Octane = 60 mmol, ratio octane/ benzaldehyde = 9:1, 10 bar oxygen, 1 wt. % AuPd/ C = 0.05 g, time = 20 h, **temperature = 80 °C to 160 °C**, stirring = 1500 rpm

4.4. Time online study

The effect of reaction time (1 h to 72 h) was subsequently investigated. Figure 3.13 shows that octane conversion increased with time reaching a maximum of c.a. 6.5 %. However, the reaction rate seems to decrease. This result may be due to deactivation of the catalyst. The formation of octanol and octanone increases until 24 h, increasing reaction time further decreases the selectivity to octanone and octanol whilst a greater amount of octylbenzoate is formed. With time the amount of cracking products increases at a faster rate than the amount of oxygenated products. The GC spectra of the gas phase shows an increasing signal for butane and the liquid phase an increase of alkyl benzoates especially C$_3$, C$_4$ and C$_5$.
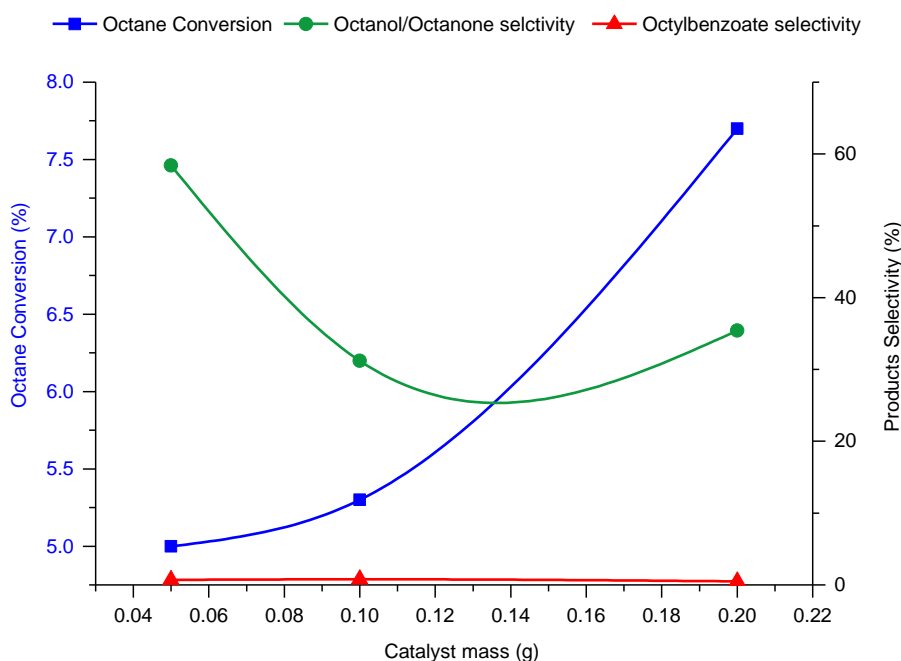

Figure 3.13: Effect of time for octane oxidation

Reaction conditions: Octane = 60 mmol, ratio octane/ benzaldehyde = 9:1, 10 bar oxygen, 1 wt. % AuPd/ C = 0.05 g, **time = 1 h to 72 h**, temperature = 80 °C, stirring = 1500 rpm

The selectivity for octanol/ octanone seems to decrease while the selectivity for smaller alkane and octyl benzoate increases. The bonds scission can come from C-C bond breaking of octane but also from bond breaking from oxygenates which could also explain the drop in the amount of oxygenates. Octylbenzoate comes from the coupling between an octanol molecule and benzoic acid; the rate of formation of an ester can be promoted by many ways such as temperature and acidic environment.[25] Hence the deactivation of the catalyst could occur while the ester will still be formed. It can be

assumed in this case that with catalyst deactivation the conversion for octane to oxygenated products is decreased; however, the formation of octylbenzoate and the C-C breaking being independent of the presence of catalyst continue to occur.

Figure 3.14 shows benzaldehyde conversion and benzoic acid selectivity depending on time. Rapidly the conversion of benzaldehyde reaches 98 % with a high selectivity for benzoic acid. However, this selectivity never reaches 100 % due to the benzoic acid used in the formation of the esters alkyl benzoate.

As seen previously the first product of the oxidation of benzaldehyde is not benzoic acid but perbenzoic acid.[22] This specie is a radical which could also react to couple with the alkanes present. Peroxide species being instable react quickly to form other molecules until a non-radical is reached. Hence, peroxide species are difficult to isolate and quantify. Radical trap could be use in order to detect the species formed in function of time. Benzaldehyde is mostly consumed after 7 h while octane conversion continues to increase. Benzaldehyde is not directly responsible of octane oxidation. Hence, a turnover of peroxy and radical species in the mixture are activating octane.
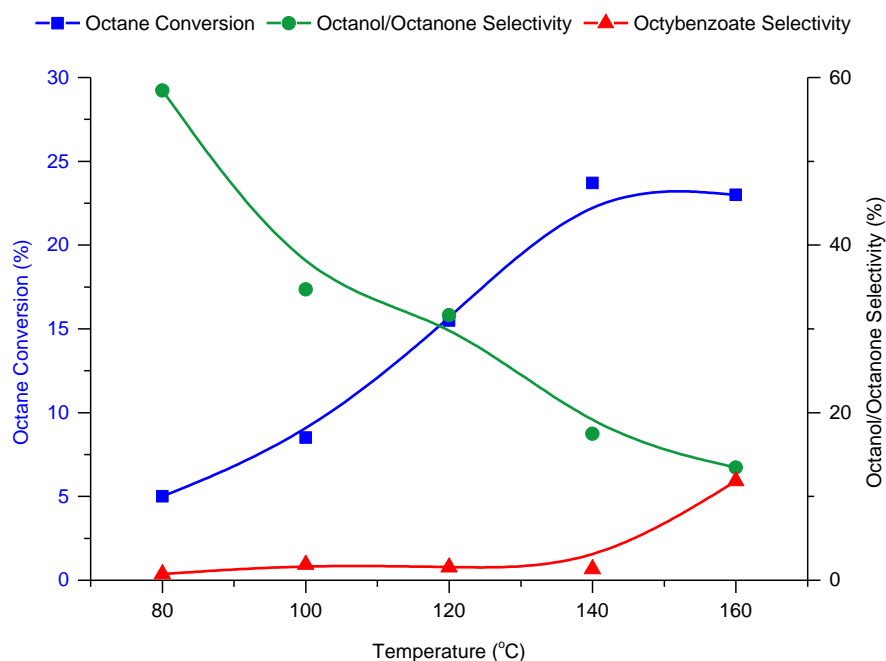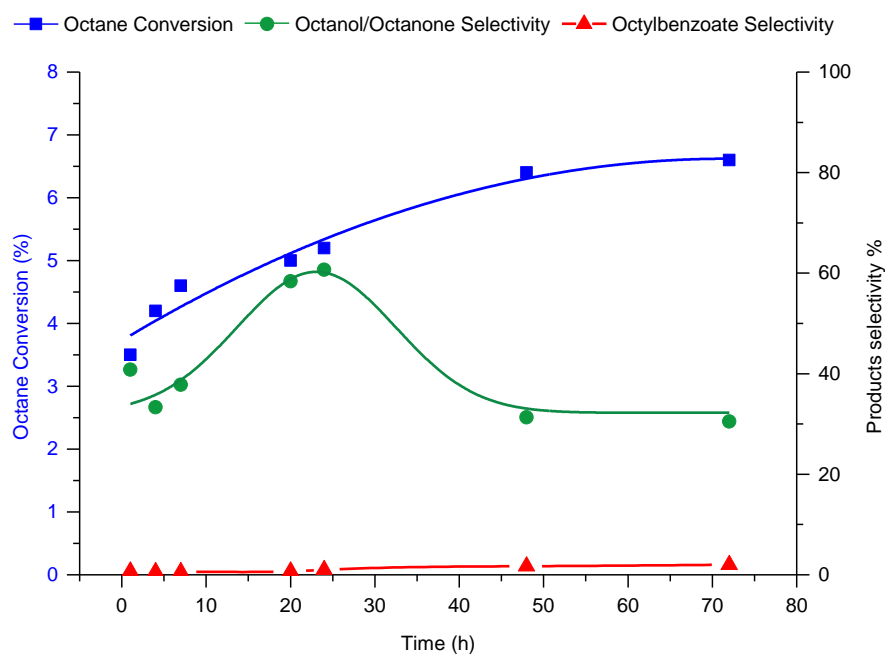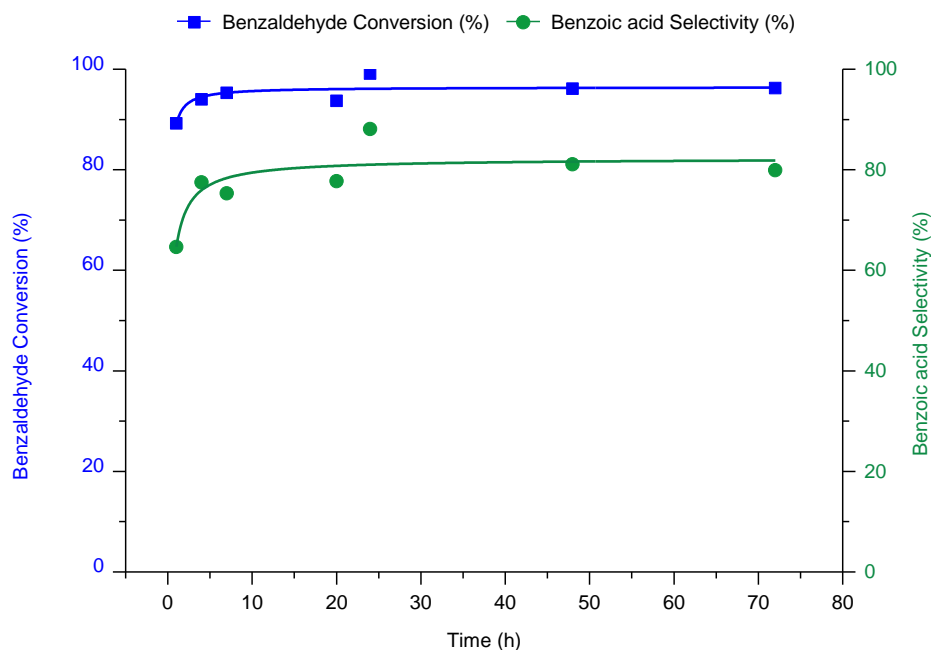

Figure 3.14: Effect of time for benzaldehyde conversion

Reaction conditions: Octane = 60 mmol, ratio octane/ benzaldehyde = 9:1, 10 bar oxygen, 1 wt. % AuPd/ C = 0.05 g, **time = 1 h to 72 h**, temperature = 80 °C, stirring = 1500 rpm

4.5. Conclusion on the reaction conditions

Reaction conditions have been changed in order to understand the effect of pressure, catalyst mass, temperature and time on the reaction. In general with an increasing of these conditions the conversion of octane increases. The selectivity towards oxygenated products tends to decrease whereas for octylbenzoate time and temperature increase their selectivity.

A general trend is the higher formation of cracking products from octane with increasing conversion. Hence, the selectivity for oxygenates decreases. However, the amount of moles of products does not decrease or only slightly which cannot explain the drop of selectivity. One possibility is that oxygenates can still be produced with higher conversion but can also be cracked. Formation and scission of oxygenates may not have the same kinetic mechanism which could explain why there is no direct relation between the amount of products and their selectivity.

The formation of octylbenzoate shows the proposed coupling between octanol and benzoic acid. This coupling prevents over oxidation of the alcohol to aldehyde or ketone by blocking the alcohol site. A subsequent hydrolyse of the ester, octylbenzoate in this case, would generate the desired alcohol.

It can be concluded that benzaldehyde plays two roles; first it can initiate the oxidation of octane from low temperature (50 ℃). The second role is to oxidise to benzoic acid which subsequently couples with octanol to form octylbenzoate, thus protecting the alcohol from over-oxidation and C-C scission.

5. *Generalise the concept*

The concept to couple octane with benzaldehyde has been proved. Octanol, the product of octane oxidation and target molecule of this study can be coupled with benzoic acid, the oxidation product of benzaldehyde. It is known that benzaldehyde is easily oxidised to acid, and often, in the presence of molecular O_2, is used to commence reactions.[22] In fact different research groups reported activation of various substrates due to the mixture aldehyde/ O_2. The oxidative desulfurisation of dibenzothiophene have been successful using this system; Garg and co-workers used isobutyraldehyde, [12] octanal have been used by Dumont *et al.*, [26] while Murata *et al.* used different aldehyde showing the general application of this system.[13] The oxidation of organic molecules has also been reported using the system aldehyde/ O_2 by Ishii and co-workers.[27] The following

experiments were performed using different aldehydes and different alkanes to prove the general applicability of the concept.

5.1. Other aldehydes

Formaldehyde, butanal and propanal was investigated in the oxidation of octane under the same conditions; the results are shown in Figure 3.15. In the case of formaldehyde no products were detected. It is believed that formaldehyde did not initiate the oxidation of octane, due to the formaldehyde being in the gas phase under the reaction conditions utilised. The boiling point of formaldehyde is -19 °C,[28] and at 80 °C even under 20 bar pressure, formaldehyde is in the gas phase whilst octane is in the liquid phase. This does not allow any significant interaction between the aldehyde and octane in order to initiate the oxidation. In the presence of propanal and butanal oxidation products from octane were observed. The formation of the ester, octylpropanoate and octylbutanoate were detected. These experiments indicate that the system aldehyde/ O_2 can be applied using other aldehyde instead of benzaldehyde as long as they are in the same phase.
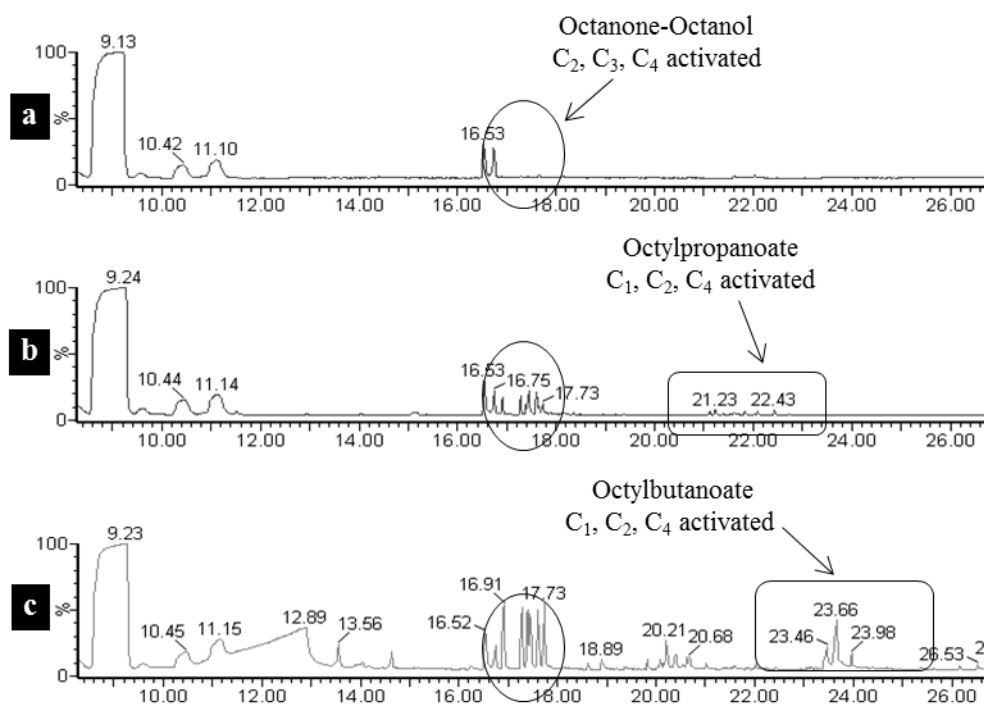
Figure 3.15: GC-MS spectra of octane co-oxidation with (a) formaldehyde, (b) propanal and (c) butanal
Reaction conditions: Octane = 60 mmol, ratio octane/ benzaldehyde = 9:1, 10 bar oxygen, 1 wt % AuPd/ C = 0.05 g, time = 20 h, temperature = 80 °C, stirring = 1500 rpm

5.2. Other alkanes

Oxidation of other alkanes in presence and absence of benzaldehyde was further investigated in order to prove the general applicability of the co-oxidant. Since shorter alkanes under given reaction conditions can be explosive, higher alkanes were chosen for oxidation reactions. Hence, decane, dodecane and cyclooctane were tested. In every instance the GC-MS chromatogram, Figure 3.16, showed the presence of oxidation products which were not present in the absence of benzaldehyde. A small amount of ester has also been detected. All these reactions show that in the presence of benzaldehyde, octane and higher alkane can be oxidized under these conditions. Hence the system benzaldehyde/ O₂ is applicable but the general applicability is not proved as under these conditions smaller alkane cannot be tested. Further investigation would be essential in order to check the applicability for lower alkane.
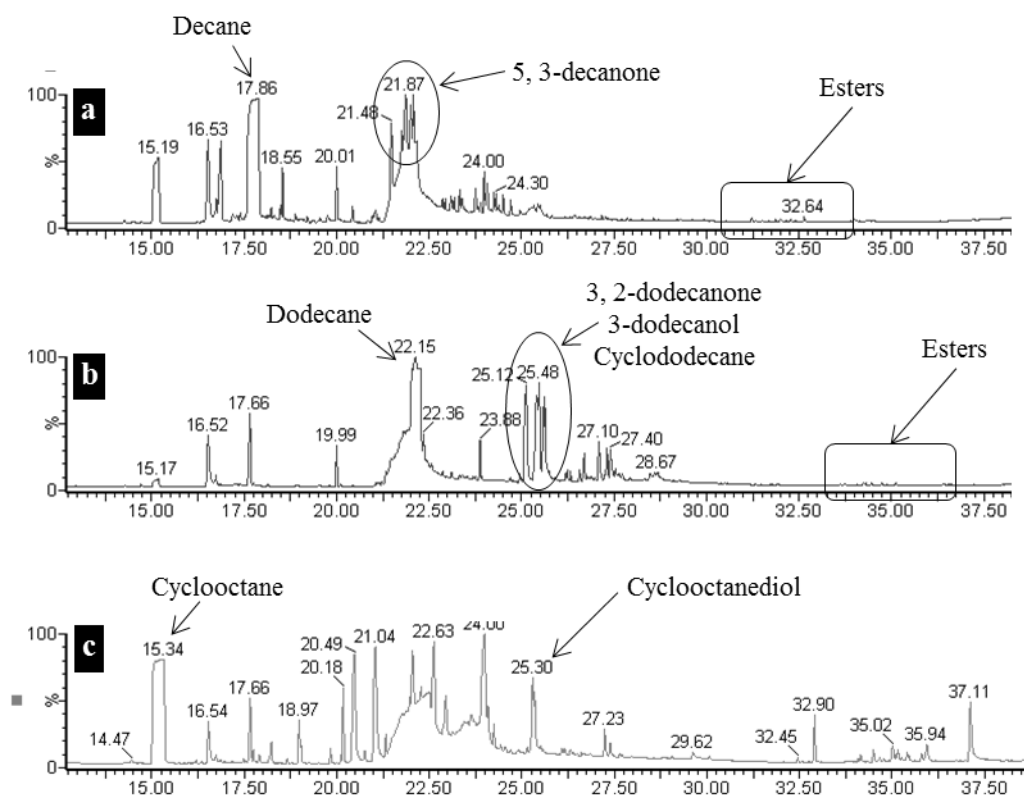
Figure 3.16: GC-MS spectra of (a) decane, (b) dodecane and (c) cyclooctane co-oxidation with benzaldehyde
Reaction conditions: Octane = 60 mmol, ratio octane/ benzaldehyde = 9:1, 10 bar oxygen, 1 wt. % AuPd/ C = 0.05 g, time = 20 h, temperature = 80 °C, stirring = 1500 rpm

5.3. Back to the initial concept

The original concept was to oxidise an alkane using toluene. The radical species from toluene oxidation would be able to activate the alkane and form the corresponding alcohol. This alcohol could then couple with benzoic acid (oxidation product from toluene) in order to form the ester. Hence, overoxidation of alcohol would be prevented. In a first attempt, a system toluene/ O$_2$/ methane has been investigated with no success. The modification of the alkane and the co-oxidant; benzaldehyde instead of toluene, has been successful. The use of other aldehydes also showed the possibility to activate octane. Next section is about integrating toluene and methane in the previous system.

5.3.1. Co-oxidation of octane using toluene/ propanal/ O$_2$ system

Benzaldehyde allows octane oxidation in the presence of 1 wt. % AuPd/ C catalyst at 80 ℃. This catalyst is the most active one for the oxidation of toluene.[9] Toluene is generally oxidised into four different products including benzaldehyde. The experiment trying the oxidation of octane with toluene in exactly same condition did not show any products.

It has been shown that octane could be co-oxidised in the presence of other aldehydes, propanal and butanal. Hence, propanal was added in this last reaction. The idea was to activate octane in the presence of toluene and an aldehyde. Kesavan *et al.* showed that under these conditions less than 1% of toluene can be oxidised.[9] However, the aldehyde present could initiate octane but also toluene. Then the formation of octanol could couple with benzoic acid formed from the oxidation of toluene.
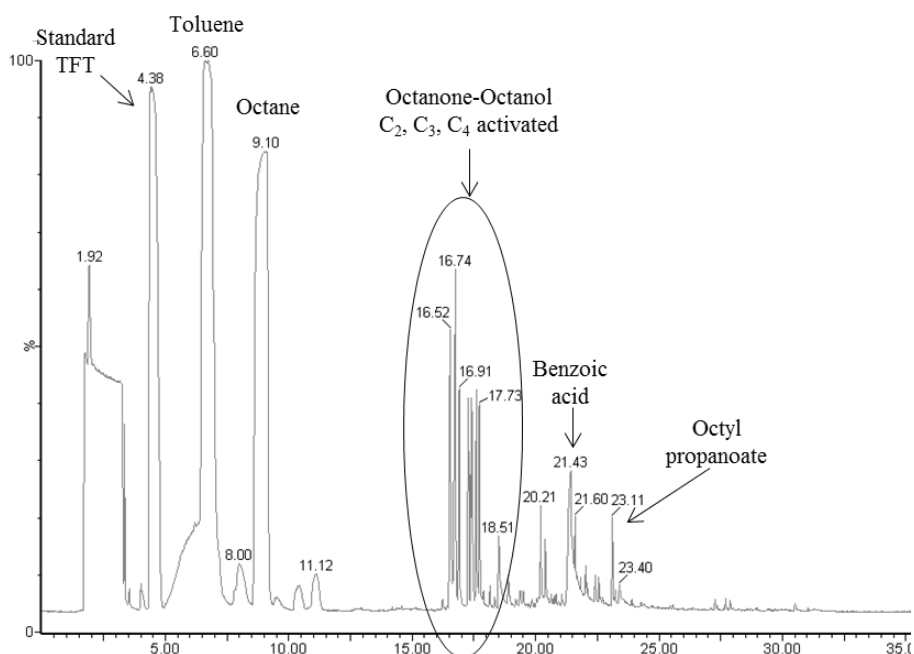
Figure 3.17: GC-MS spectra of octane co-oxidation with toluene and propanal

Reaction conditions: octane = 30 mmol, ratio octane/ toluene = 1:1, ratio octane + toluene/ propanal = 9:1, 10 bar oxygen, 1 wt. % AuPd/ C = 0.05 g, time = 20 h, temperature = 80 °C, stirring = 1500 rpm

Figure 3.17 shows the presence of oxygenated products from octane (octanol and octanone) and toluene (benzaldehyde and benzoic acid). The oxidation product of octane was expected as octane oxidation is initiate by propanal. The ester octyl propanoate was also formed. It seems that propanal is also initiating the oxidation of toluene. However, octylbenzoate was not detected. Suggesting that ester formation between propanoic acid and octanol is more favourable than with benzoic acid, unless the formation of the ester is going from the peroxide species instead of the acid. In this case, the ester would not be formed by a standard esterification mechanism but by a radical mechanism. The mixture aldehyde/ O₂ would form the peroxy radical. This specie would activate the alkane and form the ester without the need of the alcohol and acid.

5.3.2. Co-oxidation of methane using aldehyde/ O₂ system

At the beginning of this study methane was the first alkane investigated which was not activated in the presence of toluene. After exploring the reaction system using octane and benzaldehyde and showing that octyl benzoate could be formed, a further attempt was made with methane as the target molecule to oxidise. Under the conditions found previously for octane, lower alkanes cannot be tested due to the explosive limit of the

mixture alkane/ O$_2$. Hence the reaction with methane was performed with water as solvent. The general conditions stay similar; 1 wt. % AuPd/ C = 0.05 g, time = 20 h, temperature = 80 °C, stirring = 1500 rpm. The ratio methane: benzaldehyde was kept at 9:1 and the mixture of gas was methane 20 % and air 80 %. (20 bar pressure, methane = 4 mmol)

Benzaldehyde is oxidized to benzoic acid but methane is not activated as no product from methane was observed. Methane is known to be a very stable molecule and these conditions do not permit the activation of methane. Few papers report the oxidation of methane using H$_2$O$_2$.[29, 30] Hence methane is activated by peroxide species; however, the presence of an activating catalyst is essential. This shows that the C-H bond of methane cannot be modelled on the C-H bond of octane in the co-oxidation system used in this study. However, further investigation keeping this system could be done. Usually the system aldehyde/ O$_2$ is used to activate a substrate and the ratio aldehyde: substrate is superior to the one use in this work, in this case the aldehyde is called "sacrificial aldehyde".[12, 13, 26, 27] It could be possible to use benzaldehyde as solvent instead of water which should be in sufficient amount to act like a sacrificial aldehyde.

6. Conclusions

The co-oxidation of alkane has been studied in this chapter in order to activate the C-H bond of alkanes. The co-oxidant role would be to promote the activation of the alkane but also be used to couple with the primary oxygenate product from the alkane to prevent overoxidation. A system using methane and toluene was first investigated with no success. However, the same reaction with the corresponding alcohol shows the formation of the ester indicating that the role of toluene to prevent the overoxidation of alcohol is working. Nevertheless, toluene is not activating the C-H bond from the alkane. Aldehyde was then tried instead of toluene with success and the reaction conditions have been improved demonstrating the feasibility of the concept. An aldehyde is able to activate an alkane at low temperature and in the presence of a green oxidant, molecular O$_2$. This concept was then further developed using range of aldehydes and alkanes showing the generality of this reaction as long as the conditions stay the same. The addition of propanal to a toluene/ O$_2$ system activates octane but does not permit the ester formation from toluene and octane. Methane activation was finally tried without success.

This study has been based on work done on toluene oxidation. In the presence of 1 wt. % AuPd/ C toluene could form benzyl benzoate with a very high selectivity. It was assumed that the way to form benzyl benzoate was going through the formation of benzyl alcohol, benzaldehyde and benzoic acid.[9] Sankar *et al.* showed that the formation of benzoic acid from benzaldehyde oxidation with oxygen was quenched in the presence of benzyl alcohol by inhibiting the formation of perbenzoic radical.[31] Hence, toluene is oxidised into benzyl benzoate by another pathway where benzoic acid is not formed as shown in scheme 3.5. This explains why this concept of co-oxidation cannot occur with toluene but can with benzaldehyde as benzyl alcohol is not present.

In the current study aldehyde was not in large excess but the main role of the aldehyde was also to form a peroxide species which would activate the wanted reaction. The aim to activate alkane in the presence of a co-catalyst was reached with high alkane chain ($> C_8$). However, using benzaldehyde as a "sacrificial aldehyde" in the usual condition (larger excess of benzaldehyde) could improve the reaction. Further investigations such as the use of different co-catalysts or catalysts have to be done to increase the conversion and selectivity as well as improving conditions in order to use smaller alkane chains.
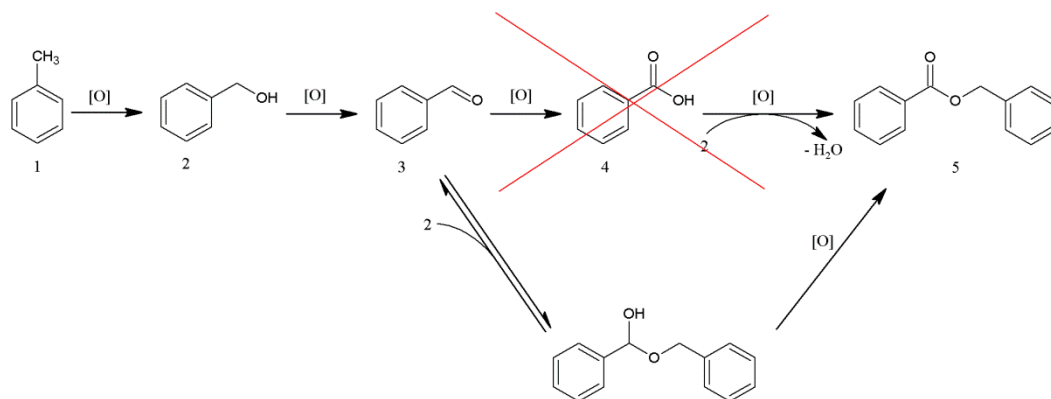
Scheme 3.5: Revised reaction scheme for toluene oxidation at 160 ºC using O$_2$ as oxidant (From reference [9])

7. *References*

1.   Monfared, H.H. and Amouei, Z., *Journal of Molecular Catalysis A: Chemical,* 2004. **217** (1-2), p. 161-164.

2.   Das, S., Bhowmick, T., Punniyamurthy, T., Dey, D., Nath, J. and Chaudhuri, M.K., *Tetrahedron Letters,* 2003. **44** (26), p. 4915-4917.

3.	Hammond, C., Dimitratos, N., Jenkins, R.L., Lopez-Sanchez, J.A., Kondrat, S.A., Hasbi ab Rahim, M., Forde, M.M., Thetford, A., Taylor, S.H., Hagen, H., Stangland, E.E., Kang, J.H., Moulijn, J.M., Willock, D.J. and Hutchings, G.J., *ACS Catalysis,* 2013. **3** (4), p. 689-699.

4.	Gallezot, P., *Catalysis Today,* 1997. **37**, p. 405-418.

5.	Murahashi, S.-I., Komiya, N., Hayashi, Y. and Kumano, T., *Pure Appl. Chem.,* 2001. **73** (2), p. 311-314.

6.	Theyssen, N., Hou, Z. and Leitner, W., *Chem. Eur. J.,* 2006. **12**, p. 3401-3409.

7.	De Vos, D.E. and Sels, B.F., *Angewandte Chemie,* 2004. **44** (1), p. 30-2.

8.	Bond, G.C., Louis, C. and Thompson, D.T., *Catalysis by Gold*, in *Catalytic Science Series*, G.J. Hutchings, Editor. 2006, Imperial College Press: London.

9.	Kesavan, L., Tiruvalam, R., Ab Rahim, M.H., bin Saiman, M.I., Enache, D.I., Jenkins, R.L., Dimitratos, N., Lopez-Sanchez, J.A., Taylor, S.H., Knight, D.W., Kiely, C.J. and Hutchings, G.J., *Science,* 2011. **331** (6014), p. 195-199.

10.	Carley, A.F., Dimitratos, N., Hutchings, G.J., Jenkins, R.L., Rahim, H.A.B., Lopez-Sanchez, J.A., Taylor, S.H. and Willock, D.J. *Hydrocarbon Selective Oxidation with Heterogenous Gold Catalysts*. W.I.P. Organization 2011. WO 2011/051642 A1

11.	Ab Rahim, M.H., Forde, M.M., Jenkins, R.L., Hammond, C., He, Q., Dimitratos, N., Lopez-Sanchez, J.A., Carley, A.F., Taylor, S.H., Willock, D.J., Murphy, D.M., Kiely, C.J. and Hutchings, G.J., *Angewandte Chemie,* 2013. **52** (4), p. 1280-4.

12.	Rao, T.V., Sain, B., Kafola, S., Nautiyal, B.R., Sharma, Y.K., Nanoti, S.M. and Garg, M.O., *Energy anf Fuels,* 2007. **21**, p. 3420-3424.

13.	Murata, S., Murata, K., Kidena, K. and Nomura, M., *Energy anf Fuels,* 2004. **18**, p. 116-121.

14.	Hammond, C., Jenkins, R.L., Dimitratos, N., Lopez-Sanchez, J.A., Rahim, M.H.a., Forde, M.M., Thetford, A., Murphy, D.M., Hagen, H., Stangland, E.E., Moulijn, J.M., Willock, S.H.T.J. and Hutchings, G.J., *Chemistry-A European Journal,* 2012. **18** (49), p. 15735-15745.

15.	Saiman, M.I.b., Brett, G.L., Tiruvalam, R., Forde, M.M., Sharples, K., Thetford, A., Jenkins, R.L., Dimitratos, N., Lopez-Sanchez, J.A., Murphy, D.M., Bethell, D., Willock, D.J., Taylor, S.H., Knight, D.W., Kiely, C.J. and Hutchings, G.J., *Angewandte Chemie, International Edition,* 2012. **51**, p. 5981-5985.

16.	Cheng, X.-M., Wang, Q.-D., Li, J.-Q., Wang, J.-B. and Li, X.-Y., *Journal of Physical Chemistry,* 2012. **116**, p. 9811-9818.

17.   Sander, W., Roy, S., Bravo-Rodriguez, K., Grote, D. and Sanchez-Garcia, E., *Chemistry-A European Journal,* 2014. **20**, p. 1-8.

18.   Eberhardt, M.K., *Journal of the American Chemical Society,* 1981. **103**, p. 3876-3878.

19.   Sheng-Gui, L., Xian-Tai, Z. and Hong-Bing, J., *Catalysis Communication,* 2013. **37**, p. 60-63.

20.   Ogata, Y., Tezuka, H. and Kamei, T., *Journal of Organic Chemistry,* 1969. **34** (4), p. 845-847.

21.   Timmermans, J., *Physico-Chemical Constant of Pure Organic Compounds*. Vol. **2**. 1965: Elsevier.

22.   Mill, T. and Hendry, D.G., *Comprehensive Chemical Kinetics*, in *Liquid Phase Oxidation*, C.H. Bamford and C.H.F. Tipper, Editors. 1980, Elsevier Scientific p. 64.

23.   Garcia-Ochoa, F., Romero, A. and Querol, J., *Industrial & Engineering Chemistry Research,* 1989. **28** (1), p. 43-48.

24.   Valden, M., Lai, X. and Goodman, D.W., *Science,* 1998. **281**, p. 1647-1650.

25.   Bamford, C.H. and Tipper, C.F.H., *Ester Formation and Hydrolysis and Related Reactions*. Vol. **10**. 1972, Amsterdam: Elsevier.

26.   Dumont, V., Oliviero, L., Mauge, F. and Houalla, M., *Catalysis Today,* 2008. **130**, p. 195-198.

27.   Hamamoto, M., Nakayama, K., Nishiyama, Y. and Ishii, Y., *Journal of Organic Chemistry,* 1993. **58**, p. 6421-6425.

28.   Ledgard, J., *A Laboratory History of Narcotics: Amphetamines and Derivatives*. Vol. **1**.

29.   Park, E.D., Hwang, Y.-S., Lee, C.W. and Lee, J.S., *Applied Catalysis A: General,* 2003. **247**, p. 269-281.

30.   Park, E.D., Hwang, Y.-S. and Lee, J.S., *Catalysis Communication,* 2001. **2**, p. 187-190.

31.   Sankar, M., Nowicka, E., Carter, E., Murphy, D.M., Knight, D.W., Bethell, D. and Hutchings, G.J., *Nature Communications,* 2014, p. Article 3332.

Toluene Oxidation using TBHP 4

1. Introduction

Benzaldehyde, benzyl alcohol, benzoic acid and benzyl benzoate are valorised oxidation products from toluene. Many studies have been reported for toluene oxidation. Without a catalyst, toluene oxidation shows a high selectivity for benzaldehyde and benzoic acid. Hence, other oxidation products are difficult to reach. Benzyl alcohol is the first oxidation products and really easy to oxidise under atmospheric condition. Various studies show high selectivity for benzyl alcohol, however only low conversions are obtained.

Zhao *et al.* reported more than 65 % selectivity for benzyl alcohol and benzaldehyde keeping a low conversion; under 9 %.[1] Gong-de and co-workers achieved 81.4 % selectivity for benzyl alcohol using a F-modified CuNiAl hydrotalcite compounds, despite a low conversion of 8.4 %.[2]

An efficient system using O_2 to oxidise toluene has been reported. 94 % conversion and 95 % selectivity for benzyl benzoate have been reach at 160 ºC using AuPd supported on C.[3] Figure 4.1 shows the possible reaction mechanism going through a number of intermediate products.

It has been shown that the oxidation of benzaldehyde to benzoic acid is quenched by the presence of benzyl alcohol.[4] Hence, the direct way to form benzyl benzoate, through the formation of benzoic acid, is not possible in the presence of O_2.
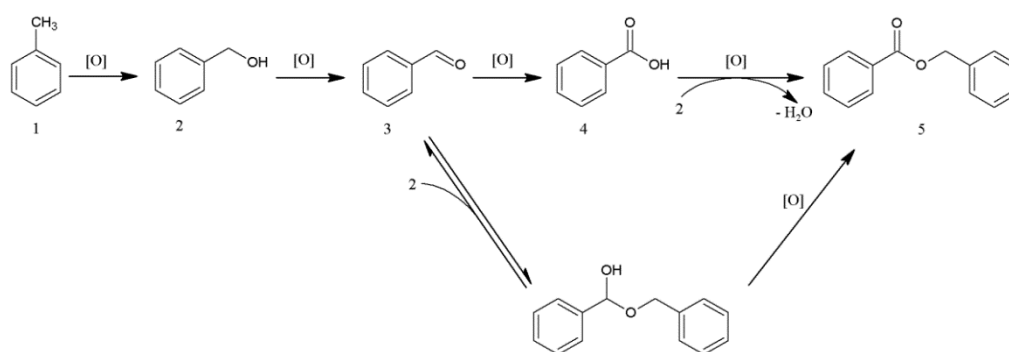
Figure 4.1: Reaction scheme of toluene oxidation to benzyl benzoate (from reference [3])

Huang and co-workers selectively oxidise toluene using TBHP as initiator and O_2 as an oxidant at 60 °C. Depending on reaction condition, 40 % conversion was reached. At low conversion benzaldehyde was the major product, and benzoic acid was the major product at higher conversion.[5]
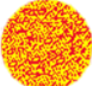
The principal focus of this chapter was to use mild conditions to oxidise toluene using Au, Pd and Pt nanoparticles. *tert*-Butyl hydroperoxide (TBHP) is an initiator and oxidant, consequently O_2 is not necessary. As an initiator, TBHP can form radical species able to activate toluene and form oxidation products.

A sol-immobilisation method (described in the experimental section 4.1) was used to prepare sets of Au, Pt and Pd supported catalysts. These catalysts have been characterised and their morphology confirmed by XPS and microscopy. They have been used to oxidise toluene with TBHP at 80 °C under atmospheric pressure. The effect of the catalyst morphology has been studied in order to relate the activity to the structure of the catalyst.

A second part of this study was to investigate and understand the reactivity using the most active catalyst from the materials tested. Time and concentration of TBHP have been investigated as well as the integration of O_2 in the system.

2. *Catalyst characterisation*

Sets of catalysts were prepared by sol immobilisation, the theoretical structure are reported in Table 4.1. Au, Pd and Pt were supported on TiO_2 and C. A metal weight ratio 1:1 was used with 1 wt. % total metal in final catalyst.

Table 4.1: Summary table of Au-Pd-Pt catalysts supported on TiO$_2$ and C

Monometallic			Au/ TiO$_2$	Au/ C
			Pt/ TiO$_2$	Pt/ C
			Pd/ TiO$_2$	Pd/ C
Bimetallic	Homogeneous alloy structures		AuPd/ TiO$_2$	AuPd/ C
			AuPt/ TiO$_2$	AuPt/ C
			PtPd/ TiO$_2$	PtPd/ C
	Core-Shell structures shell(core)/support		Au(Pd)/ TiO$_2$	Au(Pd)/ C
			(Au)Pd/ TiO$_2$	(Au)Pd/ C
			Au(Pt)/ TiO$_2$	Au(Pt)/ C
			(Au)Pt/ TiO$_2$	(Au)Pt/ C
			Pt(Pd)/ TiO$_2$	Pt(Pd)/ C
			(Pt)Pd/ TiO$_2$	(Pt)Pd/ C
Trimetallic homogeneous alloy structures			AuPdPt/ TiO$_2$	AuPdPt/ C

2.1. XPS

All the catalysts were characterised using XPS and the data concerning binding energies and surface atomic metal ratios are presented in Tables 4.2 to 4.6. As seen Figure 4.2, XPS signal can be observed at 84 eV for Au $4f_{7/2}$, corresponding to metallic Au. Similarly, Pd $3d_{5/2}$ at 335 eV and Pt $4f_{7/2}$ at 70 eV are also corresponding to metallic compound.[6-8] In all cases the measured binding energies indicate that the majority of the species are in the zero-valent state, *i.e.* all the nanoparticles are metallic in nature, which might be expected considering the vigorous chemical reduction steps used in the preparation of the sol-immobilised catalysts.
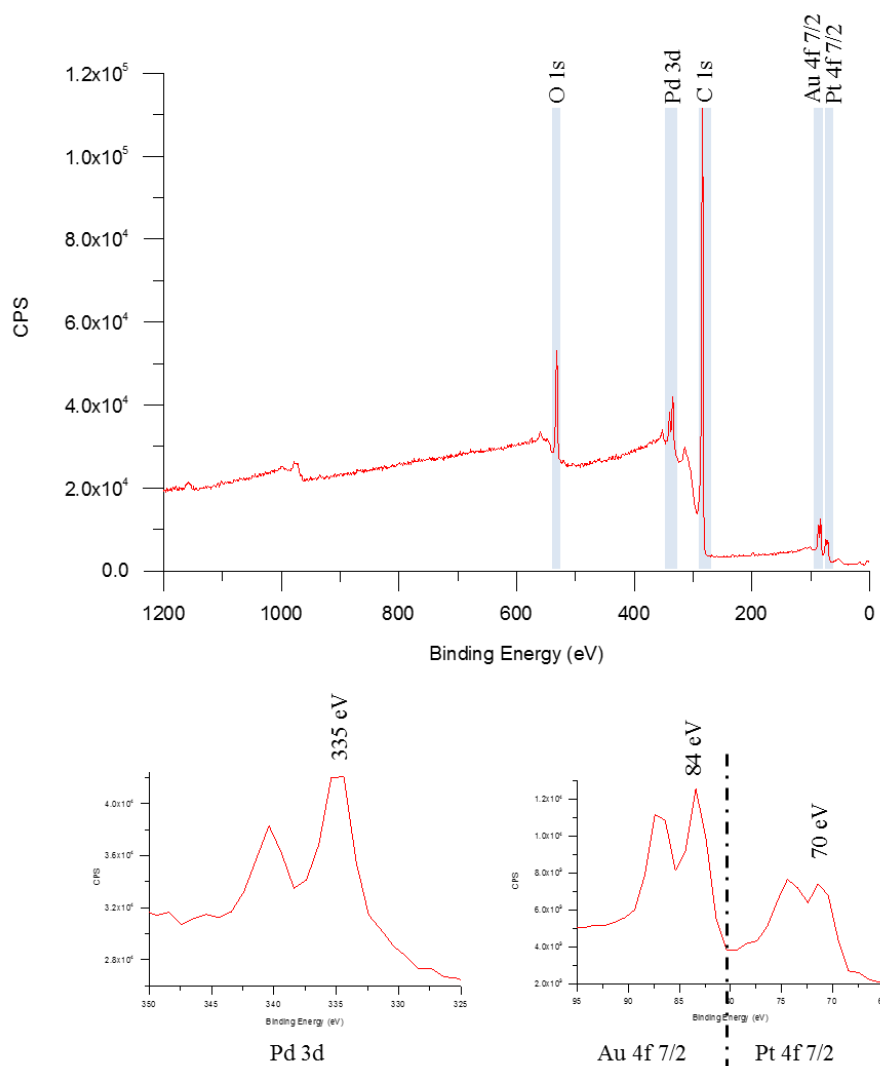
Figure 4.2: XPS spectrum of trimetallic AuPdPt catalyst

2.1.1. Monometallic catalysts

For monometallic materials, the XPS data in table 4.2 indicate the presence of the metal and their oxidation state. XPS analysis being a surface method, the totality of the support is not detected. The atomic percentage cannot be correlated to the weight percentage; hence, from these data, it is not possible to determine the amount of metal supported.

Table 4.2: XPS surface compositional data from monometallic catalysts supported on TiO$_2$ and C

Catalyst	Binding Energy (eV)[a]			Surface Content (atom %)		
	Au(4f$_{7/2}$)	Pd(3d$_{5/2}$)	Pt(4f$_{7/2}$)	Au(4f$_{7/2}$)	Pd(3d$_{5/2}$)	Pt(4f$_{7/2}$)
Au/ TiO$_2$	80.1	_	_	0.17	_	_
Au/ C	80.9	_	_	0.74	_	_
Pd/ TiO$_2$	_	334.0	_	_	0.14	_
Pd/ C	_	331.5	_	_	0.65	_
Pt/ TiO$_2$	_	_	70.6	_	_	0.04
Pt/ C	_	_	71.5	_	_	0.25

[a] All binding energies referenced to C 1s=284.7 eV

2.1.2. Bimetallic catalysts

For each bimetallic catalyst the formation of the core-shell morphology can be proven by a change in the surface metal ratio compared to homogeneous alloy morphology. However this has to be treated carefully as XPS analysis is a surface method which means that the core layer could not be totally detected. Furthermore molar mass of Au, Pt and Pd is different meaning that for a same weight percentage the number of moles would be different. Hence, the thickness of layers will be different for the three metals which could change the percentage detected.

Table 4.3 shows the XPS data for a set of PdPt catalysts. The Pd/Pt ratio for the alloy catalyst is close to the theoretical atomic value (= 1.85) confirming the 1:1 weight metal ratio. For the materials supported on C, the Pd(Pt)/ C catalyst has a similar Pd/Pt surface atomic ratio to the Pd-Pt random alloy, 1.74 and 1.79 respectively, but the Pt(Pd) particle shows a lower Pd/Pt ratio, with 1.34. This data suggests an increase of Pt on the surface confirming the change of morphology. In the case of TiO$_2$ support materials, the Pd/Pt ratio for Pd(Pt)/ TiO$_2$ is higher (= 2.42) than the homogeneous alloy (= 1.9), indicating a variation in surface composition and confirming the difference in morphology. The Pd/Pt ratio for Pt(Pd)/ TiO$_2$ decreases from 1.9 to 1.5, indicating a Pt surface enrichment.

Table 4.3: XPS surface compositional data from 1 wt. % PdPt (1.85:1 at) bimetallic catalysts supported on TiO$_2$ and C

Catalyst	Binding Energy (eV)[a]		Surface Content (atom %)		Ratio
	Pd(3d$_{5/2}$)	Pt(4f$_{7/2}$)	Pd(3d$_{5/2}$)	Pt(4f$_{7/2}$)	Pd/Pt
PdPt/ TiO$_2$	334.8	70.7	0.38	0.20	1.9
(Pt)Pd/ TiO$_2$	335.2	71.1	0.29	0.12	2.42
Pt(Pd)/ TiO$_2$	334.9	70.9	0.33	0.22	1.50
PdPt/ C	335.4	71.2	1.27	0.73	1.74
(Pt)Pd/ C	335.4	71.3	0.97	0.54	1.79
Pt(Pd)/ C	335.5	71.3	1.00	0.72	1.34

[a] All binding energies referenced to C 1s=284.7 eV

In the case of AuPt materials, presented in Table 4.4, the ratio Au/Pt for homogeneous alloy supported on either TiO$_2$ or C is 0.96. This value, being close to one, confirms the 1:1 weight metal ratio and the homogeneity of the alloy catalyst. The Au/Pt surface ratio for Au(Pt) supported on both TiO$_2$ and C decreased compared to the homogeneous alloy, suggesting a change in morphology which we interpret as resulting from the formation of a core-shell configuration. The reverse results are observed for the (Au)Pt confirming the formation of core-shell morphology.

Table 4.4: XPS surface compositional data from 1 wt. % AuPt (1:1 at) bimetallic catalysts supported on TiO$_2$ and C

Catalyst	Binding Energy (eV)[a]		Surface Content (atom %)		Ratio
	Au(4f$_{7/2}$)	Pt(4f$_{7/2}$)	Au(4f$_{7/2}$)	Pt(4f$_{7/2}$)	Au/Pt
AuPt/ TiO$_2$	83.6	71.0	0.24	0.25	0.96
Au(Pt)/ TiO$_2$	83.7	71.0	0.16	0.19	0.84
(Au)Pt/ TiO$_2$	83.6	70.8	0.17	0.14	1.21
AuPt/ C	83.9	71.2	0.53	0.55	0.96
Au(Pt)/ C	84.0	71.5	0.33	0.44	0.75
(Au)Pt/ C	84.0	71.3	0.88	0.56	1.57

[a] All binding energies referenced to C 1s=284.7 eV

XPS data for the AuPd set are found in Table 4.5. It was anticipated that results would be comparable to those obtained with the PdPt materials. The theoretical atomic ratio for Au/Pd alloy is 0.54. For materials supported on TiO$_2$, the ratio Au/Pd is close to 0.54 confirming the 1:1 weight metal ratio. The atomic ratio for (Au)Pd supported on TiO$_2$ increases compared to the alloy, also suggesting the formation of the core-shell morphology. In the case of Au(Pd) supported on TiO$_2$ the ratio is similar to the alloy making it difficult to draw conclusion about its morphology. However, STEM analysis could be used to help interpret the morphology. In the case of the homogeneous alloy supported on C, the ratio Au/Pd for homogeneous alloy AuPd is higher than expected (= 0.76). However, the ratio Au/Pd increases to 0.91 for (Au)Pd and decreases to 0.54 for Au(Pd) suggesting that core-shell morphology may have been formed.

Table 4.5: XPS surface compositional data from 1 wt. % AuPd (1:1.85 at) bimetallic catalysts supported on TiO$_2$ and C

Catalyst	Binding Energy (eV)[a]		Surface Content (atom %)		Ratio
	Au(4f$_{7/2}$)	Pd(3d$_{5/2}$)	Au(4f$_{7/2}$)	Pd(3d$_{5/2}$)	Au/Pd
AuPd/ TiO$_2$	82.7	334.4	0.06	0.12	0.50
Au(Pd)/ TiO$_2$	83.0	334.6	0.08	0.14	0.57
(Au)Pd/ TiO$_2$	83.0	334.5	0.12	0.11	1.09
AuPd/ C	84.1	335.6	0.57	0.75	0.76
Au(Pd)/ C	84.2	335.7	0.71	1.32	0.54
(Au)Pd/ C	84.2	335.8	0.69	0.76	0.91

[a] All binding energies referenced to C 1s=284.7 eV

2.1.3. Trimetallic catalyst

The XPS data for the trimetallic materials are shown in Table 4.6. The atomic ratio AuPdPt/ TiO$_2$ and AuPdPt/ C are respectively 1.2: 2.2: 1 and 1.2: 2.5: 1. This suggests that the three metals have been supported in a homogeneous way.

Table 4.6: XPS surface compositional data from 1 wt. % AuPdPt (1:1.7:1 at) trimetallic catalysts supported on TiO$_2$ and C

Catalyst	Binding Energy (eV)[a]			Surface Content (atom %)			Ratio
	Au(4f$_{7/2}$)	Pd(3d$_{5/2}$)	Pt(4f$_{7/2}$)	Au(4f$_{7/2}$)	Pd(3d$_{5/2}$)	Pt(4f$_{7/2}$)	Au:Pd:Pt
AuPdPt/ TiO$_2$	83.0	334.6	74.2	0.07	0.13	0.06	1.2:2.2:1
AuPdPt/ C	83.8	335.4	71.4	0.38	0.83	0.33	1.2:2.5:1

[a] All binding energies referenced to C 1s=284.7 eV

XPS data indicates that each catalyst seems to have the morphology expected; however it is also showing that less metal are supported on TiO$_2$ than C. The variation in weight ratio for the same set of metals on different supports could be attributed to the type of support used. This could be due to two reasons, metal diffusion to the other metal or particle size

and shape modified during the sol immobilisation method. The ability of the nanoparticle to wet the surface during deposition could lead to the change of particle shape.[3] The combination with STEM-HAADF analysis will help to elucidate the final structure of the catalyst.

2.2. Scanning transmission electron microscopy (STEM)

The random alloy Au-Pt/ C and Pt-Pd/ C bimetallic samples prepared by the sol-immobilisation method were examined by STEM analysis. AuPd/ C have also been analysed for the oxidation of octane. Images can be found in chapter 3 section 3.2. The metal particle size for AuPd/ C ranged between 1 nm and 10 nm with a mean value of 3.7 nm.

Figure 4.3 shows the data for the Au-Pt/ C catalyst system. The metal particle size ranged between 1 nm and 6 nm with a mean value of 2.3 nm. XEDS analysis showed that all the supported particles were Au-Pt random alloys.

Figure 4.3: Electron microscopy analysis of the 1 wt. % Au-Pt/ C catalyst made by sol-immobilisation
(a) a low magnification STEM-HAADF image; (b,c) higher magnification STEM-HAADF images of representative Au-Pt particles; (d) particle size distribution derived from HAADF images; (e) a typical XEDS spectrum acquired from an individual Au-Pt alloy particle. (From reference [9])

The data for the Pt-Pd/ C catalyst system is presented in Figure 4.4. The metal particle size was found to vary between 1 nm and 12 nm with a mean value of 3 nm. XEDS analysis confirmed individual supported particle to be a Pt-Pd alloy nanoparticle.
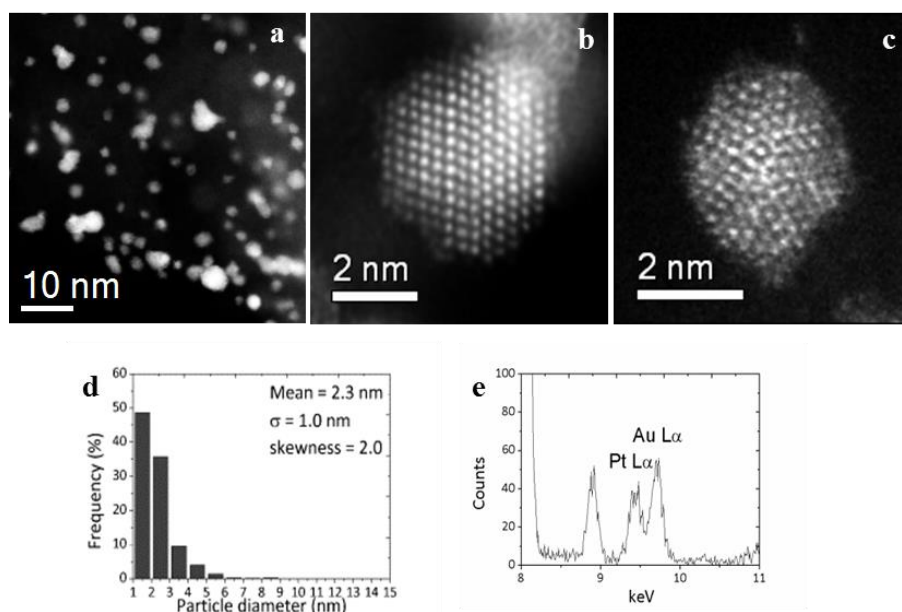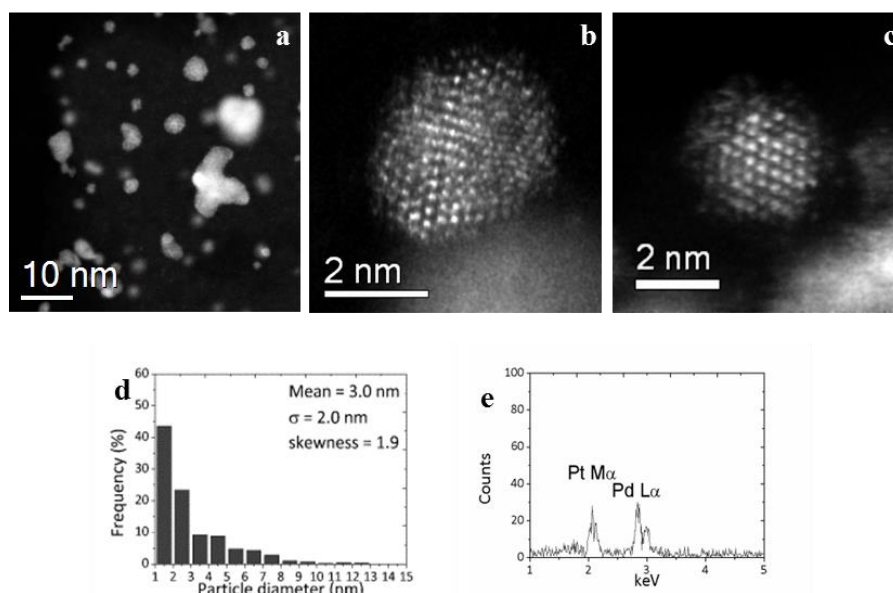

Figure 4.4: Electron microscopy analysis of the 1 wt. % Pt-Pd/ C catalyst made by sol-immobilisation
(a) a low magnification STEM-HAADF image; (b,c) higher magnification STEM-HAADF images of representative Pt-Pd particles; (d) particle size distribution derived from HAADF images; (e) a typical XEDS spectrum acquired from an individual Pt-Pd alloy particle. (From reference [9])

AuPd alloy and the corresponding core-shell supported on TiO_2 and C were characterised and showed a narrow distribution in particle size between 3.7 nm and 5 nm averages depending on the morphology and the support.[3, 10]

For all sets of catalysts the alloy or core-shell morphology has been confirmed. The particle sizes are reported Table 4.7. From monometallic to trimetallic, the particles size decreases. Monometallic catalysts have particles sizes of 4.5-6 nm while the size is 2.3-3.9 nm for bimetallic and 3.2 for trimetallic. Hence, the addition of metal plays a role on the size and shape of the particles which would certainly lead to various activities.

Table 4.7: Particles size for mono, bi and trimetallic catalyst.

Catalyst	Particles size
1 wt.% Au/ TiO$_2$	4.6
1 wt.% Au/ C	5/6.8
1 wt.% Pd/ TiO$_2$	4.8
1 wt.% AuPt/ C	2.3
1 wt.% AuPd/ TiO$_2$	3.9
1 wt.% AuPd/ C	3.7
1 wt.% PdPt/ C	3
1 wt.% Au(Pd)/ C	3
1 wt.% Au(Pd)/ TiO$_2$	3.2
1 wt.% Pd(Au)/ C	2.6
1 wt.% Pd(Au)/ TiO$_2$	4.3
1 wt.% AuPdPt/ C	3

3. Catalytic testing

All catalysts have been tested for toluene oxidation in bench reactors. Experimental description can be found chapter 2 section 6.3.

3.1. Results

3.1.1. Blank reaction

Before comparing different catalysts, several reactions were run in order to prove the actual role of the catalyst. The results are shown in Table 4.8. The first reaction, Entry 1, with neither catalyst or TBHP was run and shows as expected no reactivity. A reaction with toluene and TBHP only (Entry 2), was run and shows a conversion of 1.1 %. Without catalyst the activity for toluene oxidation is very low. Then the two supports with no metals were run; TiO$_2$-only has almost no activity with 1.4 % conversion. However carbon-only gives 14.2 % conversion of toluene with 59 % selectivity for benzoic acid and TBHP decomposition of 19 %. Activated C is usually used as a support; however it has been reported that some activated C without metals can be active. Utrilla and Polo reported the decomposition of ozone into highly oxidative species by activated C. Trace of metals present in activated C could be responsible. They also proposed that activated C does not act as a catalyst but rather as an initiator leading the transformation of ozone to

·OH radicals.[11, 12] This suggests that C could interact with TBHP, explaining the rise of TBHP consumption, and form some active species to oxidise toluene.

Table 4.8: Blank reaction for toluene oxidation at 80 ºC using TBHP

Entry	Catalyst	Conversion (%)		selectivity (%)				
		Toluene	TBHP	Benzyl alcohol	Benzal-dehyde	Benzoic acid	Benzaldehyde dimethyl acetal	Methyl ester
1	no TBHP/no catalyst	0	–	0	0	0	0	0
2	no catalyst	1.1	1	28	72	0	0	0
3	TiO$_2$	1.4	1	25	75	0	0	0
4	Carbon	14.2	19	13	23	59	3	2

Reaction conditions: Toluene = 5 mL, substrate/ TBHP ratio (mol) = 1:1, temperature = 80 °C, time = 24 h

3.1.2. Monometallic

Each metal, Au, Pd and Pt were supported on TiO$_2$ and C. These metals were first prepared alone, by sol immobilisation, to give monometallic catalysts. Table 4.9 shows the toluene oxidation results with these catalysts. The addition of Au on the support shows an important enhancement of the conversion either on TiO$_2$ or C (Entry 1 and 2) with 20.2 % and 23.1 % conversion respectively. These two catalysts have a high selectivity for benzoic acid (≈ 90 %). A similar conversion of 24.4 % is reached with Pt/ C (Entry 6), however the selectivity for benzoic acid is lower with 73 %, in comparison Pd/ C decreases the conversion of toluene (Entry 4). Pd/ TiO$_2$ and Pt/ TiO$_2$ also decrease the conversion (Entry 3 and 5). Au and Pt catalysts show a high consumption of TBHP, approximately two to three times more than toluene conversion. Pd catalysts show a similar consumption of TBHP than toluene is converted. However this means that, in all cases, more molecules of TBHP than necessary are used to oxidise toluene. The higher activity of metals supported on C compared to supported TiO$_2$ reflects the activity of the unsupported catalyst. The higher activity of C support has already been reported for toluene oxidation, benzyl alcohol oxidation and the direct production of H$_2$O$_2$.[3, 10] However it is important to note that C is active in absence a metals (14% conversion). Hence, the activity of metal supported on carbon might not be as important as the activity of the metal supported on TiO$_2$, non-active support.

Table 4.9: Comparison of the activity of monometallic Au, Pd, and Pt catalyst supported on TiO$_2$ and C for toluene oxidation at 80 ºC using TBHP

Entry	Catalyst	Conversion (%)		selectivity (%)				
		Toluene	TBHP	Benzyl alcohol	Benzal-dehyde	Benzoic acid	Benzaldehyde dimethyl acetal	Methyl ester
1	1 wt. % Au/ TiO$_2$	20.2	68	2	5	90	1	2
2	1 wt. % Au/ C	23.1	58	2	3	91	1	3
3	1 wt. % Pd/ TiO$_2$	4.1	2	26	50	12	12	0
4	1 wt. % Pd/ C	11.1	10	15	27	51	5	2
5	1 wt. % Pt/ TiO$_2$	4.2	14	22	40	30	8	0
6	1 wt. % Pt/ C	24.4	42	5	17	73	2	3

Reaction conditions: Toluene = 5 mL, substrate/ TBHP ratio (mol) = 1:1, substrate/ metal ratio (mol) = 6500, temperature = 80 °C, time = 24 h

3.1.3. Bimetallic

The activity of the Au, Pd and Pt, bimetallic catalysts were tested for toluene oxidation, the results were compared in Table 4.10. For all cases the C support showed a higher activity. AuPd combination shows a higher activity than the AuPt or PdPt bimetallic catalysts. This could be explained by the fact that Pt seems to destabilise the O-O bond while Au would stabilise it. Gewirth and co-workers tested H$_2$O$_2$ electroreduction and showed that the O-O bond from H$_2$O$_2$ is elongated on active Pt surface whereas the elongation does not change on inactive Au surface.[13] The core-shell morphology does not make an obvious difference to the activity compared to the corresponding bimetallic alloy catalysts. AuPd bimetallic alloy supported on C is the best bimetallic catalyst.

The AuPd bimetallic compared to the Au monometallic catalyst shows a slight increase in activity. For all bimetallic catalysts supported on C the TBHP consumption is higher than for catalysts supported on TiO$_2$. The lower consumption of TBHP is linked with a low conversion of toluene.

The promoting effect of adding a second metal has been previously reported. Alloying PdPt and AuPd shows a better activity than monometallic catalysts for various reduction or oxidation reactions. Kong and co-workers showed an improvement of activity for ethanol electro-oxidation by adding Au into Pd catalyst. This improvement would be dependent on the position and amount of Au.[14] Toluene oxidation also shows an enhancement of activity for all sets of bimetallic catalysts. Papers have attributed the

change of activity to the formation of core-shell nanoparticles.[15, 16] Tedsree *et al* reported an increase of activity for the production of H_2 from formic acid. By coating Ag nanoparticles with a thin layer of Pd, the presence of terrace sites in the Pd layer and electronic effect with Ag lead to higher activity.[17] However in the current work, the change in nanoparticle morphology of the catalyst is not showing an important variation of activity. The formation of core-shells for the AuPd and AuPt set of catalysts is slightly less active, contrary to the (Pt)Pd core-shell which gives better activity than the alloy PdPt. Even so this core-shell catalyst is not better than the AuPd alloy catalyst. It has already been reported by Hutchings *et al* that, for the direct production of H_2O_2, the AuPd alloy catalyst was showing the highest activity compared to other core-shell catalysts.[10]

Table 4.10: Comparison of the activity of bimetallic Au, Pd, and Pt catalyst supported on TiO$_2$ and C for toluene oxidation at 80 ºC using TBHP

Entry	Catalyst	Conversion (%)		selectivity (%)				
		Toluene	TBHP	Benzyl alcohol	Benzal-dehyde	Benzoic acid	Benzaldehyde dimethyl acetal	Methyl ester
1	1 wt. % AuPd/ TiO$_2$	19.8	16	20	7	71	1	1
2	1 wt. % AuPd/ C	25.3	59	2	5	86	1	6
3	1 wt. % Au(Pd)/ TiO$_2$	22.2	52	2	5	90	1	2
4	1 wt. % Au(Pd)/ C	22.7	78	1	4	87	1	6
5	1 wt. % (Au)Pd/ TiO$_2$	13.5	32	4	9	82	2	3
6	1 wt. % (Au)Pd/ C	22.9	69	1	5	85	1	8
7	1 wt. % AuPt/ TiO$_2$	8.9	58	9	9	82	0	0
8	1 wt. % AuPt/ C	20.7	85	5	3	89	2	1
9	1 wt. % Au(Pt)/ TiO$_2$	8.8	45	9	12	79	0	0
10	1 wt. % Au(Pt)/ C	15.5	77	5	4	84	2	5
11	1 wt. % (Au)Pt/ TiO$_2$	13.4	63	5	6	89	0	0
12	1 wt. % (Au)Pt/ C	16.9	89	5	4	80	2	9
13	1 wt. % PtPd/ TiO$_2$	4.5	23	23	38	39	0	0
14	1 wt. % PtPd/ C	13.2	79	8	7	75	2	8
15	1 wt. % Pt(Pd)/ TiO$_2$	5.7	12	21	40	39	0	0
16	1 wt. % Pt(Pd)/ C	14.6	70	10	7	74	2	7
17	1 wt. % (Pt)Pd/ TiO$_2$	6.3	11	20	35	45	0	0
18	1 wt. % (Pt)Pd/ C	18.2	90	6	4	86	2	2

Reaction conditions: Toluene = 5 mL, substrate/ TBHP ratio (mol) = 1:1, substrate/ metal ratio (mol) = 6500, temperature = 80 °C, time = 24 h

3.1.4. Trimetallic

Finally, trimetallic catalysts were tested for the oxidation of toluene (Table 4.11). As reported in the previous sections the C supported materials have a better activity than the TiO$_2$ supported materials. AuPdPt/ C is the best catalyst with 27.3 % conversion and 93 % selectivity for benzoic acid. A reason for this could be the electronic effect due to a Pt atom interacting with Au and Pd. This interaction would change the electronic properties and thus the catalytic properties.

The size of the nanoparticles could also have an effect on toluene oxidation. Particle's size decreases with addition of metals exposing different surface of nanoparticles. Hence, the higher activity could come from lower particles size.

Table 4.11: Comparison of the activity of trimetallic Au, Pd, and Pt catalyst supported on TiO₂ and C for toluene oxidation at 80 ºC using TBHP

Entry	Catalyst	Conversion (%)		Selectivity (%)				
		Toluene	TBHP	Benzyl alcohol	Benzal-dehyde	Benzoic acid	Benzaldehyde dimethyl acetal	Methyl ester
1	1 wt. % AuPdPt / TiO₂	15.8	53	4	8	86	1	1
2	1 wt. % AuPdPt/ C	27.3	86	1	3	93	1	2

Reaction conditions: Toluene = 5 mL, substrate/ TBHP ratio (mol) = 1:1, substrate/ metal ratio (mol) = 6500, temperature = 80 °C, time = 24 h

3.1.5. Conclusion on catalytic test

Toluene oxidation was done with TBHP using sets of catalysts made by sol-immobilisation. Au, Pd and Pt metals were supported on TiO₂ and C. Mono, bi and trimetallic catalysts were made and tested. In all cases, the C supported materials were more active than TiO₂ supported catalysts. Carbon seems to have, for most cases, a promotional effect. Catalysts based on Au present the best activity for toluene oxidation with an increase of activity for each extra metal added (monometallic < bimetallic < trimetallic). Hence, we can conclude that Au nanoparticles have an important role for this reaction and Pd and Pt must have a promotional effect. Further investigation would help to elucidate: (i) what are the active sites (ii) whether the active site is changed by the addition of new atoms and (iii) whether interaction between atoms causes the electronic change of active sites.

3.2. Mechanism

In most reactions reported above, benzoic acid is the major product. However, at low conversion the major products are benzaldehyde and benzyl alcohol, suggesting the first oxidation products are benzyl alcohol and benzaldehyde. This is to be expected since the C-H bond is first oxidised to an alcohol, then an aldehyde and finally an acid. The reaction scheme is shown Figure 4.5

For most of the catalysts, benzaldehyde-dimethylacetal and methyl benzoate were also observed as reaction products, as shown in Figure 4.4. These products were not present in previous work by Kesavan *et al,* when using O_2 as the oxidant, which may suggest a different mechanism potentially resulting from the use of different oxidant.[3] The catalytic test results presented previously showed that these products are made in the reaction when the conversion is highest. Hence, more products are formed with C supported catalysts, which in general have higher conversion than TiO_2 equivalents (see previous section 3.1). TBHP decomposition has also increased with the same trend. Therefore it is presumed that TBHP is decomposed into products such as methanol or radical species which will then interact with toluene to form the final product instead of only being an initiator.
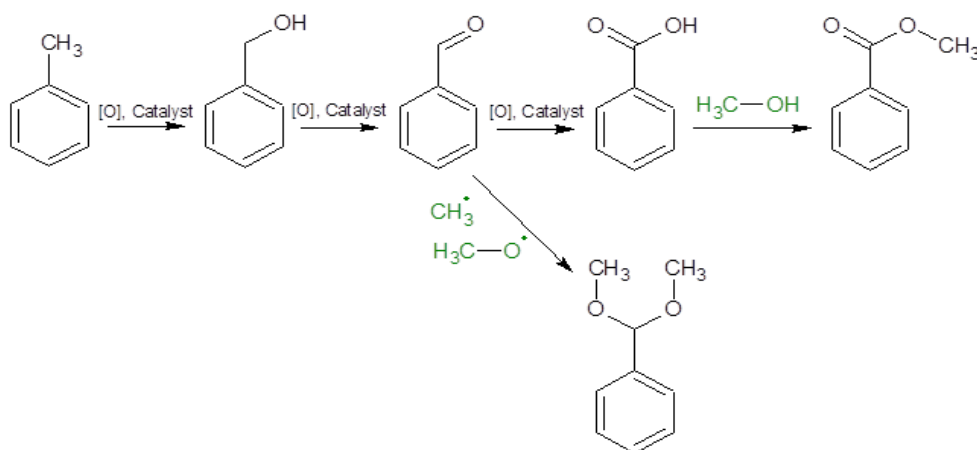

Figure 4.5: Reaction scheme for toluene oxidation at 80 ºC using TBHP (from reference [9])

The scission of TBHP into two radical molecules activates the oxidation of toluene into benzyl alcohol, benzaldehyde and benzoic acid. In the presence of O_2 as an oxidant, it has been shown that benzoic acid is not produced due to the presence of benzyl alcohol quenching the oxidation of benzaldehyde to benzoic acid. However, the conditions in this study are different as TBHP is used as the oxidant, forming radical species able to activate toluene and benzaldehyde. TBHP can decompose into a number of different products as shown in Figure 4.6[18] Some of these are radical products, they can interact with toluene and its products of oxidation. For example the formation of benzaldehyde dimethylacetal, via the interaction of methyl and methoxy radicals (•CH_3 and •OCH_3) derived from TBHP, with benzaldehyde or benzoic acid.

The possibility that -CH_3 is cleaved from toluene in the oxidation process resulting in •CH_3 and benzyl radicals is also considered.[19] However, no biphenyl (coupled product of two benzyl radicals) were formed, suggesting that •CH_3 (Entry 4) and •OCH_3 (Entry 3 apply to molecule 7) methoxy radical species were produced from TBHP.
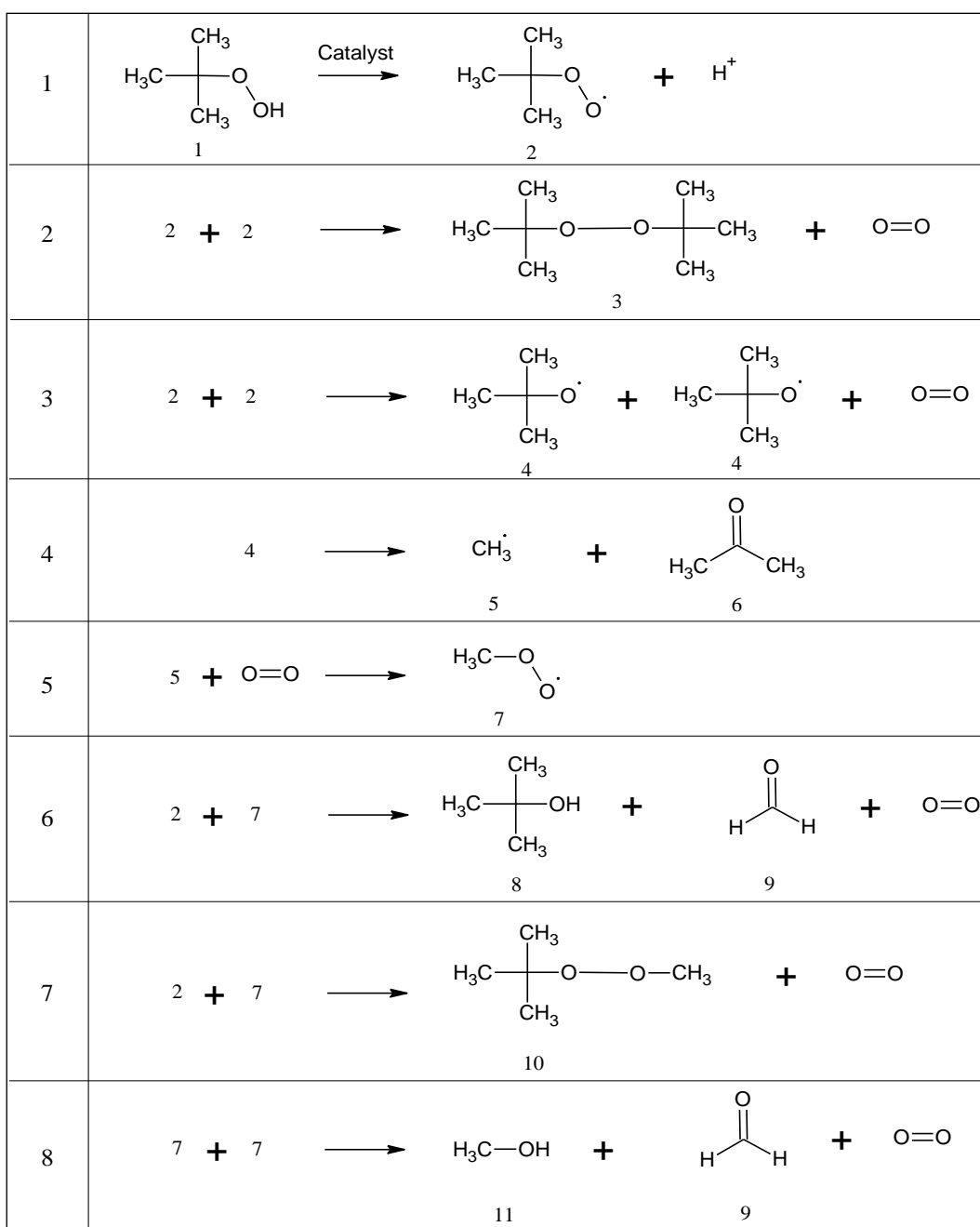

Figure 4.6: Reaction scheme for TBHP decomposition

4. Investigation of Au catalysts supported on carbon

As seen previously in section 3.1, catalysts supported on C are the most active for the oxidation of toluene. For each catalyst, from monometallic to trimetallic, those containing Au gave the best activity. In this section, the three different catalysts based on Au were used to investigate the time online, the amount of TBHP and the reusability of the catalyst.

4.1. Effect of time

Au, AuPd and AuPdPt supported on C have been used for the oxidation of toluene over different times, 4 h to 72 h. Each catalyst follows the same trend; the conversion increases with time. The rate of conversion seems to decrease with time, leading to a stabilisation of conversion as shown in Figure 4.7.
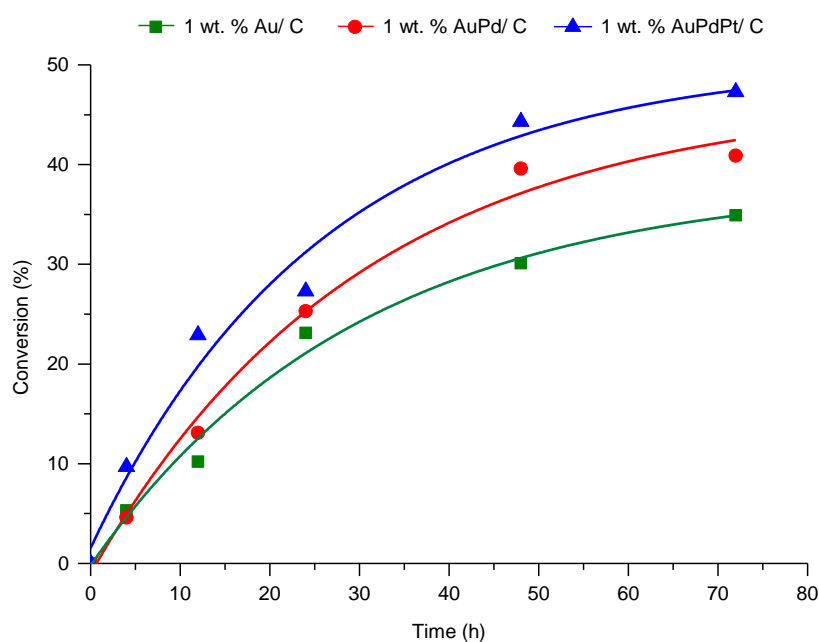

Figure 4.7: Effect of time for toluene oxidation at 80 ºC using TBHP and Au catalysts

Reaction conditions: Toluene = 5 mL, substrate/ TBHP ratio (mol) = 1:1, substrate/ metal ratio (mol) = 6500, temperature = 80 °C

When the reaction is conducted for 4 h, the monometallic catalyst is slightly better than the bimetallic material. However, after 4 h the bimetallic shows a higher activity than the monometallic. The trimetallic catalyst is the best over the whole time range.

110

Monometallic, bimetallic and trimetallic give 35 %, 41 % and 47 % conversion with 84 %, 81 % and 97 % selectivity for benzoic acid respectively after 72 h.

It seems that the addition of Pd and the combination of Pd and Pt enhance the activity. XPS results, section 2.1, indicate a slightly higher amount of Pd compare to Au for AuPd bimetallic catalyst. However the monometallic Pd catalyst has a low conversion of 11.1 %. Pd by itself is not as good as Au for the oxidation of toluene but the interaction of Pd with Au makes a more active catalyst. The same effect is seen with the addition of Pt.

All catalysts show a decrease in reaction rate after 24 h reaction. Two reason can cause the drop of activity; (i) the amount of TBHP left is not high enough to continue the activation of toluene. (ii) The catalyst is deactivated caused by poisoning, leaching or coking. Further experiments have to be conducted to understand the mechanism of deactivation.

4.2. Effect of TBHP

TBHP is used as the oxidant as well as the initiator in this reaction. The next experiment was to increase the amount of TBHP in order to increase the conversion. The amount of TBHP was increased to twice the usual amount. Table 4.12 shows that for each set of catalysts the activity decreases with the increasing amounts of TBHP. It's most obvious with Au/ C where there is 12 % conversion instead of 23.1 % in standard conditions. TBHP was also titrated after each reaction to calculate the conversion. Except for the trimetallic catalyst, TBHP consumption was higher when the amount of initial TBHP concentration was doubled.

As seen in section 3.2, TBHP decomposes easily into radical species; the more TBHP decomposed, the more radical species produced. These radical species are able to react with toluene but also together to form non radical species. Hence, TBHP could be consumed but not used to oxidise toluene.

The presence of Au nanoparticles by themselves is less active than the bimetallic and trimetallic catalyst in the presence of double amount of TBHP.

Table 4.9 in section 3.1 shows the consumption of TBHP by monometallic catalysts. Au catalysts seem the most effective to decompose TBHP. This decomposition leads to higher TBHP consumption with lower toluene conversion as seen Table 4.12.

For the three catalysts, doubling the amount of TBHP decreases the conversion and TBHP consumption increases. A competition of active size between toluene and TBHP could explain why toluene conversion decreases. Also, in the presence of Pd and Pt the

conversion difference is not as obvious as Au monometallic catalysts. This could suggest that Pd and Pt are not as active as Au for TBHP decomposition, but are active for toluene oxidation. Also their presence on the catalyst could hide Au which would stop the interaction between Au and TBHP, hence slowing down the rate of decomposition.

Another thought was that products from TBHP decomposition could poison the catalyst. If this was the case, high concentrations of TBHP would give more decomposition products which would poison the catalyst and explain why activity does not increase with higher amount of TBHP.

Table 4.12: Comparison of the activity with various amount of TBHP for toluene oxidation at 80 ºC

Entry	Metals	Toluene :TBHP	Conversion (%)		Selectivity (%)				
			Toluene	TBHP	Benzyl alcohol	Benzal-dehyde	Benzoic acid	Benzaldehyde dimethyl acetal	Methyl ester
1	Au	1:1	23.1	58	2	3	91	1	3
2		1:2	12	76	2	8	78	2	10
3	AuPd	1:1	25.3	59	2	5	86	1	6
4		1:2	22.9	79	2	6	86	2	4
5	AuPdPt *	1:1	36.9	66	2	4	88	2	4
6		1:2	34.1	61	2	5	87	1	5

Reaction conditions: Toluene = 5 mL, substrate/ metal ratio (mol) = 6500, temperature = 80 °C, time = 24 h, catalysts = 1 wt. % M/ C (M = Au, AuPd and AuPdPt)
* Substrate/ metal ratio (mol) = 13000

4.3. Reusability

From all catalysts tested so far, AuPdPt/ C shows the best activity for toluene oxidation with 47 % conversion and 97 % selectivity for benzoic acid after 72 h. The high conversion and selectivity for this catalyst is interesting. However, one principal specification for a good catalyst is to be reusable. Reusability tests have been run and the activity compared. The results are reported Figure 4.8. After each use, the catalyst was cleaned with acetone to remove products which stay on the surface. Toluene conversion decreases for each use as well as the selectivity for benzoic acid and methyl benzoate while benzyl alcohol and benzaldehyde selectivity increases. The general trend for

selectivity follows the low conversion profile; hence the change in selectivity can be explained by this.

The decrease of conversion suggests a deactivation of the catalyst. Deactivation could occur for many reasons. TGA analysis was performed on the catalyst before and after use. Figure 4.9 shows a difference of loss of weight after use between 100 ºC and 400 ºC. The TGA of the unused catalyst shows a loss of weight around 100 ºC which can be attributed to a loss of water. In the case of the used catalyst, the loss of weight around 100 ºC is not as important. However another loss of weight occurs between 200 ºC and 360 ºC. Toluene reaction is carried out in organic conditions; hence, no water is in the reaction explaining the small loss at 100 ºC. The second loss of weight shows that other compounds are present on the catalyst after use and could explain the deactivation of the catalyst by poisoning. A TGA-MS analysis would determine which compounds are chemisorbed on the surface.

Another way to determine the deactivation of the catalyst would be to analyse the presence of metal particles in the filtrate after reaction using ICP analysis. The presence of metals would confirm catalyst leaching.
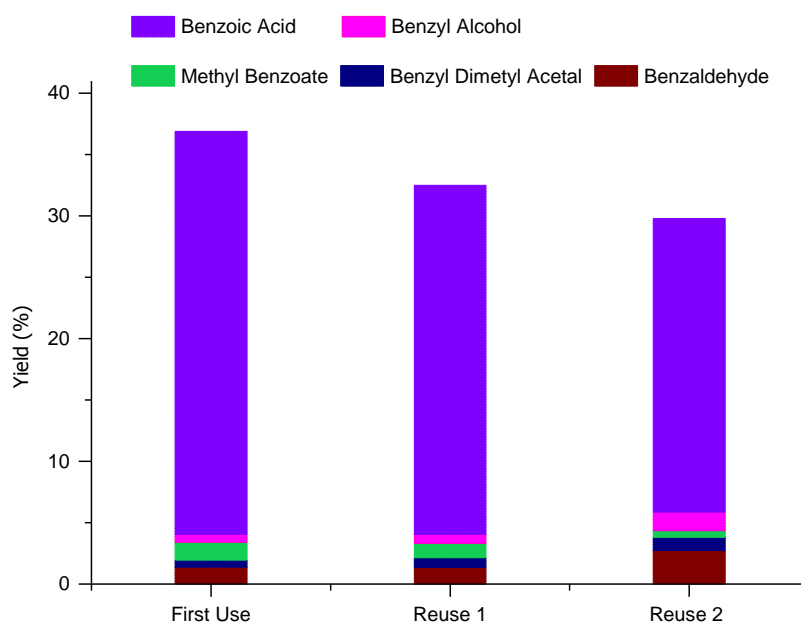

Figure 4.8: Reuse test for toluene oxidation at 80 ºC using TBHP and 1 wt. % AuPdPt/ C catalysts

Reaction conditions: Toluene = 5 mL, substrate/ TBHP ratio (mol) = 1:1, substrate/ metal ratio (mol) = 13000, temperature = 80 °C, time = 24 h
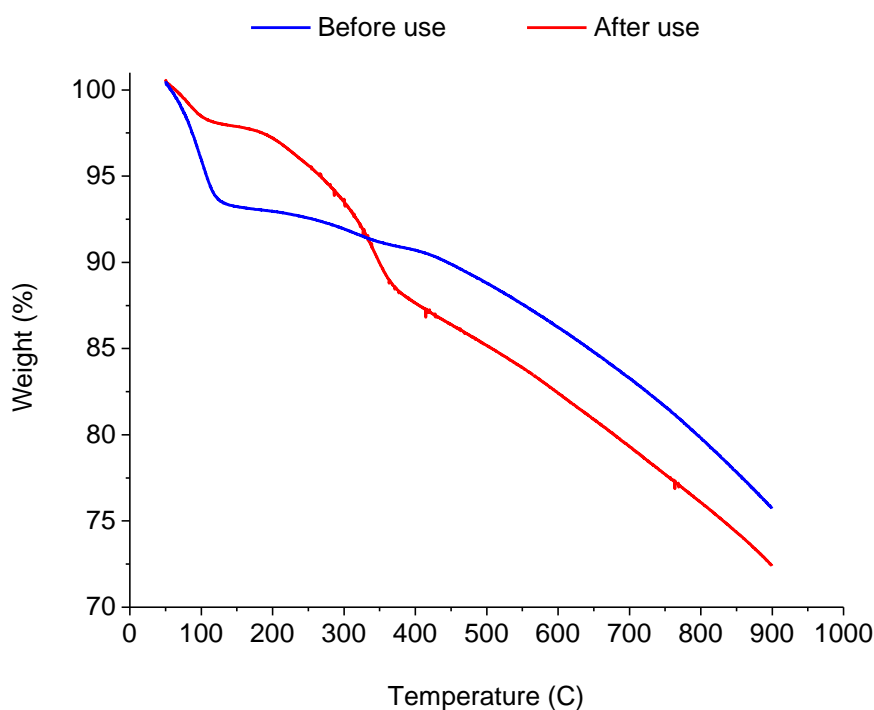

Figure 4.9: TGA analysis of 1 wt. % AuPdPt/ C used and unused.

5. H_2O_2 as oxidant

Toluene oxidation was run with TBHP as the oxidant and the initiator; however TBHP could potentially deactivate the catalyst. Hence it would be interesting to find another initiator in order to compare the reactivity. H_2O_2 is known to be a good oxidant and initiator due to its ability to form radical species (i.e. hydroperoxy and hydroxyl radicals). Also a AuPd/ C catalyst was used to synthesise *in situ.* H_2O_2, therefor it might be interesting to check what would happen in the reaction conditions used for toluene oxidation.[20-22] H_2O_2 being a very simple molecule the only by-product form would be water.

Toluene oxidation was run under the same conditions than previously with H_2O_2 instead of TBHP, however no product was detected. An experiment was conducted to understand why this was the case. An equal volume of toluene and TBHP or H_2O_2 was mixed and stirred. In both cases two equal phases could be distinguished before stirring. After a few minutes of stirring the mixture of toluene and TBHP showed a radical change; two layers

of different volume were present as shown in Figure 4.10. TBHP solution is 70 % of TBHP in water, it appears that the TBHP has gone into the toluene phase and the second phase is water only. In order to prove this assumption the TBHP was titrated for both phases. The toluene phase had a higher concentration of TBHP than the water phase which suggests that TBHP has a better solubility in toluene than water. In the case of H_2O_2 and toluene mixture, even after a few hours stirring the volume of each phases stayed equal. H_2O_2 of each phase was titrated, with ceria solution as explained in chapter 2 section 6.6. No H_2O_2 was transferred to the toluene phase, H_2O_2 stayed in the aqueous phase. Hence, H_2O_2 is not soluble in toluene and this explains why the reaction did not occur.
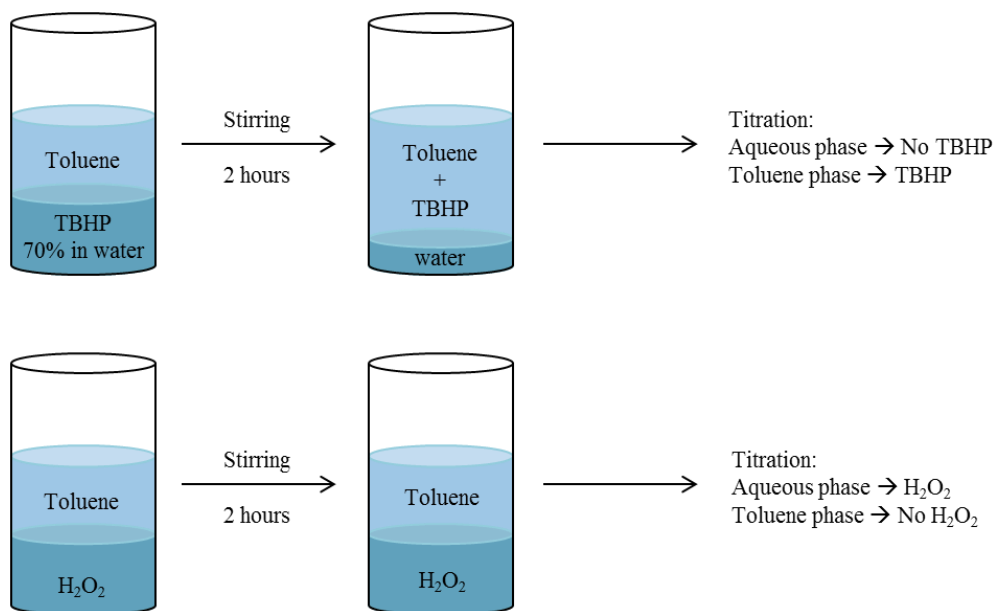

Figure 4.10: Solubility test of oxidant, TBHP and H_2O_2 in toluene

6. Toluene oxidation reaction, in an autoclave, using TBHP as oxidant

All reactions, in the previous sections of this chapter, have been run in a bench reactor equipped with a round bottom flask and condenser. The presence of the condenser enables the reaction mixture to be kept at 80 ºC without losing volatile molecules. However, some molecules such as CO_2 are in the gas phase at -56.6 °C under atmospheric pressure, meaning this will not be trapped by the condenser. Therefore, in order to detect the presence of the gas phase the reaction was run in an autoclave.

After charging the autoclave with toluene and TBHP, the autoclave was closed, purged and charged with 20 bar of synthetic air (mixture 20 % O_2/ N_2). The results are reported in Table 4.13. Toluene conversion in the autoclave is slightly higher than in the bench reactor with 36.9 % and 40.3 % conversion. This difference can be explained by the presence of CO_2 in the gas phase as the autoclave reaction shows 10 % selectivity for CO_2.

Table 4.13: Comparison of the activity of toluene oxidation in bench and autoclave at 80 ºC

Entry	System	Pressure (bar)	Conversion (%)		Selectivity (%)		
			Toluene	TBHP	Benzoic acid	Others	CO_2
1	Bench	–	36.9	66	88	12	?
2	Autoclave	20	40.3	86	78	12	10

Reaction conditions: Toluene = 5 mL, substrate/ TBHP ratio (mol) = 1:1, catalyst = 1 wt. % AuPdPt/ C, substrate/ metal ratio (mol) = 13000, temperature = 80 °C, time = 24 h

7. Oxygen activation

All previous reactions have been run in the presence of air and it is known that the AuPd/ C catalyst can activate O_2 at 160 ºC under 10 bar O_2 for the oxidation of toluene.[3] Regarding AuPdPt/ C catalyst, Hutchings and co-workers reported the oxidation by molecular O_2 at 120 ºC.[23] Pathan *et al* studied the mechanism of various alcohol oxidation reactions with TBHP and O_2 at 80 ºC. In absence of TBHP the reaction is slower. However, O_2 from TBHP is not used to oxidise alcohol, TBHP act as a radical initiator and O_2 as oxidant.[24]

From the previous work, it is known that toluene is oxidised by TBHP itself. However the possibility to activate and integrate O_2 on toluene products at 80 ºC using 1 wt. % AuPdPt/ C has to be investigated. Some calculations were done to determine the O_2 balance and check the possibility of O_2 activation occurring. However it is very difficult as TBHP is decomposed to a few products as seen previously Figure 4.6. The following reactions have been done in order to confirm the activation of O_2 in this system. For all reactions 1 wt. % AuPdPt/ C was used as catalyst.

7.1. Effect of oxygen

An experiment was run to compare toluene oxidation in the presence or absence of air. Table 4.14 shows the results. Under nitrogen, toluene conversion is clearly lower than under air condition with 18.3 % and 40.3 % conversion respectively. The selectivity of benzoic acid decreases under nitrogen whereas methyl ester increases. Under nitrogen the only source of oxidant is TBHP, only O_2 from TBHP decomposition can be introduced into the products. As shown Figure 4.6, TBHP can decompose into several different species. It is assumed that these species couple with toluene and/ or activate toluene to form coupling products. Hence, methyl ester could be formed by the coupling of methanol (molecule 7, Figure 4.5 Entry 5) and benzoic acid.

Table 4.14: Toluene oxidation in presence of air or nitrogen

		Conversion (%)		Selectivity (%)					
Entry	Condition	Toluene	TBHP	Benzyl alcohol	Benzal-dehyde	Benzoic acid	Benzaldehyde dimethyl acetal	Methyl benzoate	CO_2
1	N_2	18.3	80	2	9	51	4	30	4
2	Air (O_2/ N_2)	40.3	86	4	6	78	2	0	10

Reaction conditions: Toluene = 5 mL, substrate/ TBHP ratio (mol) = 1:1, catalyst = 1 wt. % AuPdPt/ C, substrate/ metal ratio (mol) = 13000, 20 bar pressure, temperature = 80 °C, time = 24 h

It has been demonstrated that the presence of air is crucial to get a higher conversion. The following experiments investigate the effect of O_2 in this reaction. In order to quantify O_2 these reactions were run with a mixture of He and O_2. The gas phase was analysed after reaction to quantify the amount of O_2 left. Results are shown in Table 4.15. The conversion increases from 16.1 % conversion in the absence of O_2 to 49.3 % conversion with 80 % O_2. Increasing the amount of O_2 to 100 % does not increase conversion further. The analysis of the gas phase shows the use of O_2 in the reaction, almost 10 mmol of O_2 can be introduced into the reaction products (Entry 3). TBHP decomposition involves the formation of O_2 (Figure 4.6). In the absence of O_2 in gas phase, O_2 from TBHP would participate in the oxidation of toluene. The increase of conversion in the presence of O_2 in gas phase suggests the combination of O_2 and TBHP has a promoting effect for the oxidation of toluene. Moreover, this proved the activation of molecular O_2 at 80 °C.

Regarding to Pathan *et al* study, where TBHP is only an initiator and O_2 the only oxidant, in the current work TBHP would be the initiator and the oxidant as well as O_2.

Table 4.15: Role of oxygen for toluene oxidation: Oxygen quantification

Entry	Condition	Conversion (%)		O_2 in reactor (mmol)	O_2 used from O_2 gas (%)
		Toluene	TBHP		
1	He	16.1	87	0	–
2	He/ O_2 (20%)	30.7	76	4	100
3	He/ O_2 (50%)	39.7	76	10	98
4	He/ O_2 (80%)	49.3	77	17	52
5	O_2	49.6	85	20	34

Reaction conditions: Toluene = 5 mL, substrate/ TBHP ratio (mol) = 1:1, catalyst = 1 wt. % AuPdPt/ C, substrate/ metal ratio (mol) = 13000, 20 bar pressure, temperature = 80 °C, time = 24 h

Table 4.16 shows the selectivity to products for the reactions described in the previous paragraph.

Figure 4.11 shows the evolution of the selectivity for each product depending on conversion for toluene oxidation using 1 wt. % AuPdPt/ C. The empty symbols and the dotted lines show data and trend respectively corresponding at reaction under atmospheric pressure. The full symbols represent the data from reaction under pressure found also in Table 4.16.

Table 4.16: Role of oxygen for toluene oxidation: Products selectivity

Entry	Condition	Selectivity (%)					
		Benzyl alcohol	Benzal-dehyde	Benzoic acid	Benzaldehyde dimethyl acetal	Methyl benzoate	CO_2
1	He	5	11	48	3	30	3
2	He/ O_2 (20%)	2	3	81	2	5	7
3	He/ O_2 (50%)	2	4	82	1	0	11
4	He/ O_2 (80%)	3	5	82	1	0	9
5	O_2	3	4	86	1	0	6

Reaction conditions: Toluene = 5 mL, substrate/ TBHP ratio (mol) = 1:1, catalyst = 1 wt. % AuPdPt/ C, substrate/ metal ratio (mol) = 13000, 20 bar pressure, temperature = 80 °C, time = 24 h
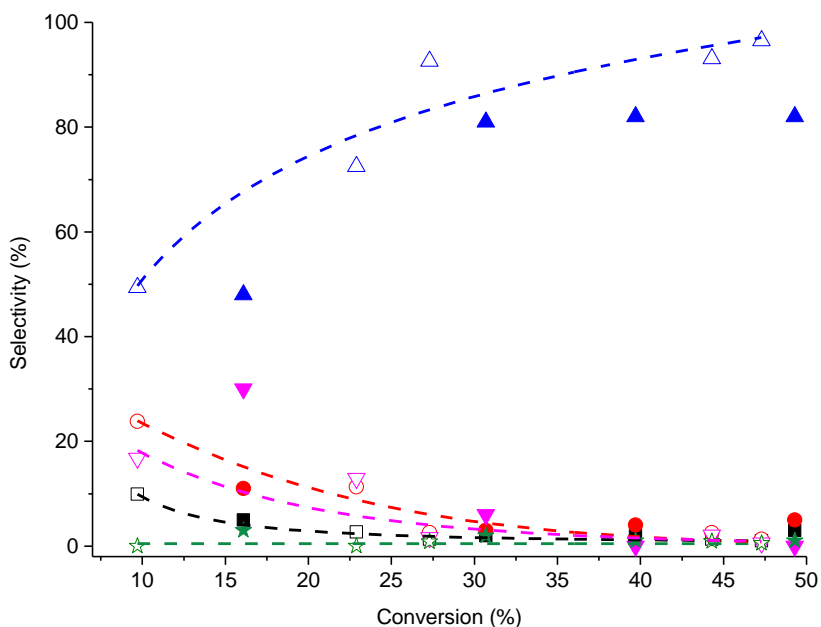

Figure 4.11: Products selectivity function of conversion for bench and autoclave reactions.
Empty symbol and dotted line: Selectivity and trend for bench reactions. Full symbol: Autoclave reactions

In autoclave, the selectivity follows a similar trend to that obtained using the bench reaction. Benzoic acid selectivity increases with the conversion whereas others products decrease. Methyl benzoate is the second major product when there is no O_2 in the reaction but its selectivity decreases as soon as O_2 is present and methyl benzoate is not produced when O_2 increases in the reaction.

The absence of methyl ester with addition of O_2 indicates a change of mechanism from TBHP decomposition. Methyl ester is supposed to be formed by the coupling of benzoic acid with methanol, suggesting the absence of methanol in the reaction mixture. This could be explained by Le Chatelier's principle shifting the equilibrium, such as O_2 wouldn't be formed in favour of the peroxide species (Figure 4.6, Molecule 7) instead of forming methanol (Figure 4.6, Entry 8, Molecule 11). The same process could happen for the other peroxy species (Figure 4.6, Entry 2, 3, 6 and 7); less by-products would be formed from TBHP, resulting in no formation of methylester.

Experiments were conducted to investigate the decomposition of TBHP in the presence of pure O_2. A reaction in autoclave, with water instead of toluene and in the absence of catalyst, shows 53 % decomposition of TBHP. The addition of catalyst to this system increases the decomposition up to 96 %. Same experiment under atmospheric pressure had a TBHP decomposition of 1 %, indicating that TBHP decomposition is facilitate by the presence of O_2. Hence, the presence of O_2 does not stop TBHP decomposition. Further experiments and analysis would be essential to ascertain the mechanism.

7.2. Effect of different TBHP/ Toluene ratios

The effect of TBHP/ toluene ratio has been investigated previously under atmospheric pressure showing that doubling the amount of TBHP did not increase the conversion. For this experiment a range (0.3 to 1.4) of different ratios were tested in order to find the best conditions for this reaction. Figure 4.12 shows an increase in conversion with the ratio increasing. However, the rate decreases with a ratio higher than 1, a TBHP/ toluene ratio does not increase the conversion significantly.

As seen previously, TBHP decomposition produces O_2 and can also integrate O_2 to produce other molecules. Increasing the TBHP/ toluene ratio increases the consumption of O_2, as shown in Figure 4.12 (number in bracket). The presence of O_2 is important as, without it, a lower conversion is obtained. The mechanism of O_2 integration is not certain, however it can be presumed that in the presence of TBHP, O_2 is activated and

subsequently incorporated into the products. Further experiments using $^{18}O_2$ in the gas phase would help to understand the mechanism and confirm the origin of O_2.
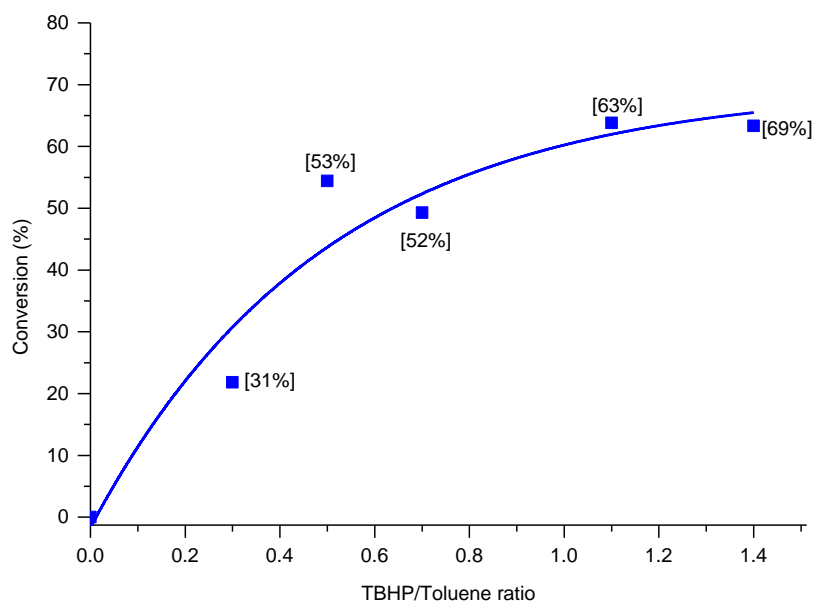

Figure 4.12: Toluene oxidation at 80 ºC using various amount of TBHP and 1 wt. % AuPdPt/ C [X %]: amount of O_2 converted
Reaction conditions: Toluene = 5 mL, substrate/ TBHP ratio (mol) = 1:1, substrate/ metal ratio (mol) = 13000, 20 bar pressure (80 % O_2/ 20 % He), temperature = 80 °C, time = 24 h

7.3. Effect of temperature

The previous results show activation and incorporation of O_2 into products at 80 ºC. An experiment at 50 ºC was run to confirm the possibility of O_2 activation at lower temperatures. Entry 2 Table 4.17 shows the result of the oxidation of O_2 at 50 ºC, 15.8 % of toluene was converted with 53 % TBHP consumption. Decreasing the temperature decreases the conversion and also the selectivity for benzoic acid. A reaction at 50 ºC with no O_2 was run (Entry 3) to compare the presence and absence of O_2. The conversion decreases in the absence of O_2 while the TBHP consumption increases. As in the previous result with no O_2 a high amount of methyl ester is produced with no benzoic acid. It is clear that at 50 ºC the presence of O_2 is crucial to increase the conversion and the selectivity for direct products from toluene. It is assumed that O_2 is also being activated under these conditions.

121

Table 4.17: Toluene oxidation at 50 ºC

Entry	T (ºC)	Gas	Conversion (%)		Selectivity (%)					
			Toluene	TBHP	Benzyl alcohol	Benzal-dehyde	Benzoic acid	Benzaldehyde dimethyl acetal	Methyl benzoate	CO_2
1	80	O_2	49.6	85	3	4	86	1	0	5
2	50	O_2	15.8	53	10	14	67	6	0	2
3	50	N_2	6.9	81	8	26	0	10	49	8

Reaction conditions: Toluene = 5 mL, substrate/ TBHP ratio (mol) = 1:1, substrate/ metal ratio (mol) = 13000, 20 bar pressure, temperature = 80 °C, time = 24 h

8. Conclusions

Au, Pd and Pt have been used to make sol-immobilisation catalysts supported on TiO_2 and C. The morphology of the catalyst has been modified by changing the order of reduction process during the sol-immobilisation method. XPS and STEM were used to characterise them and to confirm the morphology expected.

These catalysts were used for the oxidation of toluene at 80 °C and atmospheric pressure. It was previously shown that at 80 ºC no activation happened in the presence of O_2. H_2O_2 was tested but the insolubility in toluene didn't allow the reaction to occur. Hence, TBHP was used as an oxidant and an initiator for this reaction. Carbon supported catalysts gave better activity than TiO_2 supported. The presence of Au seems to be crucial with promotional effects resulting from the addition of Pd and Pt. A conversion of 27.3 % after 24 h with benzoic acid as a major product was achieved with 1 wt. % AuPdPt/ C at 80 ºC. In the literature, few studies have been done under the same conditions (i.e. oxidant, temperature, time) using a different catalyst. Tilley and co-workers reported 7.97 % toluene conversion with 63.8 % selectivity for benzaldehyde using CoSBA-15.[25] Singh *et al* used chromium silicalite-1 (CrS-1) to oxidise 18.4 % of toluene into benzaldehyde (23.3 %), benzoic acid (25.7 %) and dibenzyl (45.1 %).[26] Finally, 67.5 % conversion of toluene and 45 % selectivity for benzoic acid were reached by Ma and co-workers using a nitrogen-doped sp^2-hybridised carbon catalyst.[27]

The selectivity for products is dependent on the conversion. At low conversion, the first products of oxidation, benzyl alcohol and benzaldehyde are in majority whereas at higher conversion benzoic acid is the major product.

The time online of catalysts based on Au was investigated. 1 wt. % Au/ C, 1 wt. % AuPd/ C and 1 wt. % AuPdPt/ C show an increase of conversion with time but the rate decreases. With 1 wt. % AuPdPt/ C a conversion of 47 % was reached after 72 h with 97 % selectivity for benzoic acid. This catalyst was tested for reproducibility in order to prove its stability. However the conversion decreased after each use indicating a loss of activity. Deactivation of the catalyst could occur for a couple of reasons: (i) poisoning by by-product or (ii) leaching of the metals. Further experiments need to be done to understand this effect. Characterisation of the catalyst before and after use should be done by microscopy and TGA-MS. Leaching tests would confirm the poisoning of the catalyst or show a deactivation also due to loss of metals.

The same reaction was performed in an autoclave to investigate the use of O_2. Under inert atmosphere the conversion decreases while the addition of O_2 increases the conversion, indicating the activation of O_2 in this reaction. The formation of CO_2 has also been revealed. The amount of TBHP and temperature were investigated showing the activation of O_2 with increasing TBHP and the possibility of O_2 activation at 50 ℃. Therefore this reaction use both TBHP and O_2 in order to oxidise toluene. Reactions at lower temperature (i.e. room temperature) would show the possibility to activate O_2 for toluene oxidation.

Further characterisations of catalyst would be important to determine the active sites. It would also reveal the role of the addition of each metal; Pd then Pt, and their interaction with each other.

Finally, investigations with labelled $^{18}O_2$ experiments are needed to understand the mechanism. However it is already been shown that (i) without catalyst the reaction cannot occurs (ii) without TBHP the reaction cannot occurs either (iii) O_2 is activated and allows the formation of toluene oxidation products.

9. References

1. Huang, G., Wang, A.P., Liu, S.Y., Guo, Y.A., Zhou, H. and Zhao, S.K., *Catalysis Letters,* 2007. **114**, p. 174-177.

2. Wen, S., Xiao-li, W., Zhen-hua, Z., Ke-qiang, D., Xian-feng, L. and Gong-de, W., *Journal of Molecular Catalysis,* 2013.

3. Kesavan, L., Tiruvalam, R., Ab Rahim, M.H., bin Saiman, M.I., Enache, D.I., Jenkins, R.L., Dimitratos, N., Lopez-Sanchez, J.A., Taylor, S.H., Knight, D.W., Kiely, C.J. and Hutchings, G.J., *Science,* 2011. **331** (6014), p. 195-199.

4.   Sankar, M., Nowicka, E., Carter, E., Murphy, D.M., Knight, D.W., Bethell, D. and Hutchings, G.J., *Nature Communications,* 2014, p. Article 3332.

5.   Li, Y., Huang, X., Li, Y., Xu, Y., Wang, Y., Zhu, E., Duan, X. and Huang, Y., *Scientific Reports,* 2013. **3**, p. 1-7.

6.   Attekum, P.M.T.M.v. and Trooster, J.M., *Journal of Physics F: Metal Physics,* 1979. **9** (11), p. 2287-2300.

7.   Casaletto, M.P., Longo, A., Martorana, A., Prestianni, A. and Venezia1, A.M., *Surface and Interface Analysis,* 2006. **38**, p. 215-218.

8.   Vedrine, J.c., Dufaux, M., Naccache, C. and Imelik, B., *Journal of the Chemical Society, Faraday Transactions 1: Physical Chemistry in Condensed Phases,* 1978. **74**, p. 440-449.

9.   Peneau, V., He, Q., Shaw, G., Kondrat, S.A., Davies, T.E., Miedziak, P., Forde, M., Dimitratos, N., Kiely, C.J. and Hutchings, G.J., *Physical Chemistry Chemical Physics,* 2013. **15** (26), p. 10636-10644.

10.   Tiruvalam, R.C., Pritchard, J.C., Dimitratos, N., Lopez-Sanchez, J.A., Edwards, J.K., Carley, A.F., Hutchings, G.J. and Kiely, C.J., *Faraday Discussions,* 2011. **152**, p. 63.

11.   Sanchez-Polo, M., Gunten, U.v. and Rivera-Utrilla, J., *Water Research,* 2005. **39**, p. 3189-3198.

12.   Rivera-Utrilla, J. and Sánchez-Polo, M., *Applied Catalysis B: Environmental,* 2002. **39**, p. 319-329.

13.   Li, X., Heryadi, D. and Gewirth, A.A., *Langmuir : the ACS journal of surfaces and colloids,* 2005. **21**, p. 9251-9259.

14.   Feng, Y.-Y., Liu, Z.-H., Xu, Y., Wang, P., Wang, W.-H. and Kong, D.-S., *Journal of Power Sources,* 2013. **232**, p. 99-105.

15.   Brodsky, C.N., Young, A.P., Ng, K.C., Kuo, C.-H. and Tsung, C.-K., *ACS Nano,* 2014. **8** (9), p. 9368-9378.

16.   Taufany, F., Pan, C.-J., Rick, J., Chou, H.-L., Tsai, M.-C., Hwang, B.-J., Liu, D.-G., Lee, J.-F., Tang, M.-T., Lee, Y.-C. and Chen, C.-I., *ACS Nano,* 2001. **5** (12), p. 9370-9381.

17.   Tedsree, K., Li, T., Jones, S., Chan, C.W.A., Yu, K.M.K., Bagot, P.A.J., Marquis, E.A., Smith, G.D.W. and Tsang, S.C.E., *Nature Nanotechnology,* 2011. **6**, p. 302-307.

18.   Bennett, J.E., *Journal of the Chemical Society, Faraday Transactions,* 1990. **86** (19), p. 3247-3252.

19.   Cheng, X.-M., Wang, Q.-D., Li, J.-Q., Wang, J.-B. and Li, X.-Y., *Journal of Physical Chemistry,* 2012. **116**, p. 9811-9818.

20.   Edwards, J.K., Ntainjua, E., Carley, A.F., Herzing, A.A., Kiely, C.J. and Hutchings, G.J., *Angewandte Chemie,* 2009. **48** (45), p. 8512-5.

21.   Pritchard, J., Kesavan, L., Piccinini, M., He, Q., Tiruvalam, R., Dimitratos, N., Lopez-Sanchez, J.A., Carley, A.F., Edwards, J.K., Kiely, C.J. and Hutchings, G.J., *Langmuir: the ACS journal of surfaces and colloids,* 2010. **26** (21), p. 16568-77.

22.   Edwards, J.K., Carley, A.F., Herzing, A.A., Kiely, C.J. and Hutchings, G.J., *Faraday Discussions,* 2008. **138**, p. 225-239.

23.   He, Q., Miedziak, P.J., Kesavan, L., Dimitratos, N., Sankar, M., Lopez-Sanchez, J.A., Forde, M.M., Edwards, J.K., Knight, D.W., Taylor, S.H., Kiely, C.J. and Hutchings, G.J., *Faraday Discussions,* 2013. **162**, p. 365-378.

24.   Pathan, S. and Patel, A., *Chemical Engineering Journal,* 2014. **243**, p. 183-191.

25.   Brutchey, R.L., Drake, I.J., Bell, A.T. and Tilley, T.D., *Chemical Communications,* 2005, p. 3736-3738.

26.   Singh, A.P. and Selvam, T., *Journal of Molecular Catalysis A: Chemical,* 1996. **113**, p. 489-497.

27.   Gao, Y., Hu, G., Zhong, J., Shi, Z., Zhu, Y., Su, D.S., Wang, J., Bao, X. and Ma, D., *Angewandte Chemie, International Edition,* 2013. **52**, p. 2109-2113.

Propane Oxidation using H$_2$O$_2$ 5

1. Introduction

The valorisation of propane into partially oxygenated products allows the formation of plastic or synthetic fibres as well as fine chemical.[1]

As seen previously, the partial oxidation of alkane requires the activation of C-H bond. High energy is needed to activate C-H bond and often this energy is enough to over-oxidise the first oxygenates or to break C-C bonds.[2, 3] Hence, low condition reactions are desirable.

Previously, the direct oxidation of low alkane to partially oxygenated products was carried out at high temperature and operates at low conversion.[4] The oxidation of propane in the gas phase to acrylic acid or acrolein using mixed metal oxides has been well studied.[5]

Few studies have looked at liquid phase reactions. Clerici reported the oxidation of propane using H$_2$O$_2$ and various solvent. Acetone and isopropyl alcohol are produced in presence of TS-1 catalyst. TS-1 as also been used to produce H$_2$O$_2$ *in situ.* from gaseous H$_2$ and O$_2$ by Oyama. H$_2$O$_2$ was then utilised for the oxidation of propane. Although *in situ*. H$_2$O$_2$ is cheaper than H$_2$O$_2$, propane conversions and rates are low, at the temperatures utilised.[6, 7]

The aim of this project is to oxidise propane to C$_3$ oxygenate products (propanol, isopropanol, acetone, propanal and propanoic acid) using H$_2$O$_2$ as oxidant. Ideally the utilisation of H$_2$O$_2$ should be 100 % meaning that all H$_2$O$_2$ decomposed should be used in target products.

Following the previous work on methane and ethane oxidation, treated in chapter 1, the catalyst Fe/ ZSM-5 will be used for the liquid phase oxidation of propane.[8, 9] C-C scission are expected with the formation of C_2 (Ethane, ethene, ethanol and acetic acid) and C_1 (methane, methanol, formic acid) products as well as the C_3 products (oxygenates and propene). A systematic study of the effect of reaction condition has been performed to find the best condition in order to reach high conversion and high selectivity for C_3 oxygenate. An acid treatment has been performed on the catalyst in order to remove the metal in surface and test its activity. Catalysts were characterised and compared to the untreated catalyst leading to identify active sites.

Various supports have been tested with different framework; amorphous, mesoporous and MFI structure. Support acidity and treatment of the support have been investigated. And finally the use of other metals alongside a bimetallic system has been studied to gain a wider understanding of this complex oxidation.

2. Fe supported on ZSM-5(30)

Fe/ ZSM-5 (30) was the initial catalyst tested for the oxidation of propane based on previous results for methane and ethane oxidation under the same conditions.[8, 9] Various parameters have been changed to identify the optimum conditions for the oxidation of propane. For all graphs the amount of H_2O_2 consumed and utilised is shown; with the amount consumed being the percentage of H_2O_2 decomposed during the reaction, and utilised the percentage of H_2O_2 from the amount consumed present in the products. Each set of conditions have been tested with the same batch of catalyst and same reactor in order to make a direct comparison.

2.1. Investigation on conditions

2.1.1. Fe loading

Various amount of Fe, from 0 wt. % to 5 wt. %, have been supported on ZSM-5 using a CVI method as describe chapter 2 section 4.2. These catalysts have been tested for the oxidation of propane; the results are shown in Figure 5.1. The conversion of propane increases from 0.9 % to 8 % with Fe content. 8 % is reached with 2.5 wt. % Fe supported on ZSM-5 (30); a higher amount of Fe does not increase the conversion further. The selectivity for oxygenates is approximately 96 % and is stable independently of

conversion. In absence of Fe the consumption of H_2O_2 decreased; however, the utilisation of H_2O_2 is also low as the conversion for propane is low. Increasing the amount of Fe does not increase the use of H_2O_2. But H_2O_2 consumption increases which suggests that H_2O_2 is decomposed by Fe species that are not active for the oxidation of propane. A higher Fe loading increased the amount of active sites for propane conversion in parallel with the decomposition of H_2O_2.

It can be concluded that until 2.5 wt. % loading; the Fe species deposited on ZSM-5 are forming more active species. However, a higher loading than 2.5 wt. % only increase the amount of Fe species that are inactive for propane oxidation.
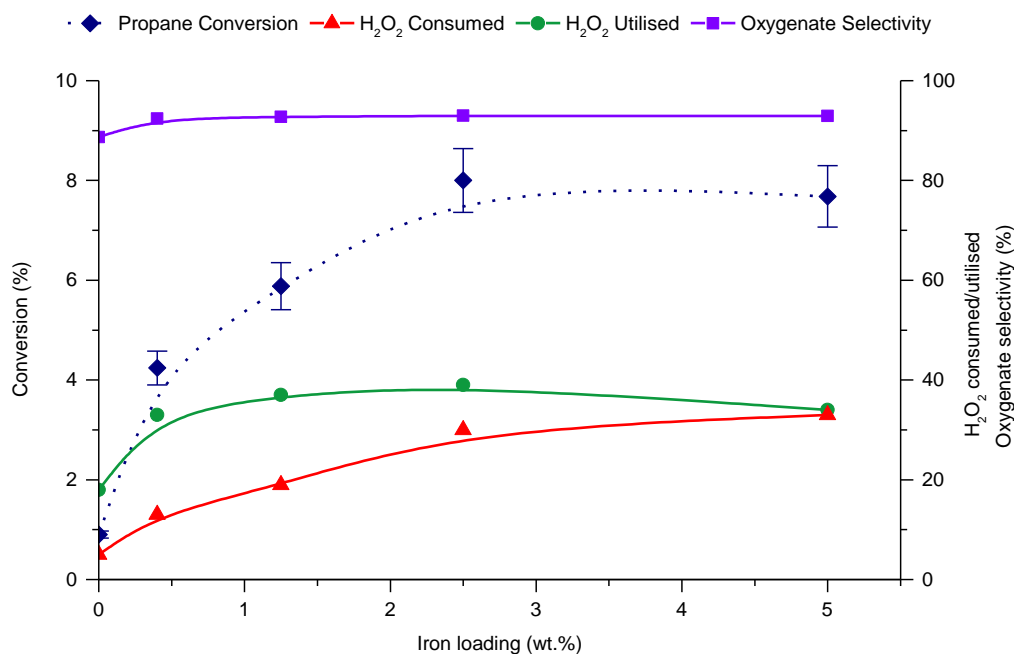
Figure 5.1: Effect of Fe loading on propane oxidation

Reaction condition: $[H_2O_2]$ = 5000 µmol, volume = 10 mL, **0 wt. % to 5 wt. % Fe**/ ZSM-5 (30) = 27 mg, 50 °C, 0.5 h, $P_{Propane}$ = 4 bar (4000 µmol), P_{Total} = 20 bar, stirring = 1500 rpm

For the following experiments all reactions were done with 2.5 wt. % Fe/ ZSM-5 (30) unless otherwise stated.

2.1.2. Effect of temperature

A range of temperatures from 30 ºC to 90 ºC have been tested for propane oxidation using 2.5 wt. % Fe/ ZSM-5 (30) as catalyst. Propane conversion increases with the temperature until 70 ºC where the conversion reaches a maximum of 20 % as shown in Figure 5.2. H_2O_2 follows the same trend and increases until total decomposition at 90 ºC. As the temperature increases the activity for propane conversion and H_2O_2 consumption increases; however, the majority of H_2O_2 being decomposed is not used in products. The amount of H_2O_2 used increases between 30 ºC to 50 ºC; the decrease after suggests that after this temperature H_2O_2 is decomposed at a faster rate than its being utilised. Increasing temperature increases the amount of collision between molecules in the mixture, hence H_2O_2 decomposition increases which subsequently increases the conversion of propane. At too high a temperature, H_2O_2 decomposition into water is higher hence no active species are produce and can be used to convert propane.
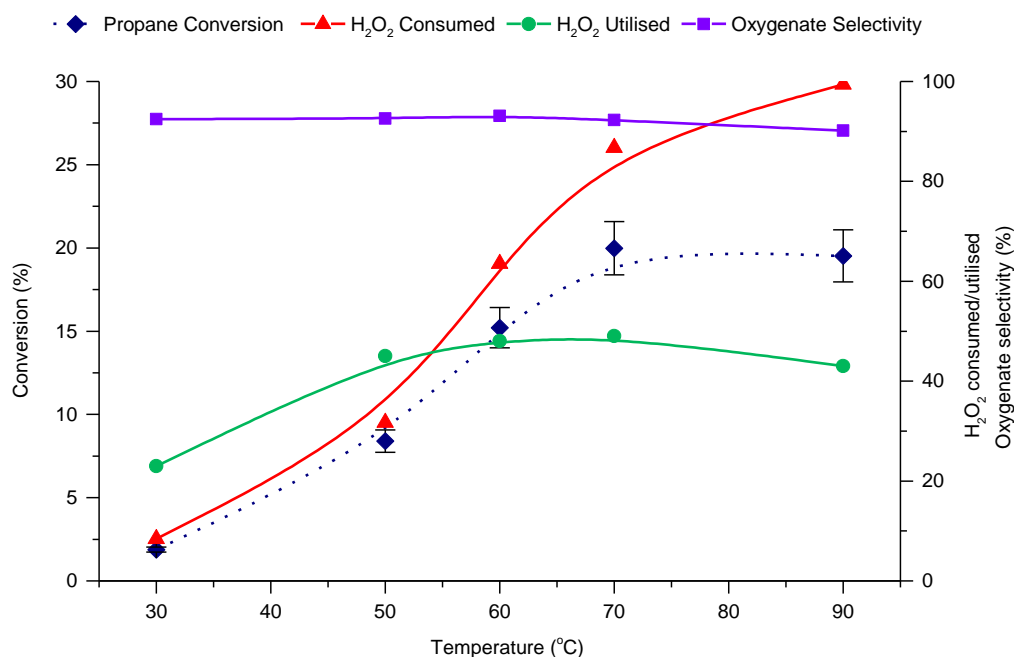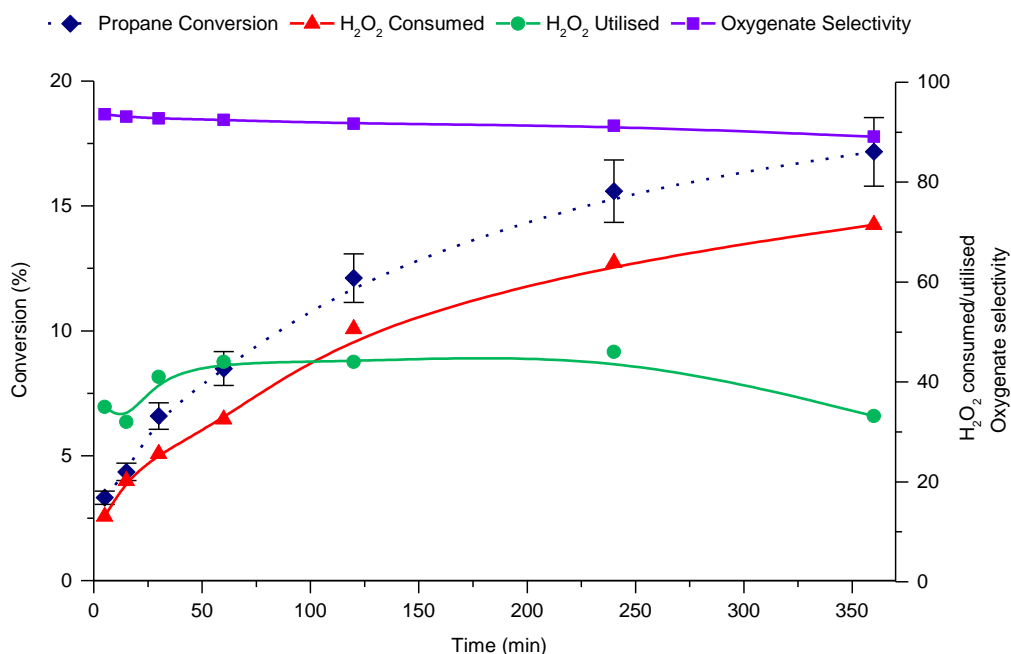

Figure 5.2: Effect of temperature on propane oxidation

Reaction condition: $[H_2O_2]$ = 5000 μmol, volume = 10 mL, 2.5 wt. % Fe/ ZSM-5 (30) = 27 mg, **30 ºC to 90 ºC**, 0.5 h, $P_{Propane}$ = 4 bar (4000 μmol), P_{Total} = 20 bar, stirring = 1500 rpm

2.1.3.   Effect of reaction time

The next parameter evaluated was propane oxidation reaction time, reactions were run from 5 minutes up to 4 h. Figure 5.3 shows that the conversion and H_2O_2 consumed are increasing with time. 17 % conversion is reached after 4 h. This increase is stronger in the first hour and slightly less thereafter. After more time, the conversion reach a limit which will not increase anymore due to the high decomposition of H_2O_2. Conversion does not increase linearly with time, which suggest that the catalyst activity is reduced with time. Previously, when using this system for the oxidation of methane, it has been reported that a small amount of acetone and methanol poisoned the catalyst for methane oxidation.[10] This could explain the decreasing rate of reaction with time. Another explaination could come from the concentration of H_2O_2, it is suppose that a minimal concentration of H_2O_2 could be needed in order to react.

Figure 5.3: Effect of time on propane oxidation

Reaction condition: $[H_2O_2]$ = 5000 µmol, volume = 10 mL, 2.5 wt. % Fe/ ZSM-5 (30) = 27 mg, 50 ºC, **5min to 4h**, $P_{Propane}$ = 4 bar (4000 µmol), P_{Total} = 20 bar, stirring = 1500rpm

2.1.4. Effect of catalyst mass

The effect of catalyst mass on the oxidation of propane was investigated; the results are reported in Figure 5.4. The conversion increases with the mass of catalyst; however, the consumption of H_2O_2 is increasing at a faster rate which accounts for the decrease in H_2O_2 utilisation. Increasing the catalyst mass increases the amount of active sites, thus conversion increases.

Propane is in gas phase; according to Chapoy *et al.* the experimental propane mole fractions in the aqueous phase of the propane–water system at 50 ^{o}C and 20 bar is 1.957.[11] Hence, less than 3% of the total amount propane on the reactor can be dissolve in the liquid phase whereas all catalyst is in the liquid phase decomposing H_2O_2 in a faster rate than converted propane.
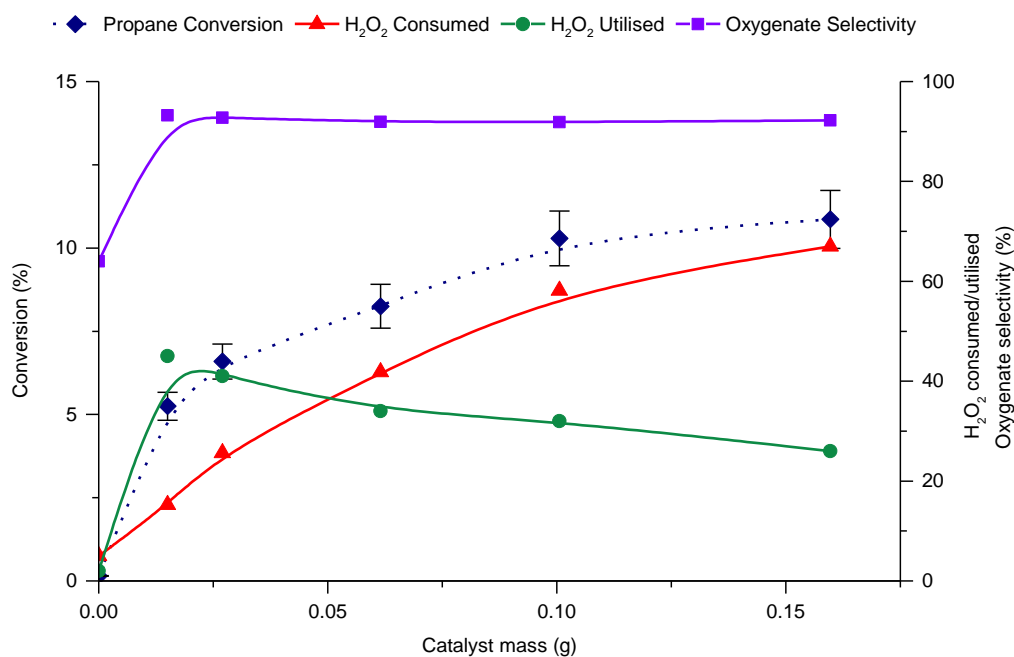
Figure 5.4: Effect of mass of 2.5 wt. % Fe/ ZSM-5 (30) on propane oxidation

Reaction condition: $[H_2O_2]$ = 5000 μmol, volume = 10 mL, 2.5 wt. % Fe/ ZSM-5 (30) = **0 to 170 mg**, 50 ºC, 0.5 h, $P_{Propane}$ = 4 bar (4000 μmol), P_{Total} = 20 bar, stirring = 1500rpm

2.1.5. Effect of H_2O_2

A range of different H_2O_2 concentrations were studied for the oxidation of propane. As shown in Figure 5.5 at low concentration (0.2 mol/ L) the conversion is lower than under standard conditions (0.5 mol/ L). Increasing the concentration increases the conversion linearly until 1 mol/ L, for a higher concentration the rate of conversion is slower with minimal increase between 1 mol/ L and 1.8 mol/ L. H_2O_2 is decomposed by the catalyst; hence, a same active site could be used for H_2O_2 decomposition and propane oxidation. At too high concentration of H_2O_2, the catalyst active sites could be blocked not allowing the activation of propane.

The consumption of H_2O_2 is approximately the same percentage when H_2O_2 concentration increases which means that more H_2O_2 is consumed. With regard to the use of H_2O_2, it decreases slightly with concentration. Increasing H_2O_2 increases the conversion, but at too high concentration the consumption of H_2O_2 is higher than the increase in conversion.
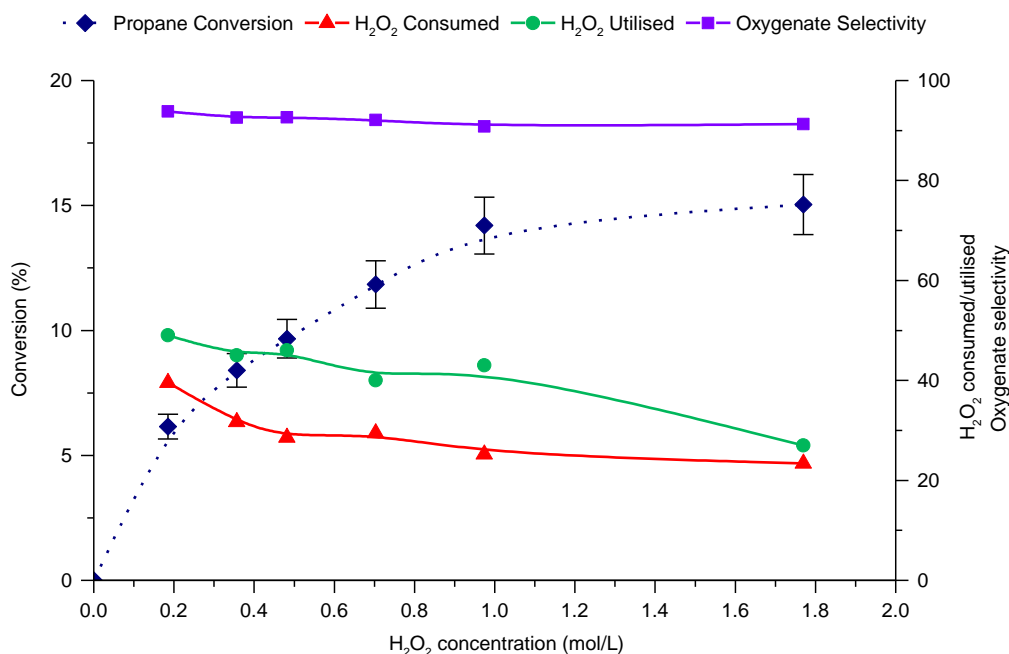

Figure 5.5: Effect of H_2O_2 concentration on propane oxidation

Reaction condition: **[H_2O_2] = 2000 to 18000 µmol**, volume = 10 mL, 2.5 wt. % Fe/ ZSM-5 (30) = 27 mg, 50 ºC, 0.5 h, $P_{Propane}$ = 4 bar (4000 µmol), P_{Total} = 20 bar, stirring = 1500rpm

2.1.6. Effect of stirring speed

The effect of stirring speed on the oxidation of propane was investigated and the results are represented in Figure 5.6. Conversion and H_2O_2 consumption decreases with increasing stirring speed. This is believed to be due to the contact time between substrate and catalyst. It is confirmed with the over oxidation of propane, at low stirring selectivity for acetic acid, formic acid and CO_2 is higher as shown Table 5.1.
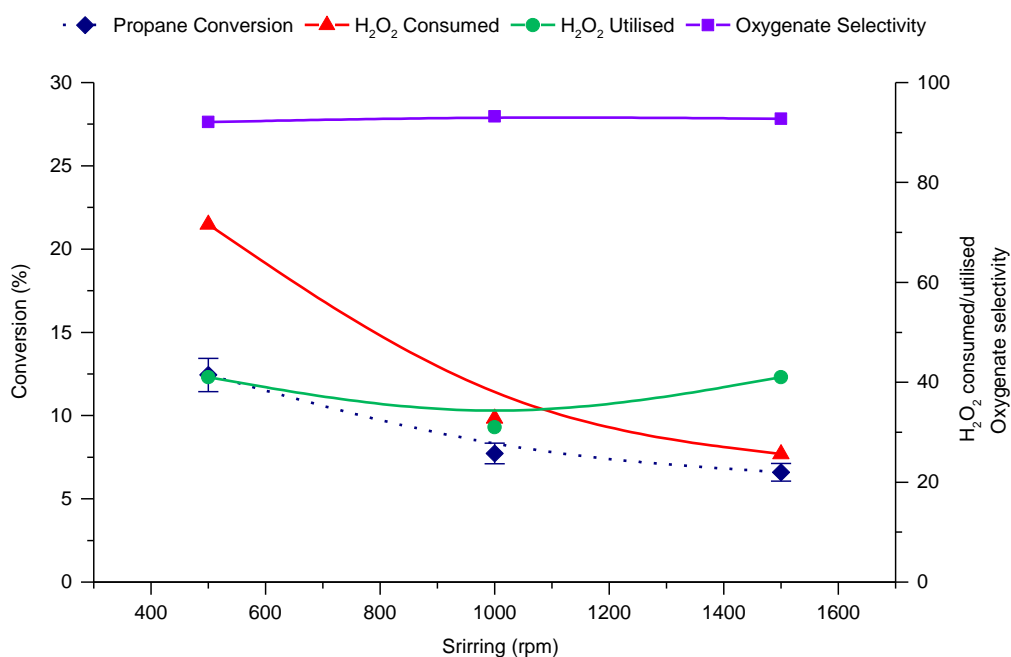

Figure 5.6: Effect stirring on propane oxidation

Reaction condition: $[H_2O_2]$ = 5000 µmol, volume = 10 mL, 2.5 wt. % Fe/ ZSM-5 (30) = 27 mg, 50 ºC, 0.5 h, $P_{Propane}$ = 4 bar (4000 µmol), P_{Total} = 20 bar, **stirring = 500 to 1500rpm**

		Stirring (rpm)		
		500	1000	1500
Selectivity (%)	Acetic acid	25	14	10
	Formic acid	47	35	29
	CO_2	5	2	1

Table 5.1: Selectivity for propane products depending on stirring

Reaction condition: $[H_2O_2]$ = 5000 µmol, volume = 10 mL, 2.5 wt. % Fe/ ZSM-5 (30) = 27 mg, 50 ºC, 0.5 h, $P_{Propane}$ = 4 bar (4000 µmol), P_{Total} = 20 bar, **stirring = 500 to 1500rpm**

2.1.7. Effect of total reaction pressure and partial pressure of propane

Two types of pressure effect were investigated. First the total pressure effect with a constant pressure of propane (4 bar) while He pressure is varied from 0 bar to 16 bar. Changing the total pressure does not have an effect on propane and H_2O_2 conversion and the selectivity is not changed either.

The second investigation, shown Figure 5.7, is the effect of partial pressure of propane (from 1 to 4 bar). Each reaction was topped up with helium to get a total pressure of 20 bar. The conversion increases with a decrease of propane pressure. However, a decrease of pressure means a decrease of moles of propane. The number in bracket is the μmol of propane converted. The amount of final products is decreasing slightly, from 350 μmol to 320 μmol. Hence, the amount of propane converted is similar and independent of the initial propane pressure.
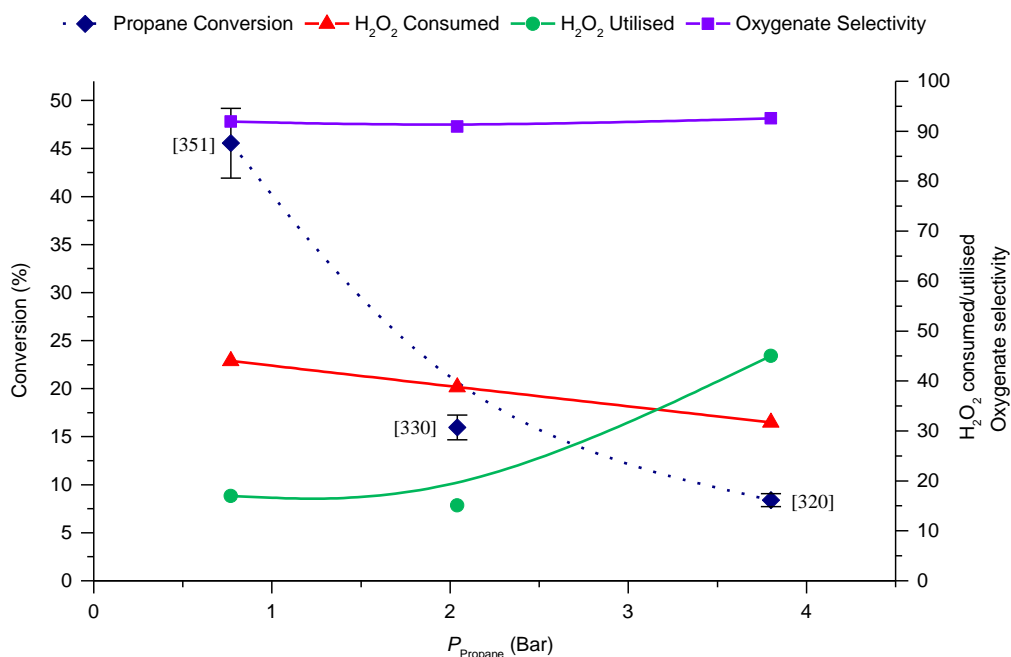

Figure 5.7: Effect partial pressure of propane for propane oxidation

Reaction condition: $[H_2O_2]$ = 5000 μmol, volume = 10 mL, 2.5 wt. % Fe/ ZSM-5 (30) = 27 mg, 50 ºC, 0.5 h, P_{Total} = 20 bar, stirring = 1500 rpm

2.1.8. Optimising the reaction conditions for propane oxidation

To get optimal conditions for propane oxidation reaching a higher conversion is necessary. However, selectivity, consumption of H_2O_2 and its utilisation are also important criteria to consider. A high conversion, high selectivity for C_3 products and low consumption of H_2O_2 with high utilisation on products would be optimal. Using the previous results, the conditions were optimised to try to reach these requirements; the results are reported Table 5.2.

Table 5.2: High conversion condition for propane oxidation

Entry	Conditions	Conversion (%)	Selectivity (%)				H_2O_2 (%)	
			Oxy	C_1	C_2	C_3	Con	Util
1	27 mg cat, 0.5M H_2O_2, 50 °C, 30 min, 4 bar Propane	8.4	95	38	28	34	33	37
2	100 mg cat, 1M H_2O_2, 70 °C, 30 min, 4 bar Propane	33	87	56	27	17	99	29
3	100 mg cat, 1M H_2O_2, 50 °C, 30 min, 4 bar Propane	19	90	48	28	24	52	27
4	100 mg cat, 1M H_2O_2, 50 °C, 120 min, 4 bar Propane	23	88	49	28	23	75	26
5	100 mg cat, 1M H_2O_2, 70 °C, 30 min, 0.8 bar Propane	52	58	64	34	2	97	12

Reaction condition: Volume = 10 mL, 2.5 wt. % Fe/ ZSM-5 (30), P_{Total} = 20 bar, stirring = 1500 rpm

The best conditions from the individual studies were combined and tested. Entry 1 is the data from a standard reaction. Entry 2 shows a 33 % conversion is reached with 87 % oxygenate selectivity after 30 min reaction. However, under these conditions the majority of H_2O_2 is consumed. Decreasing the temperature to 50 °C, Entry 3, slows the H_2O_2 decomposition. In order to increase the conversion, a longer reaction time of 120 min was performed (Entry 4). Between 30 min and 120 min there is only a slight increase in conversion and selectivities remain similar. The reasons for this maybe the decreased H_2O_2 concentration, the decrease in propane pressure and/ or catalyst deactivation. Then, propane pressure was decrease to 0.8 bar, Entry 5, a conversion of 52 % is reached. However, selectivity is towards acetic acid, formic acid and CO_2. In all cases the majority of selectivity is to C_1 products, with low selectivity to C_3.

2.1.9. Conclusion

Selectivities for products have been plot depending on propane conversion for all reaction seen previously. All C_3 products are plot on Figure 5.8. Propanol, isopropanol and propene selectivity decrease with an increase of conversion whereas propanoic acid keep a similar selectivity independently of the conversion. Only acetone has a slight increase with conversion. However, its selectivity stabilise for conversion higher than 10 %.

C_2 products are plot on Figure 5.9. Ethanol, ethane and ethene also decrease with conversion while acetic acid increases from 8 % to 20 % selectivity. Acetic acid is a secondary oxidation product; hence the primary oxidation product such as ethanol is oxidised to form acetic acid.

C_1 products are plot on Figure 5.10. Formic acid and CO_2 increase with conversion. The selectivity for methane, methanol and CO stay low and stable. Formic acid is a product of overoxidation; hence, its increase with conversion is expected.

It can be concluded that for all conditions the trend is the same and selectivities depend on conversion. The selectivity for C_3 products decreases with increase of conversion. C_2 and C_1 products (except ethanol) increase with conversion. At low conversion propanol, IPA and ethanol are predominant. Overoxidation products increase with conversion.

All conditions lead to the same conclusion. 2.5 wt. % Fe/ ZSM-5 (30) is a catalyst with a mild activity for the oxidation of propane. Conversion of 52 % can be reach. However, with high conversion products are overoxidised.
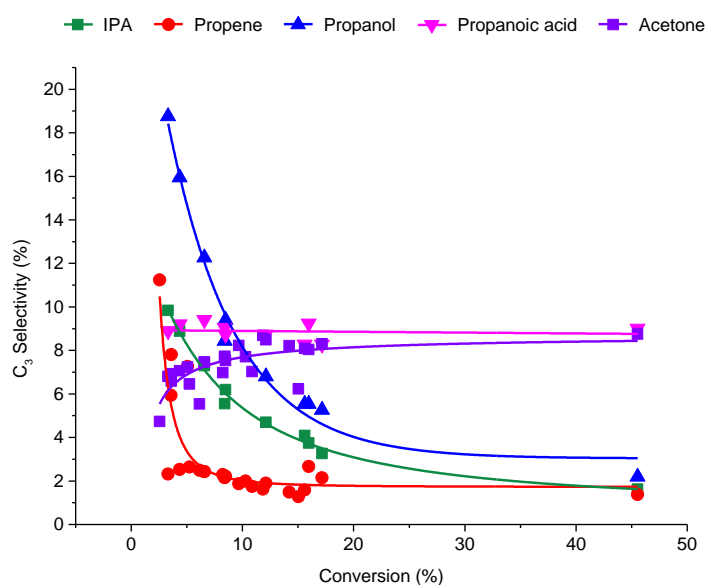

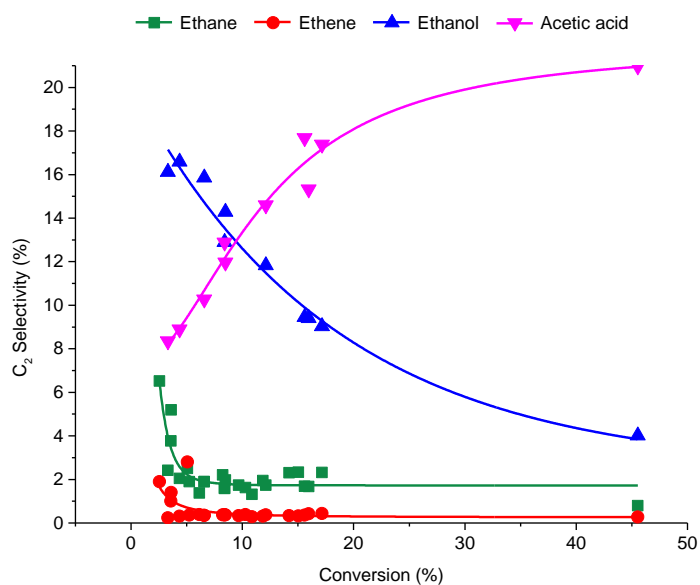**Figure 5.8: Selectivity for C_3 products in function of propane conversion**

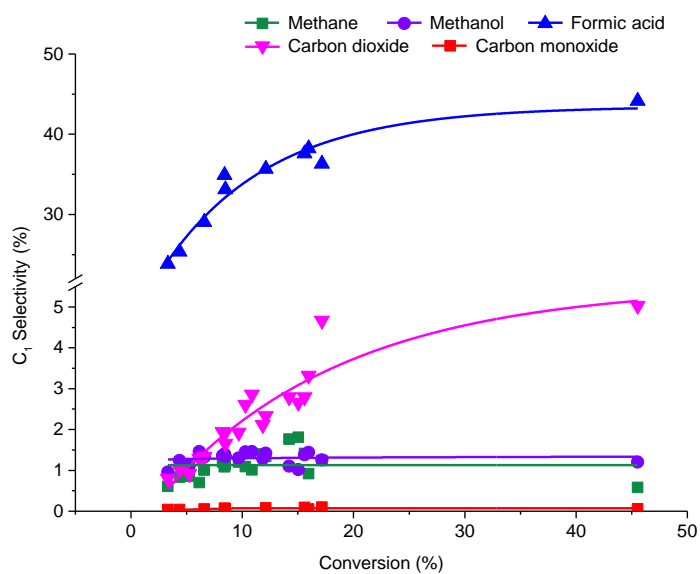**Figure 5.9: Selectivity for C_2 products in function of propane conversion**

Figure 5.10: Selectivity for C_1 products in function of propane conversion

2.2. Investigation of the active phase of 2.5 wt. % Fe/ ZSM-5 (30)

Zecchina *et al* studied the Fe species present on ZSM-5; they reported that Fe$_2$O$_3$ are in the external surface and anchored to the framework via SiOFe or AlOFe bridges as well as Fe cluster are, while Fe^{2+} and Fe^{3+} are grafted in the channel.[12] In order to investigate further the active species of 2.5 wt. % Fe/ ZSM-5 (30), this catalyst was treated by acid to remove the Fe species with a weak interaction to the zeolite and keep the Fe interacting strongly. Catalytic test and characterisation were then performed.

Different types of acid treatment were performed in order to increase or decrease the amount of Fe species removed. Various conditions were changed; time, temperature, acid concentration and finally consecutives treatment on a same sample were studied. However, all treatments have been done using nitric acid. All conditions gave the same results for propane oxidation; time was chosen to illustrate the role of this treatment on the catalyst. Hence, the standard catalyst will be named 2.5 wt. % Fe/ ZSM-5 (30) and the acid treated catalyst will be named by the time of treatment; 15 min, 1 h and 2 h.

2.2.1. Effect of acid treatment for propane oxidation

The set of catalysts prepared by acid treatment were tested for the oxidation of propane under the standard conditions as outlined in the experimental chapter section 6.6. A radical change of colour happens to 2.5 wt. % Fe/ ZSM-5 (30) after treatment, from orange to cream as shown in Figure 5.11. After 15 min treatment propane conversion decreases from 8.2 % to 6.8 % as shown Figure 5.12; conversion does not decrease after a longer time treatment. If these treatments removed Fe species from the surface this implies that most of the actives species are not removed. The aim of the treatment is to remove the surface Fe species which means that the majority of the active species would remain in the zeolite pores. These catalysts have been characterised in order to understand what active species are present and where.
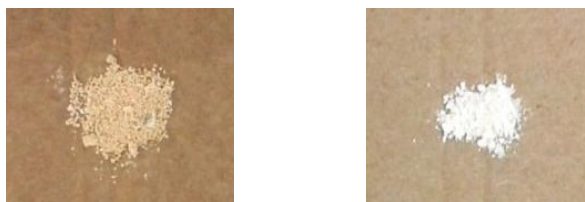

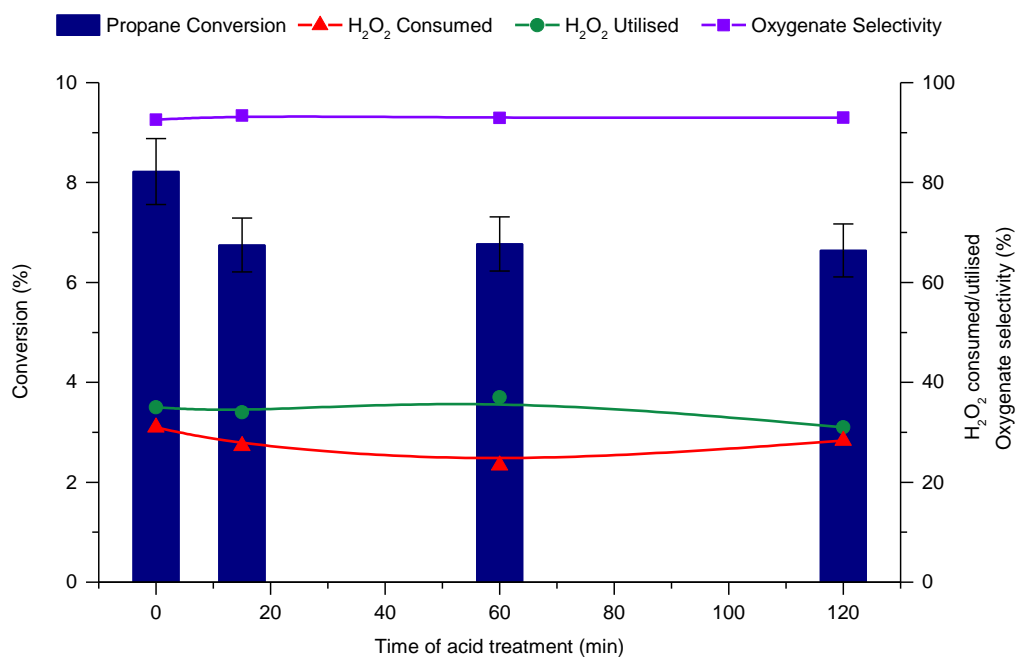**Figure 5.11: Pictures of catalyst before (left) and after treatment (right)**

Figure 5.12: Effect of acid treatment for propane oxidation

Reaction condition: $[H_2O_2]$ = 5000 μmol, volume = 10 mL, 27 mg 2.5 wt. % Fe/ ZSM-5 (30), 50 °C, 0.5 h, $P_{propane}$ = 4 bar (4000 μmol), P_{Total} = 20 bar, stirring = 1500 rpm

2.2.2. Characterisation of standard and acid treated catalysts

2.5 wt. % Fe/ ZSM-5 (30) and acid treated catalyst have been characterised in order to investigate which species are supported on the catalyst, which species are active and the interaction Fe with support. Fe loading has been determined by ICP and XPS analyses allow to ascertain the oxidation state of Fe in surface. STEM, UV-Vis, IR and TPR have been performed to find out the various species. The acid sites could be determined by TPD and solid NMR. Finally, the catalyst morphology has been defined by XRD and BET analysis. This various technique combined surface and bulk analysis in order to establish the closest characterisation of the catalysts.

2.2.2.1. *Fe loading*

Elemental analysis and XPS respectively presented in Table 5.3 and 5.4 and figure 5.13 show the decrease of Fe loading in catalysts. It is obvious that a large part of Fe is removed after acid treatment. A total of 2 wt. % Fe is detected before treatment by ICP, whereas only 0.47 wt. % is present after treatment. XPS analysis is a surface sensitive method and shows that 5.46 at. % of the surface content is made up of Fe suggesting that the repartition of Fe is not homogeneous and more Fe is present on surface than within the pores. In regards to the oxidation states, the signal detected in XPS for Fe is reported in the Table 5.4. This signal could correspond to FeO or Fe_2O_3. Hence, Fe^{II} and Fe^{III} could both be present on the catalyst.

Table 5.3: ICP analysis of acid treated catalyst

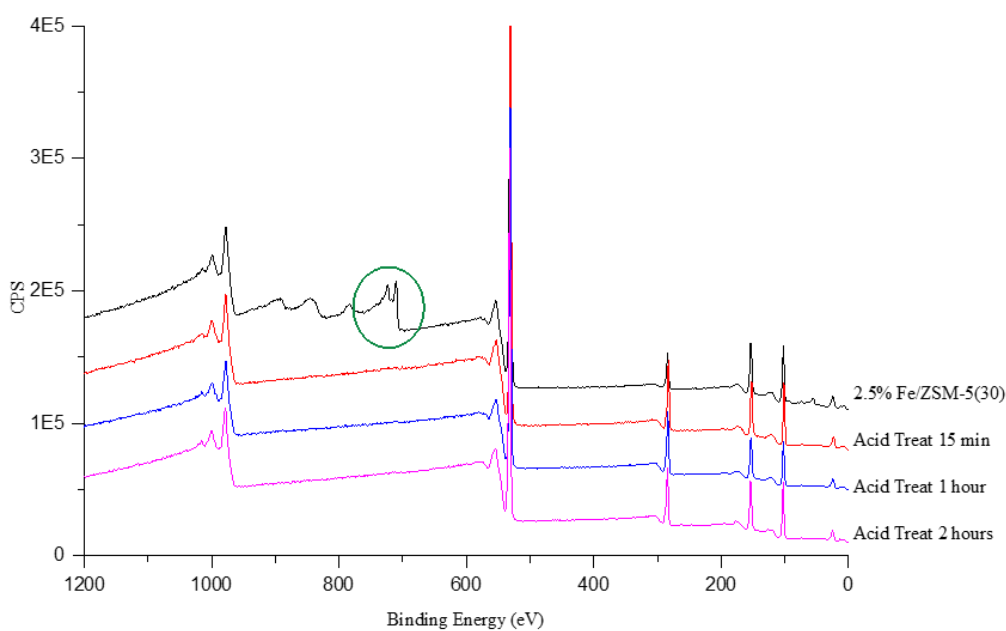| Sample	Fe %
2.5 wt. % Fe/ ZSM-5 (30)	2.06
Acid treatment 15min	0.55
Acid treatment 1 hour	0.5
Acid treatment 2 hours	0.47

Figure 5.13: XPS spectra of acid treated catalyst

Table 5.4: XPS analysis of acid treated catalyst

Catalyst	Binding Energy (eV)[a]				Surface Content (atom %)			
	Fe	O	Si	Al	Fe 2p	O 1s	Si 2p	Al 2p
2.5 wt. % Fe/ ZSM-5 (30)	709.9	530.9	101.9	73.9	5.46	68.72	25.49	0.33
15 min treatment	711.6	531.8	102.8	73.8	0.33	75.15	24.25	0.26
1hour treatment	711.6	531.6	102.6	74.6	0.30	73.37	25.96	0.36
2 hours treatment	711.6	531.6	102.6	73.6	0.18	71.27	28.28	0.28

[a] All binding energies referenced to C 1s=284.7 eV

Catalytic activity of a low loading of Fe due to acid treatment is better than the original low loading of 0.4 wt. % (result shown section 2.1). Propane conversion using 2.5 wt. % Fe/ ZSM-5 (30) after acid treatment is 6.8 % whereas propane conversion using 0.4 wt. % Fe/ ZSM-5 (30) is 4.2 %. This suggests that some specific Fe species are contributing to the activity of 2.5 wt. % Fe/ ZSM-5 (30). Also the structure of the zeolite could be modified by the acid treatment, hence further investigations on the structure of the support and the Fe species were carried out.

2.2.2.2.   *Identification of Fe species*

STEM-HAADF microscopy, Figure 5.14, shows that the surface of the catalyst appears to be coated with a semi-continuous film of Fe, which may be porous. 1 nm to 5 nm Fe$_2$O$_3$ particles are formed under the beam analysis. On image (a) and (b) brighter patches can be observed, it is probably FeOOH species.
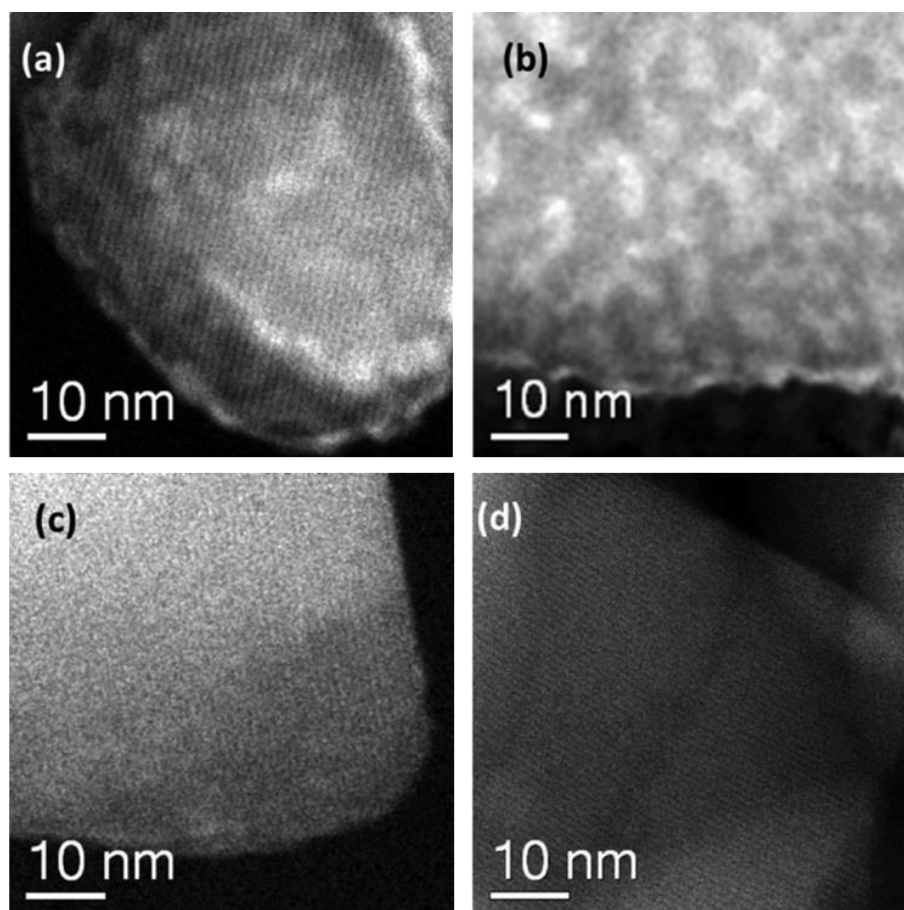

Figure 5.14: STEM-HAADF microscopy of zeolite catalyst (from reference [8])

(a) 0.4 wt. % Fe/ ZSM-5 (30) by CVI, (b) 2.5 wt. % Fe/ ZSM-5 (30) by CVI, (c) and (d) bare ZSM-5 (30) support

Fe species and their interaction with the zeolite have been studied by spectroscopy UV-Vis and infrared (IR). Figure 5.15 shows UV-visible signals. Octahedral Fe (peak at 280 nm), tetrahedral Fe (220 nm), Fe_2O_3 (500 nm) and Fe in small oligonuclear clusters (380 nm) are detected.[13] The drop of intensity between 2.5 wt. % Fe/ ZSM-5 (30) and the acid treated catalyst confirm the loss of a part of the Fe species; Fe_2O_3 and oligonuclear cluster. The signals at 220 nm and 280 nm show the presence of octahedral and tetrahedral Fe^{3+} species after acid treatment.
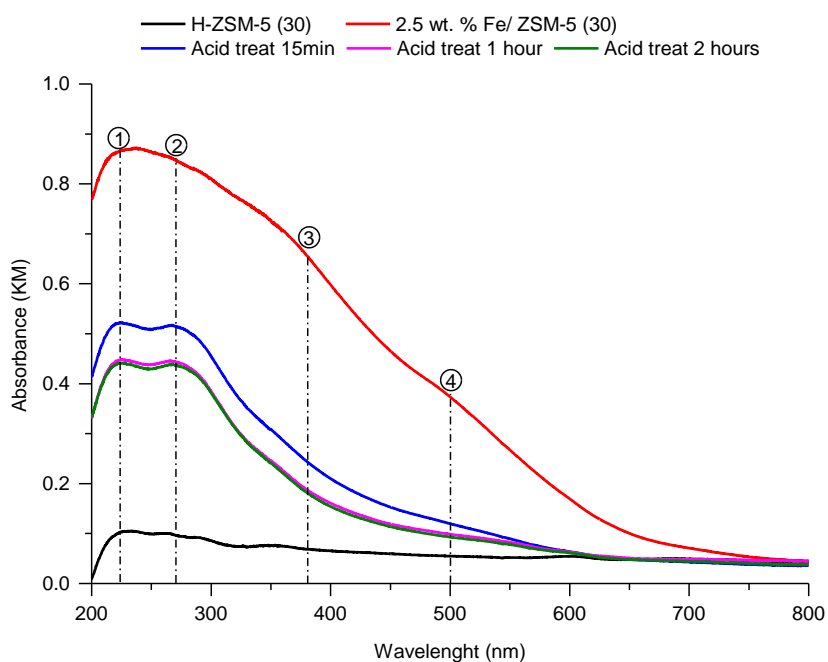

Figure 5.15: UV-Visible analysis of acid treated catalyst

Signal: (1) 220 nm, Td Fe^{3+}; (2) 280 nm, Oh Fe^{3+}; (3) 380 nm, Fe in small oligonuclear clusters; (4) 500 nm, small surface Fe_2O_3 species

The IR spectrum of H-ZSM-5 (30) and 2.5 wt. % Fe/ ZSM-5 (30) in Figure 5.16, show a decrease of the signal at 3737 cm^{-1} with addition of Fe which is attributed to terminal SiOH on ZSM-5 (30). Three other signals decrease with the addition of Fe; the peak attributed to OH groups coordinated to tetrahedrally coordinated framework Al^{3+} (3595 cm^{-1}), the peak attributed to OH groups coordinated to extra-framework T-atoms (3660 cm^{-1}). T-atoms are tetrahedral TO$_4$; T can be Al, Si or Fe in this work. And finally a total disappearance of the band attributed to OH groups in defect sites (hydroxyl nests) at 3700 cm^{-1}. Acid treatment leads to an increase of signals at 3700 cm^{-1} and 3737 cm^{-1}.[14] All signals decreasing with incorporation of Fe suggest that Fe species interact with all possible sites on ZSM-5 (30) while they are removed from a specific site during acid treatment. UV-Vis informs on the presence of Fe^{3+} tetrahedral which also could show a signal at 3660 cm^{-1} in the IR. This peak stays the same with acid treatment which mean OH groups coordinated to extra-framework T-atoms are still at the surface and could be from Fe or ZSM-5. IR spectra does not further inform on which Fe species are interacting with the zeolite and where, but it is assumed that the Fe species interacting with silanols and hydroxyl nests are not active for propane oxidation.
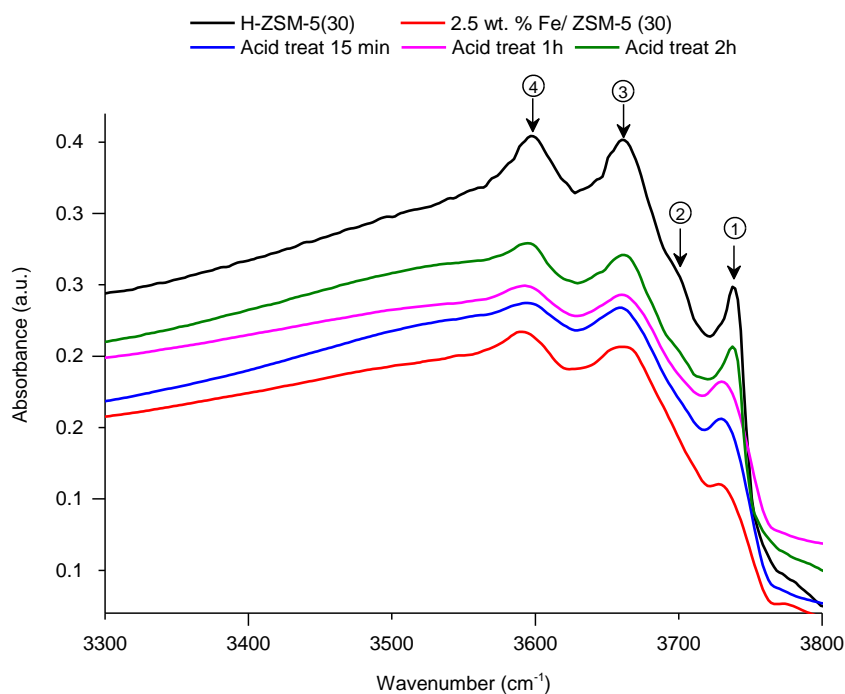

Figure 5.16: Infrared analysis of acid treated catalyst

Signal: (1) 3737 cm^{-1}, Terminal SiOH; (2) 3700 cm^{-1}, OH groups in defect sites (hydroxyl nests); (3) 3660 cm^{-1}, OH groups coordinated to extra-framework T-atoms; (4) 3595 cm^{-1}, OH groups coordinated to tetrahedrally coordinated framework Al^{3+}

In order to study the nature of Fe species present in the catalyst, H_2-TPR studies were performed on the various catalysts and are shown in Figure 5.17. 2.5 wt. % Fe/ ZSM-5 (30) exhibits two reduction peaks. The first peak is at 400 ºC representing the reduction of Fe_2O_3 in Fe_3O_4. The second peak at 520 ºC represents the reduction of Fe_3O_4 to FeO or Fe.[15, 16] These signals disappear with acid treatment suggesting that Fe oxide is removed from the catalyst by acid treatment.
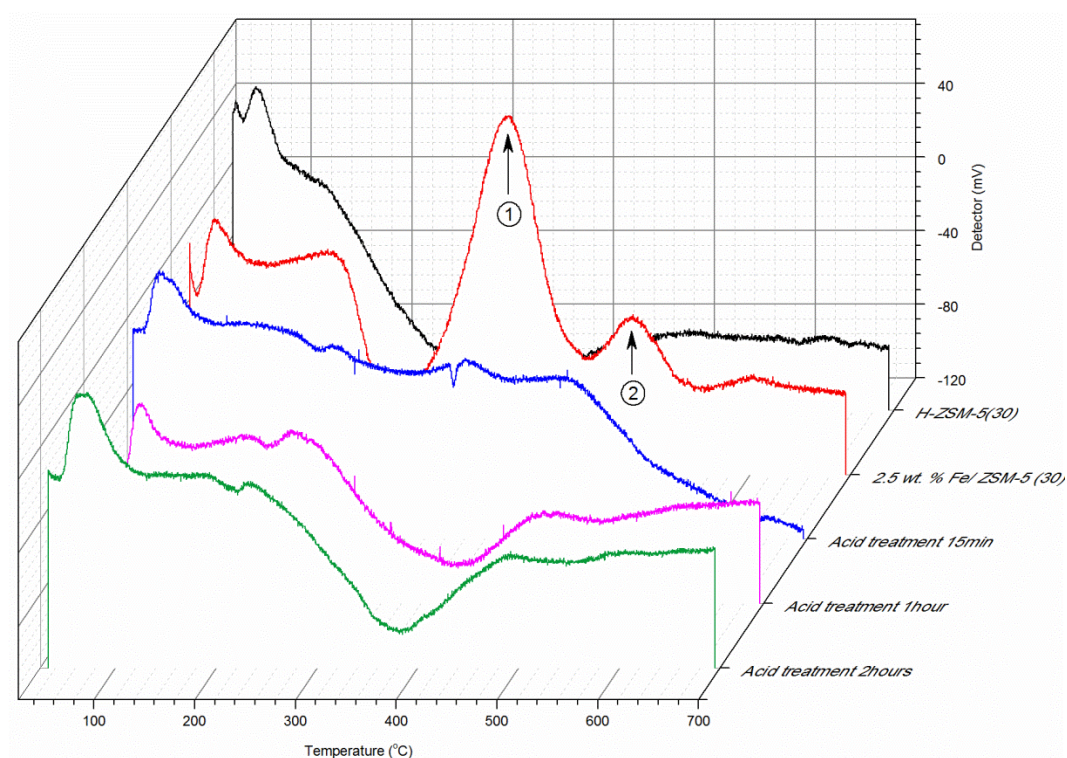

Figure 5.17: TPR analysis of acid treated catalyst
Signal (1): reduction of Fe_2O_3 to $Fe_3O_4^-$; (2): reduction of $Fe_3O_4^-$ to Fe

2.2.2.3.   Acid sites investigation

Different Fe species are interacting with the support giving the support various reactivity. NH_3-TPD was conduct in order to investigate the nature of the acid sites. Bare zeolite possesses two types of acidic sites as shown in Figure 5.18. The TPD peak at 250 ºC which corresponds to weakly adsorbed NH_3 is believed to be due to extra-framework Al (Lewis acid) and the peak at 400 ºC for strongly adsorbed NH_3 is believed to be due to Brønsted framework Al site.[17] An increase of the signal at 250 ºC with Fe loading is

attributed the formation of Fe_2O_3 particle which exposes Lewis acid sites.[18] With acid treatment this signal decreases then increases slightly. With a short acid treatment Fe_2O_3 is removed from the surface, after longer treatment it is believed that dealumination begins to occur giving more Al extra-framework. The strong acidity disappears upon integration of Fe due to the interaction of Fe species with these sites. After acid treatment the loss of Fe causes an increase of these sites. A longer treatment does not have effect. Propane conversion decreases only slightly with acid treatment indicating that the Fe species anchoring at these strong acid sites are not active for propane oxidation.
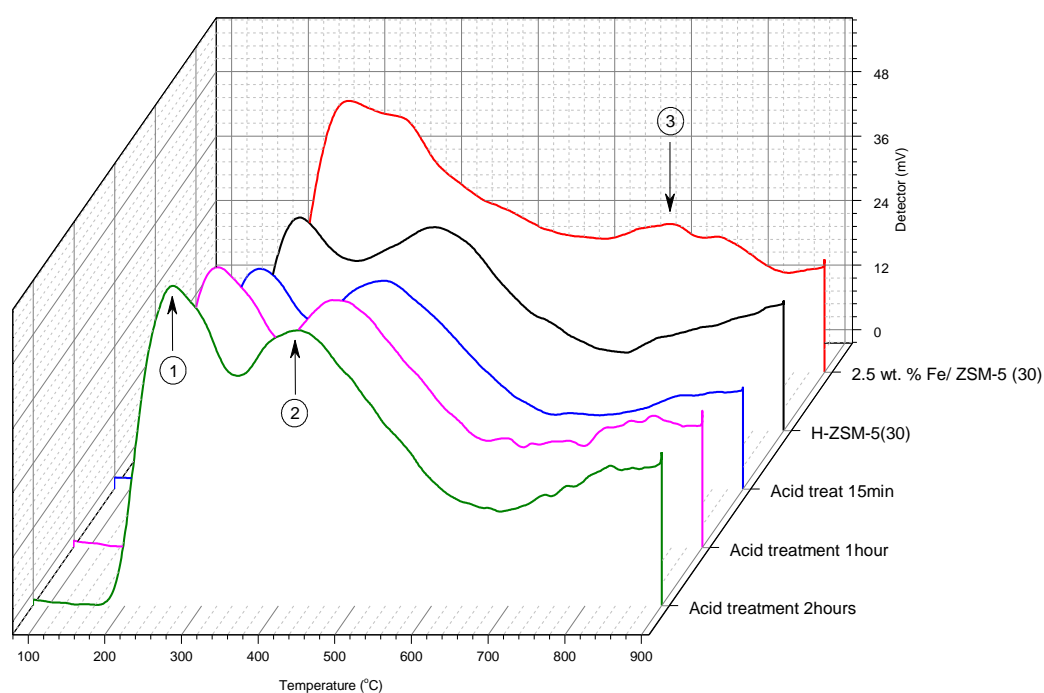

Figure 5.18: TPD analysis of acid treated catalyst
Signal: (1) Weak acid, (2) Strong acid, (3) Fe decomposition

Solid state NMR was performed to identify changes in Al species. Table 5.5 shows a decrease of tetrahedral coordinated Al while the octahedral increases. Due to its paramagnetic properties Fe is not detectable in solid state NMR. Moreover all atoms bond with Fe will be screened, hence they cannot be detected. This explains the significant drop of tetrahedral Al character. Some of these tetrahedral sites can also come out of the framework during the preparation to give octahedral extra-framework Al which goes some way to explain their increase. After acid treatment, large amounts of Fe species are

removed which allow the tetrahedral Al to be detectable in the NMR. The decrease of ratio Td/Oh between H-ZSM-5 (30) and the catalyst acid treated, 10.9 and 8.9 respectively, suggest a dealumination of the catalyst which leads to an increase of octahedral Al.

Table 5.5: Solid NMR of acid treated catalysts

Sample	Td four-coordinated framework*	Oh six-coordinated extra-framework*	Ratio Td/Oh
H-ZSM-5	28044	2576	10.9
2.5 wt. % Fe/ ZSM-5 (30)	18631	3160	5.9
Acid treatment 2 hours	31712	3555	8.9

*Normalised data

2.2.2.4.   Catalyst morphology

XRD analysis provides information about the structure of the zeolite as the nanoparticle sizes are out of the detection limit. Bare zeolite, 2.5 wt. % Fe/ ZSM-5 (30) and acid treated catalysts give a similar spectrum which suggests that the general structure is not affected by acid treatment (Figure 5.19). However the crystallite size has been calculated using the Scherrer equation. Table 5.6 shows results found for each catalyst treated and non-treated. Le crystallite size increases with addition of Fe and decreases after acid treatment. It seems that the acid treatment does not change the crystallite size ZSM-5 support.

Table 5.6: Crystallite size from XRD pattern

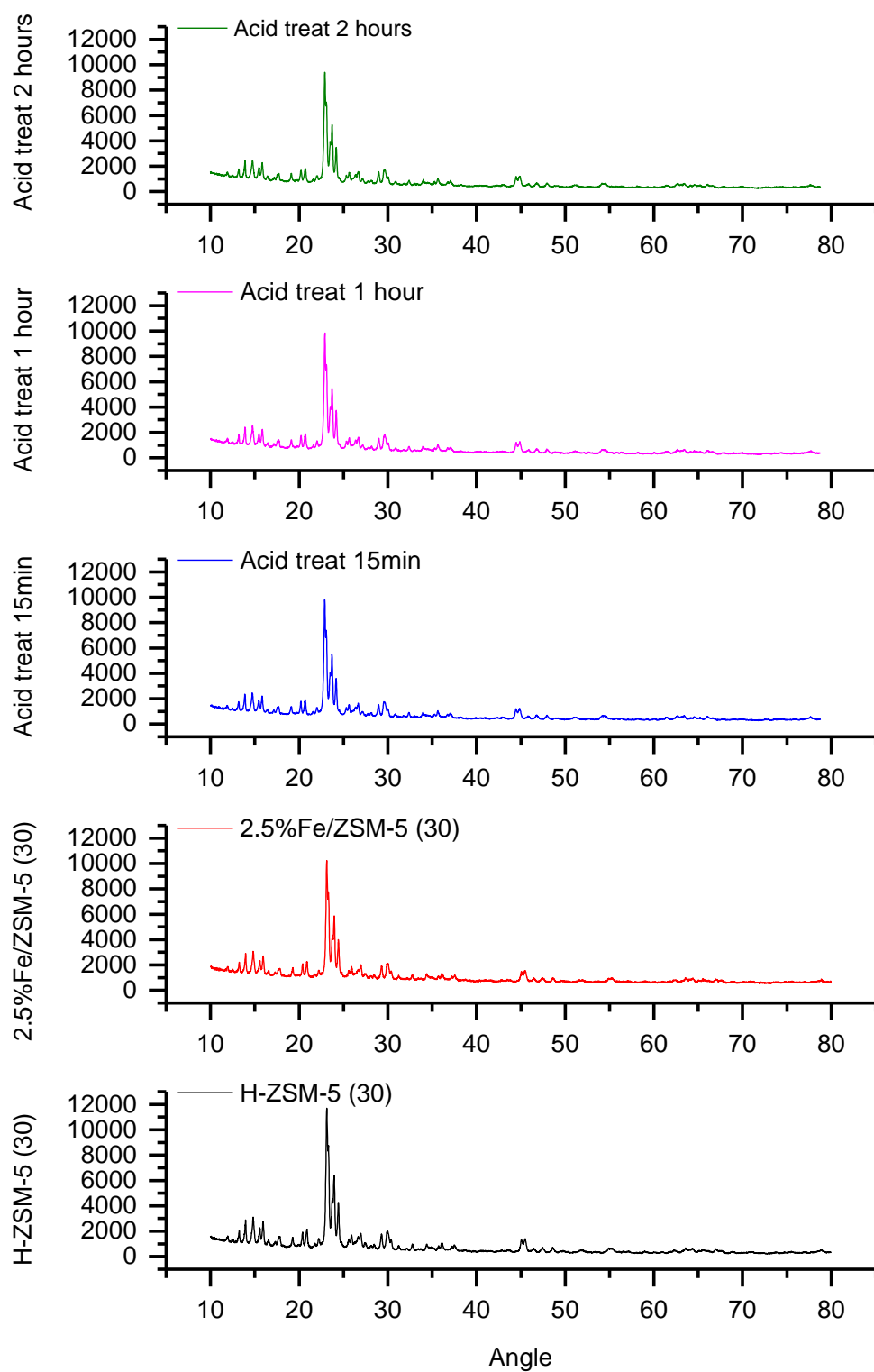| Catalyst	Crystallite size (Å) (highest signal)
H-ZSM-5	619
2.5 wt. % Fe/ ZSM-5 (30)	987
Acid treatment 15min	588
Acid treatment 1 h	629
Acid treatment 2 h	614

Figure 5.19: XRD patterns of acid treated catalyst

Finally the porosity of the acid treated and non-treated catalysts was studied using N_2 adsorption; the results are shown in Figure 5.20. Changes in high mesoporous regions (> 300 Å), are likely the result of N_2 condensation between particles. Picture 1 and 2 represent respectively the porosity of H-ZSM-5 (30) and 2.5 wt. % Fe/ ZSM-5 (30). Slight changes in microporous regions are observed, the volume of pores from 10.0 nm to 12.6 nm decreases with addition of Fe suggesting that Fe species could be interacting in these pores of the zeolite. As shown in Table 5.7, there is a decrease of surface area from 364.2 m^2/ g for H-ZSM-5 (30) to 331.8 m^2/ g for 2.5 wt. % Fe/ ZSM-5 (30) with the addition of Fe.

With acid treatment, the micropores 7.9 nm to 10.0 nm disappear while the volume of pores 10.0 nm to 12.6 nm increases (Picture 3 and 4). This could result from the loss of Fe species from the 7.9 nm to 10.0 nm. Furthermore this treatment could break the structure of the smallest pores to giving pores of 10.0 nm to 12.6 nm. This is supported by the decrease of surface area with acid treatment. However, this has not been reported in literature. Some papers reported no changes in pore volumes after acid treatment [19] or a decrease of micropore volume and surface area with acid treatment.[20] Hence further characterisation would help to clarify this effect.

Table 5.7: BET analysis, surface area for acid treated catalysts

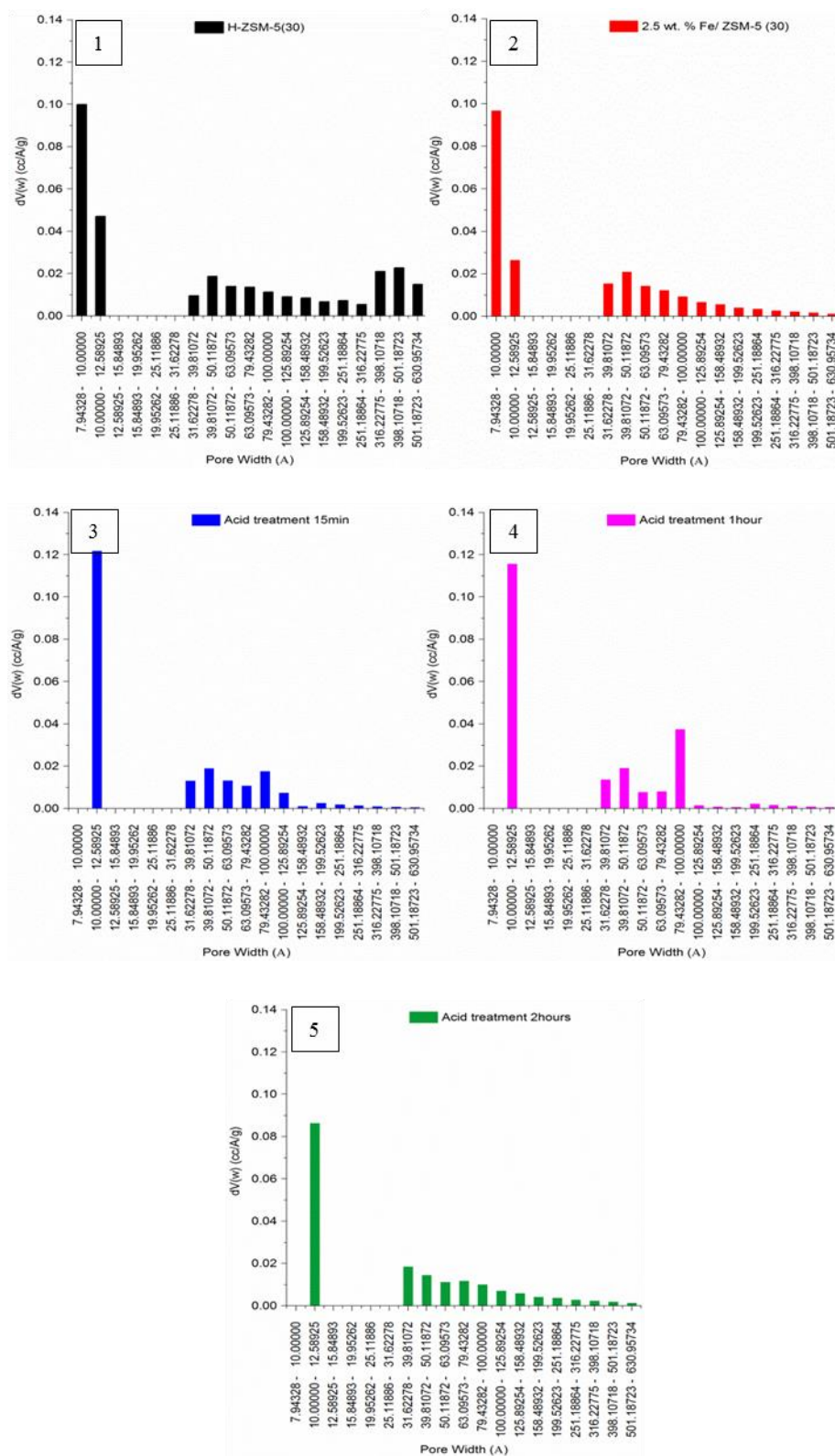| Catalyst	BET surface area (m^2/ g)
H-ZSM-5	364.2
2.5 wt. % Fe/ ZSM-5 (30)	331.8
Acid treatment 15min	319.9
Acid treatment 1 h	_
Acid treatment 2 h	256.7

Figure 5.20: Porosity analysis of acid treated catalyst

Figure (1): H-ZSM-5 (30), (2): 2.5 wt. % Fe/ ZSM-5 (30), (3): 15 min acid treatment, (4): 1h acid treatment, (5): 2h acid treatment

2.2.2.5.   Conclusion on characterisation

Finally it can be concluded that the addition of Fe by CVI to a ZSM-5 (30) support produced a number of Fe species, Fe_2O_3 film, Fe clusters, Td and Oh Fe^{3+}. These species interact with ZSM-5 via terminal SiOH, OH groups coordinated to tetrahedrally coordinated framework Al^{3+}, OH groups coordinated to extra-framework T-atoms and OH groups in hydroxyl nests. The formation of Fe_2O_3 increases the amount of Lewis acidity whereas Brønsted acidity decreases indicating that these sites are used for the interaction between the Fe species and ZSM-5.

During the acid treatment terminal silanols and defect sites increase while Fe_2O_3 and clusters are removed showing the probable interaction of Fe oxide and clusters with terminal SiOH and defect sites. From the previous analysis, it is observed that with treatment, Fe oxide is removed from catalyst and signals for Al^{3+} and SiOH increased. Hence Fe oxide could be the species interacting with Al^{3+} species and SiOH. Acid treatment causes a dealumination of the zeolite increasing the amount of Lewis acid sites. Grafted Fe species within the pores might be the ones still on the catalyst after treatment suggesting their crucial role for the oxidation of propane.

Fe_2O_3 is not the principal active species of 2.5 wt. % Fe/ ZSM-5 as without it the catalyst is still active. This could explain why a low loading as 0.4 % Fe is not as active as 2.5 wt. % Fe. Fe species supported are not only actives species but also inactive. Figure 5.1, section 2.1 of this chapter, showed that after 2.5 wt. % Fe loading, conversion does not increase anymore. The introduction of active site species cannot increase with iron loading. Hence, the interaction Fe/ support has a major role for the activity.

3. *Support investigation*

As seen previously in chapter 1 section 2.3, zeolite materials are formed by Si and Al. Zeolite supports have different properties depending on their constituting atoms and their structures, subsequent treatments can also change the properties of these materials.[21, 22] Therefore few of these properties have been studied as the SiO_2/ Al_2O_3 ratio, the role of the framework and the acidity of the surface. All reactions were performed following the description chapter 2, section 6.6.

3.1. Effect of the zeolite framework

ZSM-5 is a mesostructured MFI structure with cages, channels and uniform pore size distribution. Therefore the framework can have an important role for catalytic activity. Hence, in order to confirm the role of ZSM-5 for the oxidation of propane a number of different supports have been tried and tested.

ZSM-5 is composed of Si and Al, hence a range of supports made from Si and Al were tested. TiO_2 was also tried as it is part of TS-1; a zeolite type catalyst with a MFI structure. Moreover Bravo-Suárez *et al.* reported a high selectivity to oxygenates using Au/ TS-1 for propane oxidation.[6] The bare zeolite H-ZSM-5 (30) has a low conversion compared to the 2.5 wt. % Fe/ ZSM-5 (30) so in order to compare the other supports under the same conditions all supports were tested as bare supports and after the addition of 2.5 wt. % Fe by CVI.

3.1.1. Amorphous framework

Amorphous supports were tested as bare catalyst and with 2.5 wt. % Fe loaded. Bare catalysts show a very low activity as represented Figure 5.21. Amorphous SiO_2/ Al_2O_3 with a ratio of 10 has the best activity for the oxidation of propane, of all the amorphous support producing 8 µmol of products compared to 59 µmol with H-ZSM-5 (30). Fe loaded on these supports give the same trend with a maximum of 16 µmol of products formed with Fe/ SiO_2 compared to 660 µmol with Fe/ ZSM-5 (30) as shown Figure 5.22.
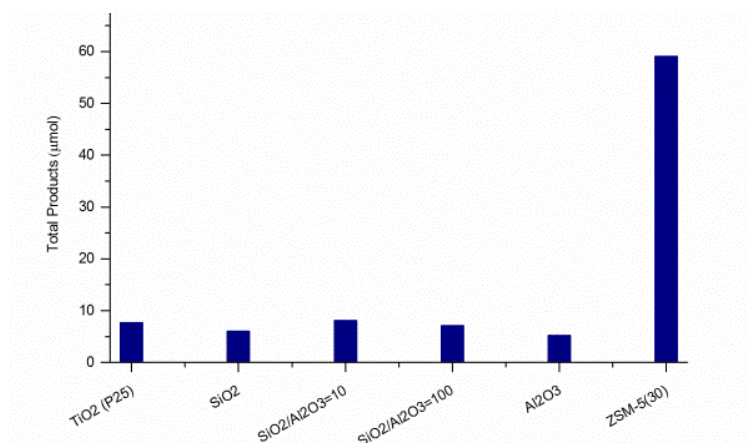

Figure 5.21: Total products for propane reaction with bare amorphous catalyst
Reaction condition: $[H_2O_2]$ = 5000 µmol, volume = 10 mL, 27 mg catalyst, 50 ºC, 0.5 h, $P_{propane}$ = 4 bar (4000 µmol), P_{Total} = 20 bar, stirring = 1500 rpm

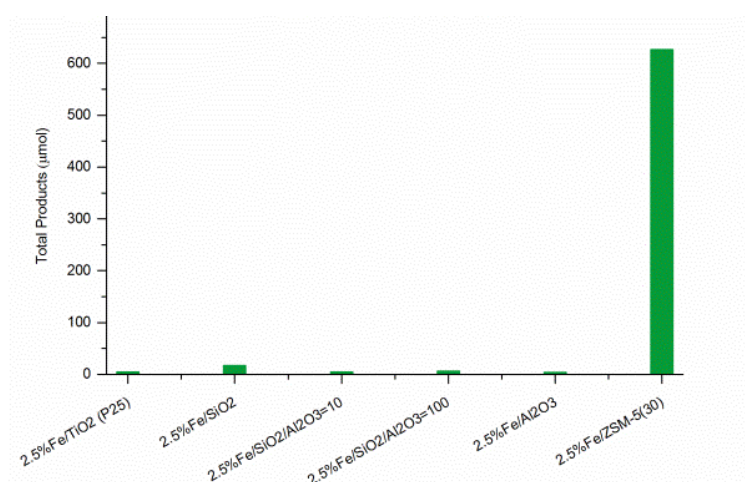**Figure 5.22: Total products for propane reaction with 2.5 wt. % Fe on amorphous support**

Reaction condition: $[H_2O_2]$ = 5000 μmol, volume = 10 mL, 27 mg catalyst, 50 ºC, 0.5 h, $P_{propane}$ = 4 bar (4000 μmol), P_{Total} = 20 bar, stirring = 1500 rpm

3.1.2. Mesoporous framework

Mesoporous catalysts were then tested and lead to similar results as shown in Figure 5.23 and 5.24. HZSM-5 (30) had the highest activity whether bare or when supported with 2.5 wt. % Fe. Bare zeolite Y (30:1) showed the best activity of the rest of mesoporous materials with 16 μmol of products formed.
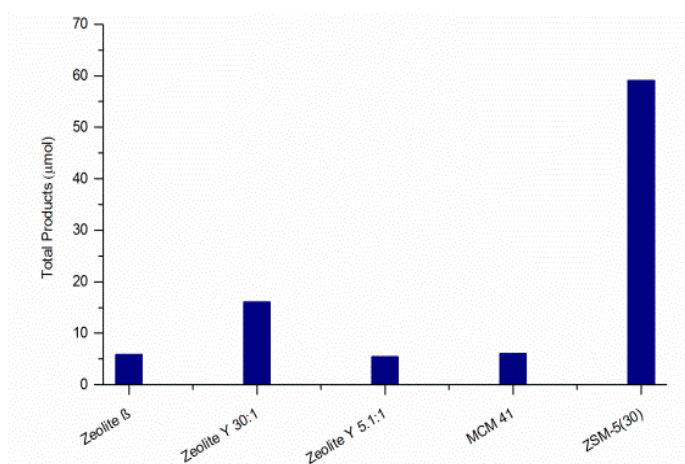

Figure 5.23: Total products for propane reaction with bare mesoporous catalyst
Reaction condition: $[H_2O_2]$ = 5000 μmol, volume = 10 mL, 27 mg catalyst, 50 ºC, 0.5 h, $P_{propane}$ = 4 bar (4000 μmol), P_{Total} = 20 bar, stirring = 1500 rpm
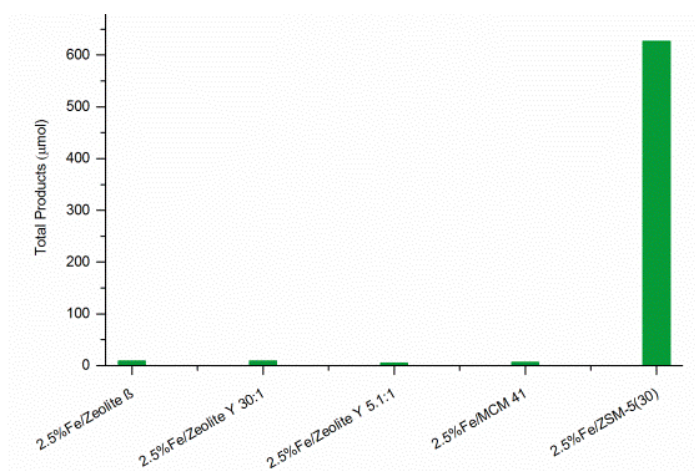
Figure 5.24: Total products for propane reaction with 2.5 wt. % Fe on mesoporous support
Reaction condition: $[H_2O_2]$ = 5000 μmol, volume = 10 mL, 27 mg catalyst, 50 ℃, 0.5 h, $P_{propane}$ = 4 bar (4000 μmol), P_{Total} = 20 bar, stirring = 1500 rpm

3.1.3. MFI framework

Finally materials with MFI framework structure (confirmed by XRD) have been tested for the oxidation of propane and the results are presented in Figure 5.25 and 5.26. Silicalite and TS-1 have the same type of structure as ZSM-5. Silicalite is made of Si, TS-1 with Si and Ti and ZSM-5 with Si and Al. Hence, the result would indicate which species composing the support are important for propane oxidation.

Results show ZSM-5 (30) is the most active catalyst whether Fe is present or not suggesting the importance of the presence of Al in the support.
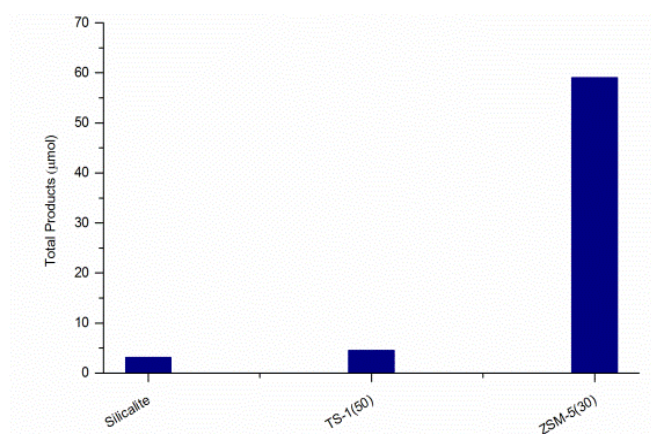

Figure 5.25: Total products for propane reaction with bare MFI catalyst
Reaction condition: $[H_2O_2]$ = 5000 μmol, volume = 10 mL, 27 mg catalyst, 50 ℃, 0.5 h, $P_{propane}$ = 4 bar (4000 μmol), P_{Total} = 20 bar, stirring = 1500 rpm
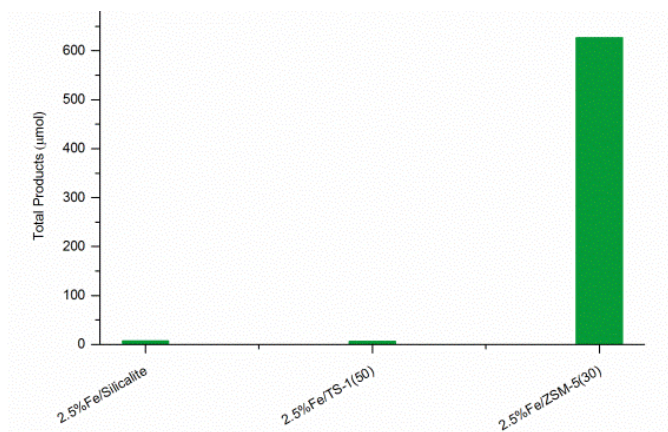
Figure 5.26: Total products for propane reaction with 2.5 wt. % Fe on MFI support
Reaction condition: $[H_2O_2]$ = 5000 µmol, volume = 10 mL, 27 mg catalyst, 50 ℃, 0.5 h, $P_{propane}$ = 4 bar (4000 µmol), P_{Total} = 20 bar, stirring = 1500 rpm

3.1.4. Conclusion

All these experiments show the importance of having a specific framework and composition. It seems that for the material to be active under the standard propane oxidation conditions, a MFI structure containing Al and Si is essential. Unsupported and supported catalysts give the same conclusion; however, the difference of activity is a lot higher for the Fe supported materials. Hence, the ZSM-5 structure must be the best for the addition of Fe in order to form the active species.

3.2. Role of the SiO₂/ Al₂O₃ ratio

Previous reactions showed ZSM-5 to be the best zeolite to oxidise propane. Various ZSM-5 exists which are differentiated by their SiO₂/ Al₂O₃ ratio. A range of ZSM-5 with SiO₂/ Al₂O₃ ratios equal to 23, 30, 50 and 280 have been tested for the oxidation of propane and compared in Figure 5.27 and 5.28. ZSM-5 (30) is still the more active catalyst whether bare or with Fe deposited. However, these catalysts also give reasonable conversion when Fe is added by CVI with 315 µmol to 450 µmol of products. Furthermore the selectivity for products changes as shown in Table 5.8. The selectivity for acetone seems to increase with increasing SiO₂/ Al₂O₃ ratio, contrary to isopropanol which is decreasing. Hence, 21 % acetone selectivity can be reached using 2.5 wt. % Fe/ ZSM-5 (280) and 46 % isopropanol using 2.5 wt. % Fe/ ZSM-5 (23). This catalyst also gives the lowest selectivity for formic acid.

Figure 5.27: Total products for propane reaction with bare ZSM-5 (X) catalyst (X = 23, 30, 50 and 280)

Reaction condition: $[H_2O_2]$ = 5000 μmol, volume = 10 mL, 27 mg catalyst, 50 ºC, 0.5 h, $P_{propane}$ = 4 bar (4000 μmol), P_{Total} = 20 bar, stirring = 1500 rpm
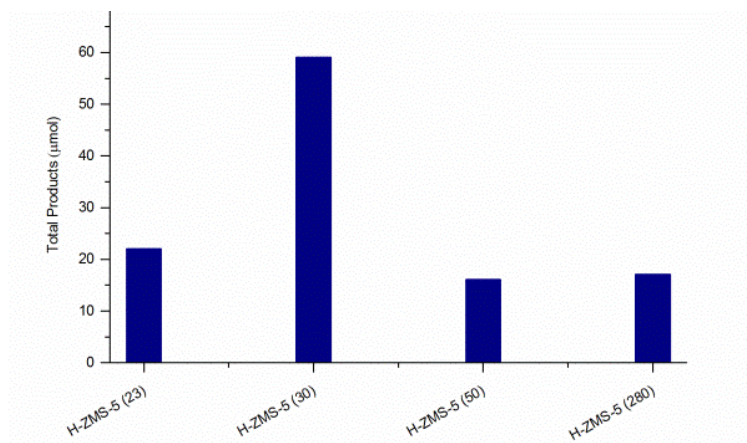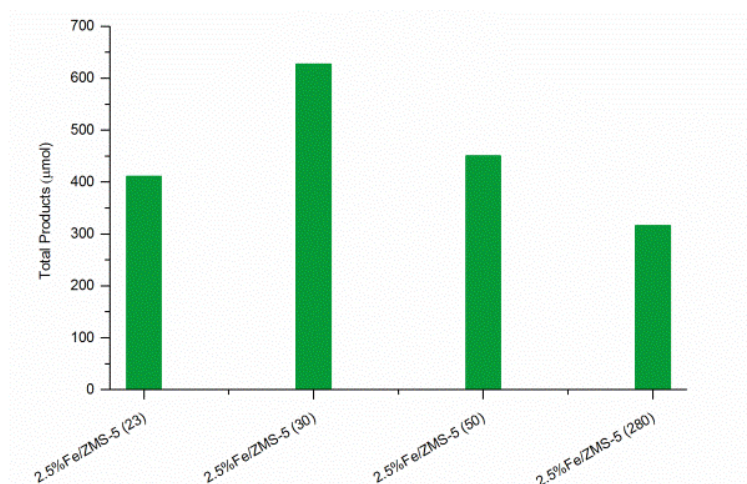

Figure 5.28: Total products for propane reaction with 2.5 wt. % Fe/ ZSM-5 (X) support (X = 23, 30, 50 and 280)

Reaction condition: $[H_2O_2]$ = 5000 μmol, volume = 10 mL, 27 mg catalyst, 50 ºC, 0.5 h, $P_{propane}$ = 4 bar (4000 μmol), P_{Total} = 20 bar, stirring = 1500 rpm

Table 5.8: Products selectivity for propane oxidation with 2.5 wt. % Fe/ ZSM-5 (X) (X = 23, 30, 50 and 280)

Catalyst	Selectivity (%)					
	C_3	Acetone	Isopropanol	C_2	C_1	Formic Acid
2.5 wt. % Fe/ ZSM-5 (23)	63	2	46	22	15	14
2.5 wt. % Fe/ ZSM-5 (30)	34	6	6	28	38	35
2.5 wt. % Fe/ ZSM-5 (50)	36	10	5	24	40	36
2.5 wt. % Fe/ ZSM-5 (280)	42	21	5	20	38	33

Reaction condition: $[H_2O_2]$ = 5000 µmol, volume = 10 mL, 27 mg catalyst, 50 °C, 0.5 h, $P_{propane}$ = 4 bar (4000 µmol), P_{Total} = 20 bar, stirring = 1500 rpm

Increasing the SiO_2/ Al_2O_3 ratio decreases the amount of Al therefore the amount of acid sites. However, the strength of individual acid site might also change which can explain the difference of selectivity. This suggests the need of the acid site for the conversion; it could also play an important role in the integration of Fe. With Al increasing, the hydrophilicity of ZSM-5 increases. This could explain the decrease of conversion for ZSM-5 (23) as propane being hydrophobic, less will diffuse into the pores of the zeolite and therefore be available to react.

3.3. Effect of various treatment on zeolite acidity

ZSM-5 (30) was found to be the best material, to support Fe for the oxidation of propane, partly due to its properties such as structure and SiO_2/ Al_2O_3 ratio. The previous section 3.2 shows that the acidity is playing an important role in the activation of propane. Corma *et al.* reported the role of Brønsted acid sites in C-C scission but also the possibility of a role of extra-framework Al species.[23] Dealumination would increase the Lewis acidity by migration of Al from tetrahedral framework to octahedral extra-framework. Hence the formation of C_2 and C_1 products could increase. Decreasing the amount of Brønsted acid sites could help to decrease the C-C scission.

Dehydration of the zeolite through heat treatment or splitting of the bridging Si-OH-Al using an alkali treatment has been reported to increase Al in extra-framework sites (Lewis acid sites). Domen and co-worker treated their zeolite with high temperature (600 °C) in order to convert Brønsted acid sites into Lewis acid sites. By water re-adsorption, they could recover the Brønsted acid sites.[24] Another group alkali treated their zeolite in

order to break the Si-OH-Al bridges. Change of pore size and increase of Lewis acid sites were observed.[25] Zhang *et al.* used an acid treatment to dissolve the non-crystalline material of ZMS-5 and subsequently removes Al species from the zeolite structure.[26]

3.3.1. Effect of heat treatment

It is known that changing the calcination temperature can cause a change in the structure of the zeolite. Tetrahedral Al comes out of the framework to give octahedral extra-framework Al.[27] Here the treatment temperature for H-ZSM-5 (30) has been varied from 550 ℃ to 750 ℃ and analysed by IR Figure 5.29. Increasing the temperature of calcination decreases the signals for terminal SiOH and OH groups coordinated to tetrahedral framework Al. The signal for OH coordinated to extra-framework T-atoms disappears. Hence, it can be concluded that dealumination occurred during the calcination but also dehydration involving the loss of OH group to form water.
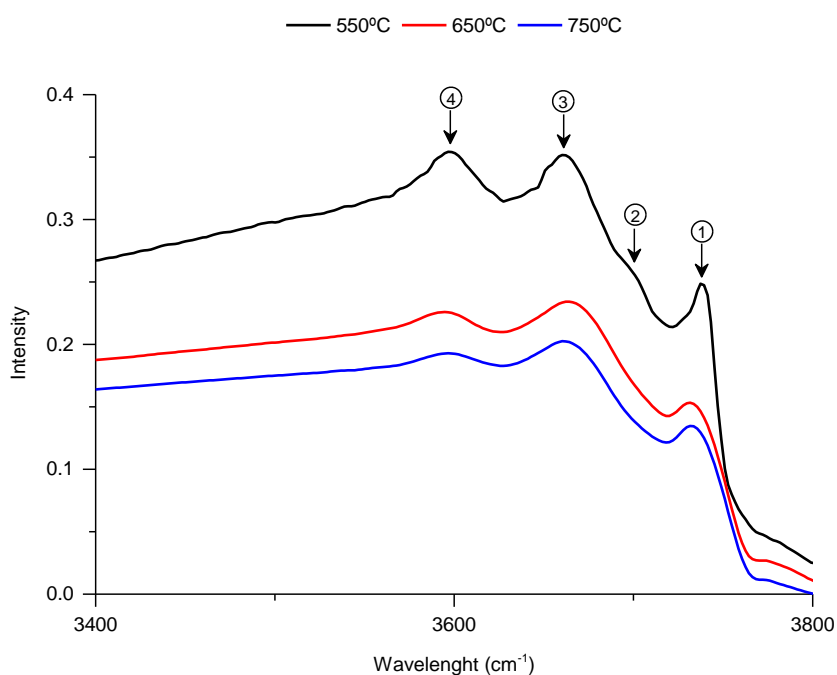

Figure 5.29: Infrared analysis of H-ZSM-5 (30) calcined at various temperatures

Signal: (1) 3737 cm^{-1}, Terminal SiOH; (2) 3700 cm^{-1}, OH groups in defect sites (hydroxyl nests); (3) 3660 cm^{-1}, OH groups coordinated to extra-framework T-atoms; (4) 3595 cm^{-1}, OH groups coordinated to tetrahedrally coordinated framework Al^{3+}

Solid-state NMR of H-ZSM-5 (30), following treatment at various temperatures, has been performed and confirms that Td framework Al decrease with temperature and Oh extra-framework Al increases. The results are represented in Table 5.9, with the Td/Oh ratio decreasing when calcination temperature decreases.

A five-coordinated extra-framework Al also appears with high calcination temperature as shown in Figure 5.30. This species is thought to be a six-coordinated extra-framework Al after losing a water molecule as illustrated in Figure 5.31.

Table 5.9: Solid NMR analysis of H-ZSM-5 (30) calcined at various temperatures

Sample H-ZSM-5 (30)	Td four-coordinated framework	Oh six-coordinated extra-framework	five-coordinated extra-framework	Ratio Td/Oh
Calcination 550 °C	3802.0	600.6	–	6.3
Calcination 650 °C	2466.9	682.2	–	3.6
Calcination 750 °C	3096.6	1369.0	339.0	2.3
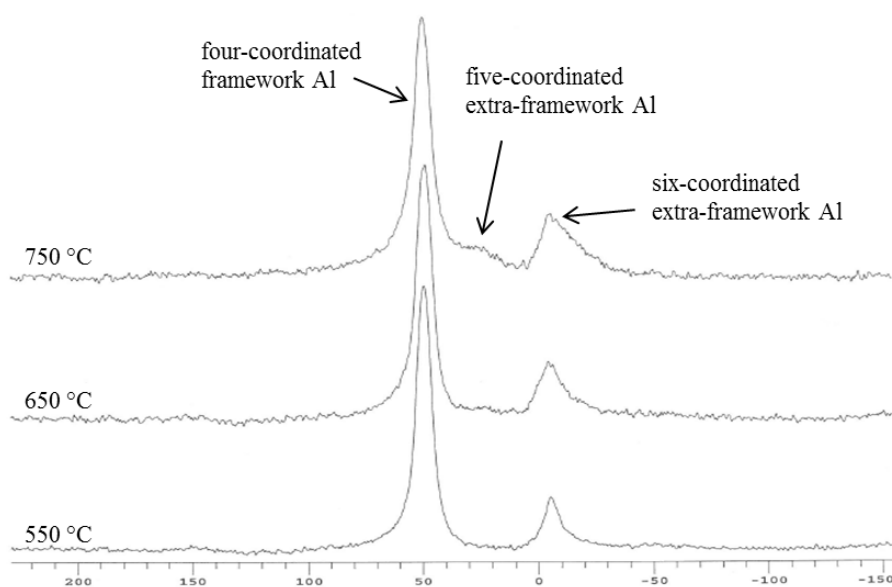
Figure 5.30: Solid NMR analysis of H-ZSM-5 (30) calcined at various temperatures
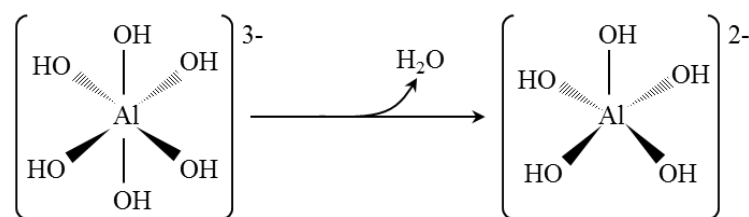
Figure 5.31: Illustration of six-coordinated Al to five-coordinated Al by loss of water

Increasing calcination leads to a decrease of Brønsted acid (Td Al) and an increase of Lewis acid (Oh Al). Further calcination involved a dehydration of the octahedral Al extra-framework. In order to correlate the activity of the catalyst with the structure, Fe was supported on these catalysts. The bare zeolites and Fe supported catalysts were tested for propane oxidation; the results are shown in Figure 5.32 and 5.33.
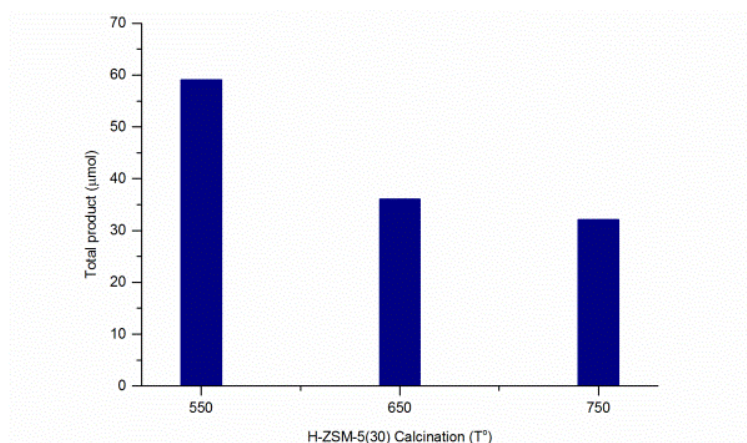
Figure 5.32: Propane conversion for reaction with H-ZSM-5 (30) calcined at various temperatures
Reaction condition: $[H_2O_2]$ = 5000 µmol, volume = 10 mL, 27 mg catalyst, 50 ºC, 0.5 h, $P_{propane}$ = 4 bar (4000 µmol), P_{Total} = 20bar, stirring = 1500 rpm

Figure 5.33: Propane conversion for reaction with 2.5 Fe % supported on ZSM-5 (30) calcined at various temperatures
Reaction condition: $[H_2O_2]$ = 5000 μmol, volume = 10 mL, 27 mg catalyst, 50 ºC, 0.5 h, $P_{propane}$ = 4 bar (4000 μmol), P_{Total} = 20bar, stirring = 1500 rpm

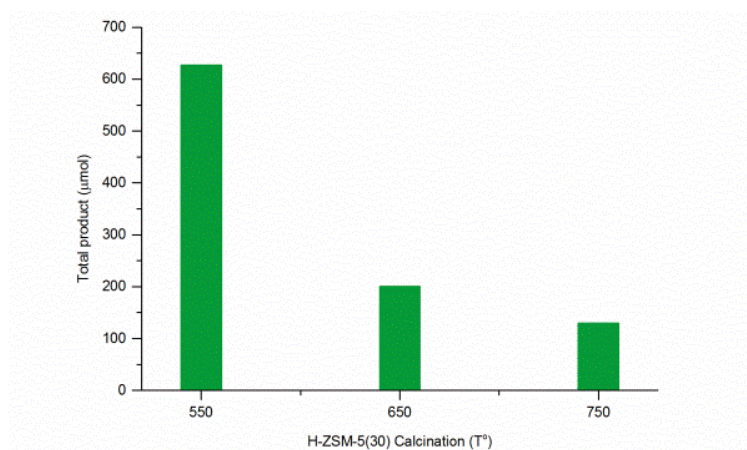The activity of bare catalysts decreases with temperature indicating that Al in framework has a better activity for propane oxidation than Al extra-framework. After supporting Fe on the zeolites the activity also decreases with calcination temperature suggesting that the active Fe species required for propane oxidation could be grafted to Al Td sites.

3.3.2. Effect of acid and basic treatments on the support

3.3.2.1. Acid treatment

The acid treatment has for purpose the dealumination of zeolite. Same as with calcination temperature, framework Al become extra-framework Al.

Figure 5.34 and 5.35 shows the activity of bare zeolite and Fe supported on ZSM-5 (30) after acid treatment respectively. A decrease of activity can be observed with the bare zeolite demonstrating that framework Al is active for the oxidisation of propane. However, in presence of Fe the activity does not change significantly. Hence, the dealumination of the support by acid treatment does not have any effect on the active Fe species. This suggests the effect of the acid treatment is different than the effect causes by heat treatment.

Figure 5.34: Propane conversion for reaction with H-ZSM-5 (30) after acid treatment
Reaction condition: $[H_2O_2]$ = 5000 μmol, volume = 10 mL, 27 mg catalyst, 50 ºC, 0.5 h, $P_{propane}$ = 4 bar (4000 μmol), P_{Total} = 20 bar, stirring = 1500 rpm

Figure 5.35: Figure 5.32: Propane conversion for reaction with 2.5 wt. % Fe loaded on H-ZSM-5 (30) after acid treatment
Reaction condition: $[H_2O_2]$ = 5000 μmol, volume = 10 mL, 27 mg catalyst, 50 ºC, 0.5 h, $P_{propane}$ = 4 bar (4000 μmol), P_{Total} = 20 bar, stirring = 1500 rpm

3.3.2.2. *Alkali treatment*

The aim of the alkali treatment is to break the Si-OH-Al in order to increase the Lewis acid sites. The activity of bare ZSM-5 (30) and 2.5 wt. % Fe/ ZSM-5 after alkali treatment are shown in Figure 5.36 and 5.37 respectively. The activity for the bare zeolite and Fe supported zeolite slightly decrease after alkali treatment. These results

show that the increase of Lewis acid from the support is not having a marginal effect for propane oxidation. As seen with the acid treatment, after alkali treatment of the support, no obvious change can be detected toward the immobilised Fe on the surface.
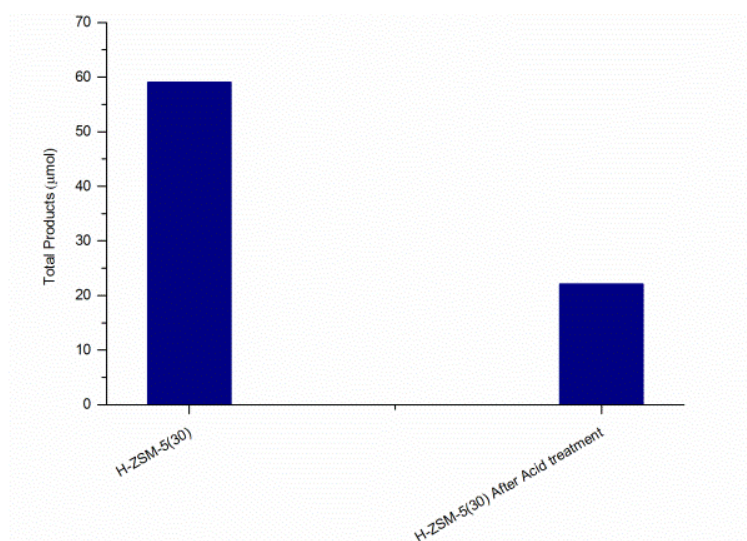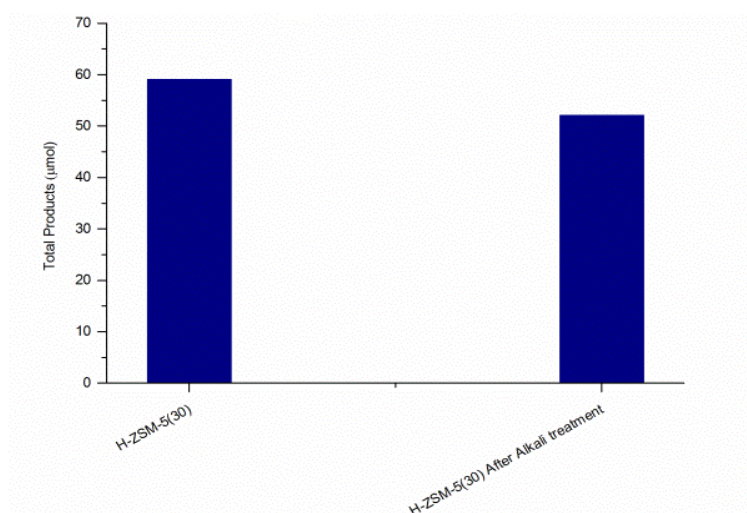

Figure 5.36: Propane conversion for reaction with H-ZSM-5 (30) after acid treatment
Reaction condition: [H$_2$O$_2$] = 5000 μmol, volume = 10 mL, 27 mg catalyst, 50 ℃, 0.5 h, P$_{propane}$ = 4 bar (4000 μmol), P$_{Total}$ = 20 bar, stirring = 1500 rpm
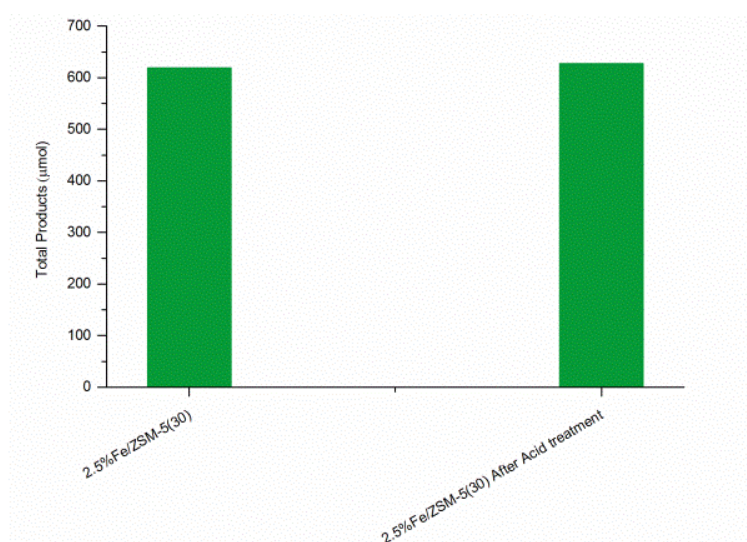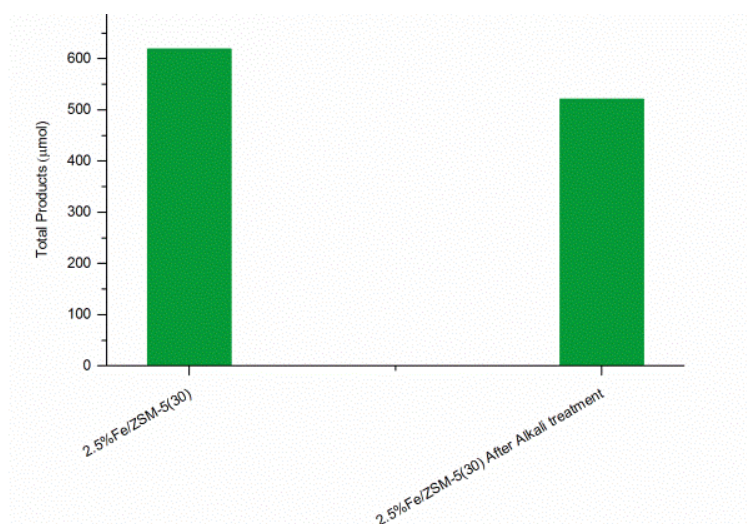

Figure 5.37: Propane conversion for reaction with 2.5 wt. % Fe loaded on H-ZSM-5 (30) after alkali treatment
Reaction condition: [H$_2$O$_2$] = 5000 μmol, volume = 10 mL, 27 mg catalyst, 50 ℃, 0.5 h, P$_{propane}$ = 4 bar (4000 μmol), P$_{Total}$ = 20 bar, stirring = 1500 rpm

163

3.3.3. Conclusion

Treatments (heat, acid and basic) were done to modify ZSM-5 (30) in order to change the site of Fe deposition and then the activity for propane.

Dealumination due to calcination implies a change of activity whereas the changes due to acid and alkali treatment do not show a difference of activity. Hence further characterisation and experiment are necessary to understand which variation of the structures could modify Fe deposition and improve the activity.

4. Investigation of the activity of other metals

2.5 wt. % Fe/ ZSM-5 is known to be active for methane and ethane oxidation and just show his activity for propane oxidation. This catalyst has been designed from a biological approach and extensively studied in this chapter; however, many other metal catalysts have been shown to be active for the oxidation of propane. Noble metals, different metals oxide and supported metals have shown the ability to oxidise propane under various conditions.[6, 28-32] Previously in this chapter the material used as support has been changed whilst keeping the same metal. The use of other metals and bimetallic systems keeping the support (ZSM-5(30)) has been investigated in the following experiments.

4.1. Homogeneous catalysts

Homogeneous catalysts have been examined for the oxidation of propane under the standard conditions, in order to investigate the possible activity of other metals. Homogeneous catalysts are known to have a different activity compared to equivalent heterogeneous catalysts as it is in the same phase and there is low possibility of mass transfer.[33, 34] Mn, Co and Cu nitrate have been tested and compared to Fe nitrate. Table 5.10 shows the results with only Fe nitrate showing activity for propane oxidisation with 8.1 % conversion.

Fe nitrate is as active as 2.5 wt. % Fe/ ZSM-5 (30), furthermore this catalyst show a better selectivity for C_3 products as presented in Table 5.11. The selectivity for acetone goes up to 57 % and formic acid selectivity decreases from 35 % to 18 %. Homogeneous catalysts are not supported; hence there is no support able to interact with the products during the reaction.

Table 5.10: Propane conversion using homogeneous catalyst

Catalyst	Total product (µmol)	Carbon balance		H_2O_2 Consumptions (%)	H_2O_2 utilisation (%) (oxygen balance)
		Conversion (%)	Selectivity to oxygenates (%)		
Iron Nitrate	489	8.1	91	53	15
Copper nitrate	6	0	0	4	1
Cobalt nitrate	14	0.1	0	0	0
Manganese nitrate	4	0	0	0	0

Reaction condition: $[H_2O_2]$ = 5000 µmol, volume = 10 mL, Amount of metal based on moles of Fe in 2.5 wt. % Fe/ ZSM-5 (30), 50 ℃, 0.5 h, $P_{propane}$ = 4 bar (4000 µmol), P_{Total} = 20 bar, stirring = 1500 rpm

Table 5.11: Comparison of Fe homogeneous and heterogeneous catalyst for propane oxidation

Catalyst	Conversion (%)	Selectivity %				
		Acetone	Propanol	Propanoic acid	Ethanol	Formic acid
2.5 wt. % Fe/ ZSM-5 (30)	8.4	6	9	11	14	35
Iron nitrate	8.1	57	0.1	0	0.1	18

Reaction condition: $[H_2O_2]$ = 5000 µmol, volume = 10 mL, equivalent moles of Fe in each reaction, 50 ℃, 0.5 h, $P_{propane}$ = 4 bar (4000 µmol), P_{Total} = 20 bar, stirring = 1500 rpm

4.2. Heterogeneous catalysts

The homogeneous catalysts tested in the previous section 4.1 do not show any activity however, this does not mean that as a heterogeneous catalyst supported on ZSM-5 these metals will not have any effect on the activity.[8] For each metal, a 2.5 wt. % metal supported on ZSM-5 (30) was made by solid-state ion-exchange, as describe chapter 2 section 4.3, and tested. The results, presented in Table 5.12, confirm the homogeneous results. Cu, Co and Mn show a very low activity for propane oxidation, similar to the corresponding homogeneous catalyst. Bare ZSM-5 (30) shows a highest activity. Hence these metals are inactive and might block the active site from H-ZSM-5 (30) during the preparation.

It is known that the addition of a second metal to monometallic catalysts can promote the activity or selectivity.[9, 35] On the contrary, the addition of Cu, Co, Mn to Fe/ ZSM-5 (30), Table 5.13, decreases the activity from 5.9 % to 3.9 %, 1.9 % and 3.8 % respectively.

Although monometallic 1.25 wt. % Fe is still the most active catalyst in terms of propane conversion, the addition of other metals changes the selectivity as shown in Table 5.14. There is an increase of C_3 products while C_1 products decrease.

Table 5.12: Propane conversion using different metal supported on ZSM-5 (30)

| Catalyst | Total product (µmol) | Carbon balance | | H_2O_2 Consumption (%) | H_2O_2 utilisation (%) (oxygen balance) |
		Conversion (%)	Selectivity to oxygenates (%)		
2.5 wt. % Fe/ ZSM-5 (30)	660	8.4	95	33	37
2.5 wt. % Cu/ ZSM-5 (30)	25	0.5	79	4	15
2.5 wt. % Co/ ZSM-5 (30)	7	0.1	52	26	0
2.5 wt. % Mn/ ZSM-5 (30)	9	0.1	69	8	2
ZSM-5(30)	60	0.9	89	5	18

Reaction condition: $[H_2O_2]$ = 5000 µmol, volume = 10 mL, 27 mg catalyst, 50 ℃, 0.5 h, $P_{propane}$ = 4 bar (4000 µmol), P_{Total} = 20 bar, stirring = 1500 rpm

Table 5.13: Propane conversion using bimetallic 1.25 wt. % Fe - 1.25 wt. % M/ ZSM-5 (30) catalyst (M = Cu, Co or Mn)

| Metals / ZSM-5 (30) | Total product (µmol) | Carbon balance | | H_2O_2 Consumption (%) | H_2O_2 utilisation (%) (oxygen balance) |
		Conversion (%)	Selectivity to oxygenates (%)		
1.25 wt. % Fe-1.25 wt. % Cu	186	3.9	63	27	6
1.25 wt. % Fe-1.25 wt. % Co	118	1.9	89	8	23
1.25 wt. % Fe-1.25 wt. % Mn	269	3.8	92	25	20
1.25 wt. % Fe	438	5.9	93	19	37

Reaction condition: $[H_2O_2]$ = 5000 µmol, volume = 10 mL, 27 mg catalyst, 50 ℃, 0.5 h, $P_{propane}$ = 4 bar (4000 µmol), P_{Total} = 20 bar, stirring = 1500 rpm

Table 5.14: Selectivity for Propane conversion using bimetallic 1.25 wt. % Fe - 1.25 wt. % M/ ZSM-5 (30) catalyst (M = Cu, Co or Mn)

Metals / ZSM-5 (30)	Selectivity (%)		
	C_3	C_2	C_1
1.25 wt. % Fe-1.25 wt. % Cu	65	29	6
1.25 wt. % Fe-1.25 wt. % Co	49	24	27
1.25 wt. % Fe-1.25 wt. % Mn	40	25	35
1.25 wt. % Fe	38	29	33

Reaction condition: $[H_2O_2]$ = 5000 μmol, volume = 10 mL, 27 mg catalyst, 50 ºC, 0.5 h, $P_{propane}$ = 4 bar (4000 μmol), P_{Total} = 20 bar, stirring = 1500 rpm

5. Fe-Cu system

Previously, the promoting effect of the addition of Cu to Fe/ ZSM-5 for ethane and methane oxidation has been reported.[8, 9, 35, 36] Cu does not interact directly for methane activation but inhibits the overoxidation, increasing the selectivity for methanol, by scavenging ·OH radical. Moreover the presence of a Cu cluster in MMO has been reported to be an active site for the oxidisation of methane to methanol.[37]

A corresponding amount of Cu metal was added as $Cu(NO_3)_2$ to a standard reaction with 1.25 % Fe/ ZSM-5 (30). The result is compared to reactions performed with 1.25 % Fe/ ZSM-5 (30) and 2.5 wt. % Fe/ ZSM-5 (30) in Figure 5.38. The addition of $Cu(NO_3)_2$ increases slightly the conversion of propane compared to the 1.25 % Fe/ ZSM-5 (30) (396 μmol and 280 μmol respectively) despite the amount of total metal being the same. The activity is lower than the corresponding 2.5 wt. % Fe/ ZSM-5 (30). The addition of homogeneous Cu seems to have a promoting effect toward the activity of the catalyst. In the previous section, homogeneous Cu and supported Cu had a very low activity.

Some characterisation after reaction would be interesting to do to determine if some Cu are supported on the catalyst during the reaction.
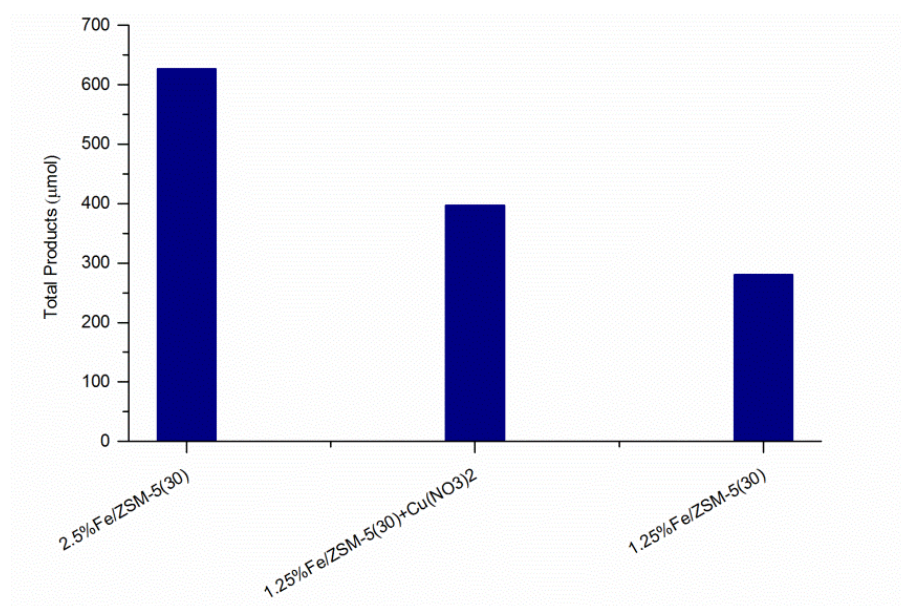
Figure 5.38: Total products for propane oxidation

Reaction condition: $[H_2O_2]$ = 5000 µmol, volume = 10 mL, 27 mg catalyst, 50 ℃, 0.5 h, $P_{propane}$ = 4 bar (4000 µmol), P_{Total} = 20 bar, stirring = 1500 rpm

The following experiment was the addition of Cu onto a Fe/ ZSM-5 (30) catalyst. The mixture Fe-Cu was deposed on ZSM-5 (30) by the CVI method as described in the experimental chapter, section 4.2 in order to obtain 1.25 % Fe - 1.25 % Cu/ ZSM-5 (30). Table 5.15 shows the results for the oxidation of propane with this catalyst as well as 2.5 wt. % Fe/ ZSM-5 (30) and 2.5 wt. % Cu/ ZSM-5 (30).

Interestingly the addition of Cu to 1.25 % Fe/ ZSM-5 (30) decreases the conversion compare to the addition of homogeneous Cu in the reaction (respectively 186 µmol and 396 µmol). This suggests that Cu could be interacting with active Fe sites which would block the interaction with the substrate.

The incorporation of Cu is not increasing the conversion of propane. However, the selectivity to C_1 products decreases to 6 % and C_3 increases to 65 %. The major part of C_1 products for 2.5 wt. % Fe/ ZSM-5 (30) is formic acid which totally disappears with the addition of Cu. C_3 product selectivity increases with an increased selectivity towards propene. Hence the mixture Fe-Cu decreases the conversion but increases the selectivity for C_3 products.

Table 5.15: Comparison of Fe, Cu and Fe-Cu catalyst for propane conversion and selectivity

Catalyst	Total product (µmol)	Carbon balance		H_2O_2 Comsuption (%)	H_2O_2 utilisation (%) (oxygen balance)
		Conversion (%)	Selectivity to oxygenates (%)		
2.5 wt. % Cu/ ZSM-5 (30)	54	0.5	79	4	15
1.25 wt. % Fe-1.25 wt. % Cu / ZSM-5 (30)	186	3.9	63	27	6
2.5 wt. % Fe/ ZSM-5 (30)	660	8.4	95	33	37

Catalyst	Selectivity				
	C3	C2	C1	Propene	Formic acid
2.5 wt. % Cu/ ZSM-5 (30)	71	15	14	8	11
1.25 wt. % Fe-1.25 wt. % Cu / ZSM-5 (30)	65	29	6	24	0
2.5 wt. % Fe/ ZSM-5 (30)	34	28	38	2	35

Reaction condition: $[H_2O_2]$ = 5000 µmol, volume = 10 mL, 27 mg catalyst, 50 ºC, 0.5 h, $P_{propane}$ = 4 bar (4000 µmol), P_{Total} = 20 bar, stirring = 1500 rpm

6. Conclusions

Propane oxidation has been investigating using 2.5 wt. % Fe/ ZSM-5 (30) under mild conditions in liquid phase using H_2O_2 as oxidant. Various reaction parameters have been investigated in order to find the best conditions to get high conversion and high selectivity for C_3 oxygenates. Both, conversion and selectivity are highly depending on the conditions used; however, with high conversion the selectivity for C_3 products is very low, with high selectivity towards formic acid and CO_2. Moreover using this catalyst involved a high consumption of H_2O_2 with a low utilisation in products.

An acidic treatment of 2.5 wt. % Fe/ ZSM-5 (30) in order to remove Fe species in surface showed that only 0.5 % Fe are left on the catalyst which marginally reduce the conversion. Various techniques have been used to characterise these catalysts; TPR, TPD, UV-Vis, IR, XRD, solid NMR and BET. From these analyses, most of the surface Fe oxide and clusters appear to be inactive for the oxidation of propane. With the presence of Fe grafted to framework Al sites being the actives species.

It has been proved that ZSM-5 (30) is the best support material for Fe to activate this reaction and achieve reasonable conversions. This may be due to a mixture of the structure and acidic properties it possess. Fe supported is interacting with Lewis and

Brønsted acid present on the support. However, more characterisation would be needed to understand which Fe species are grafted and where.

The use of other metals instead of Fe did not show successful results; however, the addition of another metal to form a bimetallic catalyst decreases the conversion but causes a change in the selectivity. Cu is the best example with an increase of C_3 product selectivity, particularly propene and a decrease of C_1 products. From previous paper it has been shown that Cu quenches the formation of $\cdot$OH radical; hence, the overoxidation is minimised.

Kinetic studies would be interesting to investigate in order to clarify the mechanism. More understanding of the active sites would allow finding other metals, support or treatment in order to improve the reaction.

7. *References*

1. Sah, S.L., *Encyclopedia of Petroleum Science and Engineering*. Vol. **4**. 2003, India: Kalpaz Publications. 16.

2. Michalkiewicz, B., *Journal of Catalysis,* 2003. **215** (1), p. 14-19.

3. Arndtsen, B.A., Bergman, R.G., Mobley, T.A. and Peterson, T.H., *J. AM. CHEM. SOC.,* 1995. **28**, p. 154-162.

4. Putra, M.D., Al-Zahrani, S.M. and Abasaeed, A.E., *Catalysis Communication,* 2011. **14**, p. 107-110.

5. Bettahar, M.M., Costentin, G., Savary, L. and Lavalley, J.C., *Applied Catalysis A: General,* 1996. **145**, p. 1-48.

6. Bravo-Suárez, J.J., Bando, K.K., Fujitani, T. and Oyama, S.T., *Journal of Catalysis,* 2008. **257**, p. 32-42.

7. Raja, R., Jacob, C.R. and Ratnasamy, P., *Catalysis Today,* 1999. **49**, p. 171-175.

8. Forde, M.M., Armstrong, R.D., Hammond, C., He, Q., Jenkins, R.L., Kondrat, S.A., Dimitratos, N., Lopez-Sanchez, J.A., Taylor, S.H., Willock, D., Kiely, C.J. and Hutchings, G.J., *Journal of the American Chemical Society,* 2013. **135**, p. 11087-11099.

9. Hammond, C., Jenkins, R.L., Dimitratos, N., Lopez-Sanchez, J.A., Rahim, M.H.a., Forde, M.M., Thetford, A., Murphy, D.M., Hagen, H., Stangland, E.E., Moulijn, J.M., Willock, S.H.T.J. and Hutchings, G.J., *Chemistry-A European Journal,* 2012. **18** (49), p. 15735-15745.

10. Forde, M.M. *Low Temperature Aqueous Phase Oxidation of Alkanes with Metal Doped Zeolites Prepared by Chemical Vapour Infiltration.* 2011. Doctor of Philosophy. Cardiff University.

11. Chapoy, A., Mokraoui, S., Valtz, A., Richon, D., Mohammadi, A.H. and Tohidi, B., *Fluid Phase Equilibria,* 2004. **226**, p. 213-220.

12. Zecchina, A., Rivallan, M., Berlier, G., Lambertia, C. and Ricchiardi, G., *Physical Chemistry Chemical Physics,* 2007. **9**, p. 3483-3499.

13. Pérez-Ramírez, J., Kumar, M.S. and Brückner, A., *Journal of Catalysis,* 2004. **223**, p. 13-27.

14. Kustov, L.M., V. B. Kazansky, Beran, S., Kubelkova, L. and Jiru, P., *Journal of Physical Chemistry,* 1987. **91**, p. 5247-5251.

15. Lin, H.-Y., Chen, Y.-W. and Li, C., *Thermochimica Acta,* 2003. **400**, p. 61-67.

16. Neri, G., Visco, A.M., Galvagno, S., Donato, A. and Panzalorto, M., *Thermochimica Acta,* 1999. **329**, p. 39-46.

17. Woolery, G.L., Kuehl, G.H., Timken, H.C., Chester, A.W. and Vartuli, J.C., *Zeolites,* 1997. **19**, p. 288-296.

18. Sirotin, S.V., Moskovskaya, I.F. and Romanovsky, B.V., *catalysis Science & Technology,* 2011. **1**, p. 971-980.

19. Sano, T., Uno, Y., Wang, Z.B., Ahn, C.-H. and Soga, K., *Microporous and Mesoporous Materials,* 1999. **31**, p. 89-95.

20. Lami, E.B., Fajula, F., Anglerot, D. and Courieres, T.D., *Microporous Materials,* 1993. **1**, p. 237-245.

21. Joo, O.-S., Jung, K.-D. and Han, S.-H., *Bulletin of the Korean Chemical Society,* 2002. **23** (8), p. 1103-1105.

22. Apelian, M.R., Fung, A.S., Kennedy, G.J. and Degnan, T.F., *Journal of Physical Chemistry,* 1996. **100**, p. 16577-16583.

23. Corma, A. and Orchilles, A.V., *Microporous and Mesoporous Materials,* 2000. **35-36**, p. 21-30.

24. Kondo, J.N., Nishitani, R., Yoda, E., Yokoi, T., Tatsumi, T. and Domen, K., *Physical Chemistry Chemical Physics,* 2010. **12**, p. 11576-11586.

25. Jia, A., Lou, L.-L., Zhang, C., Zhang, Y. and Liu, S., *Journal of Molecular Catalysis A: Chemical,* 2009. **306** (1-2), p. 123-129.

26. Zhang, W., Bi, F., Yu, Y. and He, H., *Journal of Molecular Catalysis A: Chemical,* 2013. **372**, p. 6-12.

27. Sultan, E.A. and Selim, M.M., *Journal of Chemical Society of Pakistan,* 1998. **11** (2), p. 96-102.

28. Solsona, B., Davies, T.E., Garcia, T., Vazquez, I., Dejoz, A. and Taylor, S.H., *Applied Catalysis B: Environmental,* 2008. **84**, p. 176-184.

29. Wu, X., Zhang, L., Weng, D., Liu, S., Si, Z. and Fan, J., *Journal of Hazardous Materials,* 2012. **225-226**, p. 146-154.

30. Debecker, D.P., Farin, B., Gaigneaux, E.M., Sanchez, C. and Sassoye, C., *Applied Catalysis A: General,* 2014. **481**, p. 11-18.

31. Morales, M.R., Barbero, B.P. and Cadus, L.E., *Applied Catalysis B: Environmental,* 2006. **67**, p. 229-236.

32. Heynderickx, M.P., Thybaut, J.W., Poelman, H., Poelman, D. and Marin, G.B., *Applied Catalysis B: Environmental,* 2010. **95**, p. 26-38.

33. Klaewkla, R., Arend, M. and Hoelderich, W.F., *Mass Transfer - Advanced Aspects: A Review of Mass Transfer Controlling the Reaction Rate in Heterogeneous Catalytic Systems*, ed. H. Nakajima. 2011.

34. Fadhel, A.Z., Pollet, P., Liotta, C.L. and Eckert, C.A., *Molecules,* 2010. **15**, p. 8400-8424.

35. Hammond, C., Forde, M.M., Rahim, M.H.a., Thetford, A., He, Q., Jenkins, R.L., Dimitratos, N., Lopez-Sanchez, J.A., Dummer, N.F., Murphy, D.M., Carley, A.F., Taylor, S.H., Willock, D.J., Eric E. Stangland, Kang, J., Hagen, H., Kiely, C.J. and Hutchings, G.J., *Angewandte Communications,* 2012. **51**, p. 5129-5133.

36. Hammond, C., Dimitratos, N., Jenkins, R.L., Lopez-Sanchez, J.A., Kondrat, S.A., Rahim, M.H.a., Forde, M.M., Thetford, A., Taylor, S.H., Hagen, H., Stangland, E.E., Kang, J.H., Moulijn, J.M., Willock, D.J. and Hutchings, G.J., *ACS Catalysis,* 2013. **3**, p. 689-699.

37. Jr, J.M.B., *Nature Chemistry,* 2010. **465**, p. 40-41.

Conclusions and Future Work

6

1. General conclusion

During my PhD, three subjects have been broached; Octane oxidation using O_2, toluene oxidation using TBHP and finally propane oxidation using H_2O_2.

For all projects the aim was the selective oxidation of the corresponding hydrocarbon in liquid phase using a solid catalyst in mild reaction conditions. The use of green conditions was required; solvent free or green solvent, low temperature, low pressure and green oxidant, O_2 being the best and cheapest. Primary C-H bond activation, O_2 activation and prevention of overoxidation were different points approach during these studies.

The first objective was to develop a catalytic system to oxidise the substrate with high conversion and selectivity. The second objective is to investigate effects of reaction conditions. Finally, depending on the project, modification of the system or catalyst and elucidation of active site have been investigated in order to improve catalytic activity and selectivity.

1.1. System benzaldehyde/ O_2 for the co-oxidation of octane

The aim of the first results chapter was to use a co-oxidant which would be able to initiate the activation of methane. Using previous results, toluene was the molecule of choice using 1 wt. % AuPd/ C and O_2 at 160 ºC. This system did not show positive results, it was assumed that the molecules used were not active enough. The use of octane replacing methane and benzaldehyde instead of toluene was then explored. After investigating the

reaction conditions, an optimal system was found and used to prove the feasibility of the concept.

The overall experiments show the activation of octane with molecular O_2 under mild conditions using 1 wt. % AuPd/ C. A maximum of 24 % conversion was reached at 140 °C. The presence of benzaldehyde initiates the oxidation of octane from 50 °C. The formation of octyl benzoate was detected showing the possibility of coupling the products of benzaldehyde and octane. However, increasing the reaction condition (time, temperature) increased octane conversion and C-C scission meaning that this system is not optimum to prevent overoxidation. To generalise the concept, a higher alkane and another aldehyde have been used. Reactions using reactants in the same phase were successful whereas no reaction happens with different phases reactants. A few other unsuccessful experiments have been run to integrate the first target molecules; toluene and methane.

In literature, "Sacrificial aldehydes" have been reported as good initiators for oxidation reactions. The reaction conditions used (excess of aldehyde) are slightly different than the conditions use in the current work (excess of substrate). Hence, experiments with various octane: benzaldehyde ratio would permit to investigate the role of the amount of aldehyde.

The problem of reactant being in separate phases is not resolved. Methane is more soluble in organic solvent than water. Hence using benzaldehyde as solvent could allow more methane in liquid phase and benzaldehyde would have the role of sacrificial aldehyde.

1.2. TBHP: oxidant and initiator, its role in toluene oxidation

The aim of the second chapter was to selectively oxidise toluene into benzyl alcohol, benzaldehyde or benzoic acid improving the previous research done in Cardiff Catalysis Institute.

Sets of catalysts using Au, Pd and Pt have been made, characterised and tested for toluene oxidation. Mild reaction conditions were used; 80 °C and atmospheric pressure. O_2 has been tested previously by Kesavan *et al.* in the same condition with 1 wt. % AuPd/ C and TiO_2. Less than 1 % conversion was observed.[1] TBHP and H_2O_2 have been used as oxidants in this work. H_2O_2 being not miscible with toluene, the reaction does not occur. TBHP show its best results with the trimetallic 1 wt. % AuPdPt/ C. 47 % of toluene was converted after 72 h with 97 % selectivity for benzoic acid. The participation of O_2 from air has been proved using the same system in a high pressure autoclave. The presence of

TBHP is essential to initiate the reactions. However, the insertion of O_2 in products is then possible under temperatures as low as 50 ℃. Lower temperature experiments could show the ability of this system to activate O_2 at room temperature.

1.3. Fe and ZSM-5, key products for propane oxidation

The aim of chapter 5 was to selectively oxidise propane to C_3 products using H_2O_2 as the initiator and oxidant under mild conditions. High conversion and selectivity was required with a low consumption of H_2O_2. The system used in this work came from previous research performed on methane and ethane oxidation. [2, 3] Hence, Fe/ ZSM-5 (30) was used to investigate the reaction conditions. With this system, high conversion can be reached (52 %), the selectivity is mainly toward C_2 and C_1 products and H_2O_2 is totally consumed.

Different supports and metals were tested and 2.5 wt. % Fe/ ZSM-5 (30) shows the best activity. However, the addition of Cu to this catalyst switches off the formation of formic acid and increases propene selectivity. Previous studies show that this effect is due to Cu, which quenches the formation of ·OH radical.[3] However, EPR experiment could help to understand the effect of Cu in this system.

2.5 wt. % Fe/ ZSM-5 (30) has been treated by acid in order to remove the Fe species on surface; 0.5 wt. % Fe was left from the standard catalyst. Analyses revealed that the Fe species grafted are left on the catalyst and gave its catalytic activity, whereas iron cluster and iron oxide are inactive for propane oxidation.

The active sites have been identified; nevertheless, the mechanism is not totally understood. It would be interesting to run further investigations as a kinetic reaction or using a radical scavenger in order to discover more about mechanism. Characterise a used catalyst, or IR *in situ.* reaction could also inform on which species interact with the catalyst.

More investigations on Fe homogeneous, $Fe(NO_3)_3$ and other Fe complexes, could help to find new heterogeneous catalysts with similar activity and selectivity.

Propane is a hydrophobic molecule while reaction products and H_2O_2 are hydrophilic. Few changes of the system could help to have an improvement of contact oxidant/ substrate/ products; A biphasic system where one solvent will be for the catalyst and reactant and a second solvent for the products to go before being overoxidised would be interesting to investigate.

ZSM-5(30) could be functionalised in order to have a more hydrophobic surface leading to have more propane in the zeolite.

2. *Hydrocarbon oxidation: Future work*

The purpose of these projects was the selective oxidation of C-H bond. Initiate the activation of C-H bond is a really important step for all reaction; as a consequence the choice of initiator is important. Sometimes, catalytic reactions do not use an initiator; the reaction between substrate and catalyst is enough to obtain the desire products. Nevertheless, for the three reactions investigated in this work, the use of initiator has been essential. The initiation can come from the oxidant itself or from a co-oxidant. TBHP and H_2O_2 have the ability to form radical species, whereas O_2 itself is too stable in mild conditions. In chapter 3, the addition of benzaldehyde in the system initiates octane activation, and O_2 was introduced into products. Hence, benzaldehyde has the role of initiator for octane oxidation.

C-H activation has been successfully investigated; Toluene has been converted into benzoic acid, octane and propane show conversion for the corresponding alcohols, ketones and acids. Toluene shows a high selectivity and few by-products whereas propane and octane show lower activity with a great amount of by-products; products from C-C scission. Prevention of C-C breaking remains a real challenge for linear alkanes.

Increasing the selectivity for primary C-H bonds has already been shown with a homogeneous catalyst. Two groups reported an increase of selectivity for primary C-H bond; one used various ligands in silver catalyst to increase the acidity of the active site.[4] The other group changed their iridium catalyst properties by adding a reducing agent in their system.[5] The ligand effect cannot be used so easily in heterogeneous catalysis; however adding a reagent in the system could change properties and help to be more selective.

The first two projects were linked by the presence of toluene. The idea to use toluene as a co-oxidant for the first project needed the presence of an initiator which was not present in the first step with toluene. The second chapter shows a system able to oxidise toluene to benzoic acid with TBHP/ O_2 system, using TBHP as initiator. Hence, the toluene system could be tried to oxidise octane and other alkanes. Variety of this system can also result from it.

H_2O_2 is a hydrophilic molecule which is not active in a hydrophobic system. H_2O_2 has been produced *in situ*. from H_2 and O_2 by noble metal catalysts with a good stability.[6] In the toluene project, the system is solvent free so toluene is the solvent. Hence if H_2O_2 is formed *in situ*., it will be in organic phase and might be able to activate toluene. This system could also be used for the two other projects, even so using a different catalyst might not activate the formation of H_2O_2. But if it does, it could involve a difference of reactivity.

Inversely, TBHP could be use instead of H_2O_2 in the propane system. TBHP is an organic molecule like propane and it is more hydrophobic than H_2O_2. Hence propane and TBHP might react with a different mechanism. The system would be more difficult to analyse as TBHP can decompose into smaller molecules such as methanol which is also a product from propane oxidation.Further investigation toward catalyst and mechanistic are essentials to improve each systems. In terms of catalyst, determining the active sites and how the substrate interacts with the catalyst would help to design new catalysts. More understanding of the active sites would allow finding other metals, support or treatment in order to improve the reaction. It would also reveal the role of each metal when at least two metals are supported, their interaction with each other, and explain their activity. Finding a system where the product would be desorbed from the surface of the catalyst before its overoxidation would lead to a more selective system.

Kinetic studies and *in situ.* characterisation would be interesting to clarify the mechanism. Combined the knowledge of kinetics and active sites would permit to design a system where catalyst and conditions could selectively catalyse the reactions wanted. Finally, investigations with labelled $^{18}O_2$ experiments are needed to understand the mechanism.

3. Reference

1.   Kesavan, L., Tiruvalam, R., Ab Rahim, M.H., bin Saiman, M.I., Enache, D.I., Jenkins, R.L., Dimitratos, N., Lopez-Sanchez, J.A., Taylor, S.H., Knight, D.W., Kiely, C.J. and Hutchings, G.J., *Science,* 2011. **331** (6014), p. 195-199.

2.   Forde, M.M., Armstrong, R.D., Hammond, C., He, Q., Jenkins, R.L., Kondrat, S.A., Dimitratos, N., Lopez-Sanchez, J.A., Taylor, S.H., Willock, D., Kiely, C.J. and Hutchings, G.J., *Journal of the American Chemical Society,* 2013. **135**, p. 11087-11099.

3.   Hammond, C., Forde, M.M., Rahim, M.H.a., Thetford, A., He, Q., Jenkins, R.L., Dimitratos, N., Lopez-Sanchez, J.A., Dummer, N.F., Murphy, D.M., Carley,

A.F., Taylor, S.H., Willock, D.J., Eric E. Stangland, Kang, J., Hagen, H., Kiely, C.J. and Hutchings, G.J., *Angewandte Communications,* 2012. **51**, p. 5129-5133.

4. Rangan, K., Fianchini, M., Singh, S. and Dias, H.V.R., *Inorganica Chimica Acta,* 2009. **362**, p. 4347-4352.

5. Simmons, E.M. and Hartwig, J.F., *Nature,* 2012. **483**, p. 70-73.

6. Edwards, J.K., Ntainjua, E., Carley, A.F., Herzing, A.A., Kiely, C.J. and Hutchings, G.J., *Angewandte Chemie,* 2009. **48** (45), p. 8512-5.